THÈSE POUR OBTENIR LE GRADE DE DOCTEUR
DE L'UNIVERSITÉ DE MONTPELLIER

En Mathématiques et Modélisation

École doctorale I2S - Information, Structures, Systèmes

Unité de recherche IMAG – Institut Montpelliérain Alexander Grothendieck

Modélisation des fluides multiphasiques

Présentée par Amina MECHERBET
Le 30 septembre 2019

Sous la direction de Matthieu HILLAIRET

Devant le jury composé de

Kleber CARRAPATOSO, Maître de conférences, Université de Montpellier	Examinateur
Anne-Laure DALIBARD, Professeure, Sorbonne Université	Présidente du jury
Laurent DESVILLETTES, Professeur, Université Paris Diderot	Rapporteur
Matthieu HILLAIRET, Professeur, Université de Montpellier	Directeur de thèse
Pierre-Emmanuel JABIN, Professeur, Université du Maryland	Rapporteur
Aline LEFEBVRE-LEPOT, Chargée de recherche CNRS, École polytechnique	Examinatrice
Charlotte PERRIN, Chargée de recherche CNRS, Aix-Marseille Université	Examinatrice

UNIVERSITÉ
DE MONTPELLIER

Remerciements

J'aimerais tout d'abord exprimer ma reconnaissance à mon directeur de thèse, Matthieu Hillairet, pour m'avoir accordé sa confiance en me proposant ce sujet. Merci pour sa bienveillance, sa sympathie et son soutien permanent depuis mon stage de Master. Merci pour le temps conséquent qu'il m'a accordé, ses qualités pédagogiques et scientifiques, pour avoir partagé son savoir, son expérience et ses nombreux conseils avisés. Je tiens également à le remercier pour ses (nombreuses !) relectures méticuleuses qui m'ont été d'un grand secours. J'ai beaucoup appris à ses côtés et je garderai un très bon souvenir de cette période.

J'adresse tous mes remerciements à Laurent Desvillettes et Pierre-Emmanuel Jabin de l'honneur qu'ils m'ont fait en acceptant d'être rapporteurs de cette thèse. Je remercie également Kleber Carrapatoso, Anne-Laure Dalibard, Aline Lefebvre-Lepot et Charlotte Perrin d'avoir accepté de faire partie du jury.

Durant ma thèse, j'ai eu la chance de participer à un des projets scientifiques de la CEMRACS 2018. Je remercie chaleureusement Laurent Boudin, Céline Grandmont, Sébastien Martin et Bérénice Grec de nous avoir fait bénéficier de leurs expériences et leurs conseils. Je tiens spécialement à remercier ma binôme Frédérique Nöel sans qui le travail et mon séjour au CIRM n'auraient pas été si agréables. Je garderai de très bons souvenirs de ces nombreuses heures de boulot et de discussions. Une pensée également à Tao (TNT !) rencontrée à la CEMRACS18.

J'aimerais remercier Julien Salomon rencontré au workshop RheoSuNN pour les discussions enrichissantes autour de la méthode de réflexions. Je remercie Takéo Takahashi pour l'intérêt qu'il a porté à mon travail en m'invitant au séminaire de l'équipe EDP à Nancy. Merci à Ayman Moussa pour ses précieux conseils et nos nombreux échanges scientifiques. Enfin, j'aimerais remercier David Gérard-Varet pour l'intérêt accordé à mes travaux et sa bienveillance.

Je tiens à adresser mes remerciements à tous les membres de l'institut de l'IMAG. Plus particulièrement à tous mes anciens professeurs qui ont renforcé mon amour pour les mathématiques et plus particulièrement l'analyse. Merci aux membres de l'équipe ACSIOM, notamment à Kleber Carrapatoso pour sa lecture de l'article et son intérêt pour mon travail. Un grand merci également à Simon Mendez pour son aide concernant le dernier chapitre. Une pensée particulière à Clément Gallo pour sa bienveillance et ses conseils avisés concernant l'enseignement de l'UE HLMA 102. Enfin, merci à Sophie Cazanave, Bernadette Lacan, Laurence Roux, Nathalie Collain, Carmela Madonia et Brigitte Labric pour leur gentillesse et bienveillance.

Un grand merci à tous les doctorants et post doctorants du bâtiment 9. Tiffany, Louis, Robert, Lamine, Jocelyn, Abel, Maude, Meriem, Zaineb, Pierre, Nestor, Lamis, Florent,... Une spéciale pensée à Alain et Pascal pour avoir pris le temps de répondre à mes questions et m'aider par rapport au cluster ! Merci à mes co-bureau, anciens et nouveaux, Jeremy, Matthieu, Radia et Thiziri pour les discussions et la bonne ambiance.

Une pensée spéciale pour mes amis de la promo du Master 1 rencontrés à Montpellier : Elena, Gabriel, Mario, Matthieu et Robert ! Merci également à Mathilde pour les nombreuses discussions dans le couloir du 3eme étage de la cité U ! Merci à Valérie et Yannick pour leur écoute ! Aussi une pensée à Biba (team biglousettes !) et Kamar (hobi !).

Mes remerciements les plus vifs vont à ma famille sans qui tout cela n'aurait pas été possible, mes parents, Anissa, Fatima, Yacine, Karim, Samia et Amadou. En particulier, merci de m'avoir énormément aidé pour l'organisation du pot !

Enfin, merci à toi Bastien d'avoir toujours été là, de m'avoir constamment soutenu et cru en moi bien plus que moi même. Je ne saurai décrire à quel point je te suis reconnaissante...

Résumé

Dans cette thèse, nous nous intéressons à la modélisation et l'analyse mathématique de certains problèmes liés aux écoulements en suspension.

Le premier chapitre concerne la justification du modèle de type transport-Stokes pour la sédimentation de particules sphériques dans un fluide de Stokes où l'inertie des particules est négligée et leur rotation est prise en compte. Ce travail est une extension des résultats antérieurs pour un ensemble plus général de configurations de particules.

Le deuxième chapitre concerne la sédimentation d'une distribution d'amas de paires de particules dans un fluide de Stokes. Le modèle dérivé est une équation de transport-Stokes décrivant l'évolution de la position et l'orientation des amas. Nous nous intéressons par la suite au cas où l'orientation des amas est initialement corrélée aux positions. Un résultat d'existence locale et d'unicité pour le modèle dérivé est présenté.

Dans le troisième chapitre, nous nous intéressons à la dérivation d'un modèle de type fluide-cinétique pour l'évolution d'un aérosol dans les voies respiratoires. Ce modèle prend en compte la variation du rayon des particules et leur température due à l'échange d'humidité entre l'aérosol et l'air ambiant. Les équations décrivant le mouvement de l'aérosol est une équation de type Vlasov-Navier Stokes couplée avec des équations d'advection diffusion pour l'évolution de la température et la vapeur d'eau dans l'air ambiant.

Le dernier chapitre traite de l'analyse mathématique de l'équation de transport-Stokes dérivée au premier chapitre. Nous présentons un résultat d'existence et d'unicité globale pour des densités initiales de type $L^1 \cap L^\infty$ ayant un moment d'ordre un fini. Nous nous intéressons ensuite à des densités initiales de type fonction caractéristique d'une gouttelette et montrons un résultat d'existence locale et d'unicité d'une paramétrisation régulière de la surface de la gouttelette. Enfin nous présentons des simulations numériques montrant l'aspect instable de la gouttelette.

Mots clés : écoulements de fluides multiphasiques, écoulements en suspension, écoulement de Stokes, sédimentation, équations de (Navier) Stokes, équations de type Vlasov, équations de transport, système d'interaction de particules, méthode de réflexions, théorie de champ moyen, homogéneisation, existence locale et unicité.

Abstract

This thesis is devoted to the modelling and mathematical analysis of some aspects of suspension flows.

The first chapter concerns the justification of the transport-Stokes equation describing the sedimentation of spherical rigid particles in a Stokes flow where particles rotation is taken into account and inertia is neglected. This work is an extension of former results for a more general set of particles configurations.

The second chapter is dedicated to the sedimentation of clusters of particle pairs in a Stokes flow. The derived model is a transport-Stokes equation describing the time evolution of the position and orientation of the cluster. We also investigate the case where the orientation of the cluster is initially correlated to its position. A local existence and uniqueness result for the limit model is provided.

In the third chapter, we propose a coupled fluid-kinetic model taking into account the radius growth of aerosol particles due to humidity in the respiratory system. We aim to numerically investigate the impact of hygroscopic effects on the particle behaviour. The air flow is described by the incompressible Navier-Stokes equations, and the aerosol by a Vlasov-type equation involving the air humidity and temperature, both quantities satisfying a convection-diffusion equation with a source term.

The last chapter is dedicated to the analysis of the transport-Stokes equation derived in the first chapter. First we present a global existence and uniqueness result for $L^1 \cap L^\infty$ initial densities with finite first moment. Secondly, we consider the case where the initial data is the characteristic function of a droplet. We present a local existence and uniqueness result for a regular parametrization of the droplet surface. Finally, we provide some numerical computations that show the regularity breakup of the droplet.

Keywords : multiphase fluid flows, suspension flows, Stokes flows, sedimentation, (Navier) Stokes equations, Vlasov-like equations, transport equations, system of interacting particles, method of reflections, mean field limit, homogenization, local existence and uniqueness.

Table des matières

Introduction

Le travail effectué durant cette thèse traite de la modélisation et l'analyse mathématique de certains aspects des écoulements diphasiques contenant une phase dispersée [1]. Pour ce genre d'écoulements, il s'agit de prendre en compte d'une part l'interaction entre le fluide et les particules constituant la phase dispersée et d'autre part les interactions entre particules. La prévalence d'un effet par rapport à l'autre détermine les caractéristiques principales de l'écoulement. Ainsi, les particules sont en suspension dans le fluide si les interactions fluide/particule sont prévalentes, tandis que l'écoulement est granulaire si les interactions particule/particule sont dominantes.

Dans cette thèse, nous nous concentrons sur les écoulements en suspensions et plus précisément sur les effets micro-hydrodynamiques [2]. La capacité de prédire le comportement d'un grand nombre de micro-particules en suspension dans un fluide constitue un défi crucial qui intervient dans plusieurs processus industriels et naturels. On cite par exemple le transport de sédiments en géomorphologie, génie civil et génie de l'environnement, le problème de séparation des minéraux en génie minier ou le principe de fluidisation en génie chimique. Ce problème est aussi rencontré en biologie pour la modélisation du déplacement de micro-organismes (micro-nageurs) à bas nombre de Reynolds où les aspects micro-hydrodynamiques sont importants [6, 4, 5, 48, 46, 49]. Une autre application est l'étude du mouvement des aérosols dans les voies respiratoires [61, 17, 9, 40, 7, 63, 16]. Enfin nous citons également la modélisation de certains fluides biologiques tels que le sang qui peut être vu comme une suspension de globules rouges, de globules blancs et de plaquettes dans le plasma en négligeant les phénomènes de déformation pour une première approximation [47, 26].

Dans cette thèse, nous considérons le cas d'un écoulement à bas nombre de Reynolds et négligeons l'inertie des particules. Il s'agit d'étudier les forces de frottements exercées par le fluide sur les micro-particules. À l'échelle microscopique, il est possible de décrire la phase dispersée en calculant les trajectoires de chaque particule à travers les lois de Newton. Cependant cette description peut s'avérer couteuse numériquement. Une autre approche serait de négliger le caractère discret de la phase dispersée et de la considérer comme une phase continue. La principale difficulté est alors de représenter les termes de friction à l'échelle macroscopique ou mesoscopique en effectuant une moyennisation. Dans

1. Phase occupant une région non connexe du milieu.

2. L'étude du mouvement de micro-particules en suspension dans un fluide visqueux. Le terme a été introduit par S. Kim et S. J. Karrila dans [44].

ce cas, plusieurs paramètres décrivant la configuration de la suspension rentrent en jeu : la taille des particules, leur nombre, leur géométrie, la fraction volumique de la phase dispersée et la distance minimale entre les particules. La formation d'amas de particules est aussi un phénomène à prendre en compte.

Dans la Section 0.1, nous commençons par rappeler les principales équations modélisant la suspension de particules dans un fluide de Stokes à l'échelle microscopique. Un résumé de l'état de l'art est réalisé dans la Section 0.2. Enfin dans la dernière Section, nous décrivons les principaux résultats obtenus dans cette thèse.

0.1 Principales équations en micro-hydrodynamique

On considère $N \in \mathbb{N}^*$ particules sphériques rigides notées B_i centrées en x_i et de rayon $R > 0$. On suppose que le fluide est Newtonien et incompressible. On note u sa vitesse et p la pression associée. Ces quantités satisfont les équations de Navier-Stokes

$$\left\{\begin{array}{rcl} \varrho_f\left[\partial_t u + (u\cdot\nabla)\,u\right] & = & \operatorname{div}(\sigma(u,p))\,, \\ \operatorname{div}(u) & = & 0\,, \end{array}\right. \quad \text{sur } \mathbb{R}^3\backslash\bigcup_{i=1}^N B_i,$$

où ϱ_f est la densité du fluide et σ désigne le tenseur des contraintes qui s'écrit dans le cas Newtonien:

$$\sigma(u,p) = 2\mu D(u) - p\,\mathbb{I} = \mu\left(\nabla u + \nabla^\top u\right) - p\,\mathbb{I},$$

où μ est la viscosité dynamique du fluide. On complète en considérant des conditions de non glissement

$$\left\{\begin{array}{rcl} u & = & V_i + \Omega_i \times (x - x_i), \text{sur } \partial B_i, \\ \lim\limits_{|x|\to\infty} |u(x)| & = & 0, \end{array}\right.$$

où, pour tout $1 \leqslant i \leqslant N$, $V_i \in \mathbb{R}^3$ est la vitesse linéaire décrivant la translation de la particule, $\Omega_i \in \mathbb{R}^3$ est la vitesse angulaire décrivant la rotation de la particule.
On note θ_i l'orientation de la $i^{\text{ème}}$ particule. Remarquons que comme les particules sont supposées sphériques, leur mouvement est indépendant de l'orientation. En appliquant les lois de Newton on obtient

$$\dot{x}_i = V_i \quad , \quad \dot{\theta}_i = \Omega_i,$$
$$m_i\dot{V}_i = \int_{\partial B_i} \sigma(u,p) n d\sigma + \frac{4}{3}\pi R^3(\varrho_p - \varrho_f)g \quad , \quad J_i\,\dot{\Omega}_i = \int_{\partial B_i} (x - x_i) \times [\sigma(u,p)n] d\sigma\,,$$

où ϱ_p est la densité de la particule, g l'accélération de la pesanteur, n le vecteur normal unitaire orienté vers l'extérieur de la particule. La masse m_i et le moment d'inertie J_i de la $i^{\text{ème}}$ particule sont définis par:

$$m_i = \frac{4}{3}\pi R^3 \varrho_p, \quad J_i = \tfrac{4}{5}\pi R^5 \varrho_p\,.$$

Les quantités notées

$$F_i := \int_{\partial B_i} \sigma(u,p) n d\sigma, \;\; T_i := \int_{\partial B_i} (x - x_i) \times [\sigma(u,p)n] d\sigma,$$

représentent respectivement la force de traînée et le couple appliqués par le fluide sur la particule. Une définition et quelques importantes notions associées sont présentées dans la section 0.1.2.

0.1.1 Adimensionnement

On considère L le diamètre du nuage des particules, V la vitesse moyenne de l'écoulement et $T = L/V$ le temps caractéristique du mouvement. On introduit le changement de variable suivant:

$$\tilde{u} = \frac{u}{V}, \;\; \tilde{p} = \frac{L}{\mu V} p, \;\; \tilde{x} = \frac{x}{L}, \;\; \tilde{t} = \frac{t}{T}.$$

$$\tilde{R} = \frac{R}{L}, \;\; \tilde{X}_i = \frac{X_i}{L}, \;\; \tilde{V}_i = \frac{V_i}{V}, \;\; \tilde{\Omega}_i = T\Omega_i.$$

en gardant la même notation que précédemment on trouve

$$\Delta u - \nabla p = \mathrm{Re}\left(\partial_t u + u \cdot \nabla u\right),$$

où Re est le nombre de Reynolds

$$\mathrm{Re} = \frac{\varrho_f L V}{\mu}.$$

Comme nous nous plaçons dans le cas où l'écoulement est tel que $\mathrm{Re} = \frac{\varrho_f L U}{\mu} \ll 1$, on peut négliger les effets inertiels du fluide. De même, afin de simplifier l'étude, nous négligeons l'inertie des particules.

Remark 0.1.1. *Dans [38], l'auteur montre en particulier que le nombre de Reynolds est négligeable pour des petites fractions volumiques de la suspension. D'autre part, une justification de l'écoulement de Stokes au voisinage d'une micro-particule est présentée dans [30, Chapitre 1 Section 2].*

En partant de ce modèle sans inertie et en considérant une seule particule ayant une vitesse V_p, la formule de Stokes pour la force de traînée F

$$F = 6\pi R V_p, \tag{1}$$

permet d'expliciter la vitesse de chute d'une seule particule sphérique sous l'effet de la gravité qu'on note κg

$$\kappa g = \frac{2}{9} R^2 (\varrho_p - \varrho_f) g. \tag{2}$$

Comme on le verra par la suite, les hypothèses sur la configuration des particules qu'on considère impliquent que la vitesse de chaque particule est comparable à κg. Ceci montre

que l'ordre de grandeur de la vitesse moyenne V est de l'ordre de $|\kappa g|$. D'autre part, en suivant le modèle décrit dans [24], on supposera que le rayon des particules R est proportionnel à N^{-1} de manière à ce que l'accumulation des N forces de traînée définies par la formule (1) soit d'ordre un.
Finalement, pour N fixé, on désigne par (u^N, p^N) la vitesse et pression du fluide satisfaisant l'équation de Stokes suivante

$$\left\{\begin{array}{rcl} -\Delta u^N + \nabla p^N & = & 0\,, \\ \operatorname{div}(u^N) & = & 0\,, \end{array}\right. \text{ sur } \mathbb{R}^3 \backslash \bigcup_{i=1}^{N} B_i. \tag{3}$$

$$\left\{\begin{array}{rcl} u^N & = & V_i + \Omega_i \times (x - x_i), \text{ sur } \partial B_i, \\ \lim\limits_{|x|\to\infty} |u^N(x)| & = & 0, \end{array}\right. \tag{4}$$

les centres $(x_i)_{1i\leqslant i\leqslant N}$ vérifient les lois de Newton

$$\left\{\begin{array}{rcl} \dot{x}_i & = & V_i\,, \\ 0 & = & F_i + \frac{4}{3}\pi R^3(\varrho_p - \varrho_f)\, g\,, \\ 0 & = & T_i. \end{array}\right. \tag{5}$$

Pour N fixé, les équations (3), (4), (5) admettent une unique solution (u^N, p^N) associée à d'uniques vitesses $(V_i, \Omega_i)_{1\leqslant i\leqslant N}$. En effet, il est montré dans [54] que l'application linéaire

$$\begin{pmatrix} F_i \\ T_i \end{pmatrix}_{1\leqslant i\leqslant N} \mapsto \begin{pmatrix} V_i \\ \Omega_i \end{pmatrix}_{1\leqslant i\leqslant N},$$

est bijective. Cette application est appelée matrice de résistance de Stokes et prend une part importante dans la modélisation. Dans ce qui suit, nous rappelons les principales définitions et notions associées à la matrice de résistance et son inverse la matrice de mobilité.

0.1.2 Rappel/définition de la matrice de résistance et mobilité

Dans cette section on considère un fluide ayant une vitesse u et une pression p, on note $\mathcal{B}$ une particule de forme quelconque centrée en $a \in \mathbb{R}^3$.
Les principales forces qui sont appliquées par le fluide sur la particule sont la force de traînée F et les deux composantes du moment d'ordre un M qui sont le couple T et la tension S.
La force de traînée est définie par

$$F = \int_{\partial\mathcal{B}} \sigma(u,p) n d\sigma\,, \tag{6}$$

où n est le vecteur normal unitaire sortant de $\partial\mathcal{B}$. Le moment d'ordre un est défini comme suit

$$M = \int_{\partial\mathcal{B}} (x - a) \otimes [\sigma(u,p)n]\, d\sigma\,. \tag{7}$$

La matrice M se décompose en une partie antisymétrique correspondant au couple T et une partie symétrique correspondant à la tension S. Comme la partie antisymétrique d'une matrice peut être identifiée à un unique vecteur, le couple $T \in \mathbb{R}^3$ peut aussi être défini comme le vecteur suivant

$$T = \int_{\partial \mathcal{B}} (x - a) \times [\sigma(u,p)n] \, d\sigma \, . \tag{8}$$

Par linéarité de l'équation de Stokes et donc du tenseur σ, on peut montrer que l'application

$$\begin{pmatrix} F \\ T \\ S \end{pmatrix} \mapsto \begin{pmatrix} U \\ \Omega \\ E \end{pmatrix},$$

est linéaire. Cette application peut être écrite sous forme d'une matrice par blocs

$$\begin{pmatrix} F \\ T \\ S \end{pmatrix} = -6\pi \begin{pmatrix} \mathcal{R}^{FU} & \mathcal{R}^{F\Omega} & \mathcal{R}^{FE} \\ \mathcal{R}^{TU} & \mathcal{R}^{T\Omega} & \mathcal{R}^{TE} \\ \mathcal{R}^{SU} & \mathcal{R}^{S\Omega} & \mathcal{R}^{SE} \end{pmatrix} \begin{pmatrix} U \\ \Omega \\ E \end{pmatrix} = -6\pi\mathcal{R} \begin{pmatrix} U \\ \Omega \\ E \end{pmatrix}. \tag{9}$$

$\mathcal{R}$ est appelée la matrice de résistance, voir [30, Section 3.5]. On définit également son inverse appelée matrice de mobilité $\mathcal{M} = \mathcal{R}^{-1}$ qui satisfait des propriétés similaires à $\mathcal{R}$. Il est important de noter que $\mathcal{R}^{FU}$, $\mathcal{R}^{F\Omega}$, $\mathcal{R}^{TU}$ et $\mathcal{R}^{T\Omega}$ sont des matrices 3×3 tandis que $\mathcal{R}^{FE}$, $\mathcal{R}^{TE}$, $\mathcal{R}^{SU}$ et $\mathcal{R}^{S\Omega}$ sont des tenseurs d'ordre trois et $\mathcal{R}^{SE}$ est un tenseur d'ordre quatre. La matrice de résistance est proportionnelle à la viscosité du fluide et vérifie certaines symétries selon la géométrie de la particule. De plus, en utilisant des arguments de scaling standards, on peut montrer que la matrice $\mathcal{R}^{FU}$ dépend linéairement de la taille de la particule B, les tenseurs $\left(\mathcal{R}^{T\Omega}, \mathcal{R}^{TE}, \mathcal{R}^{S\Omega}, \mathcal{R}^{SE}\right)$ dépendent de manière cubique de la taille de la particule tandis que $\left(\mathcal{R}^{F\Omega}, \mathcal{R}^{TU}, \mathcal{R}^{SU}, \mathcal{R}^{FE}\right)$ sont proportionnels au carré de la taille de la particule.

Des formules explicites pour la matrice de résistance ont étés étudiées pour certaines géométries particulières du solide. La première formule est due à Stokes pour la relation entre la force de traînée F et la vitesse de translation U dans le cas d'une particule sphérique. Cette formule est connue sous le nom de la loi de Stokes. Toujours dans le cas d'une sphère, en 1922, Faxèn étend la formule en calculant les termes additionnels correspondant à la vitesse de perturbation causée par d'autres sphères de la suspension. Cette formule est appelée la première loi de Faxèn. La seconde loi de Faxèn représente la relation entre le couple T et la vitesse angulaire Ω. Enfin, la troisième loi de Faxèn mettant en évidence la relation entre la vitesse de déformation E et la tension S est calculée par Batchelor et Green dans [12]. Plus précisément, dans le cas d'une particule à forme sphérique ayant un rayon R, la matrice de résistance est diagonale par bloc et on a

$$F = 6\pi\mu R U \, , \quad T = 4\pi\mu R^3 \Omega \, , \quad S = \frac{20}{3}\pi\mu R^3 E.$$

Toujours dans le cas sphérique, Jeffrey et Onishi [42] ont étudié la matrice de résistance et de mobilité associées à une paire de particules. En particulier, ils fournissent des expressions analytiques des matrices en fonction de la distance entre les deux centres et le quotient des rayons des deux particules. En 1971, Brenner et O'neill [18] ont calculé les formules explicites pour le cas d'une particule ellipsoïdale.

0.2 État de l'art

Dans cette thèse, on s'intérèsse à la dérivation mathématique du modèle mésoscopique partant du modèle microscopique. Il s'agit d'étudier le comportement asymptotique des équations (3), (4), (5) lorsque le nombre de particules N tend vers l'infini et le rayon R tend vers zéro. Le but est de mettre en évidence la dépendance du modèle limite par rapport à certaines caractéristiques des particules (distance minimale entre les particules et présence d'amas). Une analyse du modèle limite obtenu est aussi effectuée.

Nous présentons dans cette section un aperçu des principales contributions liées à la dynamique des suspensions. Nous citons premierement les ouvrages [32, 10, 44, 30] regroupant plusieurs aspects théoriques de l'hydrodynamique et des écoulements en suspension. Les différentes questions concernant la modélisation microscopique/mésoscopique de particules en mouvement dans un fluide visqueux ont généré une littérature très riche.

Lorsque l'on cherche à extraire le modèle mésoscopique partant du modèle microscopique, une première étape est de considérer uniquement l'équation de Stokes statique (10)-(11) et d'étudier le comportement asymptotique du couple (u^N, p^N) lorsque le nombre de particules N tend vers l'infini et le diamètre des particules tend vers zéro. Ce processus de moyennisation est appelé homogénéisation et a été introduit par A. Bensoussan, J. L. Lions et G. Papanicolaou dans [13]. Une liste non-exhaustive des ouvrages traitant de ce sujet est [2, 8, 60, 65, 69, 43], nous nous référons également au cours de G. Allaire [3]. L'application de l'homogénéisation aux équations de Stokes et Navier-Stokes dans un domaine perforé est étudiée par G. Allaire dans [1]. La méthode introduite par G. Allaire suit celle de D. Cioranescu et F. Murat [22] pour l'homogénéisation de l'équation de Laplace. Dans [1] l'homogénéisation des équations de Navier-Stokes et Stokes est effectuée pour un domaine contenant plusieurs particules périodiquement distribuées avec des conditions de type Dirichlet homogènes sur chaque particule. L'auteur distingue une caractérisation du comportement asymptotique du modèle selon le comportement asymptotique d'une quantité qui dépend de la distance minimale entre les particules et leur diamètre. Le résultat dans [1] montre que si les particules sont "denses" alors l'équation limite est une équation de Darcy, si les particules sont "diluées" alors le modèle limite est une équation de Stokes et finalement, le modèle limite est une équation de Brinkman si le régime de dilution est à la frontière entre les deux précédents. L'équation de Brinkman est une équation de Stokes à laquelle on ajoute une force de traînée. Ce terme, appelé force de Brinkman, a été identifié par H. C Brinkman [19] et représente la force de frottement collective qu'exerce les particules sur le fluide. Afin d'inclure l'évolution des particules (5) dans le modèle, une importante étape est l'extension du résultat de l'homogénéisation pour des conditions au bord non nulles (non-glissement). En effet, si on veut effectuer un relèvement des conditions au bord afin de se ramener au cas homogène etudié dans [1] cela génere un terme source oscillant dans l'équation de (Navier) Stokes dont le traitement par la méthode de [1] n'est pas immédiat. Cette extension a été effectuée par L. Desvillettes, F. Golse et V. Ricci dans [24] où les auteurs considèrent le cas d'une distribution non périodique de N particules sphériques dans un domaine borné avec des conditions de type Dirichlet non nulles sur les particules. Les principales hypothèses sur la dilution du régime des particules concernent le rayon qui est égale à $\frac{1}{N}$ tandis que la distance minimale entre les particules est de l'ordre de $N^{-1/3}$. Une autre importante généralisation est due à M. Hillairet dans [36] où l'auteur étend le résultat de l'homogénéisation pour des configurations de particules ayant une distance minimale d'ordre strictement supérieur à l'ordre des rayons. En particulier, ces hypothèses recouvrent le cas de particules aléatoirement distribuées dans l'espace. Enfin, dans [37], M. Hillairet, A. Moussa et F. Sueur considèrent le cas où la rotation des particules est prise en compte et la géométrie des obstacles est quelconque. Les auteurs montrent que dans ce cas, la force de Brinkmann se calcule par moyennisation des matrices de résistance de Stokes.

Concernant l'homogénéisation, la difficulté de la résolution de l'équation de Stokes (10) - (11) sur un domaine perforé par un large nombre d'obstacles a amené à l'utilisation de la méthode de réflexions. Cette méthode a été introduite par Smoluchowski [67] en 1911. L'idée est de formuler l'écoulement autour des N particules comme la superposition des N écoulements autour d'une seule particule. Cette formulation n'est pas correcte puisque l'écoulement autour d'une particule isolée génère une erreur sur les conditions aux bords associées aux autres particules. L'idée est alors de corriger les conditions aux bords en réitérant le procédé jusqu'à ce que le terme d'erreur soit assez petit. Formellement, la méthode converge si la suite des termes d'erreurs successifs est strictement décroissante. On définit ainsi un processus itératif qui a de bonnes propriétés de convergence selon le régime de dilution des particules. Cette méthode récursive repose sur le principe de superposition et est appliquée à plusieurs systèmes physiques tels que les équations d'électrostatique. On se refère à [32, Chapter 6 Section 1], [44, Chapter 8] ou [30, Section 4] pour une introduction. À notre connaissance, une preuve de la convergence de la méthode de réflexions pour l'équation de Stokes dans un domaine perforé est fournie pour la première fois par J. H. Luke dans [54]. La méthode décrite dans cet article est formulée grâce à des opérateurs de projection. On se réfère également à l'article de P. Laurent, G. Legendre et J. Salomon [45] où la preuve de convergence est effectuée dans un cadre plus général. On cite aussi l'article de R. Höfer et J. L. L. Velázquez [39] où une méthode de réflexions est développée pour l'homogénéisation de l'équation de Poisson et Stokes dans un domaine perforé.

Pour le problème d'évolution complet (10) - (12), à notre connaissance, il n'existe que deux résultats. Le premier est dû à P. E. Jabin et F. Otto dans [41] où les auteurs considèrent une configuration de particules diluées *i.e.* ayant une distance minimale très grande devant $N^{-1/3}$ et montrent qu'il n'y a pas d'intéraction entre les particules dans ce cas et que le régime est preservé au cours du temps. Plus précisément, ils montrent que la vitesse de chute de chaque particule correspond au premier ordre à la vitesse de chute d'une seule particule dans un fluide visqueux sous l'effet de la gravité. La preuve repose sur le contrôle de la distance minimale entre les particules et l'utilisation de la méthode de réflexions. Le second résultat connu est celui dû à R. Höfer [38] et qui étend le résultat dans [41] pour des configurations de particules ayant une distance minimale de l'ordre de $N^{-1/3}$. De plus, l'auteur fournit une preuve rigoureuse de la convergence de la densité discrète du nuage vers la densité continue solution d'une équation couplée de transport-Stokes.

L'étude du comportement asymptotique d'un système de N particules en interaction est un problème largement étudié en théorie des champs moyens (mean field theory). Pour une introduction au sujet on se réfère au cours de F. Golse [29] et toutes les références qui y figurent pour les nombreuses applications. Le principe est de dériver le modèle limite d'un système de N particules lorsque N tend vers l'infini. Dans ce genre de problèmes, le système d'EDO caractérisant les trajectoires des particules est explicitement donné. Le modèle limite décrivant la densité des particules est une équation de type Vlasov qui dépend de la force d'intéraction. Par exemple, une équation de Vlasov-Poisson pour la force électrostatique de Coulomb dans la théorie des plasmas, un système Vlasov-Maxwell pour la force électrique et magnétique dans la théorie du plasma magnétisé. Une autre application concerne l'approximation de l'équation d'Euler en 2D formulée par le biais de la vorticité. En effet, une version microscopique de l'équation formulée via une densité discrète correspondant à une somme de vortexs (masse de diracs de vorticité) est souvent utilisée en physique statistique pour approcher le modèle continu. Dans ce cas, la force d'intéraction est donnée par la loi de Biot-Savart. Les premiers résultats de convergence sont dus à R. Dobrushin [25] dans le cas où le noyau décrivant la force d'intéraction est lipschitzien. Cependant, les forces d'interactions physiques sont souvent singulières et les estimations de stabilité à la Dobrushin ne s'appliquent pas. Une généralisation est alors effectuée par G. Loeper dans [50] pour l'équation de Vlasov-Poisson. D'autre part, la preuve de convergence en champ moyen pour une classe de noyaux singuliers a été fournie par P. E. Jabin et M. Hauray [34, 33].

En considérant le modèle à l'échelle mésoscopique obtenu, la question de considérer une goutte comme fonction de distribution initiale se pose lorsqu'on veut retrouver le comportement de la suspension à l'échelle mésoscopique. Des études numériques et expérimentales ont été effectuées dans [55, 58, 62] et menèrent à la conclusion qu'une goutte, initialement de forme sphérique, évolue lentement vers un tore. Plus précisément, les particules au sommet du nuage s'échappent et forment un filet vertical. La diminution du nombre de particules sur l'axe vertical du nuage conduit à l'apparition de la forme toroïdale. De plus, il a été observé que le tore instable se brise en deux gouttelettes secondaires qui se déforment en tores elles-mêmes en cascade répétitive.

0.3 Description du contenu de la thèse

Dans cette thèse, nous nous intéressons à certains aspects liés à la modélisation des écoulements en suspension. Les principales études sont décrites dans les chapitres un, deux, trois et quatre et sont résumées ci-dessous. Le premier chapitre concerne la justification de la convergence du modèle microscopique décrivant la sédimentation de particules sans inertie dans un fluide de Stokes vers un modèle mésoscopique. Plus précisément, le premier chapitre est une extension du résultat de R. M. Höfer [38] pour un ensemble de configurations de particules plus général. Dans le deuxième chapitre, nous nous intéressons à la dérivation d'un modèle mésoscopique pour la description d'amas de paires de particules et présentons un résultat d'existence et d'unicité pour le modèle limite. La principale motivation de ce travail est de mettre en évidence l'influence des amas de particules sur la vitesse moyenne de chute à travers les matrices de résistance de Stokes. Le troisième chapitre est dédié à la dérivation d'un modèle pour le mouvement d'aérosols dans les voies respiratoires en prenant en compte la variation du rayon des particules et l'échange de température dans le système. Ce travail est une collaboration avec L. Boudin, C. Grandmont, B. Grec, S. Martin et F. Noël dans le cadre de la CEMRACS 2018. Une étude numérique de la déposition des particules dans une bifurcation en 2D est présentée. Finalement, Le dernier chapitre est dédié à l'analyse du modèle limite dérivé dans le premier chapitre. Plus précisément nous présentons un résultat d'existence et d'unicité permettant de traiter des densités initiales de type $L^1 \cap L^\infty$ ayant un moment d'ordre un fini. Nous nous intéressons ensuite à l'étude de la régularité du bord d'une gouttelette dans un fluide de Stokes. Nous montrons un résultat d'existence locale et d'unicité d'une paramétrisation régulière de la gouttelette et présentons quelques tests numériques montrant l'aspect instable de la gouttelette.

0.3.1 Sédimentation de particules dans un fluide de Stokes

Dans ce chapitre, nous considérons N particules identiques rigides et sphériques notées $(B_i)_{1\leqslant i\leqslant N}$ en sédimentation dans un écoulement de Stokes soumis à une force gravitationnelle. Les effets inertiels du fluide et des particules sont négligés et la rotation des particules est prise en compte. Pour N donné, la vitesse du fluide et la pression sont notées (u^N, p^N) et satisfont l'équation suivante

$$\left\{\begin{array}{rcl} -\Delta u^N + \nabla p^N &=& 0, \\ \operatorname{div} u^N &=& 0, \end{array}\right. \quad \text{sur } \mathbb{R}^3 \backslash \bigcup_{i=1}^{N} \overline{B_i}, \tag{10}$$

complétée par des conditions de non-glissement

$$\left\{\begin{array}{rcl} u^N &=& V_i + \Omega_i \times (x - x_i), \text{ sur } \partial B_i, \\ \lim\limits_{|x|\to\infty} |u^N(x)| &=& 0, \end{array}\right. \tag{11}$$

où $(V_i, \Omega_i) \in \mathbb{R}^3 \times \mathbb{R}^3$, $1 \leqslant i \leqslant N$ sont les vitesses linéaires et angulaires des particules. Les particules sont définies comme suit

$$B_i := B(x_i, R) \quad , \quad R = \frac{r_0}{N},$$

où r_0 est une constante positive. On décrit le mouvement des particules $(B_i)_{1\leqslant i\leqslant N}$ en considérant les lois de Newton où on a négligé les termes inertiels

$$\left\{\begin{array}{rcl} \dot{x}_i & = & V_i, \\ F_i + mg & = & 0, \\ T_i & = & 0, \end{array}\right. \tag{12}$$

m est la masse de la particule normalisée afin de prendre en compte la poussée d'Archimède, g l'accélération de la pesanteur, la force de traînée F_i et le couple T_i sont définis par (6), (8).
Il a été montré dans [38] que la densité spatiale discrète du nuage ϱ^N définie par

$$\varrho^N(t,x) = \frac{1}{N}\sum_{i=1}^{N}\delta_{x_i(t)}(x) \quad , \quad \varrho_0^N := \varrho^N(0,x),$$

converge vers l'unique densité continue ϱ solution de l'équation couplée transport-Stokes suivante

$$\left\{\begin{array}{rcl} \frac{\partial \varrho}{\partial t} + \operatorname{div}((\kappa g + u)\varrho) & = & 0\,, \\ -\Delta u + \nabla p & = & 6\pi r_0 \kappa \varrho g\,, \\ \operatorname{div}(u) & = & 0\,, \\ \varrho(0,\cdot) & = & \varrho_0\,, \end{array}\right. \tag{13}$$

où (u,p) sont la vitesse et pression du fluide. κg, définie par (2), est la vitesse de chute d'une seule particule dans un fluide sous l'effet de la gravité.
L'auteur montre également l'existence et l'unicité de la solution de l'équation de transport-Stokes (13)

Theorem 0.3.1 (R. Höfer)**.** *Soit $\varrho_0 \in X_\beta^1$ pour $\beta > 2$. Alors il existe une unique solution $\varrho \in W^{1,\infty}((0,T), X_\beta)$ pour tout $T > 0$. De plus $\nabla\varrho \in L^\infty((0,T), X_\beta)$.*

L'espace X_β est défini par

Definition 0.3.1. *Soit $\beta > 0$, on définit l'espace X_β comme suit*

$$X_\beta := \{h \in L^\infty(\mathbb{R}^3)\,,\, \|h\|_{X_\beta} < \infty\},$$

avec

$$\|h\|_{X\beta} := \operatorname*{esssup}_x (1 + |x|^\beta)|h(x)|.$$

De plus, on utilisera la notation $h \in X_\beta^1$ pour désigner les éléments h tels que $h, \nabla h \in X_\beta$.

Le résultat de convergence de ϱ^N vers ϱ présenté dans [38] est valable sous l'hypothèse que la distance minimale entre les particules est de l'ordre de $N^{-1/3}$. Cependant, le seuil idéal pour la distance minimal entre les particules est $N^{-2/3}$. En effet, ce seuil permet de traiter le cas de particules aléatoirement distribuées. La motivation principale du premier chapitre est donc d'étendre le résultat de convergence à un ensemble plus général de configurations de particules.
Avant de présenter les principaux résultats de ce chapitre nous commençons par définir l'ensemble des configurations de particules que nous considérons dans ce chapitre.

Definition 0.3.2. *Soit* $(X^N)_{N\in\mathbb{N}^*}$ *une configuration de particules où* $X^N := (x_1, \cdots, x_N)$. *Étant donné deux constantes positives* $\bar{M}, \mathcal{E}$ *on définit* $\mathcal{X}(\bar{M}, \mathcal{E})$ *comme l'ensemble des configurations de particules pour lesquelles il existe une suite positive* $(\lambda^N)_{N\in\mathbb{N}^*}$ *telle que la concentration* $(M^N)_{N\in\mathbb{N}^*}$ *définie par*

$$M^N := \sup_{x\in\mathbb{R}^3}\{\#\{i \in \{1, \cdots, N\} \text{ such that } x_i \in \overline{B_\infty(x, \lambda^N)}\}\}, \forall N \in \mathbb{N}^*,$$

et la distance minimale $(d^N_{\min})_{N\in\mathbb{N}^*}$ *définie par*

$$d^N_{\min} := \min_{\substack{i\neq j \\ 1\leqslant i,j\leqslant N}} \{|x_i - x_j|\}, \forall N \in \mathbb{N}^*,$$

vérifient les hypothèses suivantes:

$$\sup_{N\in\mathbb{N}} \frac{M^N}{N|\lambda^N|^3} \leqslant \bar{M}, \tag{14}$$

$$\sup_{N\in\mathbb{N}} \frac{|\lambda^N|^3}{|d^N_{\min}|^2} \leqslant \mathcal{E}. \tag{15}$$

λ^N *vérifie les conditions de compatibilité suivantes:*

$$\lambda^N \geqslant d^N_{\min}/2 \quad , \quad \lim_{N\to\infty} \lambda^N = 0. \tag{16}$$

Remark 0.3.1. *Selon la définition de* M^N *et l'hypothèse* (14) *on a*

$$\frac{1}{N|\lambda^N|^3} \leqslant \bar{M}, \tag{17}$$

ce qui implique grâce à (15)

$$d^N_{\min} \geqslant \frac{1}{\sqrt{\mathcal{E}}\bar{M}^{1/2}} \frac{1}{\sqrt{N}}. \tag{18}$$

Comme $R \sim \frac{1}{N}$, *on a*

$$\lim_{N\to\infty} \frac{R}{d^N_{\min}} = 0, \tag{19}$$

ce qui garantit la non-collision des particules dans le régime $\mathcal{X}(\bar{M}, \mathcal{E})$.

Enfin, nous avons besoin de l'hypothèse suivante pour la preuve du second Théorème 0.3.3

$$\lim_{N\to\infty} \frac{|\lambda^N|^2}{d^N_{\min}(0)} = 0. \tag{20}$$

Exemple: Dans le cas où $\lambda^N := N^{-1/3}$, le régime $\mathcal{X}(\bar{M}, \mathcal{E})$ correspond aux particules telles que leur distance minimale $d^N_{\min}$ est supérieure au seuil $N^{-1/2}$ et leur concentration par cube de longueur $N^{-1/3}$ est uniformément bornée. Ce cas de figure correspond à une extension des configurations de particules considérées dans les articles [41] et [38].

Le rôle de la suite λ^N est intimement lié à la notion de distance de Wasserstein infinie, voir la discussion plus détaillée sur les hypothèses dans la section 1.2 du premier chapitre et le lemme 1.A.4.
Le premier résultat de ce chapitre est la conservation du régime sur un temps court indépendant de N.

Theorem 0.3.2. *Soit $(X^N(0))_{N\in\mathbb{N}^*}$ une configuration initiale de particules. Supposons qu'il existe deux constantes $\bar{M}$, $\mathcal{E}$ et une suite $(\lambda^N)_{N\in\mathbb{N}^*}$ telles que $(X^N(0))_{N\in\mathbb{N}^*}$ appartient à l'ensemble $\mathcal{X}(\bar{M},\mathcal{E})$ i.e. les hypothèses (14), (15), (16) sont satisfaites initialement.*
Si $\bar{M}^{1/3}r_0$ est assez petit, il existe un rang $N^* = N(r_0,\bar{M},\mathcal{E}) \in \mathbb{N}^*$ et $T = T(r_0,\mathcal{E},\bar{M},\kappa|g|)$ tels que pour tout $t \in [0,T]$ et $N \geqslant N^*$

$$d_{\min}^N(t) \geqslant \frac{1}{2} d_{\min}^N(0),$$

$$M^N(t) \leqslant 8^4 M^N(0).$$

Le second résultat est la justification de la convergence de la densité ϱ^N vers ϱ lorsque N tend vers l'infini.

Theorem 0.3.3. *Considérons le temps maximal $T > 0$ introduit au premier Théorème 0.3.2 et l'hypothèse additionnelle (20). Soit $\beta > 2$, on suppose que $\varrho_0 \in X_\beta^1$ est une densité positive telle que $\int_{\mathbb{R}^3} \varrho_0 = 1$. On note par (ϱ, u) l'unique solution de l'équation de transport-Stokes (13).*
Il existe deux constantes positives $C_1, C_2 = C(r_0,\bar{M},\mathcal{E},\|\varrho_0\|_{L^\infty},\kappa|g|)$ indépendantes de N et un rang $N^* = N(r_0,\bar{M},\mathcal{E},\|\varrho_0\|_{L^\infty},\kappa|g|,T) \in \mathbb{N}^*$ tels que pour tout $t \in [0,T]$ et tout $N \geqslant N^*$

$$W_1(\varrho^N(t,\cdot),\varrho(t,\cdot)) \leqslant C_1\left(\lambda^N + d_{\min}^N(0)\,t + W_1(\varrho_0,\varrho_0^N)\right)e^{C_2 t}.$$

Ceci montre que si la densité discrète initiale ϱ_0^N converge vers une densité ϱ_0 alors la densité discrète ϱ^N converge en tout temps $0 \leqslant t \leqslant T$ vers la solution ϱ de l'équation (13). De plus, le Théorème 0.3.3 fournit une estimation quantitative de la convergence en fonction de la distance de Wasserstein initiale $W_1(\varrho_0,\varrho_0^N)$.
L'ensemble des configurations de particules introduit dans le définition 0.3.2 est basé sur l'article [36]. Les hypothèses (14) et (16) assurent l'existence d'une densité discrète uniformément bornée approchant ϱ^N. Ce qui suggère que la densité limite ϱ est L^∞ et que la constante $\bar{M}$ est équivalente à $\|\varrho\|_\infty$.
La condition de petitesse sur $r_0\bar{M}^{1/3}$ correspond au fait que l'on considère une densité de particules telle que $\|\varrho\|_\infty$ est petite mais d'ordre un. En effet, dans ce cas, la vitesse u dans l'équation de transport-Stokes (13) est proportionnelle à $\|\varrho\|_\infty$ et peut être vue comme une perturbation (d'ordre un) de la vitesse de chute κg.
La deuxième hypothèse (15) assure la conservation de la distance minimale au cours du temps. En particulier, pour $\lambda^N = N^{-1/3}$, le Théorème 0.3.2 étend les résultats antérieurs à des configurations de particules ayant une distance minimale de l'ordre d'au moins $N^{-1/2}$, voir hypothèse (15). Ce seuil minimal apparait naturellement dans nos calculs et est relié

aux propriétés de la fonction de Green de l'équation de Stokes. Nous soulignons que cette distance minimale critique apparaît également dans l'analyse de champ moyen effectuée dans [33]. Ceci est dû au lien entre λ^N et la distance de Wasserstein infinie $W_\infty(\varrho^N, \varrho)$. Cette remarque est détaillée dans la section 1.2 du premier chapitre.
La preuve des deux théorèmes repose sur le développement d'une méthode de réflexions qui permet une approximation à l'ordre un des vitesses linéaires et angulaires (V_i, Ω_i) de chaque particule.

$$V_i = \kappa g + 6\pi \frac{r_0}{N} \sum_{j \neq i} \Phi(x_i - x_j)\kappa g + O\left(d_{\min}^N\right), \quad R\Omega_i = O\left(d_{\min}^N\right), \quad 1 \leqslant i \leqslant N,$$

où Φ est la fonction de Green de l'équation de Stokes appelée tenseur d'Oseen, voir (1.26). Une fois les trajectoires des particules connues, le contrôle de la distance minimale $d_{\min}^N$ et de la concentration M^N sur un temps court se font par un argument de Gronwall. Pour la preuve du second théorème, l'idée principale est d'appliquer la théorie de champ moyens développée par M. Hauray et P. E. Jabin dans [33, 34] pour le système approché des N particules.

0.3.2 Un modèle pour la suspension d'amas de paires de particules

Dans ce chapitre, nous nous intéressons à la dérivation d'un modèle mésoscopique décrivant la suspension d'amas de paires de particules dans un fluide de Stokes. La motivation principale est la mise en évidence de l'influence de l'amas sur la vitesse de chute moyenne du nuage. La description de la configuration de l'amas se fait à travers les deux variables suivantes : la position du centre de la paire de particules $x \in \mathbb{R}^3$ et l'orientation de la paire de particules $\xi \in \mathbb{R}^3$. Dans un premier temps, nous dérivons un modèle limite décrivant l'évolution des amas à travers la fonction $f(t, x, \xi)$ représentant la densité des amas de paires centrés en x et ayant une orientation ξ au temps t. En particulier, on montre que la vitesse de chute moyenne s'écrit en fonction de la matrice de résistance de Stokes associée à une paire de particules. Dans un second temps, nous nous intéressons à des données initiales pour lesquelles l'orientation du cluster est corrélée aux positions *i.e.* $\xi = F(x)$. Le modèle dérivé est alors une équation de transport-Stokes, portant sur la première marginale de f notée ϱ, la vitesse du fluide u et la fonction F qui décrit l'évolution de l'orientation de l'amas. Nous présentons également un résultat d'existence locale et d'unicité pour le système dérivé.
Les équations de départ décrivent le mouvement du nuage à l'échelle microscopique et sont analogues à celles utilisées dans le premier chapitre. On note par N le nombre de paires de particules définies comme suit

$$B^i := B(x_1^i, R) \cup B(x_2^i, R) := B_i^1 \cup B_i^2\,, 1 \leqslant i \leqslant N,$$

où x_1^i, x_2^i les centres de la $i^{\text{ème}}$ paire, R est le rayon. On définit (u^N, p^N) l'unique solution de l'équation de Stokes:

$$\left\{\begin{array}{rcl} -\Delta u^N + \nabla p^N & = & 0, \\ \operatorname{div} u^N & = & 0, \end{array}\right. \text{sur } \mathbb{R}^3 \setminus \bigcup_{i=1}^N \overline{B}^i, \tag{21}$$

complétée par des conditions de non-glissement

$$\left\{\begin{array}{rcl} u^N & = & U_1^i \text{ sur } \partial B(x_1^i, R), \\ u^N & = & U_2^i \text{ sur } \partial B(x_2^i, R), \\ \lim\limits_{|x|\to\infty} |u^N(x)| & = & 0, \end{array}\right. \tag{22}$$

où $(U_1^i, U_2^i) \in \mathbb{R}^3 \times \mathbb{R}^3$, $1 \leqslant i \leqslant N$ sont les vitesses linéaires des particules. Dans ce modèle, on néglige la vitesse angulaire. On complète par les équations de mouvements de chaque particule

$$\left\{\begin{array}{rcl} \dot{x}_1^i & = & U_1^i, \\ \dot{x}_2^i & = & U_2^i. \end{array}\right. \tag{23}$$

Les lois de Newton impliquent les relations suivantes où l'inertie des particules est négligée

$$\begin{pmatrix} F_1^i \\ \\ F_2^i \end{pmatrix} = -\begin{pmatrix} mg \\ \\ mg \end{pmatrix}, \tag{24}$$

où m est la masse des particules normalisée afin de prendre en compte la poussée d'Archimède. g l'accélération de pesanteur, F_1^i, F_2^i sont les forces de traînée appliquées sur la $i^{\text{ème}}$ paire

$$F_1^i = \int_{\partial B(x_1^i, R)} \sigma(u^N, p^N) n \quad , \quad F_2^i = \int_{\partial B(x_2^i, R)} \sigma(u^N, p^N) n,$$

où n est le vecteur normal sortant et $\sigma(u^N, p^N) = (\nabla u^N + (\nabla u^N)^\top) - p^N \mathbb{I}$ est le tenseur des contraintes.

Avant d'énoncer les résultats nous introduisons les principales notations et hypothèses.

On suppose que le rayon des particules est donné par

$$R = \frac{r_0}{2N},$$

où r_0 est une constante positive. Nous adopterons les notations suivantes pour une paire de particules donnée $B(x_1, R)$, $B(x_2, R)$

$$x_+ := \frac{1}{2}(x_1 + x_2), \quad x_- := \frac{1}{2}(x_1 - x_2), \quad \xi := \frac{x_-}{R}.$$

Soit $T > 0$ fixé, on définit la densité discrète $\mu^N \in \mathcal{P}([0, T] \times \mathbb{R}^3 \times \mathbb{R}^3)$ par

$$\mu^N(t, x, \xi) = \frac{1}{N} \sum_1^N \delta_{\left(x_+^i(t), \xi_i(t)\right)}(x, \xi).$$

On note par ϱ^N sa première marginale

$$\varrho^N(t,x) := \frac{1}{N}\sum_i \delta_{x_+^i(t)}(x). \tag{25}$$

On définit $d_{\min}$ la distance minimale entre les centres des paires x_+^i

$$d_{\min}(t) := \min\{d_{ij}(t) := |x_+^i(t) - x_+^j(t)|\,,\, i \neq j\}.$$

On suppose qu'il existe deux constantes $M_1 > M_2 > 1$ indépendantes de N telles que:

$$M_2 \leqslant |\xi_i| \leqslant M_1 \;,\; i = 1, \cdots, N \;\; \forall\, t \in [0,T]. \tag{26}$$

On suppose que μ^N converge au sens des mesures vers une densité continue μ *i.e.* pour tout $\psi \in \mathcal{C}_b([0,T] \times \mathbb{R}^3 \times \mathbb{R}^3)$ on a

$$\int_0^T \int_{\mathbb{R}^3} \int_{\mathbb{R}^3} \psi(t,x,\xi)\mu^N(t,dx,d\xi)dt \underset{N\to\infty}{\to} \int_0^T \int_{\mathbb{R}^3} \int_{\mathbb{R}^3} \psi(t,x,\xi)\mu(t,x,\xi)dx\,d\xi\,dt. \tag{27}$$

On suppose que la première marginale de μ notée ϱ est une mesure de probabilité vérifiant $\varrho(t,\cdot) \in W^{1,1}(\mathbb{R}^3) \cap W^{1,\infty}(\mathbb{R}^3)$. On utilisera la notation

$$W_\infty(t) := W_\infty(\varrho^N(t,\cdot), \varrho(t,\cdot)),$$

pour définir la distance de Wasserstein infinie entre ϱ^N et ϱ, voir Définition 1.5.4. On suppose qu'il existe une constante positive $\mathcal{E}_1 > 0$ telle que pour tout $t \in [0,T]$

$$\sup_{N\in\mathbb{N}^*} \frac{W_\infty^3}{d_{\min}^2} \leqslant \mathcal{E}_1. \tag{28}$$

Finalement, pour le second Théorème, on suppose qu'il existe une constante positive $\mathcal{E}_2 > 0$ telle que pour tout $t \in [0,T]$

$$\sup_{N\in\mathbb{N}^*} \frac{W_\infty^3}{d_{\min}^3} \leqslant \mathcal{E}_2. \tag{29}$$

Remark 0.3.2. *La formule* (27) *implique*

$$\sup_{t\in[0,T]} W_\infty(t) \underset{N\to\infty}{\to} 0. \tag{30}$$

De plus, comme $\varrho \in L^\infty$, on a une borne inférieure pour la distance de Wasserstein

$$\frac{1}{N W_\infty^3} \lesssim \sup_{x\in\mathbb{R}^3} \frac{\varrho^N(B(x,W_\infty))}{|B(x,W_\infty)|^3} \lesssim \|\varrho\|_\infty.$$

La définition de la distance de Wasserstein infinie assure que

$$W_\infty \geqslant d_{\min}/2\,, \tag{31}$$

ce qui implique en utilisant (30)

$$\sup_{t\in[0,T]} d_{\min}(t) \underset{N\to\infty}{\to} 0. \tag{32}$$

On peut à présent énoncer les principaux théorèmes de ce chapitre.

Theorem 0.3.4. *Supposons que les hypothèses* (26), (27), (28) *sont satisfaites et que* $r_0\|\varrho_0\|_{L^1\cap L^\infty}$ *est assez petit.* μ *satisfait l'équation de transport suivante*

$$\begin{cases} \partial_t\mu + \mathrm{div}_x[(\mathbb{A}(\xi))^{-1}\kappa g + u)\mu] + \mathrm{div}_\xi[\nabla u\cdot\xi\mu] &= 0\,, & sur\ [0,T]\times\mathbb{R}^3\times\mathbb{R}^3,\\ -\Delta u + \nabla p &= 6\pi r_0\kappa\varrho g\,, & sur\ \mathbb{R}^3,\\ \mathrm{div}(u) &= 0\,, & sur\ \mathbb{R}^3. \end{cases}$$

Le second théorème concerne des données initiales pour lesquelles l'orientation des amas est corrélée aux positions.

Theorem 0.3.5. *Considérons les hypothèses du théorème* (0.3.4) *et* (29), *supposons qu'il existe une fonction* $F_0 \in W^{1,\infty}$ *telle que* $\xi_i(0) = F_0(x_+^i(0))$ *pour tout* $1 \leqslant i \leqslant N$.
Il existe $T > 0$ *indépendent de* N *et une unique fonction* $F^N \in L^\infty(0,T;W^{1,\infty})$ *telle que pour tout* $t\in[0,T]$ *on a*

$$\mu^N = \varrho^N \otimes \delta_{F^N} \quad et\ F^N(0,\cdot) = F_0.$$

De plus, la suite $(F^N)_N$ *admet une limite notée* $F \in L^\infty(|0,T],W^{1,\infty})$ *et la mesure limite* μ *est de la forme* $\mu = \varrho\otimes\delta_F$. *Le triplet* (ϱ,F,u) *satisfait le système suivant*

$$\begin{cases} \partial_t F + \nabla F\cdot(\mathbb{A}(F)^{-1}\kappa g + u) &= \nabla u\cdot F, & sur\ [0,T]\times\mathbb{R}^3,\\ \partial_t\varrho + \mathrm{div}((\mathbb{A}(F)^{-1}\kappa g + u)\varrho) &= 0, & sur\ [0,T]\times\mathbb{R}^3,\\ -\Delta u + \nabla p &= 6\pi r_0\kappa g\varrho, & sur\ \mathbb{R}^3,\\ \mathrm{div}\, u &= 0, & sur\ \mathbb{R}^3,\\ \varrho(0,\cdot) &= \varrho_0, & sur\ \mathbb{R}^3,\\ F(0,\cdot) &= F_0 & sur\ \mathbb{R}^3. \end{cases} \tag{33}$$

Remark 0.3.3. *La matrice* $\mathbb{A}$ *est définie par* $\mathbb{A} := A_1 + A_2$ *où* A_1 *et* A_2 *forment la matrice de résistance associée à une paire de particules, voir section 2.2.1 pour la définition. Le terme* $(\mathbb{A})^{-1}\kappa g$ *représente la vitesse moyenne de chute d'une paire de particules identiques en suspension dans un fluide de Stokes.*

Nous finissons par un résultat d'existence locale et d'unicité.

Theorem 0.3.6. *Soit* $p > 3$, $F_0 \in W^{2,p}$ *et* $\varrho_0 \in W^{1,p}$ *à support compact. Il existe* $T > 0$ *et un unique triplet* $(\varrho,F,u)\in L^\infty(0,T;W^{1,p})\times L^\infty(0,T;W^{2,p})\times L^\infty(0,T;W^{3,p})$ *solution du système* (33).

De même qu'au premier chapitre, l'idée de preuve des deux premiers théorèmes est d'utiliser la méthode de réflexions pour effectuer une approximation de la trajectoire des particules

$$\begin{cases} \dot{x}_+^i &\sim & (\mathbb{A}(\xi_i))^{-1}\kappa g + \frac{6\pi r_0}{N}\sum\limits_{j\neq i}\Phi(x_+^i - x_+^j)\kappa g,\\ \dot{\xi}_i &\sim & \left(\frac{6\pi r_0}{N}\sum\limits_{j\neq i}\nabla\Phi(x_+^i - x_+^j)\kappa g\right)\cdot\xi_i. \end{cases} \tag{34}$$

La force d'interaction Φ est le tenseur d'Oseen, voir formule (2.17). Comme la distance entre deux particules formant la paire est comparable au rayon, la méthode de réflexions utilisée ici consiste à approcher l'écoulement autour des N paires par la superposition des N écoulements autour d'une seule paire. Par conséquent, une analyse des solutions particulières associées à l'écoulement d'une paire de particules en translation est nécessaire. De manière similaire au premier chapitre, la convergence de la méthode de réflexions est assurée sous l'hypothèse de petitesse de $r_0\|\varrho_0\|_{L^1\cap L^\infty}$ et les hypothèses (26), (27).
Dans ce chapitre nous nous concentrons uniquement sur la dérivation des modèles limite. Nous ne traitons pas la conservation de la distance minimale $d_{\min}$ et de la distance de Wasserstein W_∞. Les propositions 2.B.3 et 2.B.1 montrent que le contrôle de la distance minimale $d_{\min}$ dépend du contrôle de la distance de Wasserstein W_∞. Cependant, l'apparition du gradient du tenseur d'Oseen $\nabla\Phi$ dans la formule (34) qui a un ordre de singularité de type $\frac{1}{|x|^2}$ génère un terme en log dans les estimations permettant de contrôler W_∞, voir proposition 2.B.2. Ceci empêche l'utilisation d'un argument de Gronwall pour la convergence en champ moyen dans l'esprit de [33, 34].

0.3.3 Modélisation de type fluide-cinétique pour des aérosols respiratoires de taille et de température variables

Dans ce chapitre nous nous intéressons à la modélisation du mouvement d'un aérosol dans les voies respiratoires. Le but est de dériver un modèle qui prend en compte la variation du rayon et de la température des particules. Cette variation est causée par l'échange d'humidité entre l'aérosol et l'air ambiant dans les voies respiratoires. Ce travail a été effectué en collaboration avec L. Boudin, C. Grandmont, B. Grec, S. Martin et F. Noël dans le cadre de la CEMRACS 2018.
L'étude du mouvement des aérosols dans les voies respiratoires est un sujet de recherche qui a engendré une large littérature de par la complexité et les nombreuses possibilités de modélisation. En effet, il est possible de considérer différentes échelles allant du microscopique, où on suit la trajectoire de chaque particule, mésoscopique où l'aérosol est représenté par une fonction de densité ou enfin macroscopique, où l'aérosol est considéré comme étant une phase continue et est caractérisé par sa concentration dans le fluide. Pour plus de détails, on se réfère à la thèse de A. Moussa [61] dédiée à l'étude mathématique et numérique du transport d'aérosols dans le poumon.
Dans cette étude, nous nous plaçons à l'échelle mésoscopique et nous considérons le modèle de type fluide-cinétique utilisé dans [17]. Dans ce modèle, le fluide représentant l'air est supposé Newtonien et incompressible et on suppose que la fraction volumique de l'aérosol dans le fluide est négligeable afin de ne pas prendre en compte les collisions entre les particules. L'équation décrivant le phénomène est une équation de Vlasov Navier-Stokes [15]. On note (u,p) la vitesse et pression du fluide, f représente la densité des particules. On note $\Omega \subset \mathbb{R}^3$ le domaine du fluide qui correspond à une bifurcation. Le bord du domaine $\partial\Omega$ est constitué de trois parties, l'entrée Γ^{in}, la sortie Γ^{out} et les parois Γ^{wall}, voir Figure

3.1. Les équations s'écrivent comme suit

$$\left\{\begin{array}{rcll} \varrho_{\mathrm{air}}[\partial_t u + (u\cdot\nabla)u] - \eta\Delta u + \nabla p &=& F, & \text{sur } \mathbb{R}^* \times \Omega, \\ \partial_t f + v\cdot\nabla_x f + \mathrm{div}_v\left(\left[\alpha(u-v) + \left(1-\frac{\varrho_{\mathrm{air}}}{\varrho_d}\right) g\right] f\right) &=& 0, & \text{sur } \mathbb{R}^* \times \Omega \times \mathbb{R}^3, \\ \mathrm{div}(u) &=& 0, & \text{sur } \mathbb{R}^* \times \Omega, \end{array}\right. \quad (35)$$

Ici ϱ_{air}, ϱ_d sont les masses volumiques de l'air et des particules, η la viscosité dynamique, g le vecteur gravité et F le terme de rétroaction défini par

$$F(t,x) = -6\pi\eta r \int_{\mathbb{R}^3} (u(t,x) - v) f(t,x,v) dv.$$

La variable $v \in \mathbb{R}^3$ représente la vitesse de l'aérosol, r leur rayon et on a

$$\alpha = \frac{6\pi\eta r}{m},$$

où m est la masse des particules. On complète (35) avec des conditions au bord et des conditions initiales

$$\left\{\begin{array}{rcll} f &=& 0, & \text{on } \mathbb{R}^+ \times \Gamma^{\mathrm{wall}} \times \mathbb{R}^3, \text{ if } v\cdot n \leqslant 0, \\ u &=& u^{\mathrm{in}}, & \text{sur } \mathbb{R}^+ \times \Gamma^{\mathrm{in}}, \\ u &=& 0, & \text{sur } \mathbb{R}^+ \times \Gamma^{\mathrm{wall}}, \\ \sigma(u,p)\cdot n &=& 0, & \text{sur } \mathbb{R}^+ \times \Gamma^{\mathrm{out}}, \\ u_{|t=0} &=& u_0, & \text{on } \Omega, \\ f_{|t=0} &=& f_{\mathrm{init}}, & \text{sur } \Omega \times \mathbb{R}^3\ . \end{array}\right. \quad (36)$$

Dans ce modèle, la variation du rayon r n'est pas prise en compte. Le but de ce chapitre est alors d'intégrer la variation de la taille des particules mais aussi leur température dans le modèle. L'idée est de considérer les articles [51, 52, 53] où un modèle $0D$ est présenté pour la modélisation de l'évolution du rayon et de la température d'une particule dans les voies respiratoires via l'échange de température et de vapeur d'eau entre l'aérosol et l'air ambiant dans le poumon.

Dans ce nouveau modèle, la densité f est fonction de $(t,x,v,r,T) \in \mathbb{R}^+ \times \Omega \times \mathbb{R}^3 \times \mathbb{R}^+ \times \mathbb{R}$ où r est le rayon des particules et T la température de la particule. Le rayon r est tel que $\frac{4}{3}\pi r^3 \varrho_d$ correspond à la masse totale de la particule. La masse volumique ϱ_d est alors une fonction de r, voir chapitre 3 formule (3.4). Comme la particule est composée de médicament, d'excipient et d'eau, nous introduisons le rayon r_{drug} pour lequel $\frac{4}{3}\pi r_{\mathrm{drug}}^3 \varrho_{\mathrm{drug}}$ représente la masse du médicament dans la particule et r_{ex} tel que $\frac{4}{3}\pi(r_{\mathrm{ex}}^3 - r_{\mathrm{drug}}^3)\varrho_{\mathrm{ex}}$ soit la masse de l'exicpient dans la particule, voir chapitre 3 Figure 3.2.

On introduit de plus la température de l'air $(t,x) \mapsto T_{\mathrm{air}}(t,x)$ et la fraction massique de vapeur d'eau dans l'air $(t,x) \mapsto Y_{\mathrm{v,air}}(t,x)$. La nouvelle équation de type Vlasov pour la densité f est exprimée comme suit

$$\partial_t f + v\cdot\nabla_x f + \left(\left[\alpha(u-v) + \left(1 - \frac{\varrho_{\mathrm{air}}}{\varrho_d}\right) g\right] f\right) + \nabla_r(af) + \nabla_T(bf) = 0,$$

où a est une fonction de $(r, T, Y_{\text{v,air}})$ et représente la variation du rayon des particules, voir chapitre 3 formule (3.6) pour la définition. b est une fonction de $(r, T, Y_{\text{v,air}}, T_{\text{air}})$ et représente la variation de la température des particules, voir chapitre 3 formule (3.7) pour la définition. Les équations additionnelles sont alors des équations d'advection-diffusion pour la température de l'air T_{air} et la fraction massique de vapeur d'eau dans l'air $Y_{\text{v,air}}$

$$\begin{aligned} \varrho_{\text{air}}[\partial_t Y_{\text{v,air}} + (u \cdot \nabla) Y_{\text{v,air}}] - \operatorname{div}(D_V(T_{\text{air}}) \nabla Y_{\text{v,air}}) &= S_Y, \\ \varrho_{\text{air}} Cp_{\text{air}}[\partial_t T_{\text{air}} + (u \cdot \nabla) T_{\text{air}}] - \kappa_{\text{air}} \Delta T_{\text{air}} &= S_T, \end{aligned}$$

où $D_V(T_{\text{air}})$, κ_{air} sont des coefficients de diffusion. Cp_{air} est la capacité thermique de l'air. Les termes sources S_Y et S_p sont définis dans le chapitre 3 par (3.20) et (3.23) et représentent l'échange de vapeur d'eau et de température entre l'aérosol et l'air ambiant dans le poumon.
Une fois les équations établies, nous montrons que le modèle couplé vérifie de bonnes propriétés de conservation. Nous discrétisons ensuite les équations par un schéma explicite en temps et effectuons des simulations numériques en deux dimensions dans une bifurcation. Nous présentons alors une étude statistique de l'influence de la croissance en rayon sur le dépôt des particules sur les paroies.

0.3.4 Analyse de l'équation de transport-Stokes

Dans ce chapitre nous nous intéressons à l'analyse de l'équation de transport-Stokes (0.3.4) dérivée au premier chapitre

$$\left\{ \begin{aligned} \frac{\partial \varrho}{\partial t} + \operatorname{div}((\kappa g + u)\varrho) &= 0\,, \\ -\Delta u + \nabla p &= 6\pi r_0 \kappa \varrho g\,, \\ \operatorname{div}(u) &= 0\,, \\ \varrho(0, \cdot) &= \varrho_0\,. \end{aligned} \right.$$

L'objectif principal de ce travail est l'étude qualitative de la solution de (0.3.4) associée à une condition initiale ϱ_0 de type indicatrice d'un domaine borné régulier. Ce travail est motivé par les études expérimentales et numériques menées dans [55, 58, 62] et qui mettent en évidence l'aspect instable d'une gouttelette en suspension dans un fluide de Stokes qui se transforme en tore avant de se scinder en deux gouttelettes reproduisant le même comportement instable.

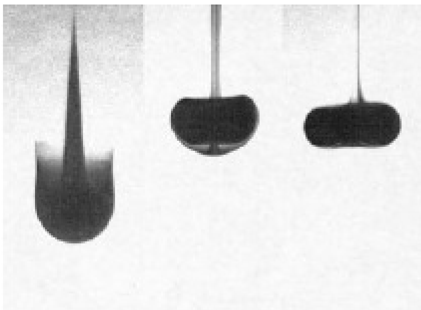

Figure 1 – Torus formation [55, Figure 2]

Le premier résultat est un théorème d'existence et d'unicité d'une solution de l'équation (0.3.4) pour des données initiales de type $L^1 \cap L^\infty$ ayant un moment d'ordre un fini.

Theorem 0.3.7. *Soit $\varrho_0 \in L^1 \cap L^\infty$ une mesure ayant un moment d'ordre un fini. Pour tout $T > 0$ il existe un unique couple $(\varrho, u) \in L^\infty(0,T; L^1(\mathbb{R}^3) \cap L^\infty(\mathbb{R}^3)) \times L^\infty(0,T; W^{1,\infty}(\mathbb{R}^3))$ solution de l'équation de transport-Stokes* (0.3.4) *et on a*

$$\varrho(t,\cdot) = X(t,0,\cdot)\#\varrho_0,$$

où X est le flot caractéristique associé à l'équation (0.3.4).

Ce résultat montre en particulier que si $\varrho_0 = 1_{B_0}$, $B_0 \subset \mathbb{R}^3$ borné, alors $\varrho(t,\cdot) = 1_{B_t}$ où B_t est le transporté de B_0 par le flot caractéristique associé à l'équation de transport-Stokes. Il est important de remarquer que la régularité Lipschitz de u implique que le flot caractéristique X est un difféomorphisme. Ainsi, ce modèle ne permet pas la rupture de la gouttelette ni la formation d'un tore. Nous nous intéressons alors aux propriétés de régularité de la surface de la gouttelette. En définissant une paramétrisation de la surface ∂B_t comme suit

$$\partial B_t = \{\tilde{X}(t,\omega), \omega \in \mathbb{S}^2\},$$

nous dérivons une équation intégro-différentielle pour $\tilde{X}$ où u est défini par (4.15)

$$\left\{ \begin{array}{rcl} \partial_t \tilde{X}(t,\omega) & = & u(t, \tilde{X}(t,\omega)) \,, \\ \tilde{X}(0,\omega) & = & \tilde{X}_0(\omega) \,, \end{array} \right. \tag{37}$$

Nous avons le résultat d'existence locale et d'unicité suivant

Theorem 0.3.8. *Soit $\tilde{X}_0 \in \mathcal{C}^1(\mathbb{S}^2; \mathbb{R}^3)$ telle que $|\tilde{X}_0|_* > 0$. Il existe un temps $T > 0$ et une unique paramétrisation $\tilde{X} \in \mathcal{C}^1(0,T; \mathcal{C}^1(\mathbb{S}^2; \mathbb{R}^3))$ solution de l'équation intégro-différentielle* (37). *De plus, l'existence globale est assurée tant que l'on a un contrôle sur les quantités $|\tilde{X}|_*$ et $\|\nabla \tilde{X}\|_0$.*

La stricte positivité de la quantité $|\cdot|_*$ définie pour tout $\tilde{X} \in \mathcal{C}^1(\mathbb{S}^2; \mathbb{R}^3)$ par

$$|\tilde{X}|_* := \inf_{\omega \neq \omega'} \frac{|\tilde{X}(\omega) - \tilde{X}(\omega')|}{|\omega - \omega'|},$$

assure que la paramétrisation est bijective et que la surface ne se croise pas.
Afin de retrouver l'aspect instable remarqué lors des études numériques et expérimentales, nous examinons le cas où $B_0 = B(0,1)$. L'invariance du flot u et de la gouttelette B_t par rotation autour de l'axe vertical permet de considérer une paramétrisation sphérique pour B_t en tout temps

$$B_t := \left\{ c + r(t,\theta) \begin{pmatrix} \cos(\phi)\sin(\theta) \\ \sin(\phi)\sin(\theta) \\ \sin(\theta) \end{pmatrix}, (\theta,\phi) \in [0,\pi] \times [0,2\pi] \right\},$$

Nous dérivons l'équation hyperbolique satisfaite par la fonction rayon r et le centre de la gouttelette $c = (0,0,c_3)$

$$\left\{ \begin{array}{rcl} \partial_t r + r' A_1[r] & = & A_2[r], \\ r(0,\cdot) & = & 1. \end{array} \right. \tag{38}$$

où $A_1[r]$ and $A_2[r]$ sont définis par les formules (4.21), (4.22) et c_3 satisfait l'équation (4.23). Nous finissons le dernier chapitre par la présentation de calculs numériques pour l'évolution de la gouttelette montrant l'aspect instable de la régularité de la surface.

0.3.5 Statut des travaux effectués lors de la thèse

Le premier chapitre a donné lieu à un article à paraître dans le journal Kinetics and related models. L'article associé au deuxième chapitre a été soumis. Enfin le troisième chapitre a fait l'objet d'un proceeding en collaboration avec L. Boudin, C. Grandmont, B. Grec, S. Martin et F. Noël accepté au journal ESAIM: Proceedings and Surveys.

Chapter 1

Sedimentation of particles in Stokes flow

Abstract

In this paper, we consider N identical spherical particles sedimenting in a uniform gravitational field. Particle rotation is included in the model while fluid and particle inertia are neglected. Using the method of reflections, we extend the investigation of [38] by discussing the threshold beyond which the minimal particle distance is conserved for a short time interval independent of N. We also prove that the particles interact with a singular interaction force given by the Oseen tensor and justify the mean field approximation in the spirit of [33] and [34].

1.1 Introduction

In this paper, we consider a system of N spherical particles $(B_i)_{1\leqslant i\leqslant N}$ with identical radii R immersed in a viscous fluid satisfying the following Stokes equation:

$$\left\{\begin{array}{rcl} -\Delta u^N + \nabla p^N & = & 0, \\ \operatorname{div} u^N & = & 0, \end{array}\right. \text{ on } \mathbb{R}^3 \backslash \bigcup_{i=1}^{N} \overline{B_i}, \tag{1.1}$$

completed with the no-slip boundary conditions

$$\left\{\begin{array}{rcl} u^N & = & V_i + \Omega_i \times (x - x_i), \text{ on } \partial B_i, \\ \lim\limits_{|x|\to\infty} |u^N(x)| & = & 0, \end{array}\right. \tag{1.2}$$

where $(V_i, \Omega_i) \in \mathbb{R}^3 \times \mathbb{R}^3$, $1 \leqslant i \leqslant N$ represent the linear and angular velocities,

$$B_i := B(x_i, R).$$

We describe the intertialess motion of the rigid spheres $(B_i)_{1\leqslant i\leqslant N}$ by adding to the instantaneous Stokes equation the classical Newton dynamics for the particles $(x_i)_{1\leqslant i\leqslant N}$

$$\left\{\begin{array}{rcl} \dot{x}_i & = & V_i, \\ F_i + mg & = & 0, \\ T_i & = & 0, \end{array}\right. \tag{1.3}$$

where m denotes the mass of the identical particles adjusted for buoyancy, g the gravitational acceleration, F_i (resp. T_i) the drag force (resp. the torque) applied by the the fluid on the i^{th} particle B_i defined by

$$\begin{aligned} F_i &:= \int_{\partial B_i} \sigma(u^N, p^N)n, \\ T_i &= \int_{\partial B_i} (x - x_i) \times [\sigma(u^N, p^N)n], \end{aligned}$$

with n the unit outer normal to ∂B_i and $\sigma(u^N, p^N) = 2D(u^N) - p^N \mathbb{I}$, the stress tensor where $2D(u^N) = \nabla u^N + \nabla u^{N\top}$.
Note that the constant velocities (V_i, Ω_i) of each particle are unknown and are determined by the prescribed force and torque $F_i = mg$ and $T_i = 0$. In [54], the author shows that the linear mapping on $\mathbb{R}^{6N}$

$$(V_i, \Omega_i)_{1 \leqslant i \leqslant N} \mapsto (F_i, T_i)_{1 \leqslant i \leqslant N},$$

is bijective for all $N \in \mathbb{N}^*$. This ensures existence and uniqueness of (u^N, p^N) and the velocities.

Remark 1.1.1 (About the modeling and nondimensionalization)**.** *Equations* (1.1)–(1.3) *describe suspensions sedimenting in a uniform gravitational field. Equations* (1.1), (1.2) *are derived starting from the Navier-Stokes equations and neglecting the inertial terms by means of the Reynolds and Stokes number, see [30, Chapter 1 Section 1], [11], [54] and all the references therein. Analogously, the ODE system* (1.3) *is obtained by neglecting particle inertia. We refer also to [24] where a formal derivation taking into account the slow motion of the system is performed.*
When considering one spherical particle sedimenting in a Stokes flow, the linear relation between the drag force F and the velocity V is given by the Stokes law

$$F = -6\pi R V\,,$$

see Section 1.2.1 for more details. Stokes law leads to the well-known formula for the fall speed of a sedimenting single particle under gravitational force denoted by

$$\kappa g := \frac{m}{6\pi R} g\,. \tag{1.4}$$

It is important to point out that in our model, a scaling with respect to the velocity fall κg has been performed. This means that the drag forces $(F_i)_{1 \leqslant i \leqslant N}$ and the gravitational force mg are terms of order R. Consequently, in this paper, κg is a constant of order one. For more details on the derivation of the model, we refer to [38, Section 1.1] where a nondimensionalization including physical units is provided. Moreover, as in [24], the particle radius R is assumed to be proportional to $\frac{1}{N}$ so that the collective force applied by the particles on the fluid is of order one. This will be made precise in the presentation of the main assumptions.

Given initial particle positions $x_i(0) := x_i^0$, $1 \leqslant i \leqslant N$, we are interested in the asymptotics of the solution when the number of particles N tends to infinity and the radius R tends to zero. The main motivation is to justifiy the representation of the motion of a dispersed phase inside a fluid using Vlasov-Stokes equations in spray theory [31], [15].
The analysis of the dynamics is done in [41] in the dilute case *i.e.* when the minimal distance between particles is at least of order $N^{-1/3}$. The authors prove that the particles do not get closer in finite time. Moreover, in the case where the minimal distance between particles is much larger than $N^{-1/3}$ the result in [41] shows that particles do not interact and sink like single particles. We refer finally to [38] where the author considers a particle system with minimal distance of order $N^{-1/3}$ and proves that, under a relevant time scale, the spatial density of the cloud converges in a certain averaged sense to the solution of a coupled transport-Stokes equation (1.15).
Since the desired threshold for the minimal distance is of order $N^{-2/3}$, which allows to tackle randomly distributed particles, we are interested in extending the results for lower orders of the minimal distance. Therefore, in this paper, we continue the investigation of [38] by looking for a more general set of particle configurations that is conserved in time and prove the convergence to the kinetic equation (1.15). Also, we include particle rotation in the modeling.

1.1.1 Main assumptions and results

In this Section, we describe the configuration of particles that we consider and present the main results : Theorem 1.1.1 and Theorem 1.1.2.
We recall that the particles B_i are spherical with identical radii R

$$B_i = B(x_i, R)\,, \quad 1 \leqslant i \leqslant N,$$

where

$$R = \frac{r_0}{N}\,, \quad r_0 > 0\,,$$

with r_0 a positive constant satisfying a smallness assumption (see Theorem 1.1.1).
Due to the quasi-static modeling, the velocities $(V_i(t), \Omega_i(t))_{1\leqslant i\leqslant N}$ at time $t \geqslant 0$ depend only on the prescribed force $(F_i)_{1\leqslant i\leqslant N}$, torque $(T_i)_{1\leqslant i\leqslant N}$ and the particles position $(x_i(t))_{1\leqslant i\leqslant N}$ at the same time t. Consequently, we drop the dependence with respect to time in the definition of the set of particle configurations. Keeping in mind that the idea is to start from a configuration of particles that lies in the set and show that it remains in it for a finite time interval.

Definition 1.1.1 (Definition of the set of particle configuration)**.** *Let $(X^N)_{N\in\mathbb{N}^*}$ be a configuration of particles, where $X^N := (x_1, \cdots, x_N)$. Given two positive constants $\bar{M}, \mathcal{E}$, we define $\mathcal{X}(\bar{M}, \mathcal{E})$ as the set of configurations for which there exists a sequence $(\lambda^N)_{N\in\mathbb{N}^*}$ such that the minimal distance $d_{\min}^N$ defined by*

$$d_{\min}^N \;\; := \;\; \min_{\substack{i\neq j\\ 1\leqslant i,j\leqslant N}} \{|x_i - x_j|\}\,, \forall N \in \mathbb{N}^*\,,$$

and the particle concentration M^N defined by

$$M^N := \sup_{x\in\mathbb{R}^3}\{\#\{i \in \{1,\cdots,N\} \text{ such that } x_i \in \overline{B_\infty(x,\lambda^N)}\}\}\,, \forall N \in \mathbb{N}^*\,,$$

satisfy the following assumptions:

$$\sup_{N\in\mathbb{N}} \frac{M^N}{N|\lambda^N|^3} \leqslant \bar{M}, \tag{1.5}$$

$$\sup_{N\in\mathbb{N}} \frac{|\lambda^N|^3}{|d^N_{\min}|^2} \leqslant \mathcal{E}\,. \tag{1.6}$$

λ^N must satisfy the following compatibility conditions:

$$\lambda^N \geqslant d^N_{\min}/2\,, \quad \lim_{N\to\infty} \lambda^N = 0\,. \tag{1.7}$$

Remark 1.1.2. *Note that, according to the definition of M^N, assumption* (1.5) *ensures that*

$$\frac{1}{N|\lambda^N|^3} \leqslant \bar{M}, \tag{1.8}$$

which yields thanks to assumption (1.6)

$$d^N_{\min} \geqslant \frac{1}{\sqrt{\mathcal{E}}\bar{M}^{1/2}}\frac{1}{\sqrt{N}}. \tag{1.9}$$

Since $R \sim \frac{1}{N}$, this leads also

$$\lim_{N\to\infty} \frac{R}{d^N_{\min}} = 0\,, \tag{1.10}$$

which ensures that the particles do not overlap.

Furthermore, for the proof of the second Theorem 1.1.2, the following assumption must be satisfied initially:

$$\lim_{N\to\infty} \frac{|\lambda^N|^2}{d^N_{\min}(0)} = 0\,. \tag{1.11}$$

Finally, we define ϱ^N the spatial density of the cloud by

$$\varrho^N(t,x) = \frac{1}{N}\sum_{i=1}^N \delta_{x_i(t)}(x)\,, \quad \varrho^N_0 := \varrho^N(0,x).$$

In the rest of this paper, if needed, we make clear the dependence with respect to time by writing for all $N \in \mathbb{N}^*$, $X^N(t)$ for the particle configuration $(x_1(t),\cdots,x_N(t))$, $d^N_{\min}(t)$ for the minimal distance and $M^N(t)$ the particle concentration at time $t \geqslant 0$.
The main results of this paper are the two following theorems. The first one ensures that the particle configurations considered herein are preserved in a short time interval depending only on the data r_0, $\bar{M}$, $\mathcal{E}$, $\kappa|g|$.

Theorem 1.1.1. *Let $(X^N(0))_{N\in\mathbb{N}^*}$ be the initial position of the particles. Assume that there exists $\bar{M}$, $\mathcal{E}$ and a sequence $(\lambda^N)_{N\in\mathbb{N}^*}$ such that $(X^N(0))_{N\in\mathbb{N}^*}$ lies in the set $\mathcal{X}(\bar{M},\mathcal{E})$ i.e. assumptions* (1.5), (1.6), (1.7) *hold true initially.*
If $\bar{M}^{1/3}r_0$ is small enough, there exists $N^* \in \mathbb{N}^*$ depending on $(r_0,\bar{M},\mathcal{E})$ and $T > 0$ depending on $(r_0,\mathcal{E},\bar{M},\kappa|g|)$ such that for all $t \in [0,T]$ and $N \geqslant N^*$

$$d^N_{\min}(t) \geqslant \frac{1}{2} d^N_{\min}(0),$$

$$M^N(t) \leqslant 8^4 M^N(0).$$

The second part of the result is the justification of the convergence of ϱ^N when N tends to infinity.

Theorem 1.1.2. *Consider the maximal time $T > 0$ introduced in Theorem 1.1.1 and the additional assumption* (1.11)*. Let ϱ_0 be a positive regular density such that $\int_{\mathbb{R}^3}\varrho_0 = 1$. We denote by (ϱ,u) the unique solution to the coupled equation* (1.15)*.*
There exists some positive constants C_1, C_2 depending on $(r_0,\bar{M},\mathcal{E},\|\varrho_0\|_{L^\infty},\kappa|g|)$ and $N^* \in \mathbb{N}^*$ depending on $(r_0,\bar{M},\mathcal{E},\|\varrho_0\|_{L^\infty},\kappa|g|,T)$ such that for all $N \geqslant N^*$ and $t \in [0,T]$

$$W_1(\varrho^N(t,\cdot),\varrho(t,\cdot)) \leqslant C_1\left(\lambda^N + d^N_{\min}(0)\,t + W_1(\varrho_0,\varrho^N_0)\right)e^{C_2 t}.$$

This shows that if the initial particle distribution ϱ^N_0 converges to ϱ_0 then the particle distribution ϱ^N converges toward the unique solution ϱ of equation (1.15) for all time $0 \leqslant t \leqslant T$. Moreover, Theorem 1.1.2 provides a quantitative convergence rate in terms of the initial Wasserstein distance $W_1(\varrho_0,\varrho^N_0)$.

Remark 1.1.3. *The regularity assumption on the initial density ϱ_0 is the one introduced by Höfer in [38] which is $\varrho_0,\ \nabla\varrho_0 \in X_\beta$, for some $\beta > 2$. See Section 1.5.1 for the definition of X_β. In particular, the assumption is satisfied if ϱ_0 is compactly supported and $\mathcal{C}^1$.*

The idea of proof of Theorem 1.1.2 is to formulate the problem considered as a mean-field problem. The mean-field theory consists in approaching equations of motion of large particles systems $(X_1,\cdots,X_N)$ when the number of particles N tends to infinity. In mean-field theory, the ODE governing the particle motion is known and is given by

$$\begin{cases} \dot{X}_i &= \frac{1}{N}\sum_{i=1}^{N} F(X_i - X_j), \\ X_i(0) &= X_i^0, \end{cases} \tag{1.12}$$

where the kernel F is the interaction force of the particles. The limit model describing the time evolution for the spatial density $\varrho(t,x)$ is given by

$$\begin{cases} \partial_t \varrho + \mathcal{K}\varrho\cdot\nabla\varrho = 0\,, \\ \mathcal{K}\varrho(x) := \int_{\mathbb{R}^3} F(x-y)\varrho(t,y)dy, \end{cases} \tag{1.13}$$

In our case, the first difficulty is to extract a system similar to (1.12) for the particle motion and to identify the interaction force F. A key step is then a sharp expansion of the velocities for large N. We obtain for each $1 \leqslant i \leqslant N$

$$V_i = \kappa g + 6\pi \frac{r_0}{N} \sum_{j \neq i} \Phi(x_i - x_j) \kappa g + O\left(d_{\min}^N\right), \quad 1 \leqslant i \leqslant N, \tag{1.14}$$

where Φ is the Green's function for the Stokes equations, also called the Oseen tensor (see formula (1.26) for a definition). κg is the fall speed of a sedimenting single particle under gravitational force and is of order one in our model, see Remark 1.1.1. This shows that the particle system satisfies *approximately* equation (1.12) with an interaction force given by the Oseen tensor. Since the convolution term $\mathcal{K}\varrho$ appearing in (1.13) corresponds to the solution of a Stokes equation in our case, the limiting model describing (1.1), (1.2), (1.3) is a coupled transport-Stokes equation

$$\left\{ \begin{array}{rcl} \frac{\partial \varrho}{\partial t} + \operatorname{div}((\kappa g + u)\varrho) & = & 0\,, \\ -\Delta u + \nabla p & = & 6\pi r_0 \kappa \varrho g\,, \\ \operatorname{div}(u) & = & 0\,, \\ \varrho(0,\cdot) & = & \varrho_0\,, \end{array} \right. \tag{1.15}$$

The proof of Theorem 1.1.2 is based on the two papers [34], [33] where, in the first one, the authors justify the mean field approximation and prove the propagation of chaos for a system of particles interacting with a singular interaction force and where the ODE governing the particle motion is second order. In [33] the author considers a different mean-field equation where the particle dynamics is a first order ODE. The results obtained hold true for a family of singular kernels and applies to the case of vortex system converging towards equations similar to the 2D Euler equation in vorticity formulation. The associated kernel in this case is the Biot-Savard kernel.

In order to extract the first order terms for the velocities (V_i, Ω_i) we apply the method of reflections. This method is introduced by Smoluchowski [67] in 1911. The main idea is to express the solution u^N of N separated particles as superposition of fields produced by the isolated N particle solutions. We refer to [44, Chapter 8] and [30, Section 4] for an introduction to the method. A convergence proof based on orthogonal projection operators is introduced by Luke [54] in 1989. We refer also to the method of reflections developped in [39] which is used by Höfer in [38].

In this paper, we design a modified method of reflections that takes into account the particle rotation and relies on explicit solutions of Stokes flow generated by a translating, rotating and straining sphere. To obtain the convergence of the method of reflections we need to identify particle configuration that can be propagated in time. The particle configuration considered herein is the one introduced in [36] to study the homogenization of the Stokes problem in perforated domains. The novelty is that the author considers the minimal distance $d_{\min}^N$ together with the particle concentration M^N as parameters to describe the cloud. The result in [36] extends in particular the validity of the homogenization problem for randomly distributed particles *i.e.* particle configurations having a minimal distance of order at least $N^{-2/3}$. Note that the notion of particle concentration appears also in [34] to describe the cloud.

1.1.2 Discussion about the particle configuration set

As stated above, the assumptions introduced in Definition 1.1.1 are based on [36]. Assumptions (1.5) and (1.7) means that there exists a uniformly bounded discrete spatial density that approximates ϱ^N. Indeed, if we define $\tilde{\varrho}^N$ by

$$\tilde{\varrho}^N(t,x) := \frac{1}{N}\sum_{i=1}^{N}\frac{1_{B(x_i,\lambda^N)}}{|B(x_i,\lambda^N)|}\,, \tag{1.16}$$

one can show that

$$W_1(\tilde{\varrho}^N,\varrho^N) \leqslant \lambda^N.$$

Assumption (1.5) ensures that there exists a sequence λ^N for which the infinite norm of $\tilde{\varrho}^N$ is bounded by $\bar{M}$, see formula (1.93). This suggests that $\|\varrho\|_\infty$ and $\bar{M}$ are equivalent. We recover the result of [41] in the case where $\lambda^N = N^{-1/3}$ and the minimal distance $d_{\min}^N$ is much larger than $N^{-1/3}$, the explicit formula for the velocities (1.14) implies in this case

$$|V_i - \kappa g| \lesssim \frac{6\pi r_0}{N}\sum_{j\neq i}\frac{1}{|x_i - x_j|}|\kappa g| \lesssim \frac{1}{N}\frac{N^{2/3}}{d_{\min}^N} \ll 1\,,$$

which is in accordance with the "non-interacting scenario" explained in [41]. In our case, the smallness assumption on $r_0\bar{M}^{1/3}$ means that we consider a density of particles such that $\|\varrho\|_\infty$ is small but of order one. Indeed, the second term in the velocity formula (1.14) can be seen as a perturbation of order one of the velocity fall κg in the case where $\bar{M}$ (or the particle density $\|\varrho\|_\infty$) is small. This can be also seen in the coupled equation (1.15) where the velocity term u is proportional to $\|\varrho\|_\infty$.
The second assumption (1.6) ensures the conservation of the minimal distance, see Proposition 1.4.2. In particular, for $\lambda^N = N^{-1/3}$, Theorem 1.1.1 extends the previous known results to configurations having minimal distance at least of order $N^{-1/2}$, see assumption (1.6). This lower bound for the minimal distance appears naturally in our analysis and is closely related to the properties of the Green's function for the Stokes equations. We emphasize that this critical minimal distance appears also in the mean-field analysis due to [33]. Precisely, computations in the proof of [33, Theorem 2.1] show the convergence for a short time interval under the assumption that

$$\frac{W_\infty(\varrho_0,\varrho_0^N)^3}{|d_{\min}^N(0)|^2},$$

is uniformly bounded, see Definition 1.5.4 for the definition of the infinite Wasserstein distance. Standard measure-theory arguments show that the Wasserstein distance ensures assumption (1.5), see Lemma 1.A.4. In other words, one can take λ^N to be the infinite

Wasserstein distance, which yields finally the same assumption (1.6). It is also important to emphasize that one can obtain a global control on the minimal distance in Theorem 1.1.1 when considering $W_\infty(\varrho^N, \varrho)$ instead of λ^N.
The first assumption in formula (1.7) means that we are interested in cases where there is more than one particle per cube of length λ^N. As pointed out by Hillairet in [36], one can choose a larger sequence $(\lambda^N)_{N\in\mathbb{N}^*}$ such that the compatibility assumption holds true. Note also that, in the case where λ^N is the infinite Wasserstein distance, this compatibility assumption is satisfied by definition.
Finally, assumption (1.11) is needed for the control of the Wasserstein distance.

1.1.3 Outline of the paper

The remaining Sections of this paper are organized as follows.
In Section 2 we recall the classical results for the existence and uniqueness of the Stokes solution u^N. We recall also the definition of the drag force F_i, torque T_i and stresslet S_i and present in Section 2.1 the particular solutions to a Stokes flow generated by a translating, a rotating or a straining sphere. Finally, the end of Section 2 is devoted to the approximation of the stresslets S_i. In Section 3 we present and prove the convergence of the method of reflections in order to compute the first order terms for the velocities $(V_i, \Omega_i)_{1\leqslant i\leqslant N}$. Section 4 is devoted to the proof of Theorem 1.1.1. In Section 5 we recall some definitions associated to the Wasserstein distance. We present then the strong existence, uniqueness and stability theory for equation (1.13). In the second part of Section 5 we show that the discrete density ϱ^N satisfies weakly a transport equation. Section 6 is devoted to the proof of the second Theorem 1.1.2. Finally, some technical Lemmas are presented in the appendix.

1.1.4 Notations

In this paper, n always refer to the unit outer normal to a surface.
The following shortcut will be often used

$$d_{ij} = |x_i - x_j|\,, 1 \leqslant i \neq j \leqslant N\,,$$

where we drop the dependence with respect to N in order to simplify the notation.
Given an exterior domain Ω with smooth boundaries, we set

$$\mathcal{C}^\infty(\overline{\Omega}) := \{v_{|\Omega}\,,\, v \in \mathcal{C}_c^\infty(\mathbb{R}^3)\},$$

and the following norm for all $u \in \mathcal{C}^\infty(\overline{\Omega})$

$$\|u\|_{1,2} := \|\nabla u\|_{L^2(\Omega)},$$

we define then the homogeneous Sobolev space $D(\Omega)$ as the closure of $\mathcal{C}^\infty(\overline{\Omega})$ for the norm $\|\cdot\|_{1,2}$ (see [27, Theorem II.7.2]). We also use the notation $D_\sigma(\Omega)$ for the subset of divergence-free $D(\Omega)$ fields

$$D_\sigma(\Omega) := \{u \in D(\Omega)\,,\, \operatorname{div} u = 0\}.$$

Which is also the closure of the subset of divergence-free $\mathcal{C}^\infty(\overline{\Omega})$ fields for the $\|\cdot\|_{1,2}$ norm. Analogously, if $\Omega = \mathbb{R}^3$ we use the notation

$$\dot{H}^1_\sigma(\mathbb{R}^3) = D_\sigma(\mathbb{R}^3).$$

For all 3×3 matrix M, we define $\mathrm{sym}(M)$ (resp. $\mathrm{ssym}(M)$) as the symmetric part of M (resp. the skew-symmetric part of M)

$$\mathrm{sym}(M) = \frac{1}{2}(M + M^\top)\,, \quad \mathrm{ssym}(M) = \tfrac{1}{2}(M - M^\top).$$

We denote by $\times$ the cross product on $\mathbb{R}^3$ and by $\otimes$ the tensor product on $\mathbb{R}^3$ which associates to each couple $(u,v)\in\mathbb{R}^3\times\mathbb{R}^3$ the 3×3 matrix defined as

$$(u\otimes v)_{ij} = u_i v_j\,,\ 1\leqslant i,j\leqslant 3.$$

For all 3×3 matrices A, B, we use the classical notation

$$A : B = \sum_{i=1}^{3}\sum_{j=1}^{3} A_{ij}B_{ij}.$$

In $\mathbb{R}^3$, $|\cdot|$ stands for the Euclidean norm while $|\cdot|_\infty$ represents the l^∞ norm. We use the notation $B_\infty(x,r)$ for the ball with center x and radius r for the l^∞ norm.
Finally, in the whole paper we use the symbol $\lesssim$ to express an inequality with a multiplicative constant independent of N and depending only on r_0, $\bar{M}$, $\mathcal{E}$ and eventually on $\kappa|g|$ which is uniformly bounded according to Remark 1.1.1.

1.2 Reminder on the Stokes problem

In this Section we recall some results concerning the Stokes equations. We remind that for all $N\in\mathbb{N}$ we denote by (u^N,p^N) the solution to (1.1) – (1.2). Keeping in mind that the linear mapping, that associates to the linear and angular velocities the forces and torques, is bijective (see [54]) together with the classical theory for the Stokes equations yields:

Proposition 1.2.1. *For all $N\in\mathbb{N}$, there exists a unique pair $(u^N,p^N)\in D_\sigma(\mathbb{R}^3\backslash\bigcup_i\overline{B_i})\times L^2(\mathbb{R}^3\backslash\bigcup_i\overline{B_i})$ and unique velocities $(V_i,\Omega_i)_{1\leqslant i\leqslant N}$ such that*

$$\begin{aligned}\int_{\partial B_i}\sigma(u^N,p^N)n + mg &= 0\,,\forall\, 1\leqslant i\leqslant N\,,\\ \int_{\partial B_i}(x-x_i)\times[\sigma(u^N,p^N)n] &= 0\,,\forall\, 1\leqslant i\leqslant N\,,\end{aligned}$$

and u realizes

$$\inf\left\{\int_{\mathbb{R}^3\backslash\bigcup_i\overline{B_i}}|\nabla v|^2\,,\ v\in D_\sigma(\mathbb{R}^3\backslash\bigcup_i\overline{B_i})\,,\ v = V_i + \Omega_i\times(x-x_i)\ \text{on}\ \partial B_i\,,\ 1\leqslant i\leqslant N\right\}. \tag{1.17}$$

The velocity field u^N can be extended to $V_i + \Omega_i \times (x - x_i)$ on each particle B_i. This extension denoted also u^N is in $\dot{H}^1_\sigma(\mathbb{R}^3)$.
We recall the definition of the force $F_i \in \mathbb{R}^3$, torque $T_i \in \mathbb{R}^3$ and stresslet $S_i \in \mathcal{M}_3(\mathbb{R})$ applied by the particle B_i on the fluid (see [30, Section 1.3])

$$\begin{aligned} F_i &= \int_{\partial B_i} \sigma(u^N, p^N) n. \\ M_i &= \int_{\partial B_i} (x - x_i) \otimes \left[\sigma(u^N, p^N) n\right]. \end{aligned} \tag{1.18}$$

The matrix M_i represents the first momentum which is decomposed into a symmetric and skew-symmetric part

$$M_i = T_i + S_i,$$

the symmetric part S_i is called stresslet, see [30, Section 2.2.3]. Since the skew-symmetric part of a 3×3 matrix M has only three independent components, it can be associated to a unique vector T such that

$$\mathrm{ssym}(M)\, x = T \times x \,,\ \forall\, x \in \mathbb{R}^3.$$

In this paper, we allow the confusion between the skew-symmetric matrix $\mathrm{ssym}(M)$ and the vector T. Hence, we define the torque $T_i \in \mathbb{R}^3$ as being the skew-symmetric part of the first momentum M_i which satisfies

$$\begin{aligned} T_i &= \mathrm{ssym}(M_i) = \int_{\partial B_i} (x - x_i) \times \left[\sigma(u^N, p^N) n\right], \\ S_i &= \mathrm{sym}(M_i). \end{aligned} \tag{1.19}$$

1.2.1 Particular Stokes solutions

The linearity of the Stokes problem allows us to develop powerful tools that will be used in the method of reflections. In particular, we investigate in what follows the analytical solution to a Stokes flow generated by a translating, a rotating or a straining sphere. The motivation in considering these cases is that the fluid motion near a point x_0 may be approximated by

$$u(x) \sim u(x_0) + \nabla u(x_0) \cdot (x - x_0),$$

hence, if we replace the boundary condition on each particle by its Taylor series of order one, we can use these special solutions to approximate the flow u. The results and formulas of this Section are detailed in [30, Section 2] and [44, Section 2.4.1]. In what follows $B := B(a, r)$ is a ball centered in $a \in \mathbb{R}^3$ with radius $r > 0$.

Case of translation

Let $V \in \mathbb{R}^3$. We consider the unique solution $(U_{a,R}[V], P_{a,R}[V])$ to the following Stokes problem:

$$\left\{\begin{array}{rcl} -\Delta U_{a,R}[V] + \nabla P_{a,R}[V] &=& 0, \\ \operatorname{div} U_{a,R}[V] &=& 0, \end{array}\right. \text{ on } \mathbb{R}^3 \backslash \overline{B}, \tag{1.20}$$

completed by the boundary condition

$$\left\{\begin{array}{rcl} U_{a,R}[V] &=& V, \text{ on } \partial B, \\ \lim\limits_{|x|\to\infty} |U_{a,R}[V](x)| &=& 0. \end{array}\right. \tag{1.21}$$

$U_{a,R}[V]$ is the flow generated by a unique sphere immersed in a fluid moving at V. The explicit formula for $(U_{a,R}[V], P_{a,R}[V])$ is derived in [44, Section 3.3.1] and also in [30, Formula (2.12) and (2.13)]. Explicit formulas imply the existence of a constant $C > 0$ such that for all $x \in \mathbb{R}^3 \backslash B(a,R)$

$$|U_{a,R}[V](x)| \leqslant CR\frac{|V|}{|x-a|}, \quad |\nabla U_{a,R}[V](x)| + |P_{a,R}[V](x)| \leqslant CR\tfrac{|V|}{|x-a|^2}. \tag{1.22}$$

$$|\nabla^2 U_{a,R}[V](x)| \leqslant CR\frac{|V|}{|x-a|^3}. \tag{1.23}$$

On the other hand, the force F, torque T and stresslet S exerted by a translating sphere B as defined in (1.18) read

$$F = -6\pi RV\ ,\ T = 0\ ,\ S = 0. \tag{1.24}$$

We recall now an important formula that links the solution to the Green's function of the Stokes problem. For all $x \in \mathbb{R}^3 \backslash B(a,R)$ we have

$$U_{a,R}[V](x) = -\left(\Phi(x-a) - \frac{R^2}{6}\Delta\Phi(x-a)\right)F\,, \tag{1.25}$$

where Φ is the Green's function for Stokes flow also called Oseen-tensor

$$\Phi(x) = \frac{1}{8\pi}\left(\frac{1}{|x|}\mathbb{I}_3 + \frac{1}{|x|^3}x\otimes x\right). \tag{1.26}$$

The 3×3 matrix $\Delta\Phi$ represents the Laplacian of Φ and is given by

$$\Delta\Phi(x) = \frac{1}{8\pi}\left(\frac{2}{|x|^3}\mathbb{I}_3 - \frac{6}{|x|^5}x\otimes x\right).$$

The first term in the right-hand side of (1.25) is the point force solution also called stokeslet, see [30, Section 3.1]. In this paper we use the term stokeslet to define the whole solution $U_{a,r}[V]$ which can bee seen as an extension of the point force solution.

Remark 1.2.1. *Formula* (1.25) *is closely related to the Faxén law which represents the relations between the force F and the velocity V. We refer to [30, Section 2.3] and [44, Section 3.5] for more details on the topic.*
Remark also that in (1.25) *the point force solution retains the most slowly decaying portion, which is of order $\frac{R}{|x|}$. This property is useful in order to extract the first order terms for the velocities $(V_i)_{1\leqslant i\leqslant N}$, see Lemma 1.3.8.*

Moreover, we recall a Lipschitz-like inequality satisfied by the Oseen tensor

$$|\Phi(x)-\Phi(y)| \leqslant C\frac{|x-y|}{\min(|y|^2\,,\,|x|^2)},\ \ \forall\, x\,,\, y \neq 0. \tag{1.27}$$

Finally, in this paper, the velocity field $U_{a,R}[V]$ is extended by V on $B(a,R)$.

Case of rotation

Let $\omega \in \mathbb{R}^3$. Denote by $(A^{(1)}_{a,R}[\omega], P^{(1)}_{a,R}[\omega])$ the unique solution to

$$\left\{\begin{array}{rcl} -\Delta A^{(1)}_{a,R}[\omega] + \nabla P^{(1)}_{a,R}[\omega] &=& 0, \\ \operatorname{div} A^{(1)}_{a,R}[\omega] &=& 0, \end{array}\right. \text{ on } \mathbb{R}^3\setminus\overline{B(a,R)}, \tag{1.28}$$

completed with the boundary conditions

$$\left\{\begin{array}{rcl} A^{(1)}_{a,R}[\omega] &=& \omega\times(x-a), \text{ on } \partial B(a,R), \\ \lim\limits_{|x|\to\infty}|A^{(1)}_{a,R}[\omega]| &=& 0. \end{array}\right. \tag{1.29}$$

$A^{(1)}_{a,R}[\omega]$ represents the flow generated by a sphere rotating with angular velocity ω. In particular we have $P^{(1)}_{a,R}[\omega]=0$ due to symmetries. The drag force F and stresslet S also vanish

$$F=0\,,\quad S=0.$$

On the other hand, the hydrodynamic torque resulting from the fluid traction on the surface defined in (1.19) is given by

$$T=-8\pi R^3\omega. \tag{1.30}$$

Finally, there exists $C>0$ such that for all $x\in\mathbb{R}^3\setminus B(a,R)$

$$|A^{(1)}_{a,R}[\omega]| \leqslant CR^3\frac{|\omega|}{|x-a|^2},\quad |\nabla A^{(1)}_{a,R}[\omega]| + |P^{(1)}_{a,R}[\omega]| \leqslant CR^3\tfrac{|\omega|}{|x-a|^3}.$$

Case of strain

Let E be a trace-free 3×3 symmetric matrix.
Denote by $(A^{(2)}_{a,R}[E], P^{(2)}_{a,R}[E])$ the unique solution to

$$\left\{ \begin{array}{rcl} -\Delta A^{(2)}_{a,R}[E] + \nabla P^{(2)}_{a,R}[E] & = & 0, \\ \operatorname{div} A^{(2)}_{a,R}[E] & = & 0, \end{array} \right. \text{ on } \mathbb{R}^3 \backslash \overline{B(a,R)}, \tag{1.31}$$

completed with the boundary conditions

$$\left\{ \begin{array}{rcl} A^{(2)}_{a,R}[E] & = & E(x-a), \text{ on } \partial B(a,R), \\ \lim\limits_{|x|\to\infty} |A^{(2)}_{a,R}[E]| & = & 0. \end{array} \right. \tag{1.32}$$

The velocity field $A^{(2)}_{a,R}[E]$ is the flow generated by a sphere submitted to the strain $E(x-a)$. In this case, the drag force and torque vanishes

$$F = 0\,, \quad T = 0. \tag{1.33}$$

On the other hand, the symmetric part of the first momentum S as defined in (1.19) is given by

$$S = -\frac{20}{3}\pi R^3 E. \tag{1.34}$$

Finally, there exists $C > 0$ such that for all $x \in \mathbb{R}^3 \backslash B(a,R)$ we have

$$|A^{(2)}_{a,R}[E]| \leqslant CR^3 \frac{|E|}{|x|^2}\,, \quad |\nabla A^{(2)}_{a,R}[E]| + |P^{(2)}_{a,R}[E](x)| \leqslant CR^3 \tfrac{|E|}{|x|^3}. \tag{1.35}$$

Final notations

Now, assume that D is a trace-free 3×3 matrix. We denote by $(A_{a,R}[D], P_{a,R}[D])$ the unique solution to

$$\left\{ \begin{array}{rcl} -\Delta A_{a,R}[D] + \nabla P_{a,R}[D] & = & 0, \\ \operatorname{div} A_{a,R}[D] & = & 0, \end{array} \right. \text{ on } \mathbb{R}^3 \backslash \overline{B(a,R)}, \tag{1.36}$$

completed by the boundary conditions

$$\left\{ \begin{array}{rcl} A_{a,R}[D] & = & D(x-a), \text{ on } \partial B(a,R), \\ \lim\limits_{|x|\to\infty} |A_{a,R}[D]| & = & 0. \end{array} \right. \tag{1.37}$$

We set then $D = E + \omega$ with $E = \operatorname{sym}(D)$ and $\omega = \operatorname{ssym}(D)$. As stated in the definition (1.19), ω represents also a $3D$ vector. Hence, the boundary condition (1.37) reads

$$A_{a,R}[D](x) = D(x-a) = E(x-a) + \omega \times (x-a), \quad \text{for all } x \in \partial B(a,R).$$

We have, thanks to the linearity of the Stokes equation, that

$$(A_{a,R}[D], P_{a,R}[D]) = (A^{(1)}_{a,R}[\omega], P^{(1)}_{a,R}[\omega]) + (A^{(2)}_{a,R}[E], P^{(2)}_{a,R}[E]).$$

Since the two solutions have the same decay-rate, this yields for all $x \in \mathbb{R}^3 \backslash B(a,R)$

$$|A_{a,R}[D]| \leqslant CR^3 \frac{|D|}{|x|^2}, \quad |\nabla A_{a,R}[D]| + |P_{a,R}[D](x)| \leqslant CR^3 \tfrac{|D|}{|x|^3}. \tag{1.38}$$

Analogously, for the second derivative we have

$$|\nabla^2 A_{a,R}[D](x)| \leqslant CR^3 \frac{|D|}{|x-a|^4}. \tag{1.39}$$

1.2.2 Approximation result

In this part we consider the unique solution (v,p) of the following Stokes problem:

$$\left\{ \begin{array}{rcl} -\Delta v + \nabla p &=& 0, \\ \operatorname{div} v &=& 0, \end{array} \right. \text{ on } \mathbb{R}^3 \backslash \bigcup_{i=1}^N \overline{B_i}, \tag{1.40}$$

completed with the boundary conditions

$$\left\{ \begin{array}{rcl} v &=& V + D(x - x_1), \text{ on } \partial B_1, \\ v &=& 0, \text{ on } \partial B_i,\ i \neq 1, \\ \lim\limits_{|x|\to\infty} |v(x)| &=& 0, \end{array} \right. \tag{1.41}$$

with $V \in \mathbb{R}^3$ and D a trace-free 3×3 matrix. We set

$$v_1 := U_{x_1,R}[V] + A_{x_1,R}[D].$$

We aim to show that the velocity field v_1 is a good approximation of the unique solution v.

Lemma 1.2.2. *For N sufficiently large, we have the following error bound:*

$$\|\nabla v - \nabla v_1\|_{L^2(\mathbb{R}^3 \backslash \bigcup_i \overline{B_i})} \lesssim \frac{R}{\sqrt{d^N_{\min}}}|V| + \frac{R^3}{|d^N_{\min}|^{3/2}}|D|.$$

Proof. We have

$$\|\nabla v - \nabla v_1\|^2_{L^2(\mathbb{R}^3 \backslash \bigcup_i \overline{B_i})} = \|\nabla v\|^2_{L^2(\mathbb{R}^3 \backslash \bigcup_i \overline{B_i})} - 2 \int_{\mathbb{R}^3 \backslash \bigcup_i \overline{B_i}} \nabla v : \nabla v_1 + \|\nabla v_1\|^2_{L^2(\mathbb{R}^3 \backslash \bigcup_i \overline{B_i})},$$

as v and v_1 satisfy the same boundary condition on ∂B_1 this yields

$$\int_{\mathbb{R}^3 \backslash \bigcup_i \overline{B_i}} \nabla v : \nabla v_1 = -\int_{\partial B_1} (\partial_n v_1 - p_1 n) \cdot v = -\int_{\partial B_1} (\partial_n v_1 - p_1 n) \cdot v_1 = \|\nabla v_1\|^2_{L^2(\mathbb{R}^3 \backslash \bigcup_i \overline{B_i})},$$

hence

$$\|\nabla v - \nabla v_1\|^2_{L^2(\mathbb{R}^3 \setminus \bigcup_i \overline{B_i})} = \|\nabla v\|^2_{L^2(\mathbb{R}^3 \setminus \bigcup_i \overline{B_i})} - \|\nabla v_1\|^2_{L^2(\mathbb{R}^3 \setminus \bigcup_i \overline{B_i})}.$$

In order to bound the first term we construct an extension $\tilde{v}$ of the boundary conditions of v and apply the variational principle. We define

$$\tilde{v} := \chi\left(\frac{\cdot - x_1}{d^N_{\min}/4}\right) v_1 - \mathcal{B}_{x_1, d^N_{\min}/4, d^N_{\min}/2}[\bar{f}],$$

where χ is a truncation function such that $\chi = 1$ on $B(0,1)$ and $\chi = 0$ out of $B(0,2)$. In what follows, we use the following shortcut $A_1 := B(x_1, d^N_{\min}/2) \setminus \overline{B(x_1, d^N_{\min}/4)}$. Thanks to formula (1.10), for N sufficiently large we have $R < d^N_{\min}/4$ and thus $\operatorname{supp} \tilde{v} \subset B(x_1, d^N_{\min}/2)$. $\bar{f}$ is defined as follows

$$\bar{f}(x) := v_1(x) \cdot \nabla \left[x \mapsto \chi\left(\frac{x - x_1}{d^N_{\min}/4}\right)\right],$$

and $\mathcal{B}_{x_1, d^N_{\min}/4, d^N_{\min}/2}$ denotes the Bogovskii operator satisfying for all $f \in L^q_0(A_1)$, $q \in (0,\infty)$

$$\operatorname{div} \mathcal{B}_{x_1, d^N_{\min}/4, d^N_{\min}/2}[f] = f,$$

we refer to [27, Theorem III.3.1] for a complete definition of the Bogovskii operator. In particular, from [36, Lemma 16], there exists a positive constant C independent of $d^N_{\min}$ such that

$$\|\nabla \mathcal{B}_{x_1, d^N_{\min}/4, d^N_{\min}/2}[\bar{f}]\|_{L^2(A_1)} \leqslant C \|\bar{f}\|_{L^2(A_1)}, \tag{1.42}$$

With this construction $\tilde{v}$ is a divergence-free field satisfying the same boundary conditions as v. Moreover, applying formula (1.42), there exists (another) constant $C > 0$ such that

$$\begin{aligned}
\|\nabla \tilde{v}\|^2_{L^2(\mathbb{R}^3 \setminus \bigcup_i \overline{B_i})} = & \int_{\mathbb{R}^3 \setminus \bigcup_i \overline{B_i}} \left| \nabla \left[x \mapsto \chi\left(\frac{x - x_1}{d^N_{\min}/4}\right) v_1(x)\right]\right|^2 dx \\
& + \int_{\mathbb{R}^3 \setminus \bigcup_i \overline{B_i}} |\nabla \mathcal{B}_{x_1, d^N_{\min}/4, d^N_{\min}/2}[\bar{f}](x)|^2 dx \\
& - 2 \int_{\mathbb{R}^3 \setminus \bigcup_i \overline{B_i}} \nabla \left[x \mapsto \chi\left(\frac{x - x_1}{d^N_{\min}/4}\right) v_1(x)\right] : \nabla \mathcal{B}_{x_1, d^N_{\min}/4, d^N_{\min}/2}[\bar{f}](x) dx\,, \\
\leqslant & \int_{\mathbb{R}^3 \setminus B_1} \left|\chi\left(\frac{x - x_1}{d^N_{\min}/4}\right) \nabla v_1(x)\right|^2 dx \\
& + C \left(\int_{A_1} |\nabla v_1(x)|^2 + \frac{1}{|d^N_{\min}|^2} \left| \nabla \chi \left(\frac{x - x_1}{d^N_{\min}/4}\right)\right|^2 |v_1(x)|^2 \right) dx.
\end{aligned}$$

Since $\chi\left(\frac{\cdot - x_1}{d^N_{\min}/4}\right) = 1$ on $B(x_1, d^N_{\min}/4)$ we get

$$\begin{aligned}\|\nabla v - \nabla v_1\|^2_{L^2(\mathbb{R}^3\setminus\bigcup_i \overline{B_i})} &\leqslant \|\nabla \tilde{v}\|^2_{L^2(\mathbb{R}^3\setminus\bigcup_i \overline{B_i})} - \|\nabla v_1\|^2_{L^2(\mathbb{R}^3\setminus\bigcup_i \overline{B_i})}\,,\\ &\lesssim \int_{A_1} |\nabla v_1(x)|^2 dx\,,\\ &+ \int_{A_1} \frac{1}{|d^N_{\min}|^2}\left|\nabla\chi\left(\frac{x-x_1}{d^N_{\min}/4}\right)\right|^2 |v_1|^2 dx,\end{aligned}$$

Thanks to (1.22) and (1.38) we have:

$$\begin{aligned}\int_{A_1} \frac{1}{|d^N_{\min}|^2}\left|\nabla\chi\left(\frac{x-x_1}{d^N_{\min}/4}\right)\right|^2 |v_1|^2 &\lesssim \|\nabla\chi\|^2_\infty \int_{A_1}\frac{1}{|d^N_{\min}|^2}\left(R^2\frac{|V|^2}{|x-x_1|^2} + R^6\frac{|D|^2}{|x-x_1|^4}\right)\,,\\ &\lesssim \frac{1}{|d^N_{\min}|^2}\int_{d^N_{\min}/4}^{d^N_{\min}/2}\left(R^2|V|^2 + R^6\frac{|D|^2}{r^2}\right)dr\,,\\ &\lesssim \frac{1}{|d^N_{\min}|^2}\left(R^2|V|^2 d^N_{\min} + R^6\frac{|D|^2}{d^N_{\min}}\right).\end{aligned}$$

Reproducing an analogous computation for the first term we obtain finally

$$\|\nabla v - \nabla v_1\|^2_{L^2(\mathbb{R}^3\setminus\bigcup_i B_i)} \lesssim \frac{R^2}{d^N_{\min}}|V|^2 + \frac{R^6}{|d^N_{\min}|^3}|D|^2. \tag{1.43}$$

This yields the expected result. $\square$

1.2.3 Estimation of the fluid stresslet

In this part we focus on approaching the stresslet S_i, $1 \leqslant i \leqslant N$, see (1.19) for the definition. Unlike the drag force F_i and torque T_i, the symmetric part of the first momentum does not appear in the ODEs governing the motion of particles, see [30, Section 2.2.3] for more details. However, in order to approximate the velocities (V_i, Ω_i), we only need to estimate its value. Precisely we have

Proposition 1.2.3. *For N sufficiently large, there exists a positive constant $C > 0$ independent of the data such that we have for all $1 \leqslant i \leqslant N$*

$$|S_i| \lesssim \frac{R^3}{|d^N_{\min}|^{3/2}} \max_{1\leqslant j\leqslant N}\left(|V_j| + R|\Omega_j|\right)\,.$$

Proof. We fix $i = 1$. Let E be a trace-free symmetric 3×3 matrix. We define v as the unique solution to the following Stokes equation

$$\left\{\begin{array}{rcl} -\Delta v + \nabla p &=& 0,\\ \operatorname{div} v &=& 0,\end{array}\right. \text{ on } \mathbb{R}^3\setminus\bigcup_{i=1}^N \overline{B_i}, \tag{1.44}$$

completed with the boundary conditions

$$\left\{\begin{array}{rcl} v & = & E(x-x_1), \text{ on } \partial B_1, \\ v & = & 0, \text{ on } \partial B_i,\, i\neq 1, \\ \lim\limits_{|x|\to\infty}|v(x)| & = & 0. \end{array}\right. \tag{1.45}$$

We also denote by (v_1, p_1) the special solution $(A^{(2)}_{x_1,R}[E], P^{(2)}_{x_1,R}[E])$. We have thanks to the symmetry of E

$$\begin{aligned} S_1 : E &= \int_{\partial B_1} \mathrm{sym}\left([\sigma(u^N,p^N)n]\otimes(x-x_1)\right) : E\,, \\ &= -\int_{\partial B_1}[\sigma(u^N,p^N)n]\cdot E(x-x_1)\,, \\ &= -\int_{\partial B_1}[\sigma(u^N,p^N)n]\cdot v\,, \\ &= 2\int_{\mathbb{R}^3\setminus\bigcup_i \overline{B_i}} D(u^N):D(v)\,, \\ &= 2\int_{\mathbb{R}^3\setminus\bigcup_i \overline{B_i}} D(u^N):D(v-v_1) + 2\int_{\mathbb{R}^3\setminus\bigcup_i \overline{B_i}} D(u^N):D(v_1)\,. \end{aligned} \tag{1.46}$$

Using an integration by parts we have for the second term in the right hand side

$$\begin{aligned} 2\int_{\mathbb{R}^3\setminus\bigcup_i \overline{B_i}} D(u^N):D(v_1) &= -\sum_{i=1}^N \int_{\partial B_i}[\sigma(v_1,p_1)n]\cdot(V_i+\Omega_i\times(x-x_i))\,, \\ = -\sum_{i=1}^N\left(\int_{\partial B_i}[\sigma(v_1,p_1)n]\right)\cdot V_i &- \left(\int_{\partial B_i}[\sigma(v_1,p_1)n]\times(x-x_i)\right)\cdot\Omega_i\,, \\ = 0\,, \end{aligned}$$

since v_1 corresponds to a flow submitted only to a strain, see (1.33). For the first term in the right hand side of (1.46), using Lemma 1.2.2 we have

$$\left|\int_{\mathbb{R}^3\setminus\bigcup_i \overline{B_i}} D(u^N):D(v-v_1)\right| \leqslant \|\nabla u^N\|_{L^2(\mathbb{R}^3\setminus\bigcup_i \overline{B_i})}\frac{R^3}{|d^N_{\min}|^{3/2}}|E|\,.$$

It remains to estimate $\|\nabla u^N\|_{L^2(\mathbb{R}^3\setminus\bigcup_i \overline{B_i})}$. One can reproduce the same arguments as for the proof of Lemma 1.2.2 or follow the same proof as [36, Lemma 10] to get

$$\|\nabla u^N\|^2_{L^2(\mathbb{R}^3\setminus\bigcup_i \overline{B_i})} \lesssim \max_i(|V_i|^2+R^2|\Omega_i|^2).$$

Gathering all the estimates we obtain

$$S_1 : E \lesssim \frac{R^3}{|d^N_{\min}|^{3/2}}|E|\max_i\left(|V_i|+R|\Omega_i|\right)\,,$$

this being true for all symmetric trace-free 3×3 matrix E, we obtain the desired result. $\square$

1.3 Analysis of the stationary Stokes equation

This Section is devoted to the analysis of a method of reflections and computation of the unknown velocities $(V_i, \Omega_i)_{1 \leqslant i \leqslant N}$. We remind that, for fixed time, u^N is the unique solution to the stationary Stokes problem

$$\left\{ \begin{array}{rcl} -\Delta u^N + \nabla p^N &=& 0, \\ \operatorname{div} u^N &=& 0, \end{array} \right. \text{ on } \mathbb{R}^3 \backslash \bigcup_{i=1}^N \overline{B_i},$$

completed with the no-slip boundary conditions

$$\left\{ \begin{array}{rcl} u^N &=& V_i + \Omega_i \times (x - x_i), \text{ on } \partial B_i, \\ \lim\limits_{|x| \to \infty} |u^N(x)| &=& 0, \end{array} \right.$$

where (V_i, Ω_i) are the unique velocities satisfying

$$F_i + mg = 0\,, \quad T_i = 0\,, \quad \forall\, 1 \leqslant i \leqslant N. \tag{1.47}$$

In this Section, we show that at each fixed time $t \geqslant 0$, the convergence of the method of reflections toward the unique solution u^N holds true in the case where $(X^N(t))_{N \in \mathbb{N}^*} \in \mathcal{X}(\bar{M}, \mathcal{E})$ and under the assumption that $r_0 \bar{M}^{1/3}$ is small enough.

1.3.1 The method of reflections

In this part, we present and prove the convergence of a modified method of reflections for the velocity field u^N for arbitrary $N \in \mathbb{N}^*$, we remind that u^N is the unique solution to the stationary Stokes problem (1.1), (1.2), with unique velocities (V_i, Ω_i) satisfying (1.47). The main idea is to express u^N as the superposition of N fields produced by the isolated N particle. Thanks to the superposition principle, we know that the velocity field

$$\sum_{i=1}^N \left(U_{x_j,R}[V_j](x) + A_{x_j,R}[\Omega_j](x) \right),$$

satisfies a Stokes equation on $\mathbb{R}^3 \backslash \bigcup\limits_i \overline{B_i}$. But this velocity field does not match the boundary conditions of u^N. Indeed, for all $1 \leqslant i \leqslant N$ and $x \in B_i$ we have

$$\begin{aligned} u_*^{(1)}(x) &:= u^N(x) - \sum_{j=1}^N \left(U_{x_j,R}[V_j](x) + A_{x_j,R}[\Omega_j](x) \right), \\ &= -\sum_{i \neq j}^N \left(U_{x_j,R}[V_j](x) + A_{x_j,R}[\Omega_j](x) \right), \end{aligned}$$

which represents the error committed on the boundary conditions when approaching u^N by the sum of the particular Stokes solutions. In this paper, for all $u_* \in \mathcal{C}^\infty(\bigcup_i \overline{B_i})$ we use the notation $U[u_*]$ to define the unique solution of the Stokes problem

$$\begin{cases} -\Delta u + \nabla p &= 0, \\ \operatorname{div} u &= 0, \end{cases} \text{ on } \mathbb{R}^3 \backslash \bigcup_{i=1}^N \overline{B_i}, \tag{1.48}$$

completed by the boundary conditions

$$\begin{cases} u &= u_*(x), \text{ on } B_i, \\ \lim\limits_{|x|\to\infty} |u(x)| &= 0, \end{cases} \tag{1.49}$$

hence, we can write

$$u^N = \sum_{i=1}^N U_{x_i,R}[V_i] + A_{x_j,R}[\Omega_j](x) + U[u_*^{(1)}].$$

Note that the boundary condition $u_*^{(1)}$ is not constant on each particle B_i, thus, the idea is to approach $u_*^{(1)}$ by

$$u_*^{(1)}(x) \sim u_*^{(1)}(x_i) + \nabla u_*^{(1)}(x_i) \cdot (x - x_i), \tag{1.50}$$

on each particle B_i and write $U[u_*^{(1)}]$ as follows:

$$U[u_*^{(1)}] = \sum_{j=1}^N \left(U_{x_j,R}[V_j^{(1)}] + A_{x_j,R}[\nabla_j^{(1)}] \right) + U[u_*^{(2)}],$$

where

$$V_i^{(1)} := u_*^{(1)}(x_i) = -\sum_{j\neq i} \left(U_{x_j,R}[V_j](x_i) + A_{x_j,R}[\Omega_j](x_i) \right),$$

$$\nabla_i^{(1)} := \nabla u_*^{(1)}(x_i) = -\sum_{j\neq i} \left(\nabla U_{x_j,R}[V_j](x_i) + \nabla A_{x_j,R}[\Omega_j](x_i) \right),$$

remark that $\nabla_i^{(1)}$ has null trace due to the fact that

$$\operatorname{div} u_*^{(1)}(x_i) = 0.$$

We set then $U[u_*^{(2)}]$ the new error term satisfying

$$u^N = \sum_{j=1}^N \left(U_{x_j,R}[V_j] + A_{x_j,R}[\Omega_j] \right) + \sum_{j=1}^N \left(U_{x_j,R}[V_j^{(1)}] + A_{x_j,R}[\nabla_j^{(1)}] \right) + U[u_*^{(2)}],$$

where for all $1 \leqslant i \leqslant N$, and $x \in B_i$

$$
\begin{aligned}
u_*^{(2)}(x) &= u_*^{(1)}(x) - \sum_{j=1}^{N} \Big(U_{x_j,R}[V_j^{(1)}](x) + A_{x_j,R}[\nabla_j^{(1)}](x) \Big) \,, \\
&= u_*^{(1)}(x) - V_i^{(1)} - \nabla_i^{(1)}(x - x_i) - \sum_{j \neq i}^{N} \Big(U_{x_j,R}[V_j^{(1)}](x) + A_{x_j,R}[\nabla_j^{(1)}](x) \Big) \,.
\end{aligned}
$$

We iterate then the process by setting for all $1 \leqslant i \leqslant N$

$$
V_i^{(0)} := V_i \,, \quad \nabla_i^{(0)} := \Omega_i, \tag{1.51}
$$

and for $p \geqslant 1$,

$$
V_i^{(p)} := u_*^{(p)}(x_i) \,, \quad \nabla_i^{(p)} := \nabla u_*^{(p)}(x_i), \tag{1.52}
$$

for the error term we set

$$
u_*^{(0)}(x) := \sum_{i}^{N} (V_i + \Omega_i \times (x - x_i)) \, 1_{B_i}, \tag{1.53}
$$

and define for all $p \geqslant 0$, $1 \leqslant i \leqslant N$, $x \in B_i$

$$
\begin{aligned}
u_*^{(p+1)}(x) &= u_*^{(p)}(x) - \sum_{j=1}^{N} \Big(U_{x_j,R}[V_j^{(p)}](x) + A_{x_j,R}[\nabla_j^{(p)}](x) \Big) \\
&= u_*^{(p)}(x) - u_*^{(p)}(x_i) - \nabla u_*^{(p)}(x_i)(x - x_i) - \sum_{j \neq i}^{N} \Big(U_{x_j,R}[V_j^{(p)}](x) + A_{x_j,R}[\nabla_j^{(p)}](x) \Big) \,.
\end{aligned} \tag{1.54}
$$

With this construction the following equality holds true for all $k \geqslant 1$

$$
u^N = \sum_{p=0}^{k} \sum_{j=1}^{N} \Big(U_{x_j,R}[V_j^{(p)}] + A_{x_j,R}[\nabla_j^{(p)}] \Big) + U[u_*^{(k+1)}]. \tag{1.55}
$$

Remark 1.3.1. *This method of reflection is obtained by expanding the error term u_* up to the first-order*

$$
u_*(x) = u_*(x_i) + \nabla u_*(x_i)(x - x_i) + o\,(|x - x_i|^2),
$$

which leads us to formula (1.55)*. If one consider an expansion of u_* up to the zeroth-order then one obtain only a stokeslet development:*

$$
u^N = \sum_{p=0}^{k} \sum_{j=1}^{N} U_{x_j,R}[V_j^{(p)}] + U[u_*^{(k+1)}].
$$

The main difference between these two expansions is that the first one allows us to tackle the particle rotation. It also helps us to obtain a converging method of reflections for a more general assumption on the minimal distance.
We emphasize that we only need to show that the series $(\sum_{p=0}^{k} V_i^{(p)})_{k\in\mathbb{N}}$ *and* $(\sum_{p=0}^{k} \nabla_i^{(p)})_{k\in\mathbb{N}}$ *for all* $1 \leqslant i \leqslant N$ *converge to obtain the convergence of the expansion* (1.55)*, see Lemma 1.3.1 and Proposition 1.3.2. Precisely, the only assumptions needed to obtain the convergence of the series are the smallness of* $\bar{M}^{1/3}r_0$*, assumption* (1.5) *and the fact that*

$$\lim_{N\to\infty} \frac{|\lambda^N|^3}{d_{\min}^N} = 0\,, \quad \lim_{N\to\infty} \frac{R|\lambda^N|^3}{|d_{\min}^N|^2} = 0,$$

which is less restrictive than (1.6)*.*
The second step is to show that the expansion is a good approximation of the unique solution u^N*. This is ensured by Proposition 1.3.4. Precisely, in addition of the previous assumptions, we need the following uniform bound*

$$\sup_{N\in\mathbb{N}^*} \frac{R|\lambda^N|^3}{|d_{\min}^N|^3} < +\infty.$$

One can show that this assumption is less restrictive than (1.6) *and allows us to consider smaller minimal distance. To reach lower bound for the minimal distance, one may develop* u_* *at higher orders.*

Preliminary estimates

Recall that the dependence in time is implicit in this Section. All the following estimates hold true under the assumption that there exists a sequence $(\lambda^N)_{N\in\mathbb{N}^*}$ and two positive constants $\bar{M}, \mathcal{E}$ such that $(X^N)_{N\in\mathbb{N}^*} \in \mathcal{X}(\bar{M}, \mathcal{E})$, see Definition 1.1.1 and $\bar{M}^{1/3}r_0$ is small enough.

Lemma 1.3.1. *Assume that there exists* $\bar{M}, \mathcal{E}$ *and a sequence* $(\lambda^N)_{N\in\mathbb{N}^*}$ *such that the particle configuration* $(X^N)_{N\in\mathbb{N}^*}$ *lies in* $\mathcal{X}(\bar{M}, \mathcal{E})$*. If* $\bar{M}^{1/3}r_0$ *is small enough, there exists a positive constant* $K < 1/2$ *and* $N(r_0, \bar{M}, \mathcal{E}) \in \mathbb{N}^*$ *such that*

$$\max_i |V_i^{(p+1)}| + R\max_i |\nabla_i^{(p+1)}| \leqslant K\left(\max_i |V_i^{(p)}| + R\max_i |\nabla_i^{(p)}|\right),$$

for all $N \geqslant N(r_0, \bar{M}, \mathcal{E})$*.*

Proof. Using formulas (1.52) and (1.54) we get

$$\begin{aligned} V_i^{(p+1)} &= u_*^{(p+1)}(x_i)\,, \\ &= -\sum_{j\neq i}^{N} \left(U_{x_j,R}[V_j^{(p)}](x_i) + A_{x_j,R}[\nabla_j^{(p)}](x_i)\right), \end{aligned} \tag{1.56}$$

and

$$\begin{aligned}\nabla_i^{(p+1)} &= \nabla u_*^{(p+1)}(x_i)\,,\\ &= -\sum_{j\neq i}^{N}\left(\nabla U_{x_j,R}[V_j^{(p)}](x_i) + \nabla A_{x_j,R}[\nabla_j^{(p)}](x_i)\right).\end{aligned} \tag{1.57}$$

This yields, for all $1 \leqslant i \leqslant N$, using the decay-rate of the special solutions (1.38), (1.22) and Lemma 1.A.1 with $k = 1$ and $k = 2$

$$\begin{aligned}|V_i^{(p+1)}| &\leqslant C\sum_{j\neq i} R\,\frac{|V_j^{(p)}|}{d_{ij}} + R^3\frac{|\nabla_j^{(p)}|}{d_{ij}^2}\\ &\leqslant Cr_0\left(\max_i |V_i^{(p)}| + R\max_i |\nabla_i^{(p)}|\right)\left(\frac{|\lambda^N|^3}{|d_{\min}^N|}\bar{M} + \bar{M}^{1/3} + \frac{R|\lambda^N|^3}{|d_{\min}^N|^2} + R\bar{M}^{2/3}\right),\end{aligned}$$

similarly, using (1.10), we have for all $1 \leqslant i \leqslant N$

$$\begin{aligned}|\nabla_i^{(p+1)}| &\leqslant C\sum_{j\neq i} R\,\frac{|V_j^{(p)}|}{d_{ij}^2} + R^3\frac{|\nabla_j^{(p)}|}{d_{ij}^3}\,,\\ &\leqslant C\left(\max_i |V_i^{(p)}| + R\max_i |\nabla_i^{(p)}|\right)\left(\sum_{j\neq i}\frac{R}{d_{ij}^2} + \frac{1}{d_{\min}^N}\sum_{j\neq i}\frac{R^2}{d_{ij}^2}\right),\\ &= C\left(\max_i |V_i^{(p)}| + R\max_i |\nabla_i^{(p)}|\right)\left(\sum_{j\neq i}\frac{R}{d_{ij}^2}\right)\left(1 + \frac{R}{d_{\min}^N}\right),\\ &\leqslant Cr_0\left(\max_i |V_i^{(p)}| + R\max_i |\nabla_i^{(p)}|\right)\left(\frac{|\lambda^N|^3}{|d_{\min}^N|^2}\bar{M} + \bar{M}^{2/3}\right).\end{aligned}$$

Finally

$$\begin{aligned}\max_i |V_i^{(p+1)}| + R\max_i |\nabla_i^{(p+1)}| &\leqslant Cr_0\left(\max_i |V_i^{(p)}| + R\max_i |\nabla_i^{(p)}|\right)\\ &\quad\times\left(\frac{|\lambda^N|^3}{d_{\min}^N}\bar{M} + \bar{M}^{1/3} + \frac{R|\lambda^N|^3}{|d_{\min}^N|^2}\bar{M} + R\bar{M}^{2/3}\right).\end{aligned}$$

For the second term on the right hand side we have

$$\frac{|\lambda^N|^3}{d_{\min}^N} + \frac{R|\lambda^N|^3}{|d_{\min}^N|^2} = \frac{|\lambda^N|^3}{|d_{\min}^N|^2}\left(d_{\min}^N + R\right),$$

which vanishes when N tends to infinity according to (1.6) and (1.7). Moreover, if $r_0\bar{M}^{1/3}$ is small enough, this ensures the existence of a positive constant $K < 1/2$ such that

$$\max_i |V_i^{(p+1)}| + R\max_i |\nabla_i^{(p+1)}| \leqslant K\left(\max_i |V_i^{(p)}| + R\max_i |\nabla_i^{(p)}|\right).$$

for N large enough and depending on r_0, $\bar{M}$ and $\mathcal{E}$. □

We have the following estimate.

Proposition 1.3.2. *Let $(U_i)_{1\leqslant i\leqslant N}$ be N vectors of $\mathbb{R}^3$ and $(D_i)_{1\leqslant i\leqslant N}$ be N trace-free 3×3 matrices. There exists $N(r_0,\bar{M},\mathcal{E})\in\mathbb{N}^*$ such that for all $N\geqslant N(r_0,\bar{M},\mathcal{E})$ we have*

$$\left\|\sum_{i=1}^N (U_{x_i,R}[U_i]+A_{x_i,R}[D_i])\right\|_{\dot{H}^1(\mathbb{R}^3\setminus\bigcup_l \overline{B}_l)} \lesssim \max_{1\leqslant i\leqslant N}(|U_i|+R|D_i|).$$

Proof. Considering only the stokeslet expansion we have

$$\left\|\sum_{i=1}^N U_{x_i,R}[U_i]\right\|^2_{\dot{H}^1(\mathbb{R}^3\setminus\bigcup_l \overline{B}_l)} = \\ \sum_{i=1}^N \|U_{x_i,R}[U_i]\|^2_{\dot{H}^1(\mathbb{R}^3\setminus\bigcup_i \overline{B}_i)} + \sum_{i=1}^N\sum_{j\neq i}^N \int_{\mathbb{R}^3\setminus\bigcup_l \overline{B}_l} \nabla U_{x_i,R}[U_i]:\nabla U_{x_j,R}[U_j]\,. \quad (1.58)$$

The first term in the right hand side of (1.58) can be computed using the fact that $U_{x_i,R}[U_i]=U_i$ on ∂B_i, $1\leqslant i\leqslant N$ and formula (1.24)

$$\begin{aligned}
\sum_{i=1}^N \|U_{x_i,R}[U_i]\|^2_{\dot{H}^1(\mathbb{R}^3\setminus\bigcup_l \overline{B}_l)} &\leqslant \sum_{i=1}^N \int_{\mathbb{R}^3\setminus\overline{B}_i} \nabla U_{x_i,R}[U_i]:\nabla U_{x_i,R}[U_i]\,,\\
&= -\sum_{i=1}^N \int_{\partial B_i} [\sigma(U_{x_i,R}[U_i],P_{x_i,R}[U_i])n]\cdot U_i\,,\\
&= \sum_{i=1}^N 6\pi R|U_i|^2\,,\\
&\leqslant 6\pi r_0\left(\max_{1\leqslant i\leqslant N}|U_i|\right)^2\,.
\end{aligned}$$

For the second term in the right hand side of (1.58) we write for all $i\neq j$

$$\begin{aligned}
\int_{\mathbb{R}^3\setminus\bigcup_l \overline{B}_l} \nabla U_{x_i,R}[U_i]:\nabla U_{x_j,R}[U_j] &= -\sum_{l=1}^N \int_{\partial B_l} [\sigma(U_{x_i,R}[U_i],P_{x_i,R}[U_i])n]\cdot U_{x_j,R}[U_j]\,,\\
&\leqslant \sum_{l=1}^N 4\pi R^2 \left\|\sigma(U_{x_i,R}[U_i],P_{x_i,R}[U_i])\right\|_{L^\infty(\partial B_l)} \left\|U_{x_j,R}[U_j]\right\|_{L^\infty(\partial B_l)}\,,\\
&:= \sum_{l=1}^N 4\pi R^2\mathcal{O}^l_{i,j}.
\end{aligned}$$

According to the decay properties of the stokeslet (1.22) we have

$$\begin{aligned}
\|\sigma(U_{x_i,R}[U_i],P_{x_i,R}[U_i])\|_{L^\infty(\partial B_l)} &\lesssim R\frac{|U_i|}{d_{il}^2}(1-\delta_{il})+\frac{|U_i|}{R}\delta_{il}\,,\\
\left\|U_{x_j,R}[U_j]\right\|_{L^\infty(\partial B_l)} &\lesssim \frac{R|U_j|}{d_{jl}}(1-\delta_{jl})+|U_j|\delta_{jl}\,,
\end{aligned}\tag{1.59}$$

where δ_{ij} is the Kronecker symbol. On the other hand, we recall that the triangle inequality $d_{ij}\leqslant d_{il}+d_{jl}$ yields for all $i\neq j\neq l$

$$\frac{1}{d_{il}d_{jl}}\leqslant\frac{1}{d_{ij}}\left(\frac{1}{d_{il}}+\frac{1}{d_{jl}}\right)\,.\tag{1.60}$$

Using (1.59), formula (1.60) twice and Lemma 1.A.1 we obtain for all $i\neq j$

$$\begin{aligned}
\sum_{l=1}^{N}4\pi R^2\mathcal{O}^l_{i,j} &= \sum_{l\neq i,j}4\pi R^2\mathcal{O}^l_{i,j}+4\pi R^2\mathcal{O}^i_{i,j}+4\pi R^2\mathcal{O}^j_{i,j}\,,\\
&\lesssim \sum_{l\neq i,j}R^2\frac{R|U_i|}{d_{il}^2}\frac{R|U_j|}{d_{jl}}+R^2\frac{|U_i|}{R}\frac{R|U_j|}{d_{ij}}+R^2\frac{R|U_i|}{d_{ij}^2}|U_j|\,,\\
&\lesssim \frac{R^3}{d_{ij}}\left(\frac{1}{d_{ij}}\left(\sum_{l\neq i,j}\frac{R}{d_{il}}+\sum_{l\neq i,j}\frac{R}{d_{jl}}\right)+\sum_{l\neq i,j}\frac{R}{d_{il}^2}\right)|U_j||U_i|\\
&+R^2\frac{|U_j||U_i|}{d_{ij}}+R^3\frac{|U_i||U_j|}{d_{ij}^2}\,,\\
&\lesssim \frac{R^3}{d_{ij}}\left(\frac{1}{d_{ij}}\left(\frac{|\lambda^N|^3}{d_{\min}^N}\bar{M}+\bar{M}^{1/3}\right)+\frac{|\lambda^N|^3}{|d_{\min}^N|^2}\bar{M}+\bar{M}^{2/3}\right)|U_j||U_i|\\
&+R^2\frac{|U_j||U_i|}{d_{ij}}+R^3\frac{|U_i||U_j|}{d_{ij}^2}\,,\\
&\lesssim \frac{R^3}{d_{ij}}\left(\mathcal{E}\bar{M}+\frac{\bar{M}^{1/3}r_0^2}{d_{\min}^N}+\bar{M}^{2/3}\right)|U_j||U_i|+R^2\frac{|U_j||U_i|}{d_{ij}}+R^3\frac{|U_i||U_j|}{d_{ij}^2}\,,\\
&\lesssim \left[\frac{R^3}{d_{ij}}\frac{1}{d_{\min}^N}+\frac{R^2}{d_{ij}}+\frac{R^3}{d_{ij}^2}\right]|U_j||U_i|\,,
\end{aligned}$$

where we kept only the largest terms using the fact that $d_{\min}^N$ vanishes according to (1.7) for N large enough. Hence, the second term in the right hand side of (1.58) yields using

Lemma 1.A.1

$$\begin{aligned}
&\sum_{i=1}^{N}\sum_{j\neq i}^{N}\int_{\mathbb{R}^3\setminus\underset{l}{\cup}\overline{B}_l}\nabla U_{x_i,R}[U_i]:\nabla U_{x_j,R}[U_j] \lesssim \sum_{i=1}^{N}\sum_{j\neq i}^{N}\left[\frac{R^3}{d_{ij}}\frac{1}{d_{\min}^N}+\frac{R^2}{d_{ij}}+\frac{R^3}{d_{ij}^2}\right]|U_j||U_i|\,,\\
&\lesssim \max_{1\leqslant i\leqslant N}\left(\sum_{j\neq i}^{N}\left[\frac{R^2}{d_{ij}}\frac{1}{d_{\min}^N}+\frac{R}{d_{ij}}+\frac{R^2}{d_{ij}^2}\right]\right)\left(\max_{1\leqslant i\leqslant N}|U_i|\right)^2,\\
&\lesssim \left[\left(\frac{R}{d_{\min}^N}+1\right)\left(\frac{|\lambda^N|^3}{d_{\min}^N}\bar{M}+\bar{M}^{1/3}\right)+\frac{R|\lambda^N|^3}{|d_{\min}^N|^2}\bar{M}+R\bar{M}^{2/3}\right]\left(\max_{1\leqslant i\leqslant N}|U_i|\right)^2,\\
&\lesssim \left(\max_{1\leqslant i\leqslant N}|U_i|\right)^2,
\end{aligned}$$

where we used the fact that $\frac{R}{d_{\min}^N}\lesssim 1$ thanks to (1.10) and $\frac{|\lambda^N|^3}{d_{\min}^N}\leqslant\frac{|\lambda^N|^3}{|d_{\min}^N|^2}d_{\min}^N\lesssim 1$ according to (1.6) and (1.7). The term involving rotating and straining solutions $A_{x_i,R}[D_i]$ is handled analogously. $\square$

Since the series $\sum\limits_{p=0}^{k}V_i^{(p)}$, $\sum\limits_{p=0}^{k}\nabla_i^{(p)}$ are convergent, we denote their limit by

$$V_i^\infty:=\sum_{p=0}^{\infty}V_i^{(p)},\quad \nabla_i^\infty:=\sum_{p=0}^{\infty}\nabla_i^{(p)}.$$

Thanks to the linearity of the Stokes equation and Proposition 1.3.2, the expansion term

$$\sum_{i=1}^{N}\left(U_{x_i,R}\left[\sum_{p=0}^{k}V_i^{(p)}\right]+A_{x_i,R}\left[\sum_{p=0}^{k}\nabla_i^{(p)}\right]\right),$$

converges in $\dot{H}^1(\mathbb{R}^3\setminus\underset{l}{\cup}\overline{B}_l)$ uniformly in N to the expansion where we replace the series by their limit. This shows that the error term $U[u_*^{(k)}]$ has a limit when $k\to\infty$. In order to quantify the error term, we begin by the following estimate

Proposition 1.3.3. *For all $k\geqslant 1$ we set*

$$\eta^{(k)}:=\max_j|V_j^{(k)}|+R\max_j|\nabla_j^{(k)}|.$$

Under the same assumptions as Lemma 1.3.1, there exists $N(r_0,\bar{M},\mathcal{E})\in\mathbb{N}^*$ such that for all $N\geqslant N(r_0,\bar{M},\mathcal{E})$ and $1\leqslant i\leqslant N$

$$\begin{aligned}
\|\nabla^2u_*^{(k+1)}\|_{L^\infty(B_i)} &\lesssim \left(1+\frac{|\lambda^N|^3}{|d_{\min}^N|^3}+|\log(\bar{M}^{1/3}\lambda^N)|\right)\max_i(|V_i|+R|\Omega_i|),\\
\|\nabla u_*^{(k+1)}\|_{L^\infty(B_i)} &\lesssim R\|\nabla^2u_*^{(k+1)}\|_{L^\infty(B_i)}+\eta^{(k)},\\
\|u_*^{(k)}\|_{L^\infty(B_i)} &\lesssim R^2\|\nabla^2u_*^{(k+1)}\|_{L^\infty(B_i)}+\eta^{(k)}.
\end{aligned}$$

Proof.
1. Estimate of $\|\nabla^2 u_*^{(k+1)}\|_{L^\infty(B_i)}$
Let $x \in B_i$, using formula (1.10) we recall that for $i \neq j$

$$|x - x_j| \geqslant |x_i - x_j| - |x - x_i| \geqslant \frac{1}{2} d_{ij}.$$

Applying this, formula (1.10), the decay properties of the second gradient of single particle solutions (1.23), (1.39) and the iteration formula (1.54) together with Lemma 1.A.1 for $k = 3$ yields

$$\begin{aligned}
|\nabla^2 u_*^{(k+1)}(x)| &\leqslant |\nabla^2 u_*^{(k)}(x)| + \sum_{j\neq i} |\nabla^2 U_{x_j,R}[V_j^{(k)}](x)| + |\nabla^2 A_{x_j,R}[\nabla_j^{(k)}](x)|\,, \\
&\lesssim \|\nabla^2 u_*^{(k)}\|_{L^\infty(B_i)} + \sum_{j\neq i} \frac{|V_j^{(k)}|}{d_{ij}^3} R + \frac{|\nabla_j^{(k)}|}{d_{ij}^4} R^3\,, \\
&\lesssim \|\nabla^2 u_*^{(k)}\|_{L^\infty(B_i)} + \left(\sum_{j\neq i} \frac{R}{d_{ij}^3} + \frac{R}{d_{\min}^N} \sum_{j\neq i} \frac{R}{d_{ij}^3} \right) \left(\max_j |V_j^{(k)}| + R \max_j |\nabla_j^{(k)}| \right)\,, \\
&= \|\nabla^2 u_*^{(k)}\|_{L^\infty(B_i)} + \left(\sum_{j\neq i} \frac{R}{d_{ij}^3} \right) \left(1 + \frac{R}{d_{\min}^N} \right) \eta^{(k)}\,, \\
&\lesssim \|\nabla^2 u_*^{(k)}\|_{L^\infty(B_i)} + r_0 \bar{M} \left(\frac{|\lambda^N|^3}{|d_{\min}^N|^3} + |\log(\bar{M}^{1/3}\lambda^N)| + 1 \right) \eta^{(k)},
\end{aligned}$$

hence, we iterate the formula and use the fact that $\nabla^2 u_*^{(0)} = 0$ according to formula (1.53), to get

$$\|\nabla^2 u_*^{(k+1)}\|_{L^\infty(B_i)} \lesssim \left(1 + \frac{|\lambda^N|^3}{|d_{\min}^N|^3} + |\log(\bar{M}^{1/3}\lambda^N)| \right) \sum_{p=0}^{k} \eta^{(p)},$$

which yields the expected result by applying Lemma 1.3.1.
2. Estimate of $\|\nabla u_*^{(k+1)}\|_{L^\infty(B_i)}$
Let $x \in B_i$, again, the decay properties of the gradient of the special solutions (1.22), (1.38), formula (1.54) and Lemma 1.A.1 yields

$$\begin{aligned}
|\nabla u_*^{(k+1)}(x)| &\leqslant |\nabla u_*^{(k)}(x) - \nabla u_*^{(k)}(x_i)| + \sum_{j\neq i} |\nabla U_{x_j,R}[V_j^{(k)}](x_i)| + |\nabla A_{x_j,R}[\nabla_j^{(k)}](x_i)|\,, \\
&\lesssim R \|\nabla^2 u_*^{(k)}\|_{L^\infty(B_i)} + \sum_{j\neq i} \frac{|V_j^{(k)}|}{d_{ij}^2} R + \frac{|\nabla_j^{(k)}|}{d_{ij}^3} R^3\,, \\
&\lesssim R \|\nabla^2 u_*^{(k)}\|_{L^\infty(B_i)} + \left(\sum_{j\neq i} \frac{R}{d_{ij}^2} + \frac{R}{d_{\min}^N} \sum_{j\neq i} \frac{R}{d_{ij}^2} \right) \left(\max_j |V_j^{(k)}| + R \max_j |\nabla_j^{(k)}| \right)\,, \\
&\lesssim R \|\nabla^2 u_*^{(k)}\|_{L^\infty(B_i)} + \left(1 + \frac{R}{d_{\min}^N} \right) \left(\frac{|\lambda^N|^3}{|d_{\min}^N|^2} \bar{M} + \bar{M}^{2/3} \right) r_0 \eta^{(k)},
\end{aligned}$$

again, according to (1.10), note that for N large enough, $1 + \frac{R}{d_{\min}^N} \leqslant 2$. We conclude using assumption (1.6) to bound the right hand side by $\eta^{(k)}$ up to constants depending on $\bar{M}$, $\mathcal{E}$, r_0.

3. Estimate of $\|u_*^{(k+1)}\|_{L^\infty(B_i)}$

Let $x \in B_i$, again, the decay property (1.22), (1.38) and formula (1.54) yields

$$\begin{aligned}
|u_*^{(k+1)}(x)| &\leqslant R^2\|\nabla^2 u_*^{(k)}\|_{L^\infty(B_i)} + \sum_{j\neq i}|U_{x_j,R}[V_j^{(k)}](x)| + |A_{x_j,R}[\nabla_j^{(k)}](x)|\,,\\
&\lesssim R^2\|\nabla^2 u_*^{(k)}\|_{L^\infty(B_i)} + \sum_{j\neq i}\frac{|V_j^{(k)}|}{d_{ij}}R + \frac{|\nabla_j^{(k)}|}{d_{ij}^2}R^3\,,\\
&\lesssim R^2\|\nabla^2 u_*^{(k)}\|_{L^\infty(B_i)} + r_0\left(\frac{|\lambda^N|^3}{d_{\min}^N}\bar{M} + \bar{M}^{1/3} + \frac{R|\lambda^N|^3}{|d_{\min}^N|^2}\bar{M} + R\bar{M}^{2/3}\right)\eta^{(k)}.
\end{aligned}$$

Using (1.6) and (1.7), the right hand side can be bounded by $\eta^{(k)}$ up to constants depending on $\bar{M}$, $\mathcal{E}$, r_0. □

Approximation result

We can now state the main result of this Section.

Proposition 1.3.4. *Assume that there exists $\bar{M}, \mathcal{E}$ and a sequence $(\lambda^N)_{N\in\mathbb{N}^*}$ such that $(X^N)_{N\in\mathbb{N}^*} \in \mathcal{X}(\bar{M}, \mathcal{E})$. Assume moreover that $\bar{M}^{1/3}r_0$ is small enough.*
There exists a positive constant $C = C(r_0, \bar{M}, \mathcal{E})$ and $N(r_0, \bar{M}, \mathcal{E}) \in \mathbb{N}^*$ satisfying for all $N \geqslant N(r_0, \bar{M}, \mathcal{E})$

$$\lim_{k\to\infty}\|\nabla U[u_*^{(k+1)}]\|_{L^2(\mathbb{R}^3\setminus\bigcup B_i)} \leqslant CR\max_i\left(|V_i| + R|\Omega_i|\right),$$

Proof. The aim is to estimate $\|\nabla U[u_*^{(k+1)}]\|_{L^2(\mathbb{R}^3\setminus\bigcup B_i)}$. To this end, we construct a suitable extension $E[u_*^{(k+1)}]$ of the boundary conditions of $u_*^{(k+1)}$ and apply the variational principle (1.17). By construction, $u_*^{(k+1)}$ is regular and well defined on each particle $B(x_i, R)$. Hence, we construct the extension piecewise in each $B(x_i, 2R)$. Let $1 \leqslant i \leqslant N$, for all $x \in B(x_i, 2R)$ we set

$$v^i(x) := u_1^{(i)}(x) + u_2^{(i)}(x),$$

where the first term $u_1^{(i)}$ matches the boundary condition on $B(x_i, R)$ and vanishes outside $B(x_i, 2R)$. The second term is the correction needed to get $\operatorname{div} v_i = 0$. In order to obtain an extension of $u_*^{(k)}$ on $B(x_i, 2R)$ we set

$$\begin{aligned}
u_1^{(i)}(x) &= u_*^{(k)}\left(x_i + R\frac{x - x_i}{|x - x_i|}\right)\chi\left(\left|\frac{x - x_i}{R}\right|\right),\ \text{if } |x - x_i| \geqslant R,\\
u_1^{(i)}(x) &= u_*^{(k)}(x),\ \text{if } x \in B(x_i, R)\ ,
\end{aligned}$$

with χ a truncation function such that $\chi = 1$ on $[0,1]$ and $\chi = 0$ outside $[0,2]$.
We have then

$$\|\nabla u_1^{(i)}\|_{L^\infty(B(x_i,2R))} \leqslant K_\chi \left(\|\nabla u_*^{(k)}\|_{L^\infty(B(x_i,R))} + \frac{1}{R}\|u_*^{(k)}\|_{L^\infty(B(x_i,R))} \right). \tag{1.61}$$

In what follows we introduce the notation $A(x,r,R) := B(x,R)\backslash\overline{B(x,r)}$ for $r < R$. For the second term we set:

$$u_i^{(2)} = \mathcal{B}_{x_i\,,\,R\,,\,2R}(-\operatorname{div} u_i^{(1)}),$$

where $\mathcal{B}$ is the Bogovskii operator, see [36, Appendix A Lemma 15 and 16] for more details.
The construction satisfies:
— supp $u_i^{(2)} \subset A(x_i, R, 2R)$
— $\operatorname{div} v_i = 0$
— $v_i = u_i^{(1)} = u_*^{(k)}$ on $B(x_i, R)$
We set then

$$E[u_*^{(k+1)}] = \sum_i^N v^i(x) 1_{B(x_i,2R)},$$

and thanks to the variational formulation we have

$$\begin{aligned}\|\nabla U[u_*^{(k+1)}]\|^2_{L^2(\mathbb{R}^3\backslash \bigcup B_i)} &\leqslant \|\nabla E[u_*^{(k+1)}]\|^2_{L^2(\mathbb{R}^3\backslash \bigcup B_i)}\,, \\ &= \sum_i^N \|\nabla v_i\|^2_{L^2(A(x_i,R,2R))},\end{aligned}$$

where we used the fact that the v_i have disjoint support.
Thanks to the properties of the Bogovskii operator $\mathcal{B}_{x_i\,,\,R\,,\,2R}$ we get

$$\begin{aligned}\|\nabla v_i\|^2_{L^2(B(x_i,R))} &\lesssim \int_{A(x_i,R,2R)} |\nabla u_1^{(i)}|^2\,, \\ &\lesssim R^3 \|\nabla u_1^{(i)}\|^2_{L^\infty(B(A(x_i,R,2R)))}\,, \\ &\lesssim R^3 \left(\|\nabla u_*^{(k)}\|_{L^\infty(B_i)} + \frac{1}{R}\|u_*^{(k)}\|_{L^\infty(B_i)} \right)^2.\end{aligned}$$

Finally

$$\|\nabla U[u_*^{(k+1)}]\|^2_{L^2(\mathbb{R}^3\backslash \bigcup B_i)} \lesssim \sum_i^N R^3 \left(\|\nabla u_*^{(k)}\|_{L^\infty(B_i)} + \frac{1}{R}\|u_*^{(k)}\|_{L^\infty(B_i)} \right)^2.$$

Thanks to Proposition 1.3.3 we have

$$\begin{aligned}\|\nabla u_*^{(k)}\|_{L^\infty(B_i)} + \frac{1}{R}\|u_*\|_{L^\infty(B_i)} \lesssim \max_i(|V_i| + R|\Omega_i|) \left(R + \frac{R|\lambda^N|^3}{|d_{\min}^N|^3} + R|\log(\bar{M}^{1/3}\lambda^N)| \right) \\ + \left(\frac{1}{R} + 1\right)\eta^{(k)}.\end{aligned}$$

Since

$$\eta^{(k)} \leqslant K^k \max_i(|V_i| + R|\Omega_i|),$$

with $K < 1$ according to Lemma 1.3.1, we get

$$\|\nabla U[u_*^{(k+1)}]\|^2_{L^2(\mathbb{R}^3\setminus\bigcup B_i)} \lesssim \max_i(|V_i| + R|\Omega_i|)^2 \left\{ R\left(R + \frac{R|\lambda^N|^3}{|d^N_{\min}|^3} + R|\log(\bar{M}^{1/3}\lambda^N)|\right) + (1+R)\,K^k \right\}^2.$$

Since $K < 1$ for N large enough the second term on the right hand side, which is uniformly bounded with respect to N, vanishes when $k \to \infty$. This yields

$$\lim_{k\to\infty} \|\nabla U[u_*^{(k+1)}]\|_{L^2(\mathbb{R}^3\setminus\bigcup B_i)} \lesssim R \max_i(|V_i| + R|\Omega_i|) \left(R + \frac{R|\lambda^N|^3}{|d^N_{\min}|^3} + R|\log(\bar{M}^{1/3}\lambda^N)|\right).$$

The second term on the right hand side can be bounded using assumptions (1.6), (1.8) and (1.10)

$$R + \frac{R|\lambda^N|^3}{|d^N_{\min}|^3} + R|\log(\bar{M}^{1/3}\lambda^N)| \lesssim R + \frac{R}{d^N_{\min}}\mathcal{E} + \frac{|\log \bar{M}| + \log N}{N} \lesssim 1,$$

Finally we obtain

$$\lim_{k\to\infty} \|\nabla U[u_*^{(k+1)}]\|_{L^2(\mathbb{R}^3\setminus\bigcup B_i)} \lesssim R \max_i(|V_i| + R|\Omega_i|),$$

which is the desired result. □

Remark 1.3.2. *According to Proposition 1.3.3 we have for all* $1 \leqslant i \leqslant N$

$$\begin{aligned} \|u_*^{(k+1)}\|_{L^\infty(B_i)} &\lesssim R^2 \|\nabla^2 u_*^{(k+1)}\|_{L^\infty(B_i)} + \eta^{(k)} \\ &\lesssim \max_i(|V_i| + R|\Omega_i|) \left\{ R\left(\frac{R|\lambda^N|^3}{|d^N_{\min}|^3} + R|\log(\bar{M}^{1/3}\lambda^N)|\right) + K^k \right\}. \end{aligned}$$

as for the proof of Proposition 1.3.4 the second term vanishes when $k \to \infty$ *and we obtain*

$$\overline{\lim_{k\to\infty}} \|u_*^{(k+1)}\|_{L^\infty(B_i)} \lesssim \max_i(|V_i| + R|\Omega_i|) R.$$

Some associated estimates

We recall that we aim to compute the velocities (V_i, Ω_i) associated to the unique solution u^N of the Stokes equation:

$$\left\{ \begin{array}{rcl} -\Delta u^N + \nabla p^N &=& 0, \\ \operatorname{div} u^N &=& 0, \end{array} \right. \text{ on } \mathbb{R}^3 \setminus \bigcup_{i=1}^N \overline{B_i},$$

completed with the no-slip boundary conditions

$$\left\{\begin{array}{rcl} u^N & = & V_i + \Omega_i \times (x - x_i), \text{ on } \partial B_i, \\ \lim\limits_{|x|\to\infty} |u^N(x)| & = & 0, \end{array}\right.$$

with

$$F_i + mg = 0\,, \quad T_i = 0\,, \quad \forall 1 \leqslant i \leqslant N.$$

The method of reflections obtained in this Section helps us to describe the velocity field u^N in terms of explicit flows

$$u^N = \sum_{j=1}^{N} \left(U_{x_j,R}\left[V_j^{(\infty)}\right] + A_{x_j,R}\left[\nabla_j^{(\infty)}\right]\right) + \lim_{k\to\infty} U[u_*^{(k)}].$$

In order to extract a formula for the unknown velocities (V_i, Ω_i), $1 \leqslant i \leqslant N$ we need to compute first the velocities $V_i^{(\infty)}$ and matrices $\nabla_i^{(\infty)}$. Applying the method of reflections and writing the force, torque and stresslet associated to the unique solution u^N in two different ways we get the following result.

Lemma 1.3.5. *Under the same assumptions as Proposition 1.3.4, there exists* $N(r_0, \bar{M}, \mathcal{E}) \in \mathbb{N}^*$ *such that for all* $N \geqslant N(r_0, \bar{M}, \mathcal{E})$

$$\begin{array}{rcl} V_i^{\infty} = & \kappa g + O\left(\max\limits_i(|V_i| + R|\Omega_i|)\frac{R}{\sqrt{d_{\min}^N}}\right), & 1 \leqslant i \leqslant N\,, \\ R\,|\nabla_i^{\infty}| = & O\left(\max\limits_i(|V_i| + R|\Omega_i|)\frac{R}{|d_{\min}^N|^{3/2}}\right), & 1 \leqslant i \leqslant N\,, \end{array}$$

where κg *is defined thanks to formula* (1.4)*.*

Proof. For the sake of clarity we fix $i = 1$ and the same result holds for all $1 \leqslant i \leqslant N$. Let $V \in \mathbb{R}^3$, D a trace-free 3×3 matrix.

The main idea is to apply an integration by parts with a suitable test function $v \in D_\sigma(\mathbb{R}^3 \backslash \bigcup\limits_i \overline{B_i})$ such that $v = V + D(x - x_1)$ on ∂B_1 and $v = 0$ on the other ∂B_j, $j \neq 1$. We choose v the unique solution to the Stokes equation:

$$\left\{\begin{array}{rcl} -\Delta v + \nabla p & = & 0, \\ \operatorname{div} v & = & 0, \end{array}\right. \text{ on } \mathbb{R}^3 \backslash \bigcup_{i=1}^{N} \overline{B_i}, \tag{1.62}$$

completed by the boundary conditions

$$\left\{\begin{array}{rcl} v & = & V + D(x - x_1), \text{ on } \partial B_1, \\ v & = & 0 \text{ on } \partial B_i,\, i \neq 1, \\ \lim\limits_{|x|\to\infty} |v(x)| & = & 0. \end{array}\right. \tag{1.63}$$

We extend u^N and v by their boundary values on all B_i, $1 \leqslant i \leqslant N$. We set $E = \mathrm{sym}(D)$, $\Omega = \mathrm{ssym}(D)$. An integration by parts yields

$$\begin{aligned}
2\int_{\mathbb{R}^3\setminus\bigcup_i B_i} D(u^N) : D(v) &= -\sum_i \int_{\partial B_i} \left[\sigma(u^N,p^N)n\right]\cdot v\,,\\
&= -\int_{\partial B_1} \left[\sigma(u^N,p^N)n\right]\cdot (V+\Omega\times(x-x_1)+E(x-x_1))\,,\\
&= -V\cdot\int_{\partial B_i}\sigma(u^N,p^N)n - \Omega\cdot\int_{\partial B_i}(x-x_i)\times\left[\sigma(u^N,p^N)n\right]\,,\\
&- E : \int_{\partial B_i}(x-x_i)\otimes\left[\sigma(u^N,p^N)n\right]\,,\\
&= -V\cdot F_1 - \Omega\cdot T_1 - E : S_1,
\end{aligned} \tag{1.64}$$

see (1.18) and (1.19) for the definition of the force F_1, torque T_1 and stresslet S_1. On the other hand, we apply the method of reflections to get

$$\begin{aligned}
&\int_{\mathbb{R}^3\setminus\bigcup_i B_i} D(u^N) : D(v) =\\
&\sum_{j=1}^N \int_{\mathbb{R}^3\setminus\bigcup_i B_i} (D(U_{x_j,R}[V_j^\infty]) + D(\nabla A_{x_j,R}[\nabla_j^\infty])) : D(v) + \lim_{k\to\infty}\int_{\mathbb{R}^3\setminus\bigcup_i B_i} D(U[u_*^k]) : D(v).
\end{aligned} \tag{1.65}$$

For the first term we integrate by parts to get for all $1 \leqslant j \leqslant N$

$$\begin{aligned}
2\int_{\mathbb{R}^3\setminus\bigcup_i B_i} D(U_{x_j,R}[V_j^\infty]) : D(v) &= -\sum_{i=1}^N\int_{\partial B_i}\left[\sigma(U_{x_j,R}[V_j^\infty],P_{x_j,R}[V_j^\infty])n\right]\cdot v.\\
2\int_{\mathbb{R}^3\setminus\bigcup_i B_i} D(A_{x_j,R}[\nabla_j^\infty]) : D(v) &= -\sum_{i=1}^N\int_{\partial B_i}\left[\sigma(A_{x_j,R}[\nabla_j^\infty],P_{x_j,R}[\nabla_j^\infty])n\right]\cdot v.
\end{aligned}$$

Recall that v vanishes on ∂B_i, $i \neq 1$ and hence, the sums above are reduced to the first term. Applying (1.34) (1.30) and (1.24) there holds for all $1 \leqslant j \leqslant N$

$$\begin{aligned}
\int_{\partial B_1}\left[\sigma(U_{x_j,R}[V_j^\infty],P_{x_j,R}[V_j^\infty])n\right]\cdot v &= -6\pi R V_1^\infty\cdot V\delta_{1j},\\
\int_{\partial B_1}\left[\sigma(A_{x_j,R}[\nabla_j^\infty],P_{x_j,R}[\nabla_j^\infty])n\right]\cdot v &= -\pi R^3\left(8\,\mathrm{ssym}(\nabla_1^\infty)\cdot\Omega + \frac{20}{3}\mathrm{sym}(\nabla_1^\infty) : E\right)\delta_{1j},
\end{aligned}$$

where δ_{1j} is the Kronecker symbol.
For the second term on the right hand side of formula (1.65), we consider $v_1 := U_{x_1,R}[V] +$

$A_{x_1,R}[D]$ and write

$$\int_{\mathbb{R}^3\setminus\bigcup_i B_i} DU[u_*^k] : D(v) = \int_{\mathbb{R}^3\setminus\bigcup_i B_i} D(U[u_*^k]) : D(v_1) + \int_{\mathbb{R}^3\setminus\bigcup_i B_i} D(U[u_*^k]) : D(v - v_1). \tag{1.66}$$

To bound the last term we apply Lemma 1.2.2 and Proposition 1.3.4

$$\begin{aligned}\lim_{k\to\infty}\left|\int_{\mathbb{R}^3\setminus\bigcup_i B_i} D(U[u_*^k]) : D(v-v_1)\right| &\lesssim \max_i(|V_i| + R[\Omega_i|)R\left(\frac{R}{\sqrt{d_{\min}^N}}|V| + \frac{R^3}{|d_{\min}^N|^{3/2}}|D|\right), \\ &\lesssim \frac{R^2}{\sqrt{d_{\min}^N}}(|V| + R|D|)\max_i(|V_i| + R|\Omega_i|).\end{aligned}$$

We focus now on the first term on the right hand side of formula (1.66), we have

$$\begin{aligned}\left|\int_{\mathbb{R}^3\setminus\underset{i}{\cup}B_i} DU[u_*^{(k)}] : D(v_1)\right| &= \left|\sum_i\int_{\partial B_i}[\sigma(v_1,p_1)\cdot n]\cdot u_*^{(k)}\right| \\ &\leqslant \sum_i 4\pi R^2\|\sigma(v_1,p_1)\|_{L^\infty(B_i)}\|u_*^{(k)}\|_{L^\infty(B_i)},\end{aligned}$$

using the decay properties (1.22), (1.38) we have

$$\begin{aligned}\|\sigma(v_1,p_1)\|_{L^\infty(B_i)} &\lesssim \frac{R|V|}{d_{i1}^2} + \frac{R^3}{d_{i1}^3}|D|, \text{ for } i\neq 1\,, \\ \|\sigma(v_1,p_1)\|_{L^\infty(B_1)} &\lesssim \frac{|V|}{R} + |D|,\end{aligned}$$

hence

$$\begin{aligned}\left|\int_{\mathbb{R}^3\setminus\underset{i}{\cup}B_i} D(U[u_*^{(k)}]) : D(v_1)\right| &\lesssim R(|V| + R|D|)\|u_*^{(k)}\|_{L^\infty(B_1)}\,, \\ &+ R\sum_{i\neq 1}\left(\frac{R^2|V|}{d_{i1}^2} + \frac{R^4|D|}{d_{i1}^3}\right)\max_i\|u_*^{(k)}\|_{L^\infty(B_i)}\,, \\ &\lesssim R(|V| + R|D|)\max_i\|u_*^{(k)}\|_{L^\infty(B_i)}.\end{aligned}$$

According to Remark 1.3.2 , we have for all $1 \leqslant i \leqslant N$

$$\overline{\lim_{k\to\infty}}\|u_*^{(k)}\|_{L^\infty(B_i)} \lesssim R\max_i(|V_i| + R|\Omega_i|).$$

Finally we get

$$\lim_{k\to\infty}\left|\int_{\mathbb{R}^3\setminus\bigcup_i B_i} D(U[u_*^k]) : \nabla v_1\right| + \left|\int_{\mathbb{R}^3\setminus\bigcup_i B_i} D(U[u_*^k]) : \nabla(v - v_1)\right| \lesssim$$
$$\max_i(|V_i| + R|\Omega_i|)\frac{R^2}{\sqrt{d_{\min}^N}}(|V| + R|D|). \tag{1.67}$$

Identifying formula (1.64) and (1.65) and gathering all the inequalities above we have for all V , $\Omega \in \mathbb{R}^3$ and symmetric trace-free 3×3 matrix E

$$
\begin{aligned}
-V \cdot F_1 - \Omega \cdot T_1 - E : S_1 = 6\pi R V_1^\infty \cdot V + 8\pi R^3 \,\mathrm{ssym}(\nabla_1^\infty) \cdot \Omega + \frac{20}{3}\pi R^3 \,\mathrm{sym}(\nabla_1^\infty) : E \\
+ O\left(\max_i (|V_i| + R|\Omega_i|) \frac{R^2}{\sqrt{d_{\min}^N}} (|V| + R|D|) \right),
\end{aligned}
$$

with $F_1 + mg = 0$, $T_1 = 0$. Note that the value of the stresslet S_i, see (1.19) for the definition, is unknown. However, we only need to approximate its value using Proposition 1.2.3. We conclude by identifying the terms involving $V \in \mathbb{R}^3$ to obtain

$$
V_i^\infty := \sum_{p=0}^{\infty} V_i^{(p)} = \frac{m}{6\pi R} g + O\left(\max_i (|V_i| + R|\Omega_i|) \frac{R}{\sqrt{d_{\min}^N}} \right),
$$

for the skew-symmetric part we get

$$
R\,|\mathrm{ssym}(\nabla_1^\infty)| \lesssim \max_i (|V_i| + R|\Omega_i|) \frac{R}{\sqrt{d_{\min}^N}} \lesssim \max_i (|V_i| + R|\Omega_i|) \frac{R}{|d_{\min}^N|^{3/2}},
$$

and for the symmetric part using Proposition 1.2.3

$$
R\,|\mathrm{sym}(\nabla_1^\infty)| = O\left(\max_i (|V_i| + R|\Omega_i|) \frac{R}{|d_{\min}^N|^{3/2}} \right),
$$

which concludes the proof. □

Corollary 1.3.6. *Under the same assumptions as Lemma 1.3.5, there exists a positive constant $C = C(\kappa|g|)$ and $N(r_0, \bar{M}, \mathcal{E}) \in \mathbb{N}^*$ such that for all $N \geqslant N(r_0, \bar{M}, \mathcal{E})$ we have*

$$
\max_{1 \leqslant i \leqslant N} (|V_i| + R\,|\Omega_i|) \leqslant C.
$$

Proof. recall that $V_i^{(0)} = V_i$, $\nabla_i^{(0)} = \Omega_i$ for all $1 \leqslant i \leqslant N$, according to Lemma 1.3.5 and Lemma 1.3.1 we obtain for all $1 \leqslant i \leqslant N$

$$
\begin{aligned}
|V_i| + R|\Omega_i| &\leqslant |V_i^\infty| + R|\nabla_i^\infty| + \sum_{p=1}^{\infty} \left(\left|V_i^{(p)}\right| + R\left|\nabla_i^{(p)}\right| \right), \\
&\leqslant |V_i^\infty| + R|\nabla_i^\infty| + K \left(\sum_{p=0}^{\infty} K^p \right) \max_i (|V_i| + R|\Omega_i|), \\
&\lesssim \kappa|g| + \left(\frac{R}{|d_{\min}^N|^{3/2}} + \frac{K}{1-K} \right) \max_i (|V_i| + R|\Omega_i|).
\end{aligned}
$$

Hence, according to Lemma 1.3.1 we have $\frac{K}{1-K} < 1$. Moreover, assumption (1.9) ensures that

$$
\frac{R}{|d_{\min}^N|^{3/2}} \lesssim \frac{\mathcal{E}^{3/4} \bar{M}^{3/4}}{N^{1/4}},
$$

which vanishes when N goes to infinity. □

1.3.2 Extraction of the first order terms for the velocities (V_i, Ω_i)

In order to control the motion of the particles, we want to provide a good approximation of the unknown velocities (V_i, Ω_i). Thanks to the method of reflections, the velocity field u^N can be approached by a superposition of analytical solutions to a Stokes flow generated by a translating, a rotating and a straining sphere (See Proposition 1.3.4) with the associated velocities $(V_i^\infty, \nabla_i^\infty)$. This allows us to compute the first order terms for (V_i, Ω_i) applying Lemma 1.3.5 and Corollary 1.3.6. Keeping in mind that all the computations are done for a fixed time $t \geqslant 0$, the main result of this Section is the following Proposition.

Proposition 1.3.7. *Assume that, for a fixed time, we have the existence of a sequence* $(\lambda^N)_{N\in\mathbb{N}^*}$ *and two positive constants* $\bar{M}, \mathcal{E}$ *such that* $(X^N)_{N\in\mathbb{N}^*} \in \mathcal{X}(\bar{M}, \mathcal{E})$. *Assume moreover that* $\bar{M}^{1/3} r_0$ *is small enough. Then, there exists* $N(r_0, \bar{M}, \mathcal{E}) \in \mathbb{N}^*$ *such that for all* $N \geqslant N(r_0, \bar{M}, \mathcal{E})$, *for all* $1 \leqslant i \leqslant N$ *we have*

$$V_i = \kappa g + 6\pi R \sum_{j\neq i}^{N} \Phi(x_i - x_j)\kappa g + O\left(d_{\min}^N\right), \;\; R\Omega_i = O\left(d_{\min}^N\right),$$

We begin by the following lemma:

Lemma 1.3.8. *For all trace-free* 3×3 *matrices* $(D_i)_{1\leqslant i \leqslant N}$, *for all* $W \in \mathbb{R}^3$ *and* $1 \leqslant i \leqslant N$ *we have*

$$\sum_{j\neq i}^{N} \left| 6\pi R \Phi(x_i - x_j)\, W - U_{x_j,R}[W](x_i) \right| \lesssim R|W|.$$

$$\sum_{j\neq i}^{N} \left| A_{x_j,R}[D_j](x_i) \right| \lesssim R \max_j R|D_j|.$$

Proof of Lemma 1.3.8. Thanks to formula (1.25) we have for $i \neq j$

$$U_{x_j,R}[W](x_i) = 6\pi R \Phi(x_j - x_i) W + \frac{1}{4} \frac{R^3}{|x_j - x_i|^3} W - \frac{3}{4} R^3 \frac{(x_j - x_i)\cdot W}{|x_j - x_i|^5}(x_j - x_i),$$

this yields

$$\left| U_{x_j,R}[W](x_i) - 6\pi R \Phi(x_j - x_i) W \right| \lesssim \frac{R^3}{d_{ij}^3}|W|.$$

Applying Lemma 1.A.1 with $k = 3$ yields

$$\begin{aligned}\sum_{j\neq i}^{N} \left| U_{x_j,R}[W](x_i) - 6\pi R \Phi(x_j - x_i) W \right| &\lesssim \sum_{j\neq i}^{N} \frac{R^3}{d_{ij}^3}|W| \\ &\lesssim R r_0 \bar{M} \left(\frac{R|\lambda^N|^3}{|d_{\min}^N|^3} + R(|\log \bar{M}| + |\log \lambda^N|) \right) |W|.\end{aligned}$$

We have thanks to assumptions (1.6), (1.8) and (1.10)

$$\frac{R|\lambda^N|^3}{|d_{\min}^N|^3} + R(|\log \bar{M}| + |\log \lambda^N|) \leqslant \frac{R}{d_{\min}^N}\mathcal{E} + R|\log \bar{M}| + R\log N \lesssim 1.$$

Analogously, we obtain the second bound by applying 1.A.1 with $k=2$ this time. $\square$

We can now prove the main result.

Proof of Proposition 1.3.7. Let fix $1 \leqslant i \leqslant N$. According to Lemma 1.3.5 and Corollary 1.3.6 we have

$$V_i^\infty = \sum_{p=0}^{\infty} V_i^{(p)} = \frac{m}{6\pi R} g + O\left(\frac{R}{\sqrt{d_{\min}^N}}\right).$$

As $V_i^{(0)} = V_i$ we get

$$V_i = -\sum_{p=1}^{\infty} V_i^{(p)} + \frac{m}{6\pi R} g + O\left(\frac{R}{\sqrt{d_{\min}^N}}\right).$$

Formula (1.56) for the velocities $V_j^{(p)}$ yields

$$\begin{aligned} V_i &= \sum_{p=1}^{\infty}\sum_{j\neq i} \left(U_{x_j,R}[V_j^{(p-1)}](x_i) + A_{x_j,R}[\nabla_j^{(p-1)}](x_i)\right) + \frac{m}{6\pi R} g + O\left(\frac{R}{\sqrt{d_{\min}^N}}\right), \\ &= \frac{m}{6\pi R} g + \sum_{j\neq i}\left(U_{x_j,R}[V_j^\infty](x_i) + A_{x_j,R}[\nabla_j^\infty](x_i)\right) + O\left(\frac{R}{\sqrt{d_{\min}^N}}\right), \end{aligned}$$

we apply Lemma 1.3.8, Lemma 1.3.5 and Corollary 1.3.6 together with (1.9) and (1.10) to get:

$$\begin{aligned} \sum_{j\neq i}\left|A_{x_j,R}[\nabla_j^\infty](x_i)\right| &\lesssim R\max_j R|\nabla_j^\infty|, \\ &\lesssim R\frac{R}{|d_{\min}^N|^{3/2}}, \\ &\leqslant d_{\min}^N \frac{\mathcal{E}^{3/4}\bar{M}^{3/4}}{N^{1/4}}, \\ &\lesssim d_{\min}^N. \end{aligned}$$

Now, we rewrite the sum as follows:

$$\sum_{j\neq i} U_{x_j,R}[V_j^\infty](x_i) = \sum_{j\neq i} U_{x_j,R}[\kappa g](x_i) + \sum_{j\neq i} U_{x_j,R}\left[V_j^\infty - \kappa g\right](x_i),$$

and we bound the error term using the decay rate (1.22), Lemma 1.3.5 and Lemma 1.A.1 with $k = 1$

$$\begin{aligned}\left|\sum_{j\neq i} U_{x_j,R}\left[V_j^\infty - \kappa g\right](x_i)\right| &\lesssim \left(\sum_{j\neq i}\frac{R}{d_{ij}}\right)\max_j \left|V_j^\infty - \kappa g\right| \,, \\ &\lesssim \frac{R}{\sqrt{d_{\min}^N}}\,, \\ &\lesssim d_{\min}^N.\end{aligned}$$

We conclude by replacing the stokeslets by the Oseen tensor thanks to Lemma 1.3.8. Finally we have for all $1 \leqslant i \leqslant N$

$$V_i = \kappa g + 6\pi R \sum_{j\neq i}^{N} \Phi(x_i - x_j)\kappa g + O\left(d_{\min}^N\right).$$

For the angular velocities we obtain thanks to Lemma 1.3.5 and formula (1.57) for $\nabla_1^{(p)}$, $p \geqslant 1$

$$\begin{aligned}R\Omega_1 &= -\sum_{p=1}^{\infty} R\,\mathrm{ssym}\,\nabla_1^{(p)} + O\left(\frac{R}{\sqrt{d_{\min}^N}}\right)\,, \\ &= R\,\mathrm{ssym}\left(\sum_{j\neq 1}\nabla U_{x_j,R}[V_j^\infty](x_1) + \nabla A_{x_j,R}[\nabla_j^\infty](x_1)\right) + O\left(\frac{R}{\sqrt{d_{\min}^N}}\right).\end{aligned}$$

As before, using Lemma 1.3.5 we bound the first term by

$$\begin{aligned}&R\left|\sum_{j\neq 1}\nabla U_{x_j,R}[V_j^\infty](x_1) + \nabla A_{x_j,R}[\nabla_j^\infty](x_1)\right| \\ &\lesssim R\left(\sum_{j\neq 1}\frac{R}{d_{1j}^2} + \frac{R^2}{d_{1j}^3}\right)\max_j(|V_j^\infty|, R|\nabla_j^\infty|)\,, \\ &\lesssim R\left(\sum_{j\neq 1}\frac{R}{d_{1j}^2}\right)\left(1 + \frac{R}{d_{\min}^N}\right)\max_j(|V_j^\infty|, R|\nabla_j^\infty|)\,, \\ &\lesssim Rr_0\left(\frac{|\lambda^N|^3}{|d_{\min}^N|^2}\bar{M} + \bar{M}^{2/3}\right)\,, \\ &\lesssim d_{\min}^N\left(\frac{R|\lambda^N|^3}{|d_{\min}^N|^3} + \bar{M}^{2/3}\right)\,, \\ &\lesssim d_{\min}^N\,,\end{aligned}$$

where we used the fact that $\frac{R|\lambda^N|^3}{|d_{\min}^N|^3}$ is uniformly bounded according to (1.6) and (1.10). □

1.4 Control of the particle distance and concentration

In this Section, we make precise the particle behavior in time. Precisely we want to prove that if initially there exists two positive constants $\bar{M}, \mathcal{E}$ and a sequence $(\lambda^N)_{N\in\mathbb{N}^*}$ such that $(X^N(0))_{N\in\mathbb{N}^*} \in \mathcal{X}(\bar{M},\mathcal{E})$ (see Definition 1.1.1), then the same holds true for a finite time. Recall that the initial distribution of particles satisfies:

— The minimal distance is at least of order $|\lambda^N|^{3/2}$.

— The maximal number of particles concentrated in a cube of width λ^N satisfies assumption (1.5).

We aim to show that there exists a small interval of time $[0,T]$ independent of N on which the particle distance and concentration stay at the same order. The idea is to use a Gronwall argument and the computation of the velocities $(V_i)_{1\leqslant i\leqslant N}$ at each fixed time $t \geqslant 0$.

1.4.1 Proof of Theorem 1.1.1

We assume that initially there exists two positive constants $\bar{M}, \mathcal{E}$ and a sequence $(\lambda^N)_{N\in\mathbb{N}^*}$ such that $(X^N(0))_{N\in\mathbb{N}^*} \in \mathcal{X}(\bar{M},\mathcal{E})$. Let $T>0$ be such that

$$d_{ij}(t) \geqslant \frac{1}{2} d_{ij}(0)\,, \forall 1 \leqslant i \neq j \leqslant N\,,\ \forall t \in [0,T[. \tag{1.68}$$

This maximal time $T>0$ exists and we aim to prove that it is independent of N. As long as $t<T$ we have a control on the particle concentration.

Lemma 1.4.1 (Control of particle concentration M^N)**.** *As long as $t\in[0,T[$ we have:*

$$M^N(t) \leqslant 8^4 M^N(0).$$

Proof. We recall the definition of $M^N(t)$

$$M^N(t) := \sup_{x\in\mathbb{R}^3}\Big\{\#\big\{i\in\{1,\cdots,N\} \text{ such that } x_i(t) \in \overline{B_\infty(x,\lambda^N)}\big\}\Big\}.$$

We introduce the following quantity:

$$L^N(t) := \max_i \#\left\{j\in\{1,\ldots,N\} \text{ such that } |x_i(t)-x_j(t)|_\infty \leqslant \lambda^N)\right\}. \tag{1.69}$$

One can show that the two definitions of concentration $L^N(t)$ and $M^N(t)$ are equivalent in the sense that

$$L^N(t) \leqslant M^N(t) \leqslant 8L^N(t)$$

see Lemma 1.A.2 for the proof. We also need to introduce the following notation for all $\beta>0$:

$$L^N_\beta(t) := \max_i \#\left\{j\in\{1,\ldots,N\} \text{ such that } |x_i(t)-x_j(t)|_\infty \leqslant \beta\lambda^N)\right\},$$

and

$$M_\beta^N(t) := \sup_x \Big\{ \#\{ i \in \{1, \cdots, N\} \text{ such that } x_i(t) \in \overline{B_\infty(x, \beta\lambda^N))} \} \Big\},$$

with the notation

$$M_1^N(t) := M^N(t)\,, \quad L_1^N(t) := L^N(t).$$

We have for all $\beta > 0$ and all $\alpha > 1$

$$L_{\alpha\beta}^N(t) \leqslant 8\lceil\alpha\rceil^3 L_\beta^N(t),$$

where $\lceil\cdot\rceil$ denotes the ceiling function. See Corollary 1.A.3 for the proof.

The idea is to show that the concentration L^N is controlled in time and hence, the same applies to M^N according to Lemma 1.A.2. Recall that we have for all $t \in [0, T[$

$$d_{ij}(t) \geqslant \frac{1}{2} d_{ij}(0).$$

Now, fix $1 \leqslant i \leqslant N$ and consider $j \neq i$ satisfying $|x_i(0) - x_j(0)|_\infty > \lambda^N$, then

$$\begin{aligned} |x_i(t) - x_j(t)|_\infty &\geqslant \frac{1}{\sqrt{3}} |x_i(t) - x_j(t)|\,, \\ &\geqslant \frac{1}{2\sqrt{3}} |x_i(t) - x_j(0)|\,, \\ &> \frac{\lambda^N}{2\sqrt{3}}. \end{aligned}$$

Which means that

$$j \notin \left\{ 1 \leqslant k \leqslant N, \text{ such that } |x_i(t) - x_k(t)| \leqslant \frac{\lambda^N}{2\sqrt{3}} \right\}.$$

We obtain

$$\begin{aligned} &\left\{ 1 \leqslant j \leqslant N\,, \text{ such that } |x_i(t) - x_j(t)| \leqslant \frac{\lambda^N}{2\sqrt{3}} \right\} \\ &\qquad \subset \left\{ 1 \leqslant j \leqslant N\,, \text{ such that } |x_i(0) - x_j(0)| \leqslant \lambda^N \right\}. \end{aligned} \tag{1.70}$$

Hence taking the maximum over $1 \leqslant i \leqslant N$ we obtain

$$L^N_{\frac{1}{2\sqrt{3}}}(t) \leqslant L^N(0),$$

thus, we apply Corollary 1.A.3 with $\beta = \frac{1}{2\sqrt{3}}$ and $\alpha = \beta^{-1} = 2\sqrt{3}$ to get

$$L^N(t) \leqslant 8^3 L^N(0).$$

According to Lemma 1.A.2, the equivalence between M^N and L^N yields finally for all $t \in [0, T[$

$$M^N(t) \leqslant 8^4 M^N(0).$$

This ends the proof. □

This shows that as long as $t < T$ we have $(X^N(t))_{N\in\mathbb{N}^*} \in \mathcal{X}(8^4\bar{M}, 4\mathcal{E})$. This implies the following control.

Proposition 1.4.2. *Assume that there exists two positive constants $\bar{M}, \mathcal{E}$ and a sequence $(\lambda^N)_{N\in\mathbb{N}^*}$ such that $(X^N)_{N\in\mathbb{N}^*} \in \mathcal{X}(8^4\bar{M}, 4\mathcal{E})$. If $r_0\bar{M}^{1/3}$ is small enough, there exists $N(r_0, \bar{M}, \mathcal{E})$ and a positive constant $C = C(r_0, \bar{M}, \mathcal{E}, \kappa|g|)$ independent of N such that for all $N \geqslant N(r_0, \bar{M}, \mathcal{E})$, for all $i \neq j$ we have*

$$|V_i - V_j| \leqslant C d_{ij}.$$

Proof. For the sake of clarity we fix $i = 1$ and $j = 2$. The computations below are independent of this choice. Thanks to Proposition 1.3.7 we obtain :

$$V_1 - V_2 = 6\pi R \sum_{i\neq 1,2}^{N} (\Phi(x_1 - x_i) - \Phi(x_2 - x_i))\kappa g + O(d_{\min}^N).$$

Hence, according to assumption (1.6), formula (1.27) and using Lemma 1.A.1 for $k = 2$ we obtain

$$\begin{aligned} |V_1 - V_2| &\lesssim R \sum_{i\neq 1,2}^{N} \left(\frac{1}{d_{1i}^2} + \frac{1}{d_{2i}^2} \right) |x_1 - x_2| + O(d_{\min}^N)\,, \\ &\lesssim r_0 \left(\bar{M} \frac{|\lambda^N|^3}{|d_{\min}^N|^2} + \bar{M}^{2/3} \right) |x_1 - x_2| + O(d_{\min}^N)\,, \\ &\lesssim d_{12}. \end{aligned}$$

We set then $C > 0$ the universal constant implicit in the above estimate. □

We have the following control.

Lemma 1.4.3 (Control of particle distance)**.** *For all $1 \leqslant i \neq j \leqslant N$, for all $t \in [0, T[$ we have*

$$d_{ij}(t) \geqslant d_{ij}(0)e^{-Ct}.$$

Proof. Thanks to (1.68) and Lemma 1.4.1 we have for all $t < T$ that

$$(X^N(t))_{N\in\mathbb{N}^*} \in \mathcal{X}(8^4\bar{M}, 4\mathcal{E}).$$

Hence, all computations from Proposition 1.4.2 hold true up to time T. In other words, there exists a positive constant $C = C(r_0, \bar{M}, \mathcal{E}, \kappa|g|)$ such that for all indices $1 \leqslant i \neq j \leqslant N$ we have

$$|V_i(t) - V_j(t)| \leqslant C\, d_{ij}(t)\ \forall t \in [0, T[,$$

thus,

$$\begin{aligned} \frac{d}{dt} d_{ij}(t) &\geqslant -|V_i(t) - V_j(t)|, \\ &\geqslant -C\, d_{ij}(t). \end{aligned}$$

This entails

$$d_{ij}(t) \geqslant d_{ij}(0)e^{-Ct}\,,$$

which is the desired result. □

Conclusion

Thanks to Lemma 1.4.3 and Lemma 1.4.1 we have for all $1 \leqslant i \neq j \leqslant N$, $t \in [0, T[$

$$\begin{array}{rcl} d_{ij}(t) & \geqslant & d_{ij}(0)e^{-Ct}, \\ M^N(t) & \leqslant & 8^4 M^N(0), \end{array}$$

this shows that T is independent of N and is at least of order $\frac{\log(2)}{C}$ where C depends on $(r_0, \bar{M}, \mathcal{E}, \kappa|g|)$.

1.5 Reminder on Wasserstein distance and analysis of the limiting equation

In this part we recall some important results of existence, uniqueness, regularity and stability concerning the mean-field equation (1.13). We recall also the definition of the Monge-Kantorovich-Wasserstein distance of order one and infinite. We refer to [70, Part I, chapter 6] for definition and properties of the order one distance W_1. To define the infinite Wasserstein distance we start with some associated notions. We refer to [20] for more details.

Definition 1.5.1 (Transference plan). *Let μ , $\nu \in \mathcal{P}(\mathbb{R}^3)$ be two probability measures. The set of transference plans from μ to ν denoted $\Pi(\mu\,,\,\nu)$ is the set of all probability measures $\pi \in \mathcal{P}(\mathbb{R}^3 \times \mathbb{R}^3)$ with first marginal μ and second marginal ν i.e.*

$$\pi \in \Pi(\mu\,,\,\nu) \Leftrightarrow \int\int_{\mathbb{R}^3\times\mathbb{R}^3} (\phi(x) + \psi(y))\pi(dxdy) = \int_{\mathbb{R}^3} \phi(x)\mu(dx) + \int_{\mathbb{R}^3} \psi(y)\nu(dy),$$

for all ϕ , $\psi \in \mathcal{C}_b(\mathbb{R}^3)$.

Recall that for all probability measure $\lambda \in \mathcal{P}(\mathbb{R}^3 \times \mathbb{R}^3)$ we have

Definition 1.5.2 (Essential supremum).

$$\lambda - \text{esssup}\,|x-y| := \inf\{t \geqslant 0 \,:\, \lambda(\{(x,y) \in \mathbb{R}^3 \times \mathbb{R}^3 \,:\, |x-y| > t\}) = 0\}.$$

We recall also the definition of the support for a (non-negative) measure.

Definition 1.5.3 (Measure support). *Given $\mu \in \mathcal{P}(\mathbb{R}^3)$ a non-negative measure, then the support of μ is defined as the set of all points x for which every open neighbourhood of x has positive measure*

$$\operatorname{supp}\mu = \{x \in \mathbb{R}^3 : \forall\, V \in \mathcal{V}(x)\,,\, \mu(V) > 0\},$$

where $\mathcal{V}(x)$ denotes the set of open neighbourhoods of x.

With this definition for the support one can show that there holds

$$\lambda - \text{esssup}\,|x-y| := \sup\{|x-y| \,:\, (x,y) \in \text{ supp } \lambda\}).$$

We can now define the infinite Wasserstein distance W_∞:

Definition 1.5.4 (Infinite Wasserstein distance)**.** *The infinite Wasserstein distance between two probability measures μ and ν is defined as follows:*

$$W_\infty(\mu\,,\,\nu) = \inf_{\pi \in \Pi(\mu\,,\nu)} \{\pi - \text{esssup}\,|x-y|\}.$$

A transference plan $\pi^* \in \Pi(\mu,\nu)$ satisfying

$$W_\infty(\mu\,,\,\nu) = \pi^* - \text{esssup}\,|x-y|,$$

is called an optimal transference plan.

We recall also the definition of a transport map.

Definition 1.5.5 (Transport map)**.** *Given two probability measures μ and ν, a transport map T is a measurable mapping $T : \text{supp}\,\mu \to \mathbb{R}^3$ such that*

$$\nu = T_{\#}\mu.$$

We emphasize that $T(\mathbb{R}^3) \subset \text{supp}\,\nu$ μ - almost everywhere. Indeed

$$\begin{aligned}
\mu\{x \in \mathbb{R}^3 : T(x) \notin \text{supp }\nu\ \} &= \mu\{T^{-1}({}^c\text{supp }\nu\ )\}\,,\\
&= \nu\{{}^c\,\text{supp}\,\nu\}\,,\\
&= 0.
\end{aligned}$$

Remark 1.5.1. *Note that, for all transport map T from μ to ν one may associate a transference plan $(Id,T)\#\mu \in \Pi(\mu\,,\,\nu)$ i.e. the pushforward of μ by the map $x \mapsto (x, T(x))$ and we have*

$$\begin{aligned}
&(Id,T)\#\mu - \text{esssup}\,|x-y|\,,\\
&= \inf\{t \geqslant 0 \,:\, (Id,T)\#\mu(\{(x,y) \in \mathbb{R}^3 \times \mathbb{R}^3 \,:\, |x-y| \geqslant t\}) = 0\}\,,\\
&= \inf\{t \geqslant 0 \,:\, \mu((Id,T)^{-1}\{(x,y) \in \mathbb{R}^3 \times \mathbb{R}^3 \,:\, |x-y| \geqslant t\}) = 0\}\,,\\
&= \inf\{t \geqslant 0 \,:\, \mu(\{x \in \mathbb{R}^3 \,:\, |x-T(x)| \geqslant t\}) = 0\}\,,\\
&= \mu - \text{esssup}\,|x-T(x)|.
\end{aligned}$$

Note that this yields

$$\inf_{\pi \in \Pi(\mu\,,\nu)} \{\pi - \text{esssup}\,|x-y|\} \leqslant \inf\{\mu - \text{esssup}\,|T(x)-x|\,,\, T : \text{supp}\,\mu \to \mathbb{R}^3\,,\, \nu = T\#\mu\}.$$

It is then natural to investigate in which conditions one has the existence of a transport map T associated to an optimal transference plan. As in [34] we refer to [20] for the following existence result.

Theorem 1.5.1 (Champion, De Pascale, Juutinen)**.** *Assume that μ is absolutely continuous with respect to the Lebesgue measure. Then there exists optimal transference plans, and at least one of them is given by a transport map T. If moreover ν is a finite sum of Dirac masses, this optimal transport map is unique.*

1.5.1 Existence, uniqueness and stability for the mean-field equation

Consider the following problem

$$\begin{cases} \frac{\partial \varrho}{\partial t} + \operatorname{div}((\kappa g + \mathcal{K}\varrho)\varrho) &= 0\,, \\ \varrho(0,\cdot) &= \varrho_0\,, \end{cases} \tag{1.71}$$

recall the definition of the kernel $\mathcal{K}$

$$\mathcal{K}\eta(x) = 6\pi r_0 \kappa \int \Phi(x-y)\, g\, \eta(y) dy,$$

for all $\eta \in L^\infty(\mathbb{R}^3) \times L^1(\mathbb{R}^3)$. We refer to the existence and uniqueness result due to Höfer [38, Theorem 9.2] in the case where the initial data ϱ_0 and its gradient $\nabla\varrho_0$ are in the space X_β for some $\beta > 2$ where

$$X_\beta := \{h \in L^\infty(\mathbb{R}^3)\,,\, \|h\|_{X_\beta} < \infty\},$$

with

$$\|h\|_{X\beta} := \operatorname*{esssup}_x (1+|x|^\beta)|h(x)|.$$

Theorem 1.5.2 (Höfer)**.** *Assume that ϱ_0, $\nabla\varrho_0 \in X_\beta$ for $\beta > 2$. There exists a unique solution $\varrho \in W^{1,\infty}((0,T), X_\beta)$ to equation (1.71) for all $T > 0$ and a unique well defined flow X satisfying*

$$\begin{cases} \partial_s X(s,t,x) &= \kappa g + \mathcal{K}\varrho(s, X(s,t,x)), \quad \forall\, s,t \in [0,+\infty[, \\ X(t,t,x) &= x, \quad \forall\, t \in [0,+\infty[, \end{cases} \tag{1.72}$$

such that

$$\varrho(t,x) = \varrho_0(X(0,t,x))\,,\ \forall\,(t,x) \in [0,+\infty[\times\mathbb{R}^3. \tag{1.73}$$

Remark 1.5.2. *The flow X is measure-preserving i.e. for a test function $\phi \in \mathcal{C}_b(\mathbb{R}^3)$ we have*

$$\int \phi(y)\varrho(s,y)dy = \int \phi(X(s,t,y))\varrho(t,y)dy,$$

for all s , $t \in [0,T]$. This allows us to separate the dependence of time s in the integral with respect to the measure $\varrho(t,\cdot)$.

Remark 1.5.3. *Note that for all $\eta \in L^\infty(\mathbb{R}^3) \cap L^1(\mathbb{R}^3)$, the velocity field $\mathcal{K}\eta$ is Lipschitz*

$$|\mathcal{K}(\eta)(x) - \mathcal{K}(\eta)(y)| \lesssim (\|\eta\|_{L^1} + \|\eta\|_{L^\infty})\,|x-y|, \quad \forall\, x \neq y \in \mathbb{R}^3.$$

Moreover, if one assume that ϱ_0 is only Lipschitz and compactly supported, then one can show the existence and uniqueness of the solution ϱ to equation (1.71) in the space $L^\infty((0,T); L^\infty(\mathbb{R}^3) \cap L^1(\mathbb{R}^3))$. The method of proof is related to the stability result due to G. Loeper in [50] which gives a stability estimate in terms of Wasserstein distance for the

Vlasov-Poisson equation. This result is adapted by M. Hauray in [33, Theorem 3.1] for a more general class of kernels K satisfying a (C^α) condition with $\alpha < d-1$ where d is the space dimension

$$\operatorname{div} K = 0,\ |K(x)|,\ |x||\nabla K(x)| < \frac{C}{|x|^\alpha},\ \forall\, x \neq 0, \tag{C^α}$$

see [33]. This condition being satisfied by the Oseen tensor Φ we have the following result.

Theorem 1.5.3 (Hauray-Loeper)**.** *Given $T > 0$, consider two solutions $\varrho_i \in L^\infty((0,T),$ $L^\infty(\mathbb{R}^3) \cap L^1(\mathbb{R}^3))$, $i = 1,2$, of equation* (1.71) *associated to two initial data $\varrho_0^i \in L^\infty(\mathbb{R}^3) \cap$ $L^1(\mathbb{R}^3)$, $i = 1,2$. There holds*

$$W_1(\varrho_1(t,\cdot), \varrho_2(t,\cdot)) \leqslant W_1(\varrho_0^1, \varrho_0^2) e^{C \max(\|\varrho_1^0\|_{L^\infty \cap L^1}, \|\varrho_2^0\|_{L^\infty \cap L^1}) t}. \tag{1.74}$$

We refer to [33, Theorem 3.1] for a complete proof which introduces the main ideas used also in [34] for the mean field approximation result.

1.5.2 ϱ^N as a weak solution to a transport equation

According to Theorem 1.1.1, there exists a time $T > 0$ independent of N for which the particles do not overlap. This shows that the empirical measure

$$\varrho^N(t,x) := \frac{1}{N} \sum_{i=1}^N \delta_{x_i(t)}(x),$$

is well defined on $[0,T]$. Recall that we are interested in the limiting behaviour of $\varrho^N \in \mathcal{P}([0,T] \times \mathbb{R}^3)$ when $N \to \infty$. According to Proposition 1.3.7, particles $(x_i)_{1 \leqslant i \leqslant N}$ satisfy the following system:

$$\left\{ \begin{array}{lcl} \dot{x}_i & = & V_i, \\ V_i & \sim & \kappa g + 6\pi R \sum\limits_{i \neq j} \Phi(x_i - x_j). \end{array} \right.$$

In order to prove Theorem 1.1.2 we want to compare the particle system to the continuous density ϱ which is solution to equation (1.71). Hence, we need to express ϱ^N as a weak solution to a transport equation. The remainder of this Section is devoted to establish such a formulation.

Analogously to the continuous case, we are interested in giving a sense to the quantity

$$\mathcal{K}\varrho^N = 6\pi r_0 \kappa \int \Phi(x-y) g \varrho^N(t,dy),$$

which is not well defined because Φ is singular. On the other hand, as the only values of Φ that matters are the terms $\Phi(x_i - x_j)$, $i \neq j$ we define the following regularization

$$\psi^N \Phi(x) := \Phi(x) \psi^N(x),$$

where $\psi^N(x) := \psi\left(\frac{x}{d^N_{\min}(0)}\right)$ and ψ is a truncation function such that $\psi = 0$ on $B(0,1/4)$ and $\psi = 1$ outside $B(0,1/2)$. We can now define the operator $\mathcal{K}^N$

$$\begin{aligned}\mathcal{K}^N \varrho^N(t,x) &:= 6\pi r_0 \kappa \int_{\mathbb{R}^3} \psi^N \Phi(x-y)\, g\, \varrho^N(t,dy)\,,\\ &= \frac{6\pi r_0\kappa}{N}\sum_i \psi^N \Phi(x - x_i(t))g.\end{aligned}$$

Since Theorem 1.1.1 ensures that the particles satisfy

$$|x_i(t) - x_j(t)| \geqslant \frac{1}{2} d^N_{\min}(0)\,,\ \ \forall i \neq j\,, \forall\, t \in [0,T],$$

we have for $x = x_i(t)$, $t \in [0,T]$, $1 \leqslant i \leqslant N$

$$\mathcal{K}^N \varrho^N(t, x_i(t)) = \frac{6\pi r_0\kappa}{N}\sum_{j\neq i}\Phi(x_j(t) - x_i(t))g.$$

Now, it remains to check that ϱ^N is a weak solution of a transport equation. We recall that ϱ^N is a weak solution of a transport equation $\frac{\partial}{\partial t} + \operatorname{div}(V\varrho^N)$ with $V \in \mathcal{C}([0,T], \mathcal{C}^1(\mathbb{R}^3))$ if for all test function $\phi \in \mathcal{C}^\infty_c([0,T]\times\mathbb{R}^3)$ we have

$$\int_0^T \int_{\mathbb{R}^3} \left(\partial_t \phi(t,x) + \nabla\phi(t,x)\cdot V(t,x)\right) \varrho^N(dx,t)dt = 0.$$

Note that this integral yields

$$\begin{aligned}&\int_0^T \int_{\mathbb{R}^3} \left(\partial_t \phi(t,x) + \nabla\phi(t,x)\cdot V(t,x)\right) \varrho^N(dx,t)dt\,,\\ &= \int_0^T \frac{1}{N}\sum_i \left(\partial_t\phi(t,x_i(t)) + \nabla\phi(t,x_i(t))\cdot V(t,x_i(t))\right).\end{aligned}$$

In particular if we choose V such that $V(t,x_i(t)) = V_i(t)$ one has

$$\begin{aligned}&= \int_0^T \frac{1}{N}\sum_i \partial_t\phi(t,x_i(t)) + \nabla\phi(t,x_i(t))\cdot V_i\,,\\ &= \frac{1}{N}\sum_i \int_0^T \frac{d}{dt}(\phi(t,x_i(t)))\,,\\ &= 0.\end{aligned}$$

On the other hand, we recall that from Proposition 1.3.7 we can write for all $1 \leqslant i \leqslant N$

$$\begin{aligned}V_i &= \kappa g + 6\pi R \sum_{j\neq i}^N \Phi(x_i - x_j)\kappa g + E_i(t)\,,\\ &= \kappa g + \mathcal{K}^N\varrho^N(t,x_i(t)) + E_i(t),\end{aligned}$$

with $E_i(t) = O(d_{\min}^N)$. Hence if we construct a divergence-free vector field E^N such that

$$E^N(t, x_i(t)) = E_i(t),$$

we can define V as

$$V(t,x) = \kappa g + \mathcal{K}^N \varrho^N(t,x) + E^N(t,x).$$

Construction of E^N We fix χ a truncation function such that $\chi = 1$ on $B(0,1)$ and $\chi = 0$ on ${}^cB(0,2)$. For all i we set

$$\mathcal{E}_i(t,x) := \operatorname{curl}\left(\chi\left(\frac{x - x_i(t)}{R}\right) E_i(t) \times \frac{x - x_i(t)}{2}\right).$$

By construction, $\mathcal{E}_i$ is a divergence-free compactly supported vector field satisfying

$$\mathcal{E}_i(t, x_i(t)) = E_i(t).$$

Furthermore, $\mathcal{E}_i$ is supported in $B(x_i(t), 2R)$. Thanks to Theorem 1.1.1, this entails that $\operatorname{supp}(\mathcal{E}_i) \cap \operatorname{supp}(\mathcal{E}_j) = \varnothing$ for $i \neq j$. We set then

$$E^N(t,x) := \sum_i \mathcal{E}_i(t,x)\,.$$

By construction, this velocity field is divergence-free and is regular $E^N \in \mathcal{C}([0,T] \times \mathbb{R}^3)$, $E^N(t,\cdot) \in \mathcal{C}^1(\mathbb{R}^3)$ for all $0 \leqslant t \leqslant T$. Moreover is satisfies for all $t \in [0,T]$

$$E^N(t, x_i(t)) = E_i(t) \text{ for all } 1 \leqslant i \leqslant N,$$

$$\|E^N(t,\cdot)\|_\infty \leqslant C_\chi \max_i |E_i(t)| \lesssim d_{\min}^N. \tag{1.75}$$

The only statement that needs further explanation is (1.75). For all $x \in B(x_i(t), R_i)$ we have

$$\mathcal{E}_i(t,x) = E_i(t),$$

and for all $x \in B(x_i, 2R) \backslash B(x_i, R)$, direct computations yields

$$\begin{aligned}\mathcal{E}_i(t,x) = \frac{1}{2}\Big[2\chi\left(\frac{x - x_i(t)}{R}\right)\mathbb{I}_3 - \frac{1}{R}\nabla\chi\left(\frac{x - x_i(t)}{R}\right) \otimes (x - x_i(t)) \\ + \frac{1}{R}(x - x_i(t)) \cdot \nabla\chi\left(\frac{x - x_i(t)}{R}\right)\mathbb{I}_3\Big]E_i(t).\end{aligned}$$

Therefore

$$|\mathcal{E}_i(t,x)| \leqslant C\left[\|\chi\|_\infty + \|\nabla\chi\|_\infty\right]|E_i(t)|.$$

We can now state the following proposition.

Proposition 1.5.4. *For arbitrary N we have that $\kappa g + \mathcal{K}^N \varrho^N + E^N \in \mathcal{C}([0,T] \times \mathbb{R}^3)$ and $\nabla \mathcal{K}^N \varrho^N + \nabla E^N \in \mathcal{C}([0,T] \times \mathbb{R}^3)$. Moreover, the velocity field satisfies*

$$|\kappa g + \mathcal{K}^N \varrho^N(t,x) + E^N(t,x)| \leqslant C \,,\ \forall (t,x) \in [0,T] \times \mathbb{R}^3, \tag{1.76}$$

for some positive constant C independent of N.

Proof. As the kernel is regularized, the two first properties are satisfied by construction. For all $(t,x) \in [0,T] \times \mathbb{R}^3$ we have

$$\begin{aligned} \mathcal{K}^N \varrho^N(x) &= \frac{6\pi r_0 \kappa}{N} \sum_i \psi^N(x) \Phi(x - x_i(t)) \,, \\ &= \frac{6\pi r_0 \kappa}{N} \sum_i \psi^N(x) 1_{\{|x_i(t) - x| > \frac{d^N_{\min}(0)}{2}\}} \Phi(x - x_i(t)). \end{aligned}$$

We set $\mathcal{I}(t,x) = \{1 \leqslant i \leqslant N \,,\ |x_i(t) - x| > \frac{d^N_{\min}(0)}{2}\}$. Reproducing the arguments of Lemma 1.A.1 for $k = 1$ together with assumptions (1.6), (1.7) and Theorem 1.1.1 yields

$$\begin{aligned} \left|\mathcal{K}^N \varrho^N(x)\right| &\lesssim \frac{1}{N} \sum_{\mathcal{I}(t,x)} \frac{1}{|x - x_i(t)|} \,, \\ &\lesssim \bar{M} \frac{|\lambda^N|^3}{d^N_{\min}(0)} + \bar{M}^{1/3} \,, \\ &\lesssim \bar{M} \frac{|\lambda^N|^3}{|d^N_{\min}(0)|^2} d^N_{\min}(0) + \bar{M}^{1/3} \,, \\ &\lesssim 1 \,. \end{aligned}$$

Furthermore, the velocity field E^N is uniformly bounded according to (1.75). □

This allows us to state the following result.

Theorem 1.5.5. *ϱ^N is a weak solution of*

$$\left\{ \begin{array}{rcl} \frac{\partial \varrho^N}{\partial t} + \operatorname{div}((\kappa g + \mathcal{K}^N \varrho^N + E^N) \varrho^N) &=& 0 \,, \\ \varrho^N(0, \cdot) &=& \varrho^N_0 \,, \end{array} \right. \tag{1.77}$$

on $[0,T] \times \mathbb{R}^3$. Moreover, the characteristic flow associated to the velocity $\kappa g + \mathcal{K}^N \varrho^N + E^N$ is of class $\mathcal{C}^1$ for all $N \geqslant 1$

$$\left\{ \begin{array}{rcll} \partial_s X^N(s,t,x) &=& \kappa g + \mathcal{K}^N \varrho^N(s, X^N(s,t,x)) + E^N(s, X^N(s,t,x)) & \forall\, s,t \in [0,T], \\ X^N(t,t,x) &=& x, & \forall\, t \in [0,T], \end{array} \right. \tag{1.78}$$

and the following classical formula holds true:

$$\varrho^N(t, \cdot) = X^N(t, 0, \cdot) \# \varrho^N_0 \ \ \forall\, t \in [0,T]. \tag{1.79}$$

Proof. As $V(t,x) := \kappa g + \mathcal{K}^N \varrho^N(t,x) + E^N(t,x) \in \mathcal{C}^1([0,T]\times\mathbb{R}^3)$ is defined such that $V(t,x_i(t)) = V_i\,,\ \forall\, 1 \leqslant i \neq N$ this ensures that for all test function $\phi \in \mathcal{C}_c^\infty([0,T]\times\mathbb{R}^3)$:

$$\int_0^T \int_{\mathbb{R}^3} \left(\partial_t \phi(t,x) + \nabla\phi(t,x)\cdot\left[\kappa g + \mathcal{K}^N \varrho^N(t,x) + E^N(t,x)\right]\right) \varrho^N(dx,t)dt = 0,$$

thus, ϱ^N is a weak solution for (1.77).
According to Proposition 1.5.4, the ode governing the characteristic flow satisfies the assumptions of the Cauchy-Lipschitz theorem. Therefore, the ode admits a unique maximal solution $X^N \in \mathcal{C}^1([0,T]\times[0,T]\times\mathbb{R}^3)$ thanks to formula (1.76). Equality (1.79) holds true thanks to the classical theory for transport equations. $\square$

1.6 Control of the Wasserstein distance

At this point, we proved that the particles interact two by two with an interaction force given by the Oseen-tensor with an additional error term.

$$\left\{\begin{array}{rcl} \dot{x}_i(t) &=& V_i(t), \\ V_i(t) &=& \kappa g + 6\pi R \sum\limits_{i\neq j} \Phi(x_i(t)-x_j(t)) + E^N(t,x_i(t)). \end{array}\right. \tag{1.80}$$

We want to estimate the Wasserstein distance $W_1(\varrho^N(t,\cdot),\varrho(t,\cdot))$ for all time $0 \leqslant t \leqslant T$. To this end, we follow the ideas of [33] and [34] and show that the additional error term E^N can be controled. As in [34], we introduce an intermediate density $\bar{\varrho}^N$.

1.6.1 Step 1. Estimate of the distance between ϱ and $\bar{\varrho}^N$

We define $\bar{\varrho}_0^N$ as the regularized density of ϱ_0^N:

$$\bar{\varrho}_0^N := \varrho_0^N * \chi_{\lambda^N}$$

where $\chi_{\lambda^N}(x) := \frac{1}{|\lambda^N|^3}\chi\left(\frac{x}{\lambda^N}\right)$ a mollifier compactly supported. Note that the support of χ is not important, we consider for instance χ such that $\operatorname{supp}\chi = B(0,1)$. We emphasize that the regularized density is uniformly bounded

$$\begin{aligned} \bar{\varrho}_0^N(x) &= \int \frac{1}{|\lambda^N|^3}\chi\left(\frac{x-y}{\lambda^N}\right)\varrho_0^N(dy)\,, \\ &= \frac{1}{N|\lambda^N|^3}\sum_{i=1}^N \chi\left(\frac{x-x_i(0)}{\lambda^N}\right)\,, \\ &\leqslant \frac{1}{N|\lambda^N|^3}\|\chi\|_\infty \sup_x \#\{i\in\{1,\dots,N\}\,,\, x_i(0)\in B(x,\lambda^N)\}\,, \\ &\leqslant \|\chi\|_\infty \bar{M}, \end{aligned} \tag{1.81}$$

according to assumption (1.5). Moreover, we have

$$\begin{aligned}\int_{\mathbb{R}^3} \bar{\varrho}_0^N(x)dx &= \frac{1}{N|\lambda^N|^3}\sum_{i=1}^{N}\int_{B(x_i(0),\lambda^N)} \chi\left(\frac{x-x_i(0)}{\lambda^N}\right) dx\,,\\ &= 1. \end{aligned} \tag{1.82}$$

Now, we define $\bar{\varrho}^N$ as the unique solution to equation (1.71) associated to the initial data $\bar{\varrho}_0^N$. The stability Theorem 1.5.3 allows us to compare ϱ and $\bar{\varrho}^N$:

$$W_1(\varrho(t,\cdot), \bar{\varrho}^N(t,\cdot)) \leqslant W_1(\varrho_0, \bar{\varrho}_0^N)e^{Ct},$$

where $C = C(\|\chi\|_\infty, \bar{M}, \|\varrho_0\|_\infty)$. We split the distance $W_1(\varrho_0, \bar{\varrho}_0^N)$ as follows

$$W_1(\varrho_0, \bar{\varrho}_0^N) \leqslant W_1(\varrho_0, \varrho_0^N) + W_1(\varrho_0^N, \bar{\varrho}_0^N),$$

and use the fact that

$$W_1(\varrho_0^N, \bar{\varrho}_0^N) \leqslant W_\infty(\varrho_0^N, \bar{\varrho}_0^N),$$

together with [34, Proposition 1]

$$W_\infty(\varrho_0^N, \bar{\varrho}_0^N) \leqslant C\lambda^N, \tag{1.83}$$

to get

$$W_1(\varrho(t,\cdot), \bar{\varrho}^N(t,\cdot)) \lesssim \left(\lambda^N + W_1(\varrho_0, \varrho_0^N)\right) e^{Ct}. \tag{1.84}$$

1.6.2 Step 2. Estimate of the distance between $\bar{\varrho}^N$ to ϱ^N

It remains to estimate $W_1(\varrho^N(t,\cdot), \bar{\varrho}^N(t,\cdot))$. We have the following result.

Lemma 1.6.1. *For N large enough, there exists a positive constant C such that for all $t \in [0,T]$*

$$W_1(\varrho^N(t,\cdot), \bar{\varrho}^N(t,\cdot)) \lesssim \left(\lambda^N + t d_{\min}^N\right) e^{Ct}.$$

Theorem 1.1.2 is a consequence of estimate (1.84) and Lemma 1.6.1. The rest of this Section is devoted to proving the above lemma.

Proof of Lemma 1.6.1. According to Theorems 1.5.2 and 1.5.5 we have the explicit formulas for all s, $t \in [0,T]$

$$\begin{aligned}\bar{\varrho}^N(t,\cdot) &= X(t,s,\cdot)\#\bar{\varrho}_s^N,\\ \varrho^N(t,\cdot) &= X^N(t,s,\cdot)\#\varrho_s^N.\end{aligned}$$

At $t = 0$ we have the existence of an optimal transport map T_0 from $\bar{\varrho}_0^N$ to ϱ_0^N thanks to Theorem 1.5.1

$$\varrho_0^N = T_0\#\bar{\varrho}_0^N,$$

satisfying

$$W_\infty(\bar{\varrho}_0^N, \varrho_0^N) = \bar{\varrho}_0^N - \text{esssup}\,|T_0(x) - x|.$$

We construct then a transport map T_t from $\bar{\varrho}^N$ to ϱ^N at all time $t \in [0, T]$ by following T_0 along the two flows X and X^N

$$T_t = X^N(t, 0, \cdot) \circ T_0 \circ X(0, t, \cdot).$$

One can remark that for all $0 \leqslant s \leqslant t$:

$$\begin{aligned} T_t &= X^N(t, s, \cdot) \circ T_s \circ X(s, t, \cdot) \\ \varrho^N(t, \cdot) &= T_t \# \bar{\varrho}^N(t, \cdot). \end{aligned}$$

As in [34] we set then

$$f^N(t) := \sup_{s \leqslant t} \bar{\varrho}^N(t, \cdot) - \text{esssup}\,|T_s(x) - x|,$$

so that

$$W_\infty(\varrho^N(t, \cdot), \bar{\varrho}^N(t, \cdot)) \leqslant f^N(t),$$

and thanks to (1.83) we have

$$f^N(0) = W_\infty(\bar{\varrho}_0^N, \varrho_0^N) \leqslant C\lambda^N. \tag{1.85}$$

We reproduce the same steps as in [34] and introduce the following notation for a generic "particle" of the continuous system with position x_t at time t such that

$$x_s = X(s, t, x_t),$$

we fix in what follows $0 \leqslant t_2 \leqslant t_1$ and recall the following formula

$$T_{t_1} \circ X(t_1, t_2, \cdot) = X^N(t_1, t_2, \cdot) \circ T_{t_2}.$$

We aim now to estimate $|T_{t_1}(x_{t_1}) - x_{t_1}|$ for all test particle x_{t_1}

$$\begin{aligned} T_{t_1}(x_{t_1}) - x_{t_1} &= X^N(t_1, t_2, T_{t_2}(x_{t_2})) - X(t_1, t_2, x_{t_2}), \\ &= T_{t_2}(x_{t_2}) - x_{t_2} + \int_{t_2}^{t_1} \dot{X}^N(s, t_2, T_{t_2}(x_{t_2})) - \dot{X}(s, t_2, x_{t_2}) ds, \\ &= T_{t_2}(x_{t_2}) - x_{t_2} + \int_{t_2}^{t_1} \big([\mathcal{K}^N \varrho^N + E^N](s, X^N(s, t_2, T_{t_2}(x_{t_2}))), \\ &- \mathcal{K}\bar{\varrho}^N(s, x_s))\big) ds, \\ &= T_{t_2}(x_{t_2}) - x_{t_2} + \int_{t_2}^{t_1} \big([\mathcal{K}^N \varrho^N + E^N](s, T_s(x_s)) - \mathcal{K}\bar{\varrho}^N(s, x_s))\big) ds, \\ &= T_{t_2}(x_{t_2}) - x_{t_2} + \int_{t_2}^{t_1} E^N(s, T_s(x_s)) ds, \\ &+ \int_{t_2}^{t_1} \int_{\mathbb{R}^3} 6\pi r_0 \kappa \left(\psi^N \Phi(T_s(x_s) - T_s(y)) - \Phi(x_s - y)\right) g\bar{\varrho}^N(s, dy) ds, \end{aligned}$$

where we used the fact that $\varrho_s^N = T_s \# \bar\varrho_s^N$ to get

$$\begin{aligned}\mathcal{K}^N \varrho^N(s, T_s(x_s)) &= 6\pi r_0 \kappa \int_{\mathbb{R}^3} \psi^N \Phi(T_s(x_s) - y) g \varrho^N(s, dy)\,,\\ &= 6\pi r_0 \kappa \int_{\mathbb{R}^3} \psi^N \Phi(T_s(x_s) - T_s(y)) g \bar\varrho^N(s, dy).\end{aligned}$$

We set then $t_1 = t$ and $t_2 = t_1 - \tau = t - \tau$, $\tau > 0$. We obtain for almost every x_t

$$\begin{aligned}|T_t(x_t) - x_t| \leqslant& |T_{t-\tau}(x_{t-\tau}) - x_{t-\tau}| + \tau \|E^N(t)\|_\infty,\\ &+ 6\pi r_0 \kappa |g| \int_{t-\tau}^t \int_{\mathbb{R}^3} \left|\psi^N \Phi(T_s(x_s) - T_s(y)) - \Phi(x_s - y)\right| \bar\varrho^N(s, dy) ds,\\ &\leqslant f^N(t-\tau) + \tau \|E^N(t)\|_\infty\,,\\ &+ C \int_{t-\tau}^t \int_{\mathbb{R}^3} \left|\psi^N \Phi(T_s(x_s) - T_s(y_s)) - \Phi(x_s - y_s)\right| \bar\varrho^N(t, dy_t) ds,\end{aligned}$$

here we used Remark 1.5.2 with $y_s = X(s, t, y_t)$. In addition we defined

$$\|E^N(t)\|_\infty := \sup_{0 \leqslant s \leqslant t} \|E^N(s, \cdot)\|_\infty.$$

This being true for almost every x_t we obtain

$$\begin{aligned}f^N(t) \leqslant& f^N(t-\tau) + \tau \|E^N(t)\|_\infty\\ &+ C \operatorname*{esssup}_{x_t} \int_{t-\tau}^t \int_{\mathbb{R}^3} \left|\psi^N \Phi(T_s(x_s) - T_s(y_s)) - \Phi(x_s - y_s)\right| \bar\varrho^N(t, dy_t) ds. \quad (1.86)\end{aligned}$$

Hence, it remains to control the last quantity. We split the integral on $\mathbb{R}^3$ into two terms: the first one denoted J_1 is the integral over the subset I and the second one denoted J_2 the integral over $\mathbb{R}^3 \backslash I$ where

$$I = \{y_t \,:\, |x_t - y_t| \geqslant 4 f^N(t) e^{\tau L}\},$$

where L will be defined later.

Step 1: Estimate of J_1

For all $t - \tau \leqslant s \leqslant t$, we have

$$\begin{aligned}|x_s - y_s| \geqslant& |x_t - y_t| - \int_s^t |\dot X(t', t, x_t) - \dot X(t', t, y_t)| dt',\\ &\geqslant |x_t - y_t| - \int_s^t |\mathcal{K}\bar\varrho^N(t', X(t', t, x_t)) - \mathcal{K}\bar\varrho^N(t', X(t', t, y_t))| dt',\\ &\geqslant |x_t - y_t| - \mathrm{Lip}\ (\mathcal{K}\bar\varrho^N) \int_s^t |X(t', t, x_t) - X(t', t, y_t)| dt'.\end{aligned}$$

Using Remarks 1.5.2 and 1.5.3, formula (1.73) and the uniform bounds (1.81), (1.82), the Lipschitz constant of $\mathcal{K}\bar{\varrho}^N$ is uniformly bounded. This allows us to define the constant L as

$$\text{Lip }(\mathcal{K}\bar{\varrho}^N) \leqslant C\|\bar{\varrho}_0^N\|_{L^\infty(L^\infty\cap L^1)} \leqslant L\,.$$

Applying Gronwall's inequality yields for all $0 \leqslant t-\tau \leqslant s \leqslant t$

$$|x_s - y_s| \geqslant |x_t - y_t|e^{-L(t-s)}.$$

We can make precise now the constant $L := \text{Lip }(\mathcal{K}\bar{\varrho}^N)$ which is uniformly bounded with respect to N and $t \in [0,T]$.
We have for all $0 \leqslant t-\tau \leqslant s \leqslant t$ and τ small enough

$$|x_s - y_s| \geqslant |x_t - y_t|e^{-L(t-s)} \geqslant |x_t - y_t|e^{-L\tau} \geqslant \frac{1}{2}|x_t - y_t|. \tag{1.87}$$

Analogously, for almost all x_s and y_s

$$\begin{aligned}|T_s(x_s) - T_s(y_s)| \geqslant |x_s - y_s| - |T_s(x_s) - x_s| - |T_s(y_s) - y_s|\,, \\ \geqslant |x_s - y_s| - 2f^N(s) \geqslant |x_s - y_s| - 2f^N(t),\end{aligned}$$

where we used the fact that $f^N(t) \geqslant f^N(s)$. According to the definition of $I = \{y_t : |x_t - y_t| \geqslant 4f^N(t)e^{\tau L}\}$, this yields for τ small enough

$$|T_s(x_s) - T_s(y_s)| \geqslant \frac{1}{4}|x_t - y_t|. \tag{1.88}$$

Moreover, recall that $T_s(x_s)$ and $T_s(y_s)$ are in the support of $\varrho^N(s,\cdot)$ *i.e.* there exists i, j such that $T_s(x_s) = x_i(s)$ and $T_s(y_s) = x_j(s)$. In addition, estimate (1.88) and the definition of I ensures that $i \neq j$. We have then

$$\psi^N\Phi(T_s(x_s) - T_s(y_s)) = \Phi(T_s(x_s) - T_s(y_s)). \tag{1.89}$$

Finally, using estimates (1.87), (1.88), formula (1.89) and the Lipschitz-like estimate (1.27) for Φ we obtain

$$\begin{aligned}J_1 &= \int_I \int_{t-\tau}^t |\Phi(T_s(x_s) - T_s(y_s)) - \Phi(x_s - y_s)|\, ds\bar{\varrho}^N(t, dy_t),\\ &\leqslant C\int_I \int_{t-\tau}^t \frac{|x_s - T_s(x)| + |y_s - T_s(y)|}{\min(|x_s - y_s|^2\,,\, |T_s(x) - T_s(y)|^2)} ds\bar{\varrho}^N(t, dy_t),\\ &\leqslant Cf^N(t)\tau \int_I \frac{1}{|x_t - y_t|^2}\bar{\varrho}^N(t, dy_t),\\ &\leqslant C\tau f^N(t)\|\bar{\varrho}^N(t)\|_{L^\infty\cap L^1}\,,\\ &\leqslant C\tau f^N(t)\|\bar{\varrho}_0^N\|_{L^\infty\cap L^1}\,,\\ &\leqslant C\tau f^N(t)\,,\end{aligned}$$

where we used Remark 1.5.2, formula (1.73) and the uniform bounds (1.81), (1.82).

Step 2: Estimate of J_2
We focus now on

$$J_2 := \operatorname*{esssup}_{x_t} \int_{t-\tau}^{t} \int_{^cI} \left|\psi^N \Phi(T_s(x_s) - T_s(y_s)) - \Phi(x_s - y_s)\right| \bar{\varrho}^N(t, dy_t) ds.$$

Again $T_s(x_s)$ and $T_s(y_s)$ are in the support of $\varrho^N(s,\cdot)$ *i.e.* there exists i , j such that $T_s(x_s) = x_i(s)$ and $T_s(y_s) = x_j(s)$. Moreover if $i = j$ then $\psi^N\Phi(T_s(x_s) - T_s(y_s)) = 0$. Hence in all cases we have

$$\begin{aligned}\left|\Phi(x_s - y_s) - \psi^N\Phi(T_s(x_s) - T_s(y_s))\right| &\leqslant |\Phi(x_s - y_s)| + |\psi^N\Phi(T_s(x_s) - T_s(y_s))|\,,\\ &\leqslant C\left(\frac{1}{|x_s - y_s|} + \frac{1}{d^N_{\min}(s)}\right),\end{aligned}$$

applying the change of variable $y_t = X(t, s, y_s)$ we get

$$\begin{aligned}\int_{^cI}\int_{t-\tau}^{t} \frac{1}{|x_s - y_s|} ds\bar{\varrho}^N(t, dy_t) &\leqslant \|\bar{\varrho}^N\|_\infty \int_{t-\tau}^{t}\int_{^cI} \frac{1}{|x_s - y_s|} dy_t ds,\\ &= C\int_{t-\tau}^{t}\int_{X(t,s,^cI)} \frac{1}{|x_s - y_s|} dy_s ds.\end{aligned}$$

Denote $K = X(t, s, {}^cI)$, as the flow X preserves the Lebesgue measure we have $|K| = |{}^cI|$. For all $s \in [t - \tau, t]$ and $a > 0$ a direct computation yields

$$\begin{aligned}\int_K \frac{1}{|x_s - y_s|} dy_s &= \left(\int_{K\cap B(x_s,a)} + \int_{K\cap {}^cB(x,a)}\right) \frac{1}{|x_s - y_s|} dy_s,\\ &\leqslant Ca^2 + \frac{1}{a}|K|,\end{aligned}$$

we choose then $a^3 = |K| = |{}^cI| \leqslant C\left|f^N(t)\right|^3 e^{3L\tau}$ to get

$$\int_{^cI}\int_{t-\tau}^{t} \frac{1}{|x_s - y_s|} ds\bar{\varrho}^N(t, dy_t) \leqslant C\tau\left|f^N(t)\right|^2 e^{2L\tau}. \tag{1.90}$$

For the remaining term we apply Theorem 1.1.1 and get for all $t - \tau \leqslant s \leqslant t$

$$\begin{aligned}\int_{^cI}\int_{t-\tau}^{t} \frac{1}{d^N_{\min}(s)} ds\bar{\varrho}^N(t, dy_t) &\leqslant \frac{2}{d^N_{\min}(0)} \int_{^cI}\int_{t-\tau}^{t} ds\bar{\varrho}^N(t, dy_t),\\ &\leqslant C\tau\frac{2e^{3\tau L}}{d^N_{\min}(0)} \left|f^N(t)\right|^3.\end{aligned}$$

Conclusion
Gathering these bounds, there exists a constant $K > 0$ independent of N such that for τ small enough and $0 < t \leqslant T$

$$f^N(t) \leqslant f^N(t - \tau) + \tau\|E^N(t)\|_\infty + K\tau f^N(t)\left[1 + f^N(t) + \frac{\left|f^N(t)\right|^2}{d^N_{\min}(0)}\right].$$

We can now apply a discrete Gronwall argument: Note that at time $t = 0$, assumption (1.11) and formula (1.85) ensures the existence of a positive constant $C_1 > 1$ such that

$$1 + f^N(0) + \frac{\left|f^N(0)\right|^2}{d^N_{\min}(0)} \leqslant \frac{C_1}{K},$$

hence, we define $T^* \leqslant T$ as the maximal time for which

$$1 + f^N(t) + \frac{\left|f^N(t)\right|^2}{d^N_{\min}(0)} \leqslant \frac{C_1}{K} \quad \forall t \in [0, T^*[. \tag{1.91}$$

Note that T^* a priori depends on N, the purpose is to show that this is not the case. We obtain for all $t \in [0, T^*[$

$$f^N(t) \leqslant f^N(t-\tau) + C_1 \tau f^N(t) + \tau \|E^N\|_\infty.$$

If τ is small enough we can write

$$f^N(t) \leqslant (1 - C_1\tau)^{-1} f^N(t-\tau) + \frac{\tau}{1 - C_1\tau}\|E^N\|_\infty,$$

iterating the formula we obtain for $M \in \mathbb{N}^*$

$$\begin{aligned} f^N(t) &\leqslant (1 - C_1\tau)^{-M} f^N(t - M\tau) + \tau \sum_{k=1}^{M} \frac{1}{(1 - C_1\tau)^k}\|E^N\|_\infty, \\ &\leqslant (1 - C_1\tau)^{-M} f^N(t - M\tau) + \tau \sum_{k=1}^{M} e^{2C_1\tau k}\|E^N\|_\infty. \end{aligned}$$

Thanks to the bound $\frac{1}{1-C_1\tau} \leqslant e^{2C_1\tau}$ for τ small enough. We set then $t - M\tau = 0$ to get

$$f^N(t) \leqslant (1 - C_1\frac{t}{M})^{-M} f^N(0) + \frac{t}{M}\sum_{k=1}^{M} e^{2C_1\frac{t}{M}k}\|E^N\|_\infty.$$

As $e^{2C_1\frac{t}{M}k} \leqslant e^{2C_1 t}$ for all $1 \leqslant k \leqslant M$ the second term yields

$$\frac{t}{M}\sum_{k=1}^{M} e^{2C_1\frac{t}{M}k}\|E^N\| \leqslant t e^{2C_1 t}\|E^N\|_\infty,$$

and for M sufficiently large

$$(1 - C_1\frac{t}{M})^{-M} \leqslant e^{2C_1 t}.$$

Finally for all $t \in [0, T^*[$

$$f^N(t) \leqslant f^N(0) e^{2C_1 t} + t e^{2C_1 t}\|E^N\|_\infty.$$

In particular we have for all $t \in [0, T^*[$

$$f^N(t) + \frac{\left|f^N(t)\right|^2}{d^N_{\min}(0)} \leqslant f^N(0)e^{2C_1 t} + \|E^N\|_\infty T e^{2C_1 t} + 2\frac{\left|f^N(0)\right|^2 e^{4C_1 t} + \|E^N\|_\infty^2 T^2 e^{4C_1 t}}{d^N_{\min}(0)},$$
$$\leqslant e^{4C_1 T}(2 + T + 2T^2)\left(f^N(0) + \|E^N\|_\infty + \frac{\left|f^N(0)\right|^2 + \|E^N\|_\infty^2}{d^N_{\min}(0)}\right).$$

Since we have $f^N(0) = O\left(\lambda^N\right)$ and thanks to (1.75)

$$\frac{\left|f^N(0)\right|^2 + \|E^N\|_\infty^2}{d^N_{\min}(0)} \lesssim \frac{|\lambda^N|^2}{d^N_{\min}(0)} + d^N_{\min},$$

which vanishes according to assumption (1.7) and (1.11). This shows that we can take N large enough and depending on T, K and C_1 such that $T^* \to T$ and formula (1.91) holds true up to time T. Hence, for N large enough we have for all $t \in [0, T]$

$$f^N(t) \leqslant f^N(0)e^{2C_1 t} + t e^{2C_1 t}\|E^N\|_\infty.$$

Using (1.85) and the fact that $W_1(\varrho^N, \bar{\varrho}^N) \leqslant W_\infty(\varrho^N, \bar{\varrho}^N) \leqslant f^N$, this implies Lemma 1.6.1. □

Appendix

1.A Technical lemmas

We state here an important lemma which is the extension of [41, Lemma 2.1] to the new assumptions on the dilution regime introduced in [36]. We introduce $\tilde{\varrho}^N$ an approximation of ϱ^N defined as

$$\tilde{\varrho}^N(t,x) := \frac{1}{N}\sum_{i=1}^{N}\frac{1_{B_\infty(x_i,\lambda^N/3)}}{|B_\infty(x_i,\lambda^N/3)|}\,. \tag{1.92}$$

$\tilde{\varrho}^N$ is L^∞ and using (1.5), one can check that

$$\|\tilde{\varrho}^N\|_{L^\infty} \lesssim \frac{1}{N|\lambda^N|^3}\sup_{x\in\mathbb{R}^3}\#\left\{i\in\{1,\cdots,N\} \text{ such that } x_i\in B_\infty(x,\lambda^N/3)\right\} \lesssim \frac{M^N}{N|\lambda^N|^3} \lesssim \bar{M}\,. \tag{1.93}$$

Moreover, $\tilde{\varrho}^N$ is L^1 and we have $\|\tilde{\varrho}^N\|_{L^1} = 1$ by construction.

Lemma 1.A.1. *For all $k \in [0,2]$, under assumptions* (1.5), (1.7)*, if N is large enough, there exists a positive constant $C > 0$ such that for all fixed $1 \leqslant i \leqslant N$:*

$$\frac{1}{N}\sum_{j\neq i}\frac{1}{d_{ij}^k} \leqslant C\bar{M}\frac{|\lambda^N|^3}{|d_{\min}^N|^k} + \bar{M}^{k/3}. \tag{1.94}$$

Moreover, if $k=3$ we have

$$\frac{1}{N}\sum_{j\neq i}\frac{1}{d_{ij}^3} \leqslant C\bar{M}\left(\frac{|\lambda^N|^3}{|d_{\min}^N|^3} + |\log(\bar{M}^{1/3}\lambda^N)| + 1\right).$$

Proof. We fix $i=1$ and the same holds true for all $1 \leqslant i \leqslant N$. We use the following shortcut

$$\mathcal{I}_1 := \{j\in\{1,\cdots,N\} \text{ such that } |x_1 - x_j|_\infty \leqslant \lambda^N\}.$$

The sum can be written as follows:

$$\begin{aligned}
\frac{1}{N}\sum_{j\neq 1}\frac{1}{d_{1j}^k} &= \frac{1}{N}\sum_{\substack{j\in\mathcal{I}_1\\ j\neq 1}}\frac{1}{d_{1j}^k} + \frac{1}{N}\sum_{j\notin\mathcal{I}_1}\frac{1}{d_{1j}^k}\,,\\
&\leqslant \frac{1}{N}\frac{M^N}{|d_{\min}^N|^k} + \frac{1}{N}\sum_{j\notin\mathcal{I}_1}\frac{1}{d_{1j}^k}\,,\\
&\leqslant \bar{M}\frac{|\lambda^N|^3}{|d_{\min}^N|^k} + \frac{1}{N}\sum_{j\notin\mathcal{I}_1}\frac{1}{d_{1j}^k}\,.
\end{aligned}$$

For the second term in the right hand side, note that, for all $y\in B_\infty(x_j,\lambda^N/3)$, $j\notin\mathcal{I}_1$ we have

$$|x_1-y|_\infty \geqslant |x_1-x_j|_\infty - |x_j-y|_\infty \geqslant 2/3\lambda^N\,,$$

this yields

$$|x_1-x_j|_\infty \geqslant |x_1-y|_\infty - \lambda^N/3 \geqslant |x_1-y|_\infty/2\,.$$

Hence, we have for all constant $L>2/3\lambda^N$

$$\begin{aligned}
\frac{1}{N}\sum_{j\notin\mathcal{I}_1}\frac{1}{d_{1j}^k} &\leqslant \frac{2^k}{N}\sum_{j\notin\mathcal{I}_1}\int_{B_\infty(x_j,\lambda^N/3)}\frac{1}{|B_\infty(x_j,\lambda^N/3)|}\frac{1}{|x_1-y|^k}dy\,,\\
&\lesssim \int_{^cB(x_1,2/3\lambda^N)}\frac{1}{|x_1-y|^k}\tilde{\varrho}^N(t,dy)\,,\\
&\leqslant \|\tilde{\varrho}^N\|_{L^\infty}\int_{2/3|\lambda^N|}^{L} r^{2-k}dr + \int_{^cB(x_1,L)}\frac{1}{|x_1-y|^k}\tilde{\varrho}^N(t,dy)\,,\\
&\leqslant \|\tilde{\varrho}^N\|_{L^\infty}\frac{L^{3-k}-\big(2/3|\lambda^N|\big)^{3-k}}{3-k} + \frac{\|\tilde{\varrho}^N\|_{L^1}}{L^k}\,,\\
&\lesssim \bar{M}\frac{L^{3-k}}{3-k} + \frac{1}{L^k}\,.
\end{aligned}$$

One can show that the optimal constant $L>2/3\lambda^N$ is $L=\frac{1}{\bar{M}^{1/3}}$. Since $\lim\limits_{N\to\infty}\lambda^N=0$, this choice of L is possible for N large enough such that $\lambda^N<\frac{3}{2\bar{M}^{1/3}}$. Hence, we obtain

$$\frac{1}{N}\sum_{j\notin\mathcal{I}_1}\frac{1}{d_{1j}^k} \lesssim \frac{4-k}{3-k}\bar{M}^{k/3}.$$

If $k=3$, we integrate the term r^{-1} keeping the same value for L as before

$$\begin{aligned}
\frac{1}{N}\sum_{j\notin\mathcal{I}_1}\frac{1}{d_{1j}^3} &\leqslant \|\tilde{\varrho}^N\|_{L^\infty}\int_{2/3|\lambda^N|}^{\frac{1}{\bar{M}^{1/3}}}\frac{dr}{r} + \int_{^cB(x_1,\frac{1}{\bar{M}^{1/3}})}\frac{1}{|x_1-y|^3}\tilde{\varrho}^N(t,dy)\,,\\
&\leqslant \bar{M}\left(\log\left(\frac{1}{\bar{M}^{1/3}|\lambda^N|}\right) + \log(3/2)\right) + \bar{M}\,,\\
&\leqslant 2\bar{M}(|\log(\bar{M}^{1/3}\lambda^N)|+1)\,,
\end{aligned}$$

for N large enough to ensure $\frac{3}{2}\leqslant\frac{1}{\bar{M}^{1/3}|\lambda^N|}$. $\square$

The following results are used for the control of the particle concentration M^N:

$$M^N(t) := \sup_{x\in\mathbb{R}^3}\Big\{\#\big\{i\in\{1,\cdots,N\} \text{ such that } x_i(t)\in\overline{B_\infty(x,\lambda^N)}\big\}\Big\}.$$

We recall the definition of L^N introduced in (1.69):

$$L^N(t) := \max_i \# \left\{j\in\{1,\dots,N\} \text{ such that } |x_i(t)-x_j(t)|_\infty \leqslant \lambda^N\right\}.$$

The following lemma shows that the two definitions are equivalent.

Lemma 1.A.2. *We have*

$$L^N(t)\leqslant M^N(t)\leqslant 8L^N(t).$$

Proof. The first inequality is trivial. To prove the second one note that we have:

$$\sup_{x\in\mathbb{R}^3}\Big\{\#\big\{i\in\{1,\cdots,N\} \text{ such that } x_i\in\overline{B_\infty(x,\lambda^N)}\big\}\Big\}\leqslant \\ 8\sup_{x\in\mathbb{R}^3}\Big\{\#\big\{i\in\{1,\cdots,N\} \text{ such that } x_i\in\overline{B_\infty(x,\lambda^N/2)}\big\}\Big\}.$$

Indeed, for all $x\in\mathbb{R}^3$ there exists $\bar{x}_k$, $k=1,\cdots,8$ such that

$$\overline{B_\infty\left(x,\lambda^N\right)}\subset\bigcup_k^8\overline{B_\infty\left(\bar{x}_k,\frac{\lambda^N}{2}\right)},$$

this yields

$$\big\{i\in\{1,\cdots,N\} \text{ such that } x_i\in\overline{B_\infty(x,\lambda^N)}\big\} \\ \subset\bigcup_k^8\big\{i\in\{1,\cdots,N\} \text{ such that } x_i\in\overline{B_\infty(\bar{x}_k,\lambda^N/2)}\big\}.$$

Taking the supremum in the right hand side and then in the left one we obtain

$$\sup_{x\in\mathbb{R}^3}\Big\{\#\big\{i\in\{1,\cdots,N\} \text{ such that } x_i\in\overline{B_\infty(x,\lambda^N)}\big\}\Big\}\leqslant \\ 8\sup_{x\in\mathbb{R}^3}\Big\{\#\big\{i\in\{1,\cdots,N\} \text{ such that } x_i\in\overline{B_\infty(x,\lambda^N/2)}\big\}\Big\}. \quad (1.95)$$

Moreover, we remark that the supremum in the right hand side over all $x\in\mathbb{R}^3$ can be reduced to the supremum over $\bigcup_i\overline{B_\infty(x_i,\frac{\lambda^N}{2})}$. Now consider $x\in\bigcup_i\overline{B_\infty(x_i,\frac{\lambda^N}{2})}$, there exists $1\leqslant i_0\leqslant N$ such that $|x-x_{i_0}|_\infty\leqslant\frac{\lambda^N}{2}$, we have then for all $j\neq i_0$ such that $|x-x_j|_\infty\leqslant\frac{\lambda^N}{2}$:

$$|x_j-x_{i_0}|_\infty\leqslant|x_j-x|_\infty+|x-x_{i_0}|_\infty\leqslant\lambda^N,$$

which means that for all $x \in \bigcup_i \overline{B_\infty(x_i, \frac{\lambda^N}{2})}$ there exists $1 \leqslant i_0 \leqslant N$ such that

$$\Big\{1 \leqslant j \leqslant N, \text{ such that } x_j \in \overline{B_\infty(x, \lambda^N/2)}\Big\} \subset \Big\{1 \leqslant j \leqslant N, \text{ such that } |x_j - x_{i_0}|_\infty \leqslant \lambda^N\Big\}.$$

Taking the maximum over all i_0 in the right hand side, and then the supremum over all $x \in \bigcup_i \overline{B_\infty(x_i, \frac{\lambda^N}{2})}$ we obtain

$$\sup_x \Big\{\#\big\{i \in \{1, \cdots, N\} \text{ such that } x_i \in \overline{B_\infty(x, \lambda^N/2)}\big\}\Big\} \leqslant \\ \max_i \# \left\{j \in \{1, \ldots, N\} \backslash \{i\} \text{ such that } |x_i - x_j|_\infty \leqslant \lambda^N\right\}. \quad (1.96)$$

Gathering inequality (1.95) and (1.96) concludes the proof. $\square$

More generally we define for all $\beta > 0$:

$$L_\beta^N(t) := \max_i \# \left\{j \in \{1, \ldots, N\} \text{ such that } |x_i(t) - x_j(t)|_\infty \leqslant \beta\lambda^N\right\},$$

and

$$M_\beta^N(t) := \sup_{x \in \mathbb{R}^3} \Big\{\#\big\{i \in \{1, \cdots, N\} \text{ such that } x_i(t) \in \overline{B_\infty(x, \beta\lambda^N)}\big\}\Big\},$$

with the notation

$$M_1^N(t) := M^N(t) \ , \ L_1^N(t) := L^N(t).$$

The previous results yields

Corollary 1.A.3. *For all $\beta > 0$ and all $\alpha > 1$ we have*

$$L_{\alpha\beta}^N(t) \leqslant 8\lceil\alpha\rceil^3 L_\beta^N(t),$$

where $\lceil\cdot\rceil$ denotes the ceiling function.

Proof. For sake of clarity we set $\beta = 1$ and the proof remains the same for all $\beta > 0$. The idea is to show an equivalent formula for M^N and use Lemma 1.A.2. Analogously to the proof of Lemma 1.A.2, for all $x \in \mathbb{R}^3$ there exists $\bar{x}_k$, $k = 1, \cdots, \lfloor\lambda\rceil^3$ such that

$$\overline{B_\infty\left(x, \alpha\lambda^N\right)} \subset \bigcup_{k=1}^{\lceil\alpha\rceil^3} \overline{B_\infty\left(\bar{x}_k, \lambda^N\right)}.$$

This yields, with the definition of M_λ^N:

$$M_\alpha^N \leqslant \lceil\alpha\rceil^3 M^N(t).$$

Finally, we apply Lemma 1.A.2 to get

$$L_\alpha^N(t) \leqslant M_\alpha^N(t) \leqslant \lceil\alpha\rceil^3 M^N(t) \leqslant 8\lceil\alpha\rceil^3 L^N(t),$$

which completes the proof. $\square$

We finish with the following Lemma showing the relation between the sequence $(\lambda^N)_{N\in\mathbb{N}}$ and the infinite Wasserstein distance.

Lemma 1.A.4. *If there exists a constant C such that*

$$W_\infty(\varrho^N, \varrho) \leqslant C\lambda^N,$$

then Assumption (1.5) *holds true.*

Proof. We recall below Assumption (1.5)

$$\sup_N \frac{M^N}{N|\lambda^N|^3} \leqslant \bar{M}.$$

Thanks to the definition of M^N, we have

$$\frac{M^N}{N|\lambda^N|^3} = \sup_x \frac{\varrho^N(B(x,\lambda^N))}{|\lambda^N|^3}.$$

Hence, we aim to estimate $\varrho^N(B(x,\lambda^N))$ for all $x \in \mathbb{R}^3$. According to the definition of the infinite Wasserstein distance, there exists an optimal transport map T such that $\varrho^N = T\#\varrho$ and

$$W_\infty(\varrho^N, \varrho) := \varrho - \text{esssup}\,|T(x) - x|.$$

Let $x \in \mathbb{R}^3$, since ϱ^N is the pushforward of ϱ one can write

$$\varrho^N(B(x,\lambda^N)) = \varrho(T^{-1}(B(x,\lambda^N))).$$

We have for almost all $y \in T^{-1}(B(x,\lambda^N))$

$$|x-y| \leqslant |x - T(y)| + |T(y) - y| \leqslant \lambda^N + W_\infty(\varrho^N, \varrho).$$

This shows that $T^{-1}(B(x,\lambda^N)) \subset B(x, \lambda^N + W_\infty(\varrho^N,\varrho))$ μ a.e. and yields

$$\frac{M^N}{N|\lambda^N|^3} = \sup_x \frac{\varrho(T^{-1}(B(x,\lambda^N)))}{|\lambda^N|^3} \lesssim \|\varrho\|_\infty \left(1 + \frac{W_\infty(\varrho^N,\varrho)^3}{|\lambda^N|^3}\right).$$

□

Chapter 2

A model for suspension of a cluster of particle pairs

Abstract

In this paper, we consider N clusters of pairs of particles sedimenting in a viscous fluid. The particles are assumed to be rigid spheres and inertia of both particles and fluid are neglected. The distance between each two particles forming the cluster is comparable to their radii $\frac{1}{N}$ while the minimal distance between the pairs is of order $\frac{1}{N^{1/3}}$. We show that, at the mesoscopic level, the dynamics are modelled using a transport-Stokes equation describing the time evolution of the position and orientation of the clusters. We also investigate the case where the orientation of the cluster is initially correlated to its position. A local existence and uniqueness result for the limit model is provided.

2.1 Introduction

We consider the problem of N rigid particles sedimenting in a viscous fluid under gravitational force. The inertia of both fluid and particles is neglected. At the microscopic level, the fluid velocity and the pressure satisfy a Stokes equation on a perforated domain. In the analysis of the associated homgenization problem, it has been proved that the interaction between particles leads to the appearance of a Brinkman force in the fluid equation. This Brinkman force depends on the dilution of the cloud but also the geometry of the particles (see [1, 24, 36, 37]). In the dynamic case, the justification of a mesoscopic model using a coupled transport-Stokes equation has been proved in [41] where authors show that the interaction between particles is negligible in the dilute case *i.e.* when the minimal distance between particles is larger than $\frac{1}{N^{1/3}}$. In [38, 57] the justification has been extended to regimes that are not so dilute but where the minimal distance between particles is still large compared to the particles radii. The coupled equations derived are:

$$\left\{\begin{array}{rcl} \partial_t \varrho + \operatorname{div}((\kappa g + u)\varrho) &=& 0 \\ -\Delta u + \nabla p &=& 6\pi r_0 \kappa g \varrho\,, \\ \operatorname{div}(u) &=& 0. \end{array}\right. \tag{2.1}$$

Here u is the fluid velocity, p its associated pressure, ϱ is the density of the cloud. $r_0 = RN$, where R is the particles radii, g the gravity vector. The velocity $\kappa g = \frac{m}{6\pi R} g$ represents the fall speed of a sedimenting single particle under gravitational force. The derivation of this model is a consequence of the method of reflections which consists in approaching the flow around several particles as the superposition of the flows associated to one particle at time, see [67], [44, Chapter 8], [54], [30, Section 4], [45], [39] for more details. This approximation is possible in the case where the minimal distance between particles is larger than the particles radii. Consequently, the velocity of each particle corresponds to the fall speed of one sedimenting particle κg to which we add the velocity contribution of all the other particles which is smaller but of order one.

In this paper, we are interested in the case where the cloud is made up of clusters. The main motivation is to show the influence of the clusters configuration on the mean velocity fall. A first investigation in this direction is to consider clusters of pairs of particles where the minimal distance between the particles forming the pair is comparable to their radii. The cluster configuration is determined by the center x and the orientation ξ of the pair. Starting from a microscopic model, the first result of this paper is the derivation of a mesoscopic fluid-kinetic model describing the fluid velocity and pressure (u, p) and the function $f(t, x, \xi)$ representing the density of clusters centered in x and having orientation ξ at time t. The mean velocity fall of clusters is formulated through the Stokes resistance matrices. The second result of this paper corresponds to the case where the orientation of the cluster is correlated to its center *i.e.* $\xi = F(t, x)$. We obtain a system of coupled equations on ϱ the first marginal of f, the fluid velocity and pressure (u, p) and the function F describing the evolution of the cluster orientation. A local existence and uniqueness result for the former system is also presented.

The starting point is a microscopic model representing suspension of $N \in \mathbb{N}^*$ identical particle pairs in a uniform gravitational field. The pairs are defined as

$$B^i := B(x_1^i, R) \cup B(x_2^i, R)\ ,\ 1 \leqslant i \leqslant N,$$

where x_1^i, x_2^i are the centers of the i^{th} pair and R the radius. We define (u^N, p^N) as the unique solution to the following Stokes problem :

$$\left\{ \begin{array}{rcl} -\Delta u^N + \nabla p^N &=& 0, \\ \operatorname{div} u^N &=& 0, \end{array} \right. \text{on } \mathbb{R}^3 \backslash \bigcup_{i=1}^N \overline{B}^i, \tag{2.2}$$

completed with the no-slip boundary conditions :

$$\left\{ \begin{array}{rcl} u^N &=& U_1^i \text{ on } \partial B(x_1^i, R), \\ u^N &=& U_2^i \text{ on } \partial B(x_2^i, R), \\ \lim\limits_{|x| \to \infty} |u^N(x)| &=& 0, \end{array} \right. \tag{2.3}$$

where $(U_1^i, U_2^i) \in \mathbb{R}^3 \times \mathbb{R}^3$, $1 \leqslant i \leqslant N$ are the linear velocities. In this model, the angular velocity is neglected and we complete the PDE with the motion equation for each couple of particles :

$$\begin{cases} \dot{x}_1^i &= U_1^i, \\ \dot{x}_2^i &= U_2^i. \end{cases} \tag{2.4}$$

Newton law yields the following equations where inertia is neglected :

$$\begin{pmatrix} F_1^i \\ \\ F_2^i \end{pmatrix} = - \begin{pmatrix} mg \\ \\ mg \end{pmatrix}, \tag{2.5}$$

where m is the mass of the identical particle adjusted for buoyancy, g the gravitational acceleration, F_1^i, F_2^i are the drag forces applied by the fluid on the i^{th} particle :

$$F_1^i = \int_{\partial B(x_1^i, R)} \sigma(u^N, p^N) n \quad , \quad F_2^i = \int_{\partial B(x_2^i, R)} \sigma(u^N, p^N) n,$$

with n the unit outer normal and $\sigma(u^N, p^N) = (\nabla u^N + (\nabla u^N)^\top) - p^N \mathbb{I}$ the stress tensor. In order to formulate our results we introduce the main assumptions on the cloud.

2.1.1 Assumptions and main results

We assume that the radius is given by $R = \frac{r_0}{2N}$. In this paper we use the following notations, given a pair of particles $B(x_1, R)$ and $B(x_2, R)$:

$$x_+ := \frac{1}{2}(x_1 + x_2)\,, \quad x_- := \tfrac{1}{2}(x_1 - x_2)\,, \quad \xi := \frac{x_-}{R}.$$

Let $T > 0$ be fixed. We introduce the empirical density $\mu^N \in \mathcal{P}([0,T] \times \mathbb{R}^3 \times \mathbb{R}^3)$:

$$\mu^N(t, x, \xi) = \frac{1}{N} \sum_1^N \delta_{\left(x_+^i(t), \xi_i(t)\right)}(x, \xi),$$

and set ϱ^N its first marginal:

$$\varrho^N(t, x) := \frac{1}{N} \sum_i \delta_{x_+^i(t)}(x). \tag{2.6}$$

We denote by $d_{\min}$ the minimal distance between the centers x_+^i:

$$d_{\min}(t) := \min\{d_{ij}(t) := |x_+^i(t) - x_+^j(t)|\,,\, i \neq j\}.$$

We assume that there exists two constants $M_1 > M_2 > 1$ independent of N such that:

$$M_2 \leqslant |\xi_i| \leqslant M_1 \ , \ i = 1, \cdots, N \ \ \forall\, t \in [0, T]. \tag{2.7}$$

We assume that μ^N converges weakly to a measure μ in the sense that for all test function $\psi \in \mathcal{C}_b([0,T]\times\mathbb{R}^3\times\mathbb{R}^3)$ we have:

$$\int_0^T\int_{\mathbb{R}^3}\int_{\mathbb{R}^3}\psi(t,x,\xi)\mu^N(t,dx,d\xi)dt \underset{N\to\infty}{\to} \int_0^T\int_{\mathbb{R}^3}\int_{\mathbb{R}^3}\psi(t,x,\xi)\mu(t,x,\xi)dx\,d\xi\,dt. \tag{2.8}$$

We assume that the first marginal of μ denoted by ϱ is a probability measure such that $\varrho \in W^{1,\infty}\cap W^{1,1}$. We use the shortcut $W_\infty(t) := W_\infty(\varrho^N(t,\cdot),\varrho(t,\cdot))$ to define the infinite-Wasserstein distance between ϱ^N and ϱ, see [20] for a definition.
We assume that there exists a positive constant $\mathcal{E}_1 > 0$ such that for all $N \in \mathbb{N}^*$ and $t \in [0,T]$:

$$\sup_{N\in\mathbb{N}^*}\frac{W_\infty^3}{d_{\min}^2} \leqslant \mathcal{E}_1. \tag{2.9}$$

Finally, we assume that there exists a positive constant $\mathcal{E}_2 > 0$ such that for all $N \in \mathbb{N}^*$ and $t \in [0,T]$:

$$\sup_{N\in\mathbb{N}^*}\frac{W_\infty^3}{d_{\min}^3} \leqslant \mathcal{E}_2. \tag{2.10}$$

Remark 2.1.1. *Note that, formula* (2.8) *ensures that:*

$$\sup_{t\in[0,T]} W_\infty(t) \underset{N\to\infty}{\to} 0. \tag{2.11}$$

Since $\varrho \in L^\infty$, this yields a lower bound for the infinite Wasserstein distance:

$$\frac{1}{NW_\infty^3} \lesssim \sup_{x\in\mathbb{R}^3}\frac{\varrho^N(B(x,W_\infty))}{|B(x,W_\infty)|^3} \lesssim \|\varrho\|_\infty. \tag{2.12}$$

The definition of the infinite Wasserstein distance ensures that

$$W_\infty \geqslant d_{\min}/2\,, \tag{2.13}$$

which yields according to (2.11)

$$\sup_{t\in[0,T]} d_{\min}(t) \underset{N\to\infty}{\to} 0. \tag{2.14}$$

Assumption (2.10) *is only needed for the second Theorem 2.1.2.*

Our main results read:

Theorem 2.1.1. *Assume that* (2.7), (2.8) *and* (2.9) *are satisfied. If $r_0\|\varrho_0\|_{L^1\cap L^\infty}$ is small enough, μ satisfies the following transport equation :*

$$\left\{\begin{array}{rcll}\partial_t\mu + \mathrm{div}_x[(\mathbb{A}(\xi))^{-1}\kappa g + u)\mu] + \mathrm{div}_\xi[\nabla u\cdot\xi\mu] & = & 0\,, & \text{on } [0,T]\times\mathbb{R}^3\times\mathbb{R}^3,\\ -\Delta u + \nabla p & = & 6\pi r_0\kappa\varrho g\,, & \text{on } \mathbb{R}^3,\\ \mathrm{div}(u) & = & 0\,, & \text{on } \mathbb{R}^3.\end{array}\right.$$

Remark 2.1.2. *Analogously to the model* (2.1)*, local existence a uniqueness result can be shown for the former model following the result of [38].*

The second result concerns the case where the vectors along the line of centers ξ_i are correlated to the positions of centers x^i_+.

Theorem 2.1.2. *We consider the additional assumption* (2.10)*. Assume that there exists a function $F_0 \in W^{1,\infty}$ such that $\xi_i(0) = F_0(x^i_+(0))$ for all $1 \leqslant i \leqslant N$. There exists $T > 0$ independent of N and unique $F^N \in L^\infty(0,T;W^{1,\infty})$ such that for all $t \in [0,T]$ we have:*

$$\mu^N = \varrho^N \otimes \delta_{F^N} \quad \text{and } F^N(0,\cdot) = F_0.$$

Moreover, the sequence $(F^N)_N$ admits a limit denoted $F \in L^\infty(0,T;W^{1,\infty})$. The limiting measure μ is of the form $\mu = \varrho \otimes \delta_F$ and the triplet (ϱ, F, u) satisfies the following system

$$\left\{\begin{array}{rcll} \partial_t F + \nabla F \cdot (\mathbb{A}(F)^{-1}\kappa g + u) &=& \nabla u \cdot F, & \text{on } [0,T] \times \mathbb{R}^3, \\ \partial_t \varrho + \operatorname{div}((\mathbb{A}(F)^{-1}\kappa g + u)\varrho) &=& 0, & \text{on } [0,T] \times \mathbb{R}^3, \\ -\Delta u + \nabla p &=& 6\pi r_0 \kappa g \varrho, & \text{on } \mathbb{R}^3, \\ \operatorname{div} u &=& 0, & \text{on } \mathbb{R}^3, \\ \varrho(0,\cdot) &=& \varrho_0, & \text{on } \mathbb{R}^3, \\ F(0,\cdot) &=& F_0 & \text{on } \mathbb{R}^3. \end{array}\right. \tag{2.15}$$

Remark 2.1.3. *The matrix $\mathbb{A}$ is defined as $\mathbb{A} := A_1 + A_2$ where A_1 and A_2 are the resistance matrices associated to the sedimentation of a couple of identical spheres, see Section 2.2.1 for the definition. The term $(\mathbb{A})^{-1}\kappa g$ represents the mean velocity of a couple of identical particles sedimenting under gravitational field. We assume herein that $\mathbb{A}^{-1} \in W^{2,\infty}$.*

We finish with a local existence and uniqueness result for the limit model.

Theorem 2.1.3. *Let $p > 3$, $F_0 \in W^{2,p}$ and $\varrho_0 \in W^{1,p}$ compactly supported. There exists $T > 0$ and unique triplet $(\varrho, F, u) \in L^\infty(0,T;W^{1,p}) \times L^\infty(0,T;W^{2,p}) \times L^\infty(0,T;W^{3,p})$ satisfying* (2.15)*.*

As in [57], the idea of proof of Theorem 2.1.1 and 2.1.2 is to provide a derivation of the kinetic equation satisfied weakly by μ^N. This is done by computing the first order terms of the velocities of each pair:

$$\left\{\begin{array}{rcl} \dot{x}^i_+ &\sim& (\mathbb{A}(\xi_i))^{-1}\kappa g + \frac{6\pi r_0}{N} \sum\limits_{j \neq i} \Phi(x^i_+ - x^j_+)\kappa g, \\ \dot{\xi}_i &\sim& \left(\frac{6\pi r_0}{N} \sum\limits_{j \neq i} \nabla \Phi(x^i_+ - x^j_+)\kappa g \right) \cdot \xi_i. \end{array}\right. \tag{2.16}$$

The interaction force Φ is the Oseen tensor, see formula (2.17). This development is a corollary of the method of reflections which consists in approaching the solution u^N of $2N$ separated particles by the superposition of fields produced by the isolated $2N$ particle solutions. We refer to [67], [54], [44, Chapter 8] and [30, Section 4], [45] for an introduction

to the topic. We also refer to [39] where a converging method of reflections is developed and is used in [38]. In this paper we reproduce the same method of reflections developed in [57, Section 3]. However this method is no longer valid in the case where the minimal distance is comparable to the particle radii. The idea is then to approach the velocity field u^N by the superposition of fields produced by the isolated N couple of particles $B^i = B(x_1^i, R) \sqcup B(x_2^i, R)$. This requires an analysis of the solution of the Stokes equation past a pair of particles. In particular, we need to show that these special solutions have the same decay rate as the Stokeslets, see [57, Section 2.1].
The convergence of the method of reflections is ensured under the condition that the minimal distance $d_{\min}$ between the centers x_+^i satisfies

$$\frac{W_\infty^3}{d_{\min}} + \frac{W_\infty^3}{d_{\min}^2} < +\infty \,,$$

and that the distance $|x_1^i - x_2^i|$ for each pair satisfies formula (2.7).
In this paper, we focus only on the derivation of the mesoscopic model. Precisely, we do not tackle the propagation in time of the dilution regime and the mean field approximation. We provide in Propositions 2.B.3 and 2.B.1 some estimates showing that the control on the minimal distance $d_{\min}$ depends on the control on the infinite Wasserstein distance W_∞. However, the gradient of the Oseen tensor appearing in equation (2.16) leads to a log term in the estimates involving the control of W_∞, see Proposition 2.B.2. This prevents us from performing a Gronwall argument in order to prove the mean field approximation in the spirit of [33, 34].

2.1.2 Outline of the paper

The remaining sections of this paper are organized as follows. In section 2 we present an analysis of the particular solution of two translating spheres in a Stokes flow. In section 3 we present and prove the convergence of the method of reflections. In section 4 we compute the particle velocities $(\dot{x}_+^i, \dot{\xi}_i)_{1\leqslant i\leqslant N}$. Sections 5 and 6 are devoted to the proofs of Theorem 2.1.1, 2.1.2 and 2.1.3. Finally, we gather all the preliminary estimates in the appendix.

2.1.3 Notations

In this paper, n always refers to the unit outer normal to a surface.
We recall that the Green's function for the Stokes problem also called the Oseen tensor is defined as:

$$\Phi(x) = \frac{1}{8\pi}\left(\frac{\mathbb{I}}{|x|} + \frac{x \otimes x}{|x|^3}\right), \tag{2.17}$$

its associated pressure P reads:

$$P(x) = \frac{1}{4\pi}\frac{x}{|x|^3}.$$

See [27, Formula (IV.2.1)] or [44, Section 2.4.1].
Given a couple of velocities $(U_1, U_2) \in \mathbb{R}^3 \times \mathbb{R}^3$ we use the following notations

$$U_+ := \frac{U_1 + U_2}{2}, U_- := \frac{U_1 - U_2}{2}.$$

Finally, in the whole paper we use the symbol $\lesssim$ to express an inequality with a multiplicative constant independent of N and depending only on r_0, $\|\varrho_0\|_{L^1 \cap L^\infty}$, $\mathcal{E}_1$, $\mathcal{E}_2$ and eventually on $\kappa|g|$ which is uniformly bounded, see [57].

2.2 Two translating spheres in a Stokes flow

In this section, we focus on the analysis of the Stokes problem in $\mathbb{R}^3$ past a pair of particles. Given $x_1, x_2 \in \mathbb{R}^3$ and $R_1, R_2 > 0$, such that $|x_1 - x_2| > R_1 + R_2$, we consider two spheres $B_\alpha := B(x_\alpha, R_\alpha)$ $\alpha = 1, 2$ and focus on the following Stokes problem:

$$\begin{cases} -\Delta u + \nabla p &= 0, \\ \operatorname{div} u &= 0, \end{cases} \text{ on } \mathbb{R}^3 \setminus \bar{B}_1 \cup \bar{B}_2, \tag{2.18}$$

completed with the no-slip boundary conditions:

$$\begin{cases} u &= U_\alpha, \text{ on } \partial B_\alpha,\ \alpha = 1, 2, \\ \lim\limits_{|x| \to \infty} |u(x)| &= 0, \end{cases} \tag{2.19}$$

where $U_\alpha \in \mathbb{R}^3$ for $\alpha = 1, 2$. Classical results on the Steady Stokes equations for exterior domains (see [27, Chapter V] for more details) ensures the existence and uniqueness of equations (2.18) – (2.19). In this section, we aim to describe the velocity field u in terms of the force applied by the fluid on the particles defined as:

$$F_\alpha := \int_{\partial B_\alpha} \sigma(u, p) n \ , \ \alpha = 1, 2.$$

We refer to the paper [42] for the following statements. Neglecting angular velocities and torque we emphasize that there exists a linear mapping called resistance matrix satisfying:

$$\begin{pmatrix} F_1 \\ F_2 \end{pmatrix} = -3\pi(R_1 + R_2) \begin{pmatrix} A_{11} & A_{12} \\ A_{21} & A_{22} \end{pmatrix} \begin{pmatrix} U_1 \\ U_2 \end{pmatrix}, \tag{2.20}$$

where $A_{\alpha\beta}$, $1 \leqslant \alpha, \beta \leqslant 2$, are 3×3 matrices depending only on the non-dimensionalized centre-to-centre separation:

$$s := 2\frac{x_1 - x_2}{R_1 + R_2},$$

and the ratio of the spheres' radii:

$$\lambda = \frac{R_1}{R_2},$$

each of these matrices is of the form:

$$A_{\alpha\beta} := g_{\alpha,\beta}(|s|,\lambda)\mathbb{I} + h_{\alpha,\beta}(|s|,\lambda)\frac{s \otimes s}{|s|^2}, \tag{2.21}$$

where $\mathbb{I}$ is the 3×3 identity matrix and $g_{\alpha,\beta}$, $h_{\alpha,\beta}$ are scalar functions. We refer to the paper of Jeffrey and Onishi [42] where the authors provide a development formulas for $g_{\alpha,\beta}$ and $h_{\alpha,\beta}$ given by a convergent power series of $|s|^{-1}$. Note that the matrices satisfy

$$\begin{array}{rcl} A_{22}(s,\lambda) & = & A_{11}(s,\lambda^{-1}), \\ A_{12}(s,\lambda) & = & A_{21}(s,\lambda), \\ A_{12}(s,\lambda) & = & A_{12}(s,\lambda^{-1}). \end{array} \tag{2.22}$$

Inversly, there exists also a linear mapping called mobility matrix such that

$$\begin{pmatrix} U_1 \\ U_2 \end{pmatrix} = -\frac{1}{3\pi(R_1+R_2)} \begin{pmatrix} a_{11} & a_{12} \\ a_{21} & a_{22} \end{pmatrix} \begin{pmatrix} F_1 \\ F_2 \end{pmatrix}. \tag{2.23}$$

The matrices $a_{\alpha,\beta}$ depend on the same parameters as matrices $A_{\alpha,\beta}$ and satisfy a formula analogous to (2.21). They are also symmetric in the sense of formula (2.22).
The resistance and mobility matrices satisfy the following formula:

$$\begin{pmatrix} A_{11} & A_{12} \\ A_{21} & A_{22} \end{pmatrix} \begin{pmatrix} a_{11} & a_{12} \\ a_{21} & a_{22} \end{pmatrix} = \begin{pmatrix} \mathbb{I} & 0 \\ 0 & \mathbb{I} \end{pmatrix}, \tag{2.24}$$

Again, we refer to [42] for more details.

2.2.1 Restriction to the case of two identical spheres

We simplify the study by assuming that $R_1 = R_2 = R$ *i.e.* $\lambda = 1$. This means that the resistance matrix depends only on the parameter s which becomes:

$$s = \frac{x_1 - x_2}{R} = 2\,\xi,$$

and we have:

$$A_{22}(s,1) = A_{11}(s,1).$$

Hence we reformulate the resistance matrix as follows:

$$\begin{pmatrix} F_1 \\ F_2 \end{pmatrix} = -6\pi R \begin{pmatrix} A_1(\xi) & A_2(\xi) \\ A_2(\xi) & A_1(\xi) \end{pmatrix} \begin{pmatrix} U_1 \\ U_2 \end{pmatrix}, \tag{2.25}$$

and the mobility matrix:

$$\begin{pmatrix} U_1 \\ U_2 \end{pmatrix} = -(6\pi R)^{-1} \begin{pmatrix} a_1(\xi) & a_2(\xi) \\ a_2(\xi) & a_1(\xi) \end{pmatrix} \begin{pmatrix} F_1 \\ F_2 \end{pmatrix}. \tag{2.26}$$

Formula (2.24) yields the following relations

$$\begin{cases} A_1 a_1 + A_2 a_2 = \mathbb{I}, \\ A_1 a_2 + A_2 a_1 = 0. \end{cases} \tag{2.27}$$

We are interested in providing a formula for the velocity u and showing some decay properties. In this paper we use the notation $(U[U_1, U_2], P([U_1, U_2])$ for the unique solution to

$$\begin{cases} -\Delta U[U_1, U_2] + \nabla P[U_1, U_2] &= 0, \\ \operatorname{div} U[U_1, U_2] &= 0, \end{cases} \quad \text{on } \mathbb{R}^3 \backslash \bar{B}_1 \cup \bar{B}_2,$$

completed with the no-slip boundary conditions:

$$\begin{cases} U[U_1, U_2] &= U_\alpha, \text{ on } \partial B_\alpha, \, \alpha = 1, 2, \\ \lim\limits_{|x| \to \infty} |U[U_1, U_2](x)| &= 0, \end{cases}$$

We have the following preliminary result:

Proposition 2.2.1. *For all $x \notin \overline{B_1 \cup B_2}$ the following formula holds true:*

$$u(x) = -\int_{\partial B_1} \Phi(\xi - x) \, [\sigma(u,p))n)](\xi) d\xi - \int_{\partial B_2} \Phi(\xi - x) \, [\sigma(u,p))n)](\xi) d\xi. \tag{2.28}$$

Proof. Without loss of generality we assume that the pair of particles is centered in the origin *i.e.* $x_+ = 0$. In what follows we use the following shortcut

$$(u, p) = (U[U_1, U_2], P[U_1, U_2]).$$

In order to prove the main property we need some preliminary decay rates. We keep the notation u for the extension of the velocity field on $\mathbb{R}^3$ by U_α on B_α, $\alpha = 1, 2$. Since $\nabla u \in L^2(\mathbb{R}^3)$, the classical steady Stokes regularity results (see [27, Theorem IV.4.1]) combined with some Sobolev embeddings ensures that $(u, p) \in \mathcal{C}^2(B(0, 3d/2) \backslash B(0, d)) \times \mathcal{C}^1(B(0, 3d/2) \backslash B(0, d))$, where d is large enough to have $\bar{B}_1 \cup \bar{B}_2 \subset B(0, 2|x_-|) \subset B(0, d)$. Hence, the idea is to consider $v = \chi_d u$, $\pi = \chi_d p$ where χ_d a regular truncation function such that $\chi_d = 0$ on $B(0, d)$ and $\chi_d = 1$ on $B(0, 3d/2)$. The couple (v, π) satisfies a Stokes equation with a source term f and a compressible condition g depending on the data and supported in $B(0, 3d/2) \backslash B(0, d)$. Hence, the convolution formula with the Oseen tensor(see [27, Formula (IV.2.1)]) holds true and we emphasize that for $|x|$ large enough we have:

$$|v(x)| = |u(x)| \lesssim \frac{1}{|x|}, \quad |\pi(x)| = |p(x)| \lesssim \tfrac{1}{|x|^2}. \tag{2.29}$$

The proof of formula (2.28) relies on the Lorentz reciprocal theorem, see [44, Section 2.3], which stands that for a given domain $\Omega \subset \mathbb{R}^3$ and two divergence free vector fields v, v' on Ω, there holds

$$\int_{\partial \Omega} v \cdot (\sigma' n) + \int_\Omega v \cdot \operatorname{div} \sigma' + \int_{\partial \Omega} v' \cdot (\sigma \, n) + \int_\Omega v' \cdot \operatorname{div} \sigma = 0 \,, \tag{2.30}$$

where σ, σ' the respective stress tensor of v and v'. On the other hand, we recall the definition of the Oseen tensor Φ and its associated pressure $\mathcal{P}$:

$$\Phi(x) = \frac{1}{8\pi}\left(\frac{\mathbb{I}}{|x|} + \frac{x \otimes x}{|x|^3}\right), \quad \mathcal{P}(x) = \tfrac{1}{4\pi}\tfrac{x}{|x|^3}.$$

We denote by Σ its (triadic) associated stress tensor :

$$\Sigma_{ijk} = (\Phi_{ij,k} + \Phi_{kj,i}) - \delta_{ik}\mathcal{P}_j = -6\frac{x_i x_j x_k}{|x|^5},$$

where $\Phi_{ij,k} = \partial_{x_k}\Phi_{ij}$. Since Φ is the Green's function, its stress tensor satisfies

$$(\operatorname{div}\Sigma)_{ij} = \sum_k \partial_{x_k}\Sigma_{ijk} = \delta_0(x)\delta_{ij},$$

in the sense that for all regular divergence-free vector field v

$$\int_\Omega \operatorname{div}\Sigma\, v = \begin{cases} v(0) & \text{if } 0 \in \Omega, \\ 0 & \text{if } 0 \notin \Omega. \end{cases} \tag{2.31}$$

We apply the reciprocal theorem, formula (2.30), for $v = u$ and $v' = \Phi(x - \cdot)$, we obtain for all domain Ω and all $x \in \Omega$:

$$u(x) = -\int_{\partial\Omega} \Phi(\xi - x)\,[\sigma(u,p))n)](\xi)d\sigma(\xi) - \int_{\partial\Omega} \Sigma(\xi - x)n(\xi)\,u(\xi)d\sigma(\xi).$$

We may then apply this formula by choosing $\Omega = B(0,\bar{R})\backslash\overline{B_1 \cup B_2}$ with $\bar{R}$ large enough to satisfy $\overline{B_1 \cup B_2} \subset B(0,\bar{R})$. We obtain then for all $x \in \Omega$:

$$\begin{aligned} u(x) = &-\int_{\partial B_1 \cup \partial B_2} \Phi(\xi - x)\,[\sigma(u,p))n)](\xi)d\sigma(\xi) - \int_{\partial B_1 \cup \partial B_2} \Sigma(\xi - x)n(\xi)\,u(\xi)d\sigma(\xi) \\ &-\int_{\partial B(0,\bar{R})} \Phi(\xi - x)\,[\sigma(u,p))n)](\xi)d\sigma(\xi) - \int_{\partial B(0,\bar{R})} \Sigma(\xi - x)n(\xi)\,u(\xi)d\sigma(\xi) \end{aligned}$$

The two last terms on the right hand side vanish when $\bar{R} \to \infty$. This is due to the fact that Φ (resp. Σ) scales like $O(\frac{1}{R})$ (resp. $O(\frac{1}{R^2})$) and, according to the decay rate (2.29), u, $R\,\sigma(u,p) \to 0$ for large $\bar{R}$.
For the term involving the stress tensor Σ and the velocity field u on $\partial B_1 \cup \partial B_2$ we recall that $u(x) = U_\alpha$ on ∂B_α $\alpha = 1, 2$. And as $x \notin \overline{B_1 \cup B_2}$ we have then:

$$\int_{\partial B_\alpha} \Sigma(\xi - x)n(\xi) = 0.$$

Finally for all $x \notin \overline{B_1 \cup B_2}$ the following formula holds true:

$$u(x) = -\int_{\partial B_1} \Phi(\xi - x)\,[\sigma(u,p))n)](\xi)d\xi - \int_{\partial B_2} \Phi(\xi - x)\,[\sigma(u,p))n)](\xi)d\xi.$$

□

Corollary 2.2.2. *The following development holds true up to order 2:*

$$U[U_1, U_2](x) = -\Phi(x - x_1)F_1 - \Phi(x_2 - x)F_2. \tag{2.32}$$

There exists a function f independent of the data such that the unique solution $(U[U_1, U_2], P[U_1, U_2])$ satisfies the following decay property for all $x \notin B(x_+, 2|x_-|)$:

$$\frac{|U[U_1, U_2](x)|}{|x_+ - x|} + |\nabla U[U_1, U_2](x)| + |P[U_1, U_2](x)| \lesssim 6\pi R|f(|\xi|)|\frac{\max(|U_1|, |U_2|)}{|x_+ - x|^2}. \tag{2.33}$$

Precisely, we have for all $x \notin B(x_+, 2|x_-|)$:

$$U[U_1, U_2](x) \lesssim 6\pi R|f(|\xi|)|\left(\frac{|U_+|}{|x_+ - x|} + \frac{|U_+| + |U_-|}{|x_+ - x|^2}|x_-|\right), \tag{2.34}$$

where $\xi = \frac{|x_-|}{R}$ and $U_+ = \frac{U_1+U_2}{2}$, $U_- = \frac{U_1-U_2}{2}$.

Proof. As in [44, Section 2.5], we take the Taylor series of $\Phi(x - \xi)$ in ξ to obtain an approximation of the velocity field u that holds true up to the order 3. We recall that if we neglect the torque we have:

$$\int_{\partial B_\alpha} [\sigma(u, p))n)](\xi)d\xi = F_\alpha, \tag{2.35}$$

$$\int_{\partial B_\alpha} [\sigma(u, p))n)](\xi) \times (\xi - x_\alpha)d\xi = 0. \tag{2.36}$$

Replacing $\Phi(x - \xi)$ by its development:

$$\Phi(\xi - x) = \Phi(x_\alpha - x) + \nabla\Phi(x_\alpha - x)\,(\xi - x_\alpha) + ...$$

in formula (2.28), we thus obtain the following formula which is exact up to second order:

$$u(x) \sim -\sum_{\alpha=1}^{2} \Phi(x - x_\alpha)F_\alpha,$$

recall that the forces are given by the following formulas:

$$\begin{aligned} F_1 &= 6\pi R(A_1U_1 + A_2U_2), \\ F_2 &= 6\pi R(A_2U_1 + A_1U_2). \end{aligned}$$

We have then the existence of a scalar function f independent of the data such that:

$$|F_\alpha| \leqslant 6\pi R\,|f(|\xi|)|\,\max(||U_1|, |U_2|).$$

This yields the following decay rate for all $x \notin \overline{B(x_1, R) \cup B(x_2, R)}$:

$$|u(x)| \lesssim 6\pi R\left(\frac{1}{|x - x_1|} + \frac{1}{|x - x_2|}\right)|f(|\xi|)|\,\max(||U_1|, |U_2|). \tag{2.37}$$

The remaining estimates are obtained using direct computations and the following formulas:

$$F_1 = F_+ + F_-, \quad F_2 = F_+ - F_-. \tag{2.38}$$

□

2.3 The method of reflections

In this section, we aim to show that the method of reflections holds true in the special case where the minimal distance and the radius R are of the same order. The idea is to approach the velocity field u^N by the particular solutions developed in the section above. We recall that u^N is the unique solution to the following Stokes problem :

$$\left\{ \begin{array}{rcl} -\Delta u^N + \nabla p^N & = & 0, \\ \operatorname{div} u^N & = & 0, \end{array} \right. \text{ on } \mathbb{R}^3 \backslash \bigcup_{i=1}^{N} \bar{B}^i,$$

completed with the no-slip boundary conditions :

$$\left\{ \begin{array}{rcl} u^N & = & U_1^i\,, \text{ on } \partial B(x_1^i, R), \\ u^N & = & U_2^i\,, \text{ on } \partial B(x_2^i, R), \\ \lim\limits_{|x| \to \infty} |u^N(x)| & = & 0, \end{array} \right.$$

where $(U_1^i, U_2^i) \in \mathbb{R}^3 \times \mathbb{R}^3$, $1 \leqslant i \leqslant N$ are such that:

$$\begin{pmatrix} F_1^i \\ \\ F_2^i \end{pmatrix} = - \begin{pmatrix} mg \\ \\ mg \end{pmatrix}, \ \forall\, 1 \leqslant i \leqslant N.$$

Thanks to the superposition principle, the sum of the N solutions $\sum_{i=1}^N U[U_1^i, U_2^i]$ satisfy a Stokes equation on $\mathbb{R}^3 \backslash \overline{\bigcup_{i=1}^{N} B^i}$, but do not match the boundary conditions. Hence, we define the error term:

$$U[u_*^{(1)}] = u - \sum_{i=1}^{N} U[U_1^i, U_2^i],$$

which satisfies a Stokes equation on $\mathbb{R}^3 \backslash \overline{\bigcup_{i=1}^{N} B^i}$ completed with the following boundary conditions for all $1 \leqslant i \leqslant N$, $\alpha = 1, 2$ and $x \in B(x_\alpha^i, R)$:

$$u_*^{(1)}(x) = - \sum_{j \neq i} U[U_1^i, U_2^i](x).$$

We set then for $\alpha = 1, 2$ and $1 \leqslant i \leqslant N$:

$$U_\alpha^{i,(1)} := u_*^{(1)}(x_\alpha^i),$$

and reproduce the same approximation to obtain:

$$U[u_*^{(2)}] := u - \sum_{i=1}^{N} \left(U[U_1^i, U_2^i] + U[U_1^{i,(1)}, U_2^{i,(1)}] \right),$$

which satisfies a Stokes equation with the following boundary conditions for all $1 \leqslant i \leqslant N$, $\alpha = 1, 2$ and $x \in B(x^i_\alpha, R)$:

$$u^{(2)}_*(x) = u^{(1)}_*(x) - u^{(1)}_*(x^i_\alpha) - \sum_{j \neq i} U[U^{i,(1)}_1, U^{i,(1)}_2](x).$$

By iterating the process, one can show that for all $k \geqslant 1$ we have:

$$u = \sum_{p=0}^{k} \sum_{i=1}^{N} U[U^{i,(p)}_1, U^{i,(p)}_2] + U[u^{(k+1)}_*],$$

where for all $\alpha = 1, 2$, $1 \leqslant i \leqslant N$ and $p \geqslant 0$:

$$\begin{aligned}
u^{(p+1)}_*(x) &= u^{(p)}_*(x) - u^{(p)}_*(x^i_\alpha) - \sum_{j \neq i} U[U^{i,(p)}_1, U^{i,(p)}_2](x)\,, \\
u^{(0)}_* &= \sum_{i=1}^{N} U^i_1 1_{B(x^i_1,R)} + U^i_2 1_{B(x^i_2,R)}\,, \\
U^{i,(p)}_\alpha &= u^{(p)}_*(x^i_\alpha)\,, \\
U^{i,(0)}_\alpha &= U^i_\alpha\,.
\end{aligned} \tag{2.39}$$

The convergence is analogous to the convergence proof in [57, Section 3.1]. We begin by the following estimates that are needed in the computations.

Lemma 2.3.1. *Under assumptions* (2.7), (2.9) *we have for all* $1 \leqslant i \neq j \leqslant N$, $1 \leqslant \alpha, \beta \leqslant 2$*:*

$$|x^i_\alpha - x^j_\beta| \geqslant \frac{1}{2}|x^i_+ - x^j_+|. \tag{2.40}$$

The first step is to show that the sequence $\max\limits_i(\max(|U^{i,(p)}_1|, |U^{i,(p)}_2|))$ converges when p goes to infinity.

Lemma 2.3.2. *Under assumptions* (2.7), (2.8), (2.9) *and the assumption that* $r_0\|\varrho_0\|_{L^1 \cap L^\infty}$ *is small enough, there exists a positive constant* $K < 1/2$ *satisfying for all* $1 \leqslant i \leqslant N$, $p \geqslant 0$

$$\max_i(\max(|U^{i,(p+1)}_1|, |U^{i,(p+1)}_2|)) \leqslant K \max_i(\max(|U^{i,(p)}_1|, |U^{i,(p)}_2|)),$$

for N large enough.

Proof. According to formulas (2.33) and Lemma 2.3.1, we have for all $\alpha = 1, 2$ and $1 \leqslant i \leqslant N$:

$$\begin{aligned}
|U^{i,(p+1)}_\alpha| &\leqslant \left| \sum_{j \neq i} U[U^{j,(p)}_1, U^{j,(p)}_2](x^i_\alpha) \right| \\
&\lesssim \frac{6\pi r_0}{N} \left(\sum_{j \neq i} \frac{|f(|\xi_j|)|}{d_{ij}} \right) \max_j \left(|U^{j,(p)}_1|, |U^{j,(p)}_2|\right) \\
&\leqslant C r_0 \|\varrho\|_{L^1 \cap L^\infty} \left(\frac{W^3_\infty}{d_{\min}} + 1 \right)\,,
\end{aligned}$$

where we used Lemma 2.A.1 and the fact that for all $1 \leqslant j \leqslant N$ and $N \in \mathbb{N}^*$

$$|f(|\xi_j|)| \leqslant \sup_{2<|s|\leqslant M_1} |f(|s|)|,$$

according to assumption (2.7). Hence, the first term in the right-hand side vanishes according to (2.9) and (2.14).
Finally, if we assume that $r_0\|\varrho\|_{L^1\cap L^\infty}$ is small enough, we obtain the existence of a positive constant $K < 1/2$ such that:

$$\max_i(\max(|U_1^{i,(p+1)}|, |U_2^{i,(p+1)}|)) \leqslant K \max_i(\max(|U_1^{i,(p)}|, |U_2^{i,(p)}|)).$$

□

We have the following result.

Proposition 2.3.3. *Under the same assumptions as Lemma 2.3.2, we have for N large enough:*

$$\lim_{k\to\infty} \|\nabla U[u_*^{(k+1)}]\|_2 \lesssim R \max_{\substack{1\leqslant i\leqslant N\\ \alpha=1,2}} |U_\alpha^i|.$$

Proof. The proof is analogous to the convergence proof of [57, Proposition 3.4]. This is due to the fact that the particular solutions have the same decay rate as the Oseen-tensor. □

2.3.1 Two particular cases

First case

Given $W \in \mathbb{R}^3$ we consider in this part w the unique solution to the Stokes equation (2.2) completed with the following boundary conditions :

$$w = \left\{ \begin{array}{rl} W & \text{on } B(x_1^1, R), \\ -W & \text{on } B(x_2^1, R), \\ 0 & \text{on } B(x_1^i, R) \cup B(x_2^i, R),\ i \neq 1. \end{array} \right. \tag{2.41}$$

We denote by $W_\alpha^{i,(p)}$, $\alpha = 1, 2$, $1 \leqslant i \leqslant N$, $p \in \mathbb{N}$ the velocities obtained from the method of reflections applied to the velocity field w. In other words :

$$w = \sum_{p=0}^{k} \sum_i U[W_1^{i,(p)}, W_2^{i,(p)}] + U[w_*^{(k+1)}].$$

We aim to show that, in this special case, the sequence of velocities $W_\alpha^{i,(p)}$ and the error term $U[w_*^{(k)}]$ are much smaller than before. This is due to the initial vanishing boundary conditions for $i \neq 1$. Indeed we have :

Proposition 2.3.4. *There exists two positive constants $C, L > 0$ such that for N large enough:*

$$\begin{aligned}
\max_{\alpha=1,2}|W_\alpha^{i,(p+1)}| &\leqslant C(2Cr_0L\|\varrho_0\|_{L^\infty\cap L^1})^p\,\frac{R|x_-^1|}{|x_+^1-x_+^i|^2}\,|W|\,,\ i\neq 1\,,\ p\geqslant 0,\\
\max_\alpha|W_\alpha^{1,(p+1)}| &\leqslant C2^{p-1}(r_0CL\|\varrho_0\|_{L^\infty\cap L^1})^p|x_-^1|\frac{R}{d_{\min}}\,|W|\,,\ p\geqslant 1,\\
\max_\alpha|W_\alpha^{i,(0)}|+\max_\alpha|W_\alpha^{1,(1)}| &= 0\,,\ i\neq 1.
\end{aligned}$$

Proof. We show that the statement holds true for $p = 0$ then we prove it for all $p \geqslant 1$ by induction. According to formula (2.39) we have for $p = 0$:

$$W_\alpha^{1,(0)} = W\delta_{\alpha 1} - W\delta_{\alpha 2},$$

and for $i \neq 1$, $\alpha = 1, 2$, $U_\alpha^{i,(0)} = 0$. This yields for $i \neq 1$, $\alpha = 1, 2$:

$$\begin{aligned}
W_\alpha^{i,(1)} &= U[W_1^{1,(0)}, W_2^{1,(0)}](x_\alpha^i),\\
&= \Phi(x_1^1 - x_\alpha^i)F_1^1 + \Phi(x_2^1 - x_\alpha^i)F_2^1,
\end{aligned}$$

where:

$$F_1^1 = -6\pi R(A_1(s^1) - A_2(s^1))W, \quad F_2^1 = -6\pi R(A_2(s^1) - A_1(s^1))W.$$

Hence, $F_2^1 = -F_1^1$ we have then using Lemma 2.3.1:

$$\begin{aligned}
|W_\alpha^{i,(1)}| &\leqslant \left|\Phi(x_1^1 - x_\alpha^i) - \Phi(x_2^1 - x_\alpha^i)\right|\,|F_1^1|,\\
&\lesssim 6\pi R\frac{|x_-^1|}{d_{i1}^2}|A_1(s^1) - A_2(s^1)|\,|W|,
\end{aligned}$$

thus, we denote by $C > 0$ the global positive constant appearing in the estimate above. This shows that the first statement holds true for $p = 0$. For the second estimate we have $|W_\alpha^{1,(1)}| = 0$ and for $p = 1$ we have:

$$\begin{aligned}
|W_\alpha^{1,(2)}| &= \left|\sum_{j\neq 1} U[W_1^{j,(1)}, W_2^{j,(1)}](x_\alpha^1)\right|,\\
&\leqslant C\sum_{j\neq 1}\frac{R}{d_{1j}}\max(|W_1^{j,(1)}|, |W_2^{j,(1)}|),\\
&\leqslant C\sum_{j\neq 1}\left(\frac{CR^2|x_-^1|}{d_{1j}^3}\right)|W|,\\
&\leqslant C\frac{|x_-^1|R}{d_{\min}}(CKr_0)\,|W|\,,
\end{aligned}$$

where we used Lemma 2.A.1 for $k=2$ and assumption (2.9). In what follows we define the constant $L>0$ as the constant satisfying:

$$\max_i \left(\frac{1}{N} \sum_{j\neq i} \left(\frac{1}{d_{ij}^2} \right) + \frac{1}{N} \sum_{j\neq 1,i} \left(\frac{1}{d_{ij}} + \frac{1}{d_{1j}} \right) \right) \leqslant L \|\varrho_0\|_{L^\infty \cap L^1}.$$

Now for all $p \geqslant 1$, $i \neq 1$ we have:

$$\begin{aligned}
|W_\alpha^{i,(p+1)}| &= \left| \sum_{j\neq i} U[W_1^{j,(p)}, W_2^{j,(p)}](x_\alpha^i) \right| \\
&\leqslant C \sum_{j\neq i} \frac{R}{d_{ij}} \max(|W_1^{j,(p)}|, |W_2^{j,(p)}|), \\
&\leqslant C \Big(\sum_{j\neq i,1} \frac{R}{d_{ij}} C (2Cr_0 L \|\varrho_0\|_{L^\infty\cap L^1})^{p-1} \, \frac{R|x_-^1|}{d_{1j}^2} \\
&+ \frac{R}{d_{i1}} \frac{R|x_-^1|}{d_{\min}} C 2^{p-2} (r_0 C L \|\varrho_0\|_{L^\infty \cap L^1})^{p-1} \Big) |W|,
\end{aligned}$$

using the fact that $\frac{1}{d_{ij}d_{kj}} \leqslant \frac{1}{d_{ik}} \left(\frac{1}{d_{ij}} + \frac{1}{d_{kj}} \right)$ we obtain

$$\begin{aligned}
|W_\alpha^{i,(p+1)}| &\leqslant C \Big(\frac{R|x_-^1|}{d_{i1}} C (2Cr_0 L \|\varrho_0\|_{L^\infty\cap L^1})^{p-1} \left(\frac{1}{d_{1i}} \sum_{j\neq i,1} \left(\frac{R}{d_{ij}} + \frac{R}{d_{1j}} \right) + \sum_{j\neq i,1} \frac{R}{d_{1j}^2} \right) \\
&+ \frac{R}{d_{i1}} \frac{R|x_-^1|}{d_{\min}} C 2^{p-2} (r_0 C L \|\varrho_0\|_{L^\infty\cap L^1})^{p-1} \Big) |W|, \\
&\leqslant C \frac{R|x_-^1|}{d_{i1}} \Big(C (2Cr_0 L \|\varrho_0\|_{L^\infty\cap L^1})^{p-1} \left(\frac{r_0 L \|\varrho_0\|_{L^\infty\cap L^1}}{d_{1i}} \right) \\
&+ \frac{R}{d_{\min}} C 2^{p-2} (r_0 C L \|\varrho_0\|_{L^\infty\cap L^1})^{p-1} \Big) |W|, \\
&\leqslant C \frac{R|x_-^1|}{d_{i1}^2} \left((Cr_0 L \|\varrho_0\|_{L^\infty\cap L^1})^p 2^{p-1} + \frac{R d_{i1}}{d_{\min}} C 2^{p-2} (r_0 C L \|\varrho_0\|_{L^\infty\cap L^1})^{p-1} \right) |W|.
\end{aligned}$$

Since $\frac{R d_{1i}}{d_{\min}} \ll r_0 L \|\varrho_0\|_{L^\infty\cap L^1}$, the second term can be bounded by $(Cr_0 L \|\varrho_0\|_{L^\infty\cap L^1})^p \, 2^{p-2}$ which yields the expected result because $2^{p-1} + 2^{p-2} \leqslant 2^p$.

We prove now the second estimate. Let $p \geqslant 1$:

$$
\begin{aligned}
|W_\alpha^{1,(p+1)}| &= \left|\sum_{j\neq 1} U[W_1^{j,(p)}, W_2^{j,(p)}](x_\alpha^1)\right|, \\
&\leqslant C\sum_{j\neq 1}\frac{R}{d_{j1}}\max(|W_1^{j,(p)}|, |W_2^{j,(p)}|), \\
&\leqslant C\left(\sum_{j\neq 1}\frac{R}{d_{1j}}C(2Cr_0L\|\varrho_0\|_{L^\infty\cap L^1})^{p-1}\,\frac{R|x_-^1|}{d_{1j}^2}\right)|W|, \\
&\leqslant C(2Cr_0L\|\varrho_0\|_{L^\infty\cap L^1})^{p-1}C\frac{R}{d_{\min}}|x_-^1|\left(\sum_{j\neq 1}\frac{R}{d_{1j}^2}\right)|W|, \\
&\leqslant C2^{p-1}(Cr_0L\|\varrho_0\|_{L^\infty\cap L^1})^p\frac{R}{d_{\min}}|x_-^1||W|.
\end{aligned}
$$

□

According to these estimates, if we assume that $r_0\|\varrho_0\|_{L^\infty\cap L^1}$ is small enough to have $2L\|\varrho_0\|_{L^\infty\cap L^1}Cr_0 < 1$ then the following result holds true :

Corollary 2.3.5. *Under the assumption that $r_0\|\varrho_0\|_{L^\infty\cap L^1}$ is small enough we have :*

$$
\begin{aligned}
\sum_{p=0}^{\infty}\max_{\alpha=1,2}|W_\alpha^{i,(p)}| &\lesssim \frac{R|x_-^1|}{|x_+^1 - x_+^i|^2}|W|\,,\ i\neq 1, \\
\sum_{p=1}^{\infty}\max_{\alpha=1,2}|W_\alpha^{1,(p)}| &\lesssim \frac{R|x_-^1|}{d_{\min}}|W|,
\end{aligned}
$$

for N large enough.

This result shows that we can obtain a better estimate for the error term of the method of reflections in this particular case:

Proposition 2.3.6. *We set $\eta := 2C\|\varrho_0\|_{L^\infty\cap L^1}Lr_0 < 1$ the constant introduced in Proposition 2.3.4. For all $i\neq 1$ we have*

$$
\begin{aligned}
\|\nabla w_*^{(k)}\|_{L^\infty(B_i)} &\lesssim \frac{R|x_-^1|}{d_{i1}^3}|W|, \\
\|w_*^{(k+1)}\|_{L^\infty(B_i)} &\lesssim R\|\nabla w_*^{(k)}\|_{L^\infty(B_i)} + \frac{R}{d_{1i}^2}|x_-^1|\eta^{k-1}|W|.
\end{aligned}
$$

And for $i = 1$ we have :

$$
\begin{aligned}
\|\nabla w_*^{(k)}\|_{L^\infty(B_1)} &\lesssim \frac{R}{d_{\min}}|x_-^1|\left(\frac{W_\infty^3}{d_{\min}^3} + |\log W_\infty|\right)|W|, \\
\|w_*^{(k+1)}\|_{L^\infty(B_1)} &\lesssim R\|\nabla w_*^{(k)}\|_{L^\infty(B_1)} + \frac{R}{d_{\min}}|x_-^1|\eta^{k-1}|W|,
\end{aligned}
$$

Proof. **Estimate for $\|\nabla w_*^{(k)}\|_\infty$.**
Let $x \in B(x_\alpha^i, R)$, with $\alpha = 1,2$ and $i \neq 1$, formula (2.39) yields:

$$
\begin{aligned}
|\nabla w_*^{(k+1)}(x)| &\leqslant |\nabla w_*^{(k)}(x)| + \sum_{j\neq i} |\nabla U[W_1^{j,(k)}, W_2^{j,(k)}](x)|,\\
&\leqslant \sum_{p=0}^{k}\sum_{j\neq i} |\nabla U[W_1^{j,(p)}, W_2^{j,(p)}](x)|,\\
&\leqslant \sum_{p=0}^{k}\sum_{j\neq i,1} |\nabla U[W_1^{j,(p)}, W_2^{j,(p)}](x)| + \sum_{p=1}^{k} |\nabla U[W_1^{1,(p)}, W_2^{1,(p)}](x)|\\
&+ |\nabla U[W_1^{1,(0)}, W_2^{1,(0)}](x)|.
\end{aligned}
$$

We estimate the first term applying Corollary 2.3.5:

$$
\begin{aligned}
\sum_{p=0}^{k}\sum_{j\neq i,1} |\nabla U[W_1^{j,(p)}, W_2^{j,(p)}](x)| &\leqslant C\sum_{p=0}^{k}\sum_{j\neq i,1}\left(\frac{R}{|x_1^j - x_\alpha^i|^2} + \frac{R}{|x_2^j - x_\alpha^i|^2}\right)\max_{\alpha=1,2}|W_\alpha^{j,(p)}|,\\
&\leqslant 2C\sum_{p=0}^{k}\sum_{j\neq i,1}\left(\frac{R}{d_{ij}^2}\right)\max_{\alpha=1,2}|W_\alpha^{j,(p)}|,\\
&\lesssim \sum_{j\neq i,1}\left(\frac{R}{d_{ij}^2}\frac{R|x_-^1|}{d_{1j}^2}\right)|W|,\\
&\lesssim \frac{R|x_-^1|}{d_{1i}^2}\sum_{j\neq i,1}\left(\frac{R}{d_{ij}^2} + \frac{R}{d_{1j}^2}\right)|W|,\\
&\lesssim \frac{R|x_-^1|}{d_{1i}^2}|W|.
\end{aligned}
$$

We reproduce the same for the second term applying Corollary 2.3.5:

$$
\begin{aligned}
\sum_{p=1}^{k} |\nabla U[W_1^{1,(p)}, W_2^{1,(p)}](x)| &\leqslant 2C\sum_{p=1}^{k}\left(\frac{R}{|x_+^1 - x_+^i|^2}\right)\max(|W_1^{1,(p)}|, |W_2^{1,(p)}|),\\
&\lesssim \frac{R}{|x_+^1 - x_+^i|^2}\frac{R}{d_{\min}}|x_-^1||W|.
\end{aligned}
$$

For the last term we recall that:

$$
\nabla U[W_1^{1,(0)}, W_2^{1,(0)}](x) = \nabla\Phi(x_1^1 - x)F_1^1 + \nabla\Phi(x_2^1 - x)F_2^1,
$$

as $(W_1^{1,(0)}, W_2^{1,(0)}) = (W, -W)$ we have:

$$
\begin{cases}
F_1^1 &= -6\pi R(A_1(\xi_1)W - A_2(\xi_1)W),\\
F_2^1 &= -6\pi R(A_2(\xi_1)W - A_1(\xi_1)W).
\end{cases}
$$

Thus $F_2^1 = -F_1^1$ and we obtain since $x \in B(x_\alpha^i, R)$, $i \neq 1$:

$$\left|\nabla U[W_1^{1,(0)}, W_2^{1,(0)}](x)\right| = \left|(\nabla\Phi(x_1^1 - x) - \nabla\Phi(x_2^1 - x))F_1^1\right|,$$
$$\lesssim \frac{R|x_-^1|}{|x_+^1 - x_+^i|^3}|W|.$$

Gathering all the inequalities we have for $i \neq 1$:

$$\|\nabla w_*^{(k)}\|_{L^\infty(B_i)} \lesssim \frac{R|x_-^1|}{|x_+^1 - x_+^i|^3}.|W|$$

Analogously for $i = 1$ we obtain:

$$|\nabla w_*^{(k+1)}(x)| \leqslant |\nabla w_*^{(k)}(x)| + \sum_{j\neq 1}|\nabla U[W_1^{j,(k)}, W_2^{j,(k)}](x)|,$$
$$\leqslant \sum_{p=0}^{k}\sum_{j\neq 1}|\nabla U[W_1^{j,(p)}, W_2^{j,(p)}](x)|,$$
$$\leqslant 2C\sum_{p=0}^{k}\sum_{j\neq 1}\left(\frac{R}{d_{1j}^2}\right)\max(|W_1^{j,(p)}|, |W_2^{j,(p)}|),$$
$$\lesssim \sum_{j\neq 1}\left(\frac{R}{d_{1j}^2}\frac{R|x_-^1|}{d_{1j}^2}\right)|W|,$$
$$\lesssim \frac{R|x_-^1|}{d_{\min}}\left(\frac{W_\infty^3}{d_{\min}^3} + |\log W_\infty|\right)|W|.$$

Estimate for $\|w_*^{(k)}\|_\infty$. Let $x \in B(x_\alpha^i, R)$, $\alpha = 1, 2$, $i \neq 1$. We have according to formula (2.39) :

$$|w_*^{(k+1)}(x)| = \left|w_*^{(k)}(x) - w_*^{(k)}(x_\alpha^i) - \sum_{j\neq i}U[W_1^{j,(k)}, W_2^{j,(k)}](x)\right|,$$
$$\leqslant R\|\nabla w_*^{(k)}\|_\infty + \sum_{j\neq i}\left|U[W_1^{j,(k)}, W_2^{j,(k)}](x)\right|,$$
$$\leqslant R\|\nabla w_*^{(k)}\|_\infty + C\sum_{j\neq i}\frac{R}{d_{ij}}\max(|W_1^{j,(k)}|, |W_2^{j,(k)}|),$$
$$\lesssim R\|\nabla w_*^{(k)}\|_\infty + \left(\sum_{j\neq i,1}\frac{R}{d_{ij}}\eta^{k-1}\frac{R}{d_{1j}^2} + \frac{R}{d_{1i}}\eta^{k-1}\frac{R}{d_{\min}}\right)|x_-^1||W|.$$

where $\eta = 2Cr_0L < 1$ is the constant appearing in Proposition 2.3.4. Reproducing the same computations as before yields:

$$\|w_*^{(k+1)}\|_{L^\infty(B_i)} \lesssim R\|\nabla w_*^{(k)}\|_\infty + \frac{R}{d_{1i}^2}|x_-^1|\eta^{k-1}|W|.$$

In the case $i=1$ we have:

$$
\begin{aligned}
|w_*^{(k+1)}(x)| &= \left| w_*^{(k)}(x) - w_*^{(k)}(x_\alpha^i) - \sum_{j\neq i} U[W_1^{j,(k)}, W_2^{j,(k)}](x) \right|, \\
&\leqslant R\|\nabla w_*^{(k)}\|_\infty + C\sum_{j\neq 1}\frac{R}{d_{1j}} \max(|W_1^{j,(k)}|, |W_2^{j,(k)}|), \\
&\lesssim R\|\nabla w_*^{(k)}\|_\infty + \sum_{j\neq 1}\frac{R}{d_{1j}}\eta^{k-1}\frac{R}{d_{1j}^2}|x_-^1||W|, \\
&\lesssim R\|\nabla w_*^{(k)}\|_\infty + \frac{R}{d_{\min}}|x_-^1|\eta^{k-1}|W|.
\end{aligned}
$$

□

Thanks to these estimates we have the following convergence rate:

Proposition 2.3.7.

$$
\lim_{k\to\infty}\|\nabla U[w_*^{(k+1)}]\|_2 \lesssim R|x_-^1||W|.
$$

Proof. Reproducing exactly the same proof as in [57, Proposition 3.4], the main difference appears in the last estimate where we apply Proposition 2.3.6:

$$
\begin{aligned}
\|\nabla U[w_*^{(k+1)}]\|_2^2 &\lesssim R^3\sum_i \left(\|\nabla w_*^{(k+1)}\|_{L^\infty(B_i)} + \frac{1}{R}\|w_*^{(k+1)}\|_{L^\infty(B_i)}\right)^2, \\
&\lesssim R^3\Bigg[\sum_{i\neq 1}\left(\frac{R^2}{d_{1i}^6} + \frac{1}{d_{1i}^4}\eta^{2(k-1)}\right) \\
&+ \frac{R^2}{d_{\min}^2}\left(\frac{W_\infty^3}{d_{\min}^3} + |\log W_\infty|\right)^2 + \frac{1}{d_{\min}^2}\eta^{2(k-1)}\Bigg]|x_-^1|^2|W|^2, \\
&\lesssim \left(\frac{R^4}{d_{\min}^3} + \frac{R^2}{d_{\min}}\eta^{2(k-1)}\right)\left(\frac{W_\infty^3}{d_{\min}^3} + |\log W_\infty|\right)|x_-^1|^2|W|^2 \\
&+ |x_-^1|^2|W|^2\frac{R^5}{d_{\min}^2}\left(\frac{W_\infty^3}{d_{\min}^3} + |\log W_\infty|\right)^2 + \frac{R^3}{d_{\min}^2}\eta^{2(k-1)}|x_-^1|^2|W|^2.
\end{aligned}
$$

Taking the limit when k goes to infinity we get:

$$
\|\nabla U[w_*^{(k+1)}]\|_2^2 \lesssim R^2|x_-^1|^2|W|^2\left\{\frac{R^2}{d_{\min}^3}\left(\frac{W_\infty^3}{d_{\min}^3} + |\log W_\infty|\right) + \frac{R^3}{d_{\min}^2}\left(\frac{W_\infty^3}{d_{\min}^3} + |\log W_\infty|\right)^2\right\}.
$$

The term inside brackets is bounded as follows:

$$
\begin{aligned}
&\frac{R^2}{d_{\min}^3}\left(\frac{W_\infty^3}{d_{\min}^3} + |\log W_\infty|\right) + \frac{R^3}{d_{\min}^2}\left(\frac{W_\infty^3}{d_{\min}^3} + |\log W_\infty|\right)^2 \\
&\qquad\leqslant \frac{R^2}{d_{\min}^2}\frac{W_\infty^3}{d_{\min}^2} + R|\log W_\infty| + \frac{R}{d_{\min}^2}\left(\frac{R}{d_{\min}}\frac{W_\infty^3}{d_{\min}^2} + R|\log W_\infty|\right)^2,
\end{aligned}
$$

we recall that $\frac{R}{d_{\min}} < +\infty$ and $\frac{R}{d_{\min}^2} \leqslant \frac{r_0}{2}\|\varrho_0\|_{L^\infty\cap L^1}\frac{W_\infty^3}{d_{\min}^2}$ according to (2.12). □

Second case

Given $W \in \mathbb{R}^3$ we consider in this part w the unique solution to the Stokes equation (2.2) completed with the following boundary conditions :

$$w = \left\{ \begin{array}{rl} W & \text{on } B(x_1^1, R), \\ W & \text{on } B(x_2^1, R), \\ 0 & \text{on } B(x_1^i, R) \cup B(x_2^i, R),\ i \neq 1. \end{array} \right. \tag{2.42}$$

Denote by $U_\alpha^{i,(p)}$, $\alpha = 1, 2$, $1 \leqslant i \leqslant N$, $p \in \mathbb{N}$ the velocities obtained from the method of reflections applied to the velocity field w. In other words :

$$w = \sum_{p=0}^{\infty} \sum_i U[W_1^{i,(p)}, W_2^{i,(p)}] + O(R).$$

We aim to show that, in this special case, the sequence of velocities $W_\alpha^{i,(p)}$ are also smaller than the general case. This is due to the initial boundary conditions which vanish for $i \neq 1$. Indeed we have :

Proposition 2.3.8. *There exists two positive constants $C, L > 0$ such that :*

$$\begin{aligned} \max_{\alpha=1,2} |W_\alpha^{i,(p+1)}| &\leqslant C(2Cr_0 L \|\varrho_0\|_{L^\infty \cap L^1})^p \frac{R}{|x_+^1 - x_+^i|} |W| \,,\ i \neq 1 \,,\ p \geqslant 0, \\ \max_\alpha |W_\alpha^{1,(p+1)}| &\leqslant C 2^{p-1} (r_0 C L \|\varrho_0\|_{L^\infty \cap L^1})^p R \,|W| \,,\ p \geqslant 1, \\ \max_\alpha |W_\alpha^{1,(1)}| &= 0, \end{aligned}$$

for N large enough.

Proof. The proof is analogous to the one of Proposition 2.3.4. □

According to these estimates, if we assume that $r_0 \|\varrho_0\|_{L^\infty \cap L^1}$ is small enough to have $2LCr_0 \|\varrho_0\|_{L^\infty \cap L^1} < 1$ then the following result holds true:

Corollary 2.3.9. *Under the assumption that $r_0 \|\varrho_0\|_{L^\infty \cap L^1}$ is small enough we have for N large enough:*

$$\begin{aligned} \sum_{k=0}^{\infty} \max_{\alpha=1,2} |W_\alpha^{i,(p+1)}| &\lesssim \frac{R}{|x_+^1 - x_+^i|} |W| \,,\ i \neq 1, \\ \sum_{k=0}^{\infty} \max_\alpha |W_\alpha^{1,(p+1)}| &\lesssim R \,|W|. \end{aligned}$$

2.4 Extraction of the first order terms for the velocities

In this section, we apply the method of reflections to the velocity field u^N as presented above and we set :

$$\sum_{p=0}^{\infty} U_\alpha^{i,(p)} = U_\alpha^{i,\infty}, 1 \leqslant \alpha \leqslant 2\,,\, 1 \leqslant i \leqslant N,$$

we also use the following notations for the forces associated to the solutions $U[U_1^{i,\infty}, U_2^{i,\infty}]$:

$$\begin{aligned} F_1^{i,\infty} &= -6\pi R(A_1(\xi_i)U_1^{i,\infty} + A_2(\xi_i)U_2^{i,\infty}), \\ F_2^{i,\infty} &= -6\pi R(A_2(\xi_i)U_1^{i,\infty} + A_1(\xi_i)U_2^{i,\infty}). \end{aligned} \tag{2.43}$$

2.4.1 Preliminary estimates

Proposition 2.4.1. *If assumptions* (2.7), (2.8) (2.9) *hold true and* $r_0\|\varrho_0\|_{L^\infty \cap L^1}$ *is small enough we have for* N *large enough and for all* $1 \leqslant i \leqslant N$

$$\begin{aligned} \frac{U_1^i + U_2^i}{2} &= (A_1(\xi_i) + A_2(\xi_i))^{-1} \frac{m}{6\pi R} g \\ &\quad + \frac{1}{2} \sum_{j \neq i} \big(U[U_1^{j,\infty}, U_2^{j,\infty}](x_1^1) + U[U_1^{j,\infty}, U_2^{j,\infty}](x_2^1) \big) + O(R) \max_{\substack{1 \leqslant i \leqslant N \\ \alpha = 1,2}} |U_\alpha^i|. \end{aligned}$$

$$\frac{U_1^{i,\infty} + U_2^{i,\infty}}{2} = (A_1(\xi_i) + A_2(\xi_i))^{-1} \frac{m}{6\pi R} g + O(R) \max_{\substack{1 \leqslant i \leqslant N \\ \alpha = 1,2}} |U_\alpha^i|.$$

Proof. We prove the formula for $i = 1$ and the same holds true for all $1 \leqslant i \leqslant N$. We set w the unique solution to the Stokes equation (2.2) completed with the following boundary conditions :

$$w = \begin{cases} W & \text{on } B(x_1^1, R), \\ W & \text{on } B(x_2^1, R), \\ 0 & \text{on } B(x_1^i, R) \cup B(x_2^i, R),\ i \neq 1, \end{cases} \tag{2.44}$$

with W an arbitrary vector of $\mathbb{R}^3$. We use the method of reflections to obtain :

$$\begin{aligned} 2mg \cdot W &= 2 \int D(u^N) : \nabla w \\ &= -(F_1^{1,\infty} + F_2^{1,\infty}) \cdot W + \lim_{k \to \infty} 2 \int D\left(U[u_*^{(k+1)}] \right) : \nabla w. \end{aligned}$$

For the last term we apply again the method of reflections to the velocity field w, see Section 2.3.1. We set:

$$w_1 = \sum_{p=0}^{k} \sum_{i=1}^{N} U[W_1^{i,(p)}, W_2^{i,(p)}],$$

with

$$\|\nabla w - \nabla w_1\|_{L^2(\mathbb{R}^3 \setminus \cup \overline{B}_i} \leqslant R|W|.$$

We obtain :

$$2\int D\left(U[u_*^{(k+1)}]\right) : \nabla w = 2\int \nabla U[u_*^{(k+1)}] : D\,(w_1) + 2\int D\left(U[u_*^{(k+1)}]\right) : \nabla (w - w_1).$$

Thanks to the method of reflections, the second term on the right hand side can be bounded by $R^2|W|\max\limits_{\substack{1\leqslant i\leqslant N\\ \alpha=1,2}}|U_\alpha^i|$ (see Proposition 2.3.3). For the first term we write :

$$\begin{aligned}\lim_{k\to\infty} 2\int D\left(U[u_*^{(k+1)}]\right) : \nabla w_1 = &\\ -\sum_{p=0}^{\infty}\sum_j\sum_i \int_{\partial B(x_1^i,R)\cup\partial B(x_2^i,R)} &\sigma(U[W_1^{j,(p)}, W_2^{j,(p)}])n\, U[u_*^{(k+1)}].\end{aligned}$$

We have

$$\begin{aligned}\|\sigma(U[W_1^{j,(p)}, W_2^{j,(p)}])\|_{L^\infty(\partial B(x_1^i,R)\cup\partial B(x_2^i,R))} &\lesssim \frac{R}{d_{ij}^2}\max(|W_1^{j,(p)}|, |W_2^{j,(p)}|)\ ,\ \forall i\neq j,\\ \|\sigma(U[W_1^{i,(p)}, W_2^{i,(p)}])\|_{L^\infty(\partial B(x_1^i,R)\cup\partial B(x_2^i,R))} &\lesssim \frac{\max(|W_1^{i,(p)}|, |W_2^{i,(p)}|)}{R}.\end{aligned}$$

for the sake of clarity we set

$$\Gamma_{i,j} := \sum_{p=0}^{\infty}\|\sigma(U[W_1^{j,(p)}, W_2^{j,(p)}])\|_{L^\infty(\partial B(x_1^i,R)\cup\partial B(x_2^i,R))}.$$

We have then

$$\lim_{k\to\infty}\left|\int \nabla U[u_*^{(k+1)}] : D\,(w_1)\right| \lesssim 4\pi R^2\left(\sum_i\sum_j \Gamma_{i,j}\right)\overline{\lim_{k\to\infty}}\|u_*^{(k+1)}\|_\infty.$$

Recall that $\|u_*^{(k+1)}\|_\infty = O(R)\max\limits_{\substack{1\leqslant i\leqslant N\\ \alpha=1,2}}|U_\alpha^i|$ when k goes to infinity. Thus, we focus only on the remaining terms by splitting the sum as follow :

$$\sum_i\sum_j\Gamma_{i,j} = \sum_{i\neq 1}\left(\sum_{j\neq 1,i}\Gamma_{i,j} + \Gamma_{i,i} + \Gamma_{i,1}\right) + \sum_{j\neq 1}\Gamma_{1,j} + \Gamma_{1,1}.$$

For the first term, we have thanks to Corollary 2.3.9 and the estimates for $\Gamma_{i,j}$:

$$\begin{aligned}\sum_{i\neq 1}\left(\sum_{j\neq 1,i}\Gamma_{i,j} + \Gamma_{i,i} + \Gamma_{i,1}\right) &\lesssim \sum_{i\neq 1}\Big(\sum_{j\neq 1,i}\frac{R}{d_{ij}^2}\frac{R}{d_{j1}} + \frac{1}{R}\frac{R}{d_{i1}} + \frac{R}{d_{i1}^2}R\Big)|W|,\\ &\lesssim \sum_{i\neq 1}\frac{1}{d_{i1}}|W|.\end{aligned}$$

For the second term we have:

$$\sum_{j\neq 1}\Gamma_{1,j} \lesssim \sum_{j\neq 1}\frac{R}{d_{1j}^2}\frac{R}{d_{1j}}|W| \lesssim |W|.$$

The third term gives finally:

$$\Gamma_{1,1} \lesssim \frac{1}{R}R|W| \lesssim |W|.$$

Gathering all the inequalities we obtain:

$$\lim_{k\to\infty}\left|\int U[u_*^{(k+1)}] : \nabla w_1\right| \lesssim R^3\left(\sum_{i\neq 1}\frac{1}{d_{i1}}\right)|W|\max_{\substack{1\leqslant i\leqslant N\\ \alpha=1,2}}|U_\alpha^i| \lesssim R^2|W|\max_{\substack{1\leqslant i\leqslant N\\ \alpha=1,2}}|U_\alpha^i|.$$

Finally, we have:

$$2mg\cdot W = -(F_1^{1,\infty}+F_2^{1,\infty})\cdot W + O(R^2)|W|\max_{\substack{1\leqslant i\leqslant N\\ \alpha=1,2}}|U_\alpha^i|.$$

This being true for all $W\in\mathbb{R}^3$ it yields:

$$2mg = -(F_1^{1,\infty}+F_2^{1,\infty}) + O(R^2)\max_{\substack{1\leqslant i\leqslant N\\ \alpha=1,2}}|U_\alpha^i|.$$

Using the definitions of $F_1^{1,\infty}$ and $F_2^{1,\infty}$, see (2.43), this becomes:

$$2mg = 6\pi R(A_1(\xi_1)+A_2(\xi_1))(U_1^{1,\infty}+U_2^{1,\infty}) + O(R^2)\max_{\substack{1\leqslant i\leqslant N\\ \alpha=1,2}}|U_\alpha^i|.$$

Recall that $A_1(\xi)$ and $A_2(\xi)$ are of the form $h_1(|\xi|)\mathbb{I}+h_2(|\xi|)\frac{\xi\otimes\xi}{|\xi|^2}$. Moreover, according to formulas (2.27) A_1+A_2 (resp. A_1-A_2) is invertible and its inverse is (a_1+a_2) (resp. a_1-a_2). Thus :

$$U_1^{1,\infty}+U_2^{1,\infty} = 2(A_1(\xi_1)+A_2(\xi_1))^{-1}\frac{m}{6\pi R}g + \frac{1}{6\pi}(A_1(\xi_1)+A_2(\xi_1))^{-1}O(R)\max_{\substack{1\leqslant i\leqslant N\\ \alpha=1,2}}|U_\alpha^i|. \quad (2.45)$$

We use the fact that $\|(A_1(\xi_1)+A_2(\xi_1))^{-1}\|$ is uniformly bounded independently of the particles and N to get

$$U_1^{1,\infty}+U_2^{1,\infty} = 2(A_1(\xi_1)+A_2(\xi_1))^{-1}\frac{m}{6\pi R}g + O(R)\max_{\substack{1\leqslant i\leqslant N\\ \alpha=1,2}}|U_\alpha^i|.$$

On the other hand, as $(U_1^{1,(0)},U_2^{1,(0)}) = (U_1^1,U_2^1)$ we rewrite formula (2.45) as :

$$U_1^1+U_2^1 = -\sum_{p=1}^{\infty}(U_1^{1,(p)}+U_2^{1,(p)}) + (A_1(\xi_1)+A_2(\xi_1))^{-1}\frac{m}{6\pi R}g$$
$$+ 2\frac{1}{6\pi}(A_1(\xi_1)+A_2(\xi_1))^{-1}O(R)\max_{\substack{1\leqslant i\leqslant N\\ \alpha=1,2}}|U_\alpha^i|.$$

Using again formula (2.39) this yields :

$$
\begin{aligned}
U_1^1 + U_2^1 &= \sum_{p=1}^{\infty}\sum_{j\neq 1} U[U_1^{j,(p-1)}, U_2^{j,(p-1)}](x_1^1) + U[U_1^{j,(p-1)}, U_2^{j,(p-1)}](x_2^1),\\
&+ 2(A_1(\xi_1) + A_2(\xi_1))^{-1}\frac{m}{6\pi R}g + \frac{1}{6\pi}(A_1(\xi_1) + A_2(\xi_1))^{-1}O(R)\max_{\substack{1\leqslant i\leqslant N\\ \alpha=1,2}}|U_\alpha^i|,\\
&= \sum_{j\neq 1}\left(U[U_1^{j,\infty}, U_2^{j,\infty}](x_1^1) + U[U_1^{j,\infty}, U_2^{j,\infty}](x_2^1)\right) + 2(A_1(\xi_1) + A_2(\xi_1))^{-1}\frac{m}{6\pi R}g,\\
&+ \frac{1}{6\pi}(A_1(\xi_1) + A_2(\xi_1))^{-1}O(R)\max_{\substack{1\leqslant i\leqslant N\\ \alpha=1,2}}|U_\alpha^i|.
\end{aligned}
$$

We conclude by emphasizing that $\|(A_1 + A_2)^{-1}\|$ can be uniformly bounded. $\square$

Applying the same ideas we obtain the following result:

Proposition 2.4.2. *for all* $1 \leqslant i \leqslant N$ *we have :*

$$
U_1^i - U_2^i = \sum_{j\neq i}\left(U[U_1^{j,\infty}, U_2^{j,\infty}](x_1^i) - U[U_1^{j,\infty}, U_2^{j,\infty}](x_2^i)\right) + O(R|x_-^i|)\max_{\substack{1\leqslant i\leqslant N\\ \alpha=1,2}}|U_\alpha^i|.
$$

$$
U_1^{i,\infty} - U_2^{i,\infty} = O(R|x_-^i|)\max_{\substack{1\leqslant i\leqslant N\\ \alpha=1,2}}|U_\alpha^i|.
$$

Proof. The proof is analogous to the one of Proposition 2.4.1. The idea is to consider this time w the unique solution to the Stokes equation (2.2) completed with the following boundary conditions :

$$
w = \begin{cases} W & \text{on } B(x_1^1, R),\\ -W & \text{on } B(x_2^1, R),\\ 0 & \text{on } B(x_1^i, R) \cup B(x_2^i, R),\ i \neq 1, \end{cases} \tag{2.46}
$$

with W an arbitrary vector of $\mathbb{R}^3$. Using the method of reflections, Propositions 2.3.7 and 2.3.3 we obtain the desired result. $\square$

2.4.2 Estimates for $\dot{x}_+^i$

Propositions 2.4.1 and 2.4.2 yields the following result:

Corollary 2.4.3. *For all* $1 \leqslant i \leqslant N$ *we have :*

$$
U_+^i := (\mathbb{A}(\xi_i))^{-1}\frac{m}{6\pi R}g + \frac{6\pi r_0}{N}\sum_{j\neq i}\Phi(x_+^i - x_+^j)\kappa g + O(R),
$$

where $\mathbb{A} = A_1 + A_2$.

Proof. First of all, from Propositions 2.4.1 and 2.4.2 we can show that the velocities U_α^i are uniformly bounded with respect to N for all $1 \leqslant i \leqslant N$ and $\alpha = 1, 2$. Indeed, using formula (2.39) together with the decay properties (2.33) and Propositions 2.4.1 and 2.4.2 we have :

$$\begin{aligned}
\max_{\substack{\alpha=1,2\\1\leqslant i\leqslant N}} |U_\alpha^i| &\leqslant \max_{1\leqslant i\leqslant N} (|U_+^i| + |U_-^i|),\\
&\lesssim 1 + \max_{1\leqslant i\leqslant N} (|U_+^{i,\infty}| + |U_-^{i,\infty}|) + O(R) \max_{\substack{\alpha=1,2\\1\leqslant i\leqslant N}} |U_\alpha^i|,\\
&\lesssim 1 + O(R) \max_{\substack{\alpha=1,2\\1\leqslant i\leqslant N}} |U_\alpha^i|.
\end{aligned}$$

This allows us to bound the terms $\max\limits_{\substack{\alpha=1,2\\1\leqslant i\leqslant N}} |U_\alpha^i|$ by a constant independent of N in the estimates of Propositions 2.4.1 and 2.4.2. From Proposition 2.4.2 we have

$$U_+^i = (A_1(\xi_i) + A_2(\xi_i))^{-1} \frac{m}{6\pi R} g + \frac{1}{2} \sum_{j\neq i} \big(U[U_1^{j,\infty}, U_2^{j,\infty}](x_1^1) + U[U_1^{j,\infty} + U_2^{j,\infty}](x_2^1) \big) + O(R),$$

with:

$$\begin{aligned}
U[U_1^{j,\infty}, U_2^{j,\infty}](x_1^1) + U[U_1^{j,\infty}, U_2^{j,\infty}](x_2^1) &= -\Phi(x_1^1 - x_1^j) F_1^{j,\infty} - \Phi(x_1^1 - x_2^j) F_2^{j,\infty}\\
&\quad - \Phi(x_2^1 - x_1^j) F_1^{j,\infty} - \Phi(x_2^1 - x_2^j) F_2^{j,\infty},\\
&= -(\Phi(x_1^1 - x_1^j) + \Phi(x_2^1 - x_1^j)) F_1^{j,\infty}\\
&\quad - (\Phi(x_1^1 - x_2^j) + \Phi(x_2^1 - x_2^j)) F_2^{j,\infty},
\end{aligned}$$

recall that:

$$\left\{ \begin{array}{lcl} F_1^{j,\infty} & = & F_+^{j,\infty} + F_-^{j,\infty} \\ F_2^{j,\infty} & = & F_+^{j,\infty} - F_-^{j,\infty} \end{array} \right., \quad \left\{ \begin{array}{lcl} F_+^{j,\infty} & = & -mg + O(R^2) \\ F_-^{j,\infty} & = & O(R^2) \end{array} \right.$$

see proof of Propositions 2.4.2 and 2.4.1. Hence, we replace F_1^j and F_2^j by their formula and bound the sum of terms involving the error term $O(R^2)$ by $O(R)$. We get

$$\begin{aligned}
&\sum_{j\neq i} U[U_1^{j,\infty}, U_2^{j,\infty}](x_1^1) + U[U_1^{j,\infty}, U_2^{j,\infty}](x_2^1) =\\
&\qquad 6\pi R \sum_{j\neq i} (\Phi(x_1^1 - x_1^j) + \Phi(x_2^1 - x_1^j) + \Phi(x_1^1 - x_2^j) + \Phi(x_2^1 - x_2^j)) \kappa g + O(R), \quad (2.47)
\end{aligned}$$

where $mg = 6\pi R\kappa g$. Now the idea is to replace each of the four terms by $\Phi(x_+^1 - x_+^j)$. Direct computations shows that for all $1 \leqslant \alpha, \beta \leqslant 2$ we have:

$$|x_\alpha^1 - x_\beta^j - x_+^1 + x_+^j| \leqslant |x_-^1| + |x_-^j|$$

which yields for all $1 \leqslant \alpha, \beta \leqslant 2$:

$$|\Phi(x_\alpha^1 - x_\beta^j) - \Phi(x_+^1 - x_+^j)| \lesssim \frac{|x_-^1| + |x_-^j|}{|x_+^1 - x_+^j|^2}.$$

Hence the error term can be bounded by $(|x_-^i| + |x_-^j|)$ which is of order R. $\square$

2.4.3 Estimates for $\dot{x}^i_-$

Analogously, Propositions 2.4.1 and 2.4.2 yields the following result:

Corollary 2.4.4. *For all* $1 \leqslant i \neq N$ *we have:*

$$\frac{U_1^i - U_2^i}{2} = \left(\frac{6\pi r_0}{N}\sum_{j\neq i}\nabla\Phi(x_+^i - x_+^j)\kappa g\right)\cdot x_-^i + O\left(|x_-^i| d_{\min}\right).$$

Proof. The first formula of Proposition 2.4.2 together with the uniform bound on the velocities (U_+^i, U_-^i), see proof of Corollary 2.4.3, yields:

$$U_1^i - U_2^i = \sum_{j\neq i} U[U_1^{j,\infty}, U_2^{j,\infty}](x_1^i) - U[U_1^{j,\infty}, U_2^{j,\infty}](x_2^i) + O(R|x_-^i|).$$

We want to estimate the first term, we have:

$$\begin{aligned}
U[U_1^{j,\infty}, U_2^{j,\infty}](x_1^i) - U[U_1^{j,\infty}, U_2^{j,\infty}](x_2^i) &= -\Phi(x_1^i - x_1^j)F_1^{j,\infty} - \Phi(x_1^i - x_2^j)F_2^{j,\infty}\\
&+ \Phi(x_2^i - x_1^j)F_1^{j,\infty} + \Phi(x_2^i - x_2^j)F_2^{j,\infty},\\
&\\
&= -\left(\Phi(x_1^i - x_1^j) - \Phi(x_2^i - x_1^j)\right)F_1^{j,\infty}\\
&- (\Phi(x_1^i - x_2^j) - \Phi(x_2^i - x_2^j))F_2^{j,\infty},\\
&\\
&= -2[\nabla\Phi(x_2^i - x_1^j)\cdot x_-^i]F_1^{j,\infty}\\
&+ 2[\nabla\Phi(x_2^i - x_2^j)\cdot x_-^i]F_2^{j,\infty} + \mathcal{E}_{i,j}^1,\\
&\\
&= -2[\nabla\Phi(x_+^i - x_+^j)\cdot x_-^i](F_1^{j,\infty} + F_2^{j,\infty}) + \mathcal{E}_{i,j}^1 + \mathcal{E}_{i,j}^2.
\end{aligned}$$

Now recall that, from the proof of Proposition 2.4.1 we have:

$$F_1^{j,\infty} + F_2^{j,\infty} = -2mg + O(R^2).$$

Thus, we get the following formula:

$$U[U_1^{j,\infty}, U_2^{j,\infty}](x_1^i) - U[U_1^{j,\infty}, U_2^{j,\infty}](x_2^i) = 2[\nabla\Phi(x_+^i - x_+^j)\cdot x_-^i]mg + \mathcal{E}_{i,j}^1 + \mathcal{E}_{i,j}^2 + \mathcal{E}_j^3,$$

with

$$\mathcal{E}_j^3 = -2[\nabla\Phi(x_+^i - x_+^j)\cdot x_-^i](F_1^{j,\infty} + F_2^{j,\infty} + 2mg).$$

Finally we obtain:

$$\frac{U_1^i - U_2^i}{2} = \sum_{j\neq i}[\nabla\Phi(x_+^i - x_+^j)\cdot x_-^i]mg + \frac{1}{2}\sum_{j\neq i}\mathcal{E}_{i,j}^1 + \mathcal{E}_{i,j}^2 + \mathcal{E}_j^3 + O(R|x_-^i|).$$

It remains to bound the error terms. We begin by the first one:

$$|\mathcal{E}^1_{i,j}| \leqslant 2\left(\sup_{y\in[x^i_1,x^i_2]}\left(|\nabla^2\Phi(x^j_1-y)|+|\nabla^2\Phi(x^j_2-y)|\right)\right)|x^i_-|^2(|F^{j,\infty}_1|+F^{j,\infty}_2|).$$

We emphasize that for all $y\in[x^i_1,x^i_2]$:

$$|y-x^j_1|\geqslant|x^i_1-x^j_1|-|x^i_1-y|\geqslant|x^i_1-x^j_1|-2|x^i_-|\geqslant\frac{1}{4}|x^i_+-x^j_+|,$$

where we used the fact that

$$|x^i_-|\leqslant\frac{C}{R}\leqslant\frac{1}{8}d_{\min}\leqslant\frac{1}{8}|x^i_+-x^j_+|,$$

and

$$|x^i_1-x^j_1|\geqslant\frac{1}{2}|x^i_+-x^j_+|,$$

This yields :

$$\sum_{j\neq i}|\mathcal{E}^1_{i,j}|\leqslant C\sum_{j\neq i}\frac{1}{d^3_{ij}}|x^i_-|^2R\kappa|g|\leqslant C|x^i_-|\frac{R}{d_{\min}}\left(\sum_{j\neq i}\frac{R}{d^2_{ij}}\right)\leqslant C|x^i_-|\frac{R}{d_{\min}}\leqslant Cd_{\min}|x^i_-|.$$

For the second error term we have:

$$\begin{aligned}\mathcal{E}^2_{i,j}=-2[\nabla\Phi(x^i_2-x^j_1)-\nabla\Phi(x^i_+-x^j_+)]\cdot x^i_-\cdot F^{j,\infty}_1&\\ -[\nabla\Phi(x^i_2-x^j_2)-\nabla\Phi(x^i_+-x^j_+)]\cdot x^i_-\cdot F^{j,\infty}_2,&\end{aligned}$$

where

$$|\nabla\Phi(x^i_2-x^j_1)-\nabla\Phi(x^i_+-x^j_+)|\leqslant C\left(\frac{1}{|x^i_2-x^j_1|^3}+\frac{1}{|x^i_+-x^j_+|^3}\right)|x^i_-+x^j_-|$$

As $|x^j_-|\sim R\sim|x^i_-|$ the second error term is bounded by:

$$\sum_{j\neq i}|\mathcal{E}^2_{i,j}|\leqslant C\sum_{j\neq i}\frac{1}{d^3_{ij}}|x^i_-|^2R\kappa|g|,$$

which yields the same estimate as for the first error term. Finally, the last error term gives:

$$\begin{aligned}\sum_{j\neq i}|\mathcal{E}^3_{i,j}|&\leqslant 2|\nabla\Phi(x^i_+-x^j_+)|\,|x^i_-|\,|F^{j,\infty}_1+F^{j,\infty}_2+2mg|,\\ &\leqslant CR^2.\end{aligned}$$

where we used the fact that $F^{j,\infty}_1+F^{j,\infty}_2=-2mg+O(R^2)$ and $|x^i_-|\sim R$. □

2.5 Proof of Theorem 2.1.1

In order to derive the transport-Stokes equation satisfied at the limit, the idea is to show that the discrete density μ^N satisfies weakly a transport equation. We introduce the following notations. Given a density ϱ, we define the operator $\mathcal{K}\varrho$ as:

$$\mathcal{K}\varrho(x) := 6\pi r_0 \int_{\mathbb{R}^3} \Phi(x-y)\kappa g\, \varrho(dy).$$

The operator is well defined and is Lipschitz in the case where $\varrho \in L^1 \cap L^\infty$. Moreover, note that $\mathcal{K}\varrho$ satisfies the Stokes equation

$$-\Delta\mathcal{K}(\varrho) + \nabla p = 6\pi r_0 \kappa g \varrho,$$

on $\mathbb{R}^3$. Analogously, we define $\mathcal{K}^N\varrho^N$ as:

$$\mathcal{K}^N\varrho^N(x) := 6\pi r_0 \int_{\mathbb{R}^3} \chi\Phi(x-y)\kappa g\, \varrho^N(dy),$$

where $\chi\Phi(\cdot) = \chi\left(\frac{\cdot}{d_{\min}}\right)\Phi(\cdot)$, χ is a truncation function such that $\chi = 0$ on $B(0,1/4)$ and $\chi = 1$ on ${}^cB(0,1/2)$.

2.5.1 Derivation of the transport-Stokes equation

The transport equation satisfied by μ^N is obtained directly using the ODE system derived for each couple (x_+^i, ξ_i). We recall that:

$$\begin{aligned} U_+^i &= (\mathbb{A}(\xi_i))^{-1}\kappa g + \mathcal{K}^N\varrho^N(x_+^i) + O(R), \\ \frac{U_-^i}{R} &= \nabla\mathcal{K}^N\varrho^N(x_+^i)\cdot\xi_i + O\left(d_{\min}\right). \end{aligned}$$

Following the idea of [57, Section 5.2], one can show that we can construct two divergence-free velocity fields E^N and $\tilde{E}^N$ such that :

$$\begin{aligned} U_+^i &= (\mathbb{A}(\xi_i))^{-1}\kappa g + \mathcal{K}^N\varrho^N(x_+^i) + E^N(x_+^i), \\ \frac{U_-^i}{R} &= \nabla\mathcal{K}^N\varrho^N(x_+^i)\cdot\xi_i + \tilde{E}^N\left(\xi_i\right), \end{aligned} \tag{2.48}$$

and there exists a positive constant independent of N such that

$$\|E^N\|_\infty = O(R), \quad \|\tilde{E}^N\|_\infty = O\left(d_{\min}\right), \quad \|\nabla E^N\|_\infty + \|\nabla\tilde{E}^N\|_\infty < C. \tag{2.49}$$

This construction yields the following result

Proposition 2.5.1. *μ^N satisfies weakly the transport equation:*

$$\partial_t\mu^N + \mathrm{div}_x[(\mathbb{A}(\xi))^{-1}\kappa g\mu^N + \mathcal{K}^N\varrho^N(x)\mu^N + E^N\mu^N] + \mathrm{div}_\xi[\nabla\mathcal{K}^N\varrho^N(x)\cdot\xi\mu^N + \tilde{E}^N\mu^N] = 0. \tag{2.50}$$

We can prove now Theorem 2.1.1.

2.5.2 proof of Theorem 2.1.1

The proof is a corollary of Proposition 2.5.1. Indeed, we want to show that for all $\psi \in \mathcal{C}_c^\infty(\mathbb{R}^3)$ we have:

$$\int_0^T \int_{\mathbb{R}^3\times\mathbb{R}^3} \Big\{\partial_t \psi(t,x,\xi) + \nabla_x \psi(t,x,\xi)\cdot[(\mathbb{A}(\xi))^{-1}\kappa g + 2\mathcal{K}\varrho(x)))] \\ + \nabla_\xi \psi(t,x,\xi)\cdot[\nabla\mathcal{K}\varrho(x)\cdot\xi]\Big\}\mu(t,dx,d\xi)dt. \quad (2.51)$$

which is obtained directly by passing through the limit in each term of formula (2.50). Indeed we recall that we have the following estimates:

$$\begin{array}{rcl} \|\mathcal{K}^N\varrho^N - \mathcal{K}\varrho\|_\infty & \lesssim & W_\infty, \\ \|\nabla\mathcal{K}^N\varrho^N - \nabla\mathcal{K}\varrho\|_\infty & \lesssim & W_\infty(1+|\log W_\infty|), \\ \|E^N\|_\infty = O(R) & , & \|\tilde{E}^N\|_\infty = O(d_{\min}). \end{array}$$

2.6 Proof of theorem 2.1.2 and 2.1.3

This section is devoted to the proof of Theorem 2.1.2 and 2.1.3. The Lipschitz-like estimates proved in Proposition 2.B.3 suggests a correlation between the vectors along the line of centers ξ_i and the centers x_+^i. In this section, we show in particular that this correlation is well propagated in time.

2.6.1 Derivation of the transport-Stokes equation

We assume now that there exists a lipschitz function F_0 such that

$$\xi_i(0) = F_0(x_+^i(0)),\ 1 \leqslant i \leqslant N,$$

which means that $\mu_0^N = \varrho_0^N \otimes \delta_{F_0}$. In order to propagate this correlation we search for a function $F^N(t,\cdot) \in W^{1,\infty}$ such that for all $t \in [0,T]$ we have

$$\xi_i(t) = F^N(t, x_+^i(t)),\ 1 \leqslant i \leqslant N.$$

According to the ODE satisfied by ξ_i, see (2.48), F^N must satisfy the following equation

$$\left\{\begin{array}{rcl} \partial_t F^N + \nabla F^N \cdot (\mathbb{A}(F^N)^{-1}\kappa g + \mathcal{K}^N\varrho^N + E^N) & = & \nabla\mathcal{K}^N\varrho^N \cdot F^N + \tilde{E}^N(F^N), \\ F^N(0,\cdot) & = & F_0. \end{array}\right.$$

The following proposition shows the existence and uniqueness of F^N.

Proposition 2.6.1. *There exists $T > 0$ such that for all $N \in \mathbb{N}^*$, there exists a unique (local) solution $F^N \in L^\infty(0,T;W^{1,\infty}(\mathbb{R}^3))$ of the following equation*

$$\left\{\begin{array}{rcl} \partial_t F^N + \nabla F^N \cdot (\mathbb{A}(F^N)^{-1}\kappa g + \mathcal{K}^N\varrho^N + E^N) & = & \nabla\mathcal{K}^N\varrho^N \cdot F^N + \tilde{E}^N(F^N), \\ F^N(0,\cdot) & = & F_0. \end{array}\right. \quad (2.52)$$

Proof. The idea is to apply a fixed-point argument. We define the mapping $\mathcal{A}$ which associates to any $F \in L^\infty(0,T;W^{1,\infty}(\mathbb{R}^3))$ the unique solution $\mathcal{A}(F) = \hat{F}$ to the transport equation

$$\begin{cases} \partial_t \hat{F} + \nabla\hat{F}\cdot(\mathbb{A}(F)^{-1}\kappa g + \mathcal{K}^N\varrho^N + E^N) &= \nabla\mathcal{K}^N\varrho^N\cdot F + \tilde{E}^N(F), \\ \hat{F}(0,\cdot) &= F_0. \end{cases} \tag{2.53}$$

We define X^N as the characteristic flow :

$$\begin{cases} \partial_s X^N(s,t,x) &= \mathbb{A}(F(s,X^N(s,t,x))^{-1}\kappa g + \mathcal{K}^N\varrho^N(s,X^N(s,t,x)) + E^N(s,X^N(s,t,x)). \\ X^N(t,t,x) &= x. \end{cases}$$

The Lipschitz property of $\mathbb{A}^{-1}$, $F, \mathcal{K}^N\varrho^N$ and E^N ensures the existence, uniqueness and regularity of such a flow, see Proposition 2.B.1 and formula (2.49). Moreover, direct estimates show that for all $0 \leqslant s \leqslant t$:

$$\|\nabla X^N(s,t,\cdot)\|_\infty \leqslant \exp(\big[|\kappa g|\|\nabla\mathbb{A}^{-1}\|_\infty\|F\|_{L^\infty(0,T;W^{1,\infty})} + \|\mathcal{K}^N\varrho^N + E^N\|_{L^\infty(0,T;W^{1,\infty})}\big](t-s)). \tag{2.54}$$

Hence, we can write

$$\begin{aligned}\hat{F}(t,x) &= F_0(X^N(0,t,x)) \\ &\quad + \int_0^t \nabla\mathcal{K}^N\varrho^N(s,X^N(s,t,x))\cdot F(s,X^N(s,t,x)) + \tilde{E}(s,F(X^N(s,t,x)))ds.\end{aligned}$$

Direct computations yield

$$\|\mathcal{A}(F)\|_{L^\infty(0,T;L^\infty)} \leqslant \|F_0\|_\infty + T\|\nabla\mathcal{K}^N\varrho^N\|_{L^\infty(0,T;L^\infty)}\|F\|_{L^\infty(0,T;L^\infty)} + \|\tilde{E}^N\|_{L^\infty(0,T;L^\infty)},$$

and

$$\begin{aligned}\|\nabla\mathcal{A}(F)\|_{L^\infty(0,T;L^\infty)} \leqslant [\|F_0\|_{1,\infty} + T\Big\{&\|\nabla\mathcal{K}^N\varrho^N\|_{L^\infty(0,T;W^{1,\infty})} \\ &+ \|\tilde{E}^N\|_{L^\infty(0,T;W^{1,\infty})}\Big\}\|F\|_{L^\infty(0,T;W^{1,\infty})}]\|\nabla X^N(\cdot,t,\cdot)\|_{L^\infty(0,T;L^\infty)},\end{aligned}$$

Gathering all the estimates and using Proposition 2.B.1 and the uniform bounds (2.49), there exists some constants independent of N such that:

$$\|\mathcal{A}(F)\|_{L^\infty(0,T;W^{1,\infty}(\mathbb{R}^3))} \leqslant (\|F_0\|_{W^{1,\infty}} + TC_1\|F\|_{L^\infty(0,T;W^{1,\infty}(\mathbb{R}^3))})e^{C_2T}. \tag{2.55}$$

On the other hand, given F_1, $F_2 \in L^\infty(0,T;W^{1,\infty}(\mathbb{R}^3))$ we set X_i the associated characteristic flow and we have

$$\begin{aligned}&\|\mathcal{A}(F_1)(t,\cdot) - \mathcal{A}(F_2)(t,\cdot)\|_\infty \leqslant \\ &\quad\Big(\|\nabla F_0\|_\infty + t\|F_1\|_{L^\infty(0,T;W^{1,\infty})}\|\mathcal{K}^N\varrho^N\|_{L^\infty(0,T;W^{2,\infty})}\Big)\|X_1(0,t,\cdot) - X_2(0,t,\cdot)\|_\infty \\ &\quad\quad + t\|\nabla\mathcal{K}^N\varrho^N\|_{L^\infty(0,T;L^\infty)}\|F_1 - F_2\|_{L^\infty(0,T;L^\infty(\mathbb{R}^3))}.\end{aligned}$$

The characteristic flows satisfies

$$|X_1(s,t,x) - X_2(s,t,x)| \leqslant \|\nabla \mathbb{A}^{-1}\|_\infty \int_s^t \|F_1(\tau,\cdot) - F_2(\tau,\cdot)\|_\infty + \\ (\|F_1\|_{L^\infty(0,T;L^\infty)}|\kappa g| + 2\|\nabla \mathcal{K}^N \varrho^N + \nabla E^N\|_{L^\infty(0,T;L^\infty)})|X_1(\tau,t,x) - X_2(\tau,t,x)| d\tau,$$

hence

$$\|X_1(s,t,\cdot) - X_2(s,t,\cdot)\|_\infty \leqslant \left(\int_s^t \|\nabla \mathbb{A}^{-1}\|_\infty \|F_1(\tau,\cdot) - F_2(\tau,\cdot)\|_\infty d\tau\right) e^{C(t-s)}.$$

This yields

$$\|\mathcal{A}(F_1) - \mathcal{A}(F_2)\|_{L^\infty(0,T;L^\infty(\mathbb{R}^3))} \leqslant C(\|F_1\|_{L^\infty(0,T;W^{1,\infty}(\mathbb{R}^3))})\, T\, \|F_1 - F_2\|_{L^\infty(0,T;L^\infty)}. \tag{2.56}$$

We construct the following sequence $(F_k)_{k\in\mathbb{N}} \subset L^\infty(0,T;W^{1,\infty}(\mathbb{R}^3))$ defined as

$$\begin{cases} F^{k+1} &= \mathcal{A}(F^k)\,, k \in \mathbb{N}\,, \\ F^0 &= F_0\,. \end{cases}$$

For T small enough and independent of N, using estimates (2.55) and (2.56), the sequence $(F^k)_k$ is bounded in $L^\infty(0,T;W^{1,\infty}(\mathbb{R}^3))$ and is a Cauchy sequence in the Banach space $L^\infty([0,T],L^\infty(\mathbb{R}^3))$. There exists a limit $F \in L^\infty(0,T;W^{1,\infty}(\mathbb{R}^3))$ such that $F^k \to F$ in $L^\infty(0,T,L^\infty)$ and $\nabla F^k \rightharpoonup \nabla F$ weakly-* in $L^\infty(0,T,L^\infty)$. It remains to show that $F = \mathcal{A}(F)$. The weak formulation of the transport equation writes

$$\int_0^T \int_{\mathbb{R}^3} \left(\partial_t \psi + \mathrm{div}\left(\psi \cdot [\mathbb{A}^{-1}(F^k)\kappa g + \mathcal{K}^N \varrho^N]\right)\right) F^k = \int_0^T \int_{\mathbb{R}^3} \left(\nabla \mathcal{K}^N \varrho^N \cdot F^k + \tilde{E}^N(F^k)\right) \cdot \psi,$$

for all $\psi \in \mathcal{C}_c^1((0,T) \times \mathbb{R}^3)$. Using the strong convergence of F^N to F and the weak-* convergence of its derivative, we get

$$\int_0^T \int_{\mathbb{R}^3} \left(\partial_t \psi + \mathrm{div}\left(\psi \cdot [\mathbb{A}^{-1}(F)\kappa g + \mathcal{K}^N \varrho^N]\right)\right) F = \int_0^T \int_{\mathbb{R}^3} \left(\nabla \mathcal{K}^N \varrho^N \cdot F + \tilde{E}^N(F)\right) \cdot \psi,$$

Uniqueness of the fixed-point is ensured thanks to estimate (2.55) and (2.56). □

Proposition 2.6.1 and formula (2.48) yield the following result

Corollary 2.6.2. *There exists a unique solution of* (2.52) $F^N \in L^\infty([0,T],W^{1,\infty})$ *such that* $\mu^N = (id, F^N)\#\varrho^N$ *and* ϱ^N *satisfies weakly*

$$\partial_t \varrho^N + \mathrm{div}[(\mathbb{A}(F^N))^{-1}\kappa g + \mathcal{K}^N \varrho^N(x) + E^N)\varrho^N] = 0. \tag{2.57}$$

2.6.2 proof of Theorem 2.1.2 and 2.1.3

In the previous part we showed the existence of a unique function F^N such that:

$$\xi_i = F^N(x_+^i).$$

In order to provide the limiting behaviour of the system, we need to extract the limiting equation satisfied by $F = \lim\limits_{N\to\infty} F^N$ and to estimate and specify the convergence. It is straightforward that the limit function F should satisfy the following equation:

$$\begin{cases} \partial_t F + \nabla F \cdot (\mathbb{A}(F)^{-1}\kappa g + \mathcal{K}\varrho) &= \nabla\mathcal{K}\varrho \cdot F, \text{ on } [0,T]\times\mathbb{R}^3, \\ F(0,\cdot) &= F_0. \end{cases} \tag{2.58}$$

We begin with the proof of local existence and uniqueness of the solution to system (2.15).

Proof of Theorem 2.1.3. Let $p > 3$, $F_0 \in W^{2,p}$, $\varrho_0 \in W^{1,p}$ having compact support. The idea is to apply a fixed-point argument. We define the operator A which associates to each $u \in L^\infty(0,T;W^{3,p})$ the following divergence free velocity

$$u \mapsto F(u) \mapsto \varrho(u) \mapsto \mathcal{A}(u),$$

where $F(u) \in L^\infty(0,T;W^{2,p})$ is the unique solution, see Proposition 2.C.1, to the following equation

$$\begin{cases} \partial_t F + \nabla F \cdot (\mathbb{A}^{-1}(F)\kappa g + u) &= \nabla u \cdot F, \quad \text{on } [0,T]\times\mathbb{R}^3, \\ F(0,\cdot) &= F_0, \quad \text{on } \mathbb{R}^3. \end{cases}$$

$\varrho(u) \in L^\infty(0,T;W^{1,p})$ is the unique solution, see Proposition 2.C.2, to the transport equation

$$\begin{cases} \partial_t\varrho + \operatorname{div}((\mathbb{A}^{-1}(F(u))\kappa g + u)\varrho) &= 0, \quad \text{on } [0,T]\times\mathbb{R}^3, \\ \varrho(0,\cdot) &= \varrho_0, \quad \text{on } \mathbb{R}^3. \end{cases}$$

and $\mathcal{A}(u) = \mathcal{K}\varrho(u) = 6\pi r_0 \Phi * (\kappa\varrho(u)g)$. The mapping is well-defined, indeed, since $\varrho_0 \in W^{1,p}$ we have $\varrho \in L^\infty(0,T;W^{1,p})$, see Proposition 2.C.2. Consequently, applying [27, Theorem IV.2.1] shows that $\nabla^3 A(u)$, $\nabla^2 A(u) \in L^p$ and we have

$$\|\nabla^3 A(u)\|_p \leqslant C\|\nabla\varrho(u)\|_p, \quad \|\nabla^2 A(u)\|_p \leqslant C\|\varrho(u)\|_p.$$

On the other hand, since $\varrho(t,\cdot) \in L^p$ and is compactly supported, see Remark 2.C.1, we have in particular $\varrho(t,\cdot) \in L^{q_1} \cap L^{q_2}$ with

$$q_1 = \frac{3p}{3+p} \in]3/2, 3[, \quad q_2 = \frac{3p}{3+2p} \in]1, 3/2[.$$

We apply again [27, Theorem IV.2.1] for $q = q_1$ (resp. $q = q_2$) to get $\nabla A(u) \in L^p$ (resp. $A(u) \in L^p$) and we have according to [27, Formula IV.2.22] (resp. [27, Formula IV.2.23])

$$\|\nabla A(u)\|_p \leqslant C\|\varrho(u)\|_{q_1}, \quad \|A(u)\|_p \leqslant C\|\varrho(u)\|_{q_2} \quad ,$$

Hence, since $q_1, q_2 < 3 < p$, Holder's inequality yields

$$\|\nabla A(u)\|_p + \|A(u)\|_p \lesssim (\sup_{[0,T]} |\operatorname{supp} \varrho(u)(t,\cdot)|^{1/3} + \sup_{[0,T]} |\operatorname{supp} \varrho(u)(t,\cdot)|^{2/3}) \|\varrho(u)\|_p,$$

where $\sup_{[0,T]} |\operatorname{supp} \varrho(u)(t,\cdot)|$ depends on T, $\|\mathbb{A}^{-1}\|_\infty$, $\|F\|_{L^\infty(0,T;W^{2,p})}$ and $\|u\|_{L^\infty(0,T;W^{2,p})}$ according to Remark 2.C.1

$$\operatorname{diam}(\operatorname{supp}(\varrho(u)(t,\cdot)) \leqslant C(\varrho_0, T, \|u\|_{L^\infty(0,T;W^{2,p})}, \|F\|_{L^\infty(0,T;W^{2,p})}), \tag{2.59}$$

Finally we have

$$\begin{aligned} \|A(u)\|_{L^\infty(0,T;W^{3,p})} &\leqslant C(1 + M(T)) \|\varrho(u)\|_{L^\infty(0,T;W^{1,p})}, & (2.60)\\ \|A(u)\|_{L^\infty(0,T;W^{2,p})} &\leqslant C(1 + M(T)) \|\varrho(u)\|_{L^\infty(0,T;L^p)}, & (2.61) \end{aligned}$$

$$M(T) = \sup_{[0,T]} |\operatorname{supp} \varrho(u)(t,\cdot)|^{1/3} (1 + \sup_{[0,T]} |\operatorname{supp} \varrho(u)(t,\cdot)|^{1/3}).$$

We recall the following bounds, see Proposition 2.C.2 and Proposition 2.C.1

$$\|\varrho(u)\|_{L^\infty(0,T;W^{1,p})} \leqslant \|\varrho_0\|_{1,p} e^{CT}, \quad C = C(\|F(u)\|_{L^\infty(0,T;W^{2,p})}, \|u\|_{L^\infty(0,T;W^{3,p})}). \tag{2.62}$$

According to Proposition 2.C.1, for a small time interval we have for a fixed $\lambda > 1$

$$\|F(u)\|_{2,p} \leqslant \lambda \|F_0\|_{2,p}. \tag{2.63}$$

On the other hand, gathering the stability estimates of Proposition 2.C.2 and Proposition 2.C.1 and (2.61) we get for $u_i \in W^{3,p}$, $i = 1, 2$

$$\begin{aligned} &\|A(u_1) - A(u_2)\|_{L^\infty(0,T;W^{2,p})} \\ &\leqslant C(1 + M(u_1,u_2)(T)) \|\varrho(u_1) - \varrho(u_2)\|_{L^\infty(0,T;L^p)} \\ &\leqslant C(1 + M(u_1,u_2)(T)) T \left(\|F(u_1) - F(u_2)\|_{L^\infty(0,T;W^{1,p})} + \|u_1 - u_2\|_{L^\infty(0,T;W^{1,p})} \right) e^{C_1 T} \\ &\leqslant C(1 + M(u_1,u_2)(T)) T (1+T) \|u_1 - u_2\|_{L^\infty(0,T;W^{2,p})} e^{C_1 T}, \end{aligned}$$

where C depends on $\|u_i\|_{L^\infty(0,T;W^{3,p})}$, $\|F(u_i)\|_{L^\infty(0,T;W^{2,p})}$, $\|\varrho(u_i)\|_{L^\infty(0,T;W^{1,p})}$ and

$$\begin{aligned} M(u_1,u_2)(T) &:= \sup_{[0,T]} |\operatorname{supp}(\varrho(u_1)) \cup \operatorname{supp}(\varrho(u_2)|^{1/3} (1 + \sup_{[0,T]} |\operatorname{supp}(\varrho(u_1)) \cup \operatorname{supp}(\varrho(u_2)|^{1/3}), \\ &\lesssim C(T, \|u_i\|_{L^\infty(0,T;W^{2,p})}, \|F_i\|_{L^\infty(0,T;W^{2,p})}, \operatorname{supp}(\varrho_0)). \end{aligned}$$

We consider the following sequence

$$\begin{cases} u^{k+1} &= \mathcal{A}(u^k)\,, k \in \mathbb{N}\,, \\ u^0 &= \mathcal{K}\varrho_0\,. \end{cases}$$

We set $F^k := A(u^k)$, $\varrho^k := \varrho(u^k)$. Previous estimates show that the sequences $(u_k)_{k\in\mathbb{N}}$, $(F_k)_{k\in\mathbb{N}}$, $(\varrho_k)_{k\in\mathbb{N}}$ are uniformly bounded in $L^\infty(0,T;W^{3,p})$, $L^\infty(0,T;W^{2,p})$, $L^\infty(0,T;W^{1,p})$, respectively, and are Cauchy sequences in $L^\infty(0,T;W^{2,p})$, $L^\infty(0,T;W^{1,p})$, $L^\infty(0,T;L^p)$, respectively for T small enough. Consequently, there exists (u,F,ϱ) such that

$$\begin{aligned} u^k &\to u \quad \text{in } L^\infty(0,T;W^{2,p}),\\ F^k &\to F \quad \text{in } L^\infty(0,T;W^{1,p}),\\ \varrho^k &\to \varrho \quad \text{in } L^\infty(0,T;L^p). \end{aligned}$$

This allows to pass through the limit in the weak formulations of u^k and ϱ^k. In addition, we use the fact that ∇F_k converges weakly-* in $L^\infty(0,T;L^\infty)$ in order to pass through the limit in the weak formulation of F^k. Hence, the triplet (u,ϱ,F) satisfies equation (2.15). We recover the regularity of each term using the a priori bounds. Uniqueness is a consequence of the previous stability estimates. □

2.6.3 Proof of Theorem 2.1.2

Proof of Theorem 2.1.2. Since $\varrho^N \rightharpoonup \varrho$ weakly in the sense of measure, this yields that $W_\infty(\varrho^N,\varrho)\to 0$. We want to show that the triplet $(\varrho^N, F^N, \mathcal{K}^N\varrho^N)$ converges to $(\varrho, F, \mathcal{K}\varrho)$ the unique solution of equation (2.15). From Proposition 2.B.2 and using the same arguments as in Proposition 2.C.1 we have

$$\|F^N(t,\cdot)-F(t,\cdot)\|_\infty \leqslant C\int_0^t W_\infty(s)\left(1+|\log W_\infty(s)|)+\frac{W_\infty^2(s)}{d_{\min}^2}\right)+\|E^N\|_\infty+\|\tilde{E}^N\|_\infty,$$

where $W_\infty(s) := W_\infty(\varrho^N(s,\cdot),\varrho(s,\cdot))$. Hence $F^N\to F$ in $L^\infty(0,T;L^\infty)$ and $\mathcal{K}^N\varrho^N\to\mathcal{K}\varrho$ in $L^\infty(0,T;W^{1,\infty})$ if the Wasserstein distance is preserved in finite time. This allows us to pass through the limit in the weak formulation of ϱ^N

$$\int_0^t\int_{\mathbb{R}^3}\left(\partial_t\psi+\nabla\psi\cdot\left(\mathcal{A}^{-1}(F^N)\kappa g+\mathcal{K}^N\varrho^N\right)\right)\varrho^N = 0.$$

□

Appendix

2.A Some preliminary estimates

This section is devoted to the proof of the following lemma which is analogous to [41, Lemma 2.1].

Lemma 2.A.1. *There exists a positive constant C such that for $k \in [0,2]$*

$$\begin{aligned} \frac{1}{N}\sum_{j\neq i}\frac{1}{d_{ij}^k} &\leqslant C\|\varrho\|_{L^1\cap L^\infty}\left(\frac{W_\infty^3}{d_{\min}^k}+1\right), \\ \frac{1}{N}\sum_{j\neq i}\frac{1}{d_{ij}^3} &\leqslant C\|\varrho\|_{L^1\cap L^\infty}\left(\frac{W_\infty^3}{d_{\min}^3}+|\log W_\infty|\right). \end{aligned}$$

Proof. We introduce a radial truncation function χ such that $\chi = 0$ on $B(0,1/2)$ and $\chi = 1$ on ${}^cB(0,3/4)$. We have for all $k \geqslant 0$:

$$\begin{aligned} \frac{1}{N}\sum_{j\neq i}\frac{1}{d_{ij}^k} &= \int_{\mathbb{R}^3}\chi\left(\frac{x_i-y}{d_{\min}}\right)\frac{1}{|x_i-y|^k}\varrho^N(t,dy), \\ &= \int_{\mathbb{R}^3}\chi\left(\frac{x_i-T(y)}{d_{\min}}\right)\frac{1}{|x_i-T(y)|^k}\varrho(t,dy), \\ &= \left(\int_{B(x_i,3W_\infty)}+\int_{{}^cB(x_i,3W_\infty)}\right)\chi\left(\frac{x_i-T(y)}{d_{\min}}\right)\frac{1}{|x_i-T(y)|^k}\varrho(t,dy). \end{aligned}$$

Recall that $W_\infty \geqslant d_{\min}/2$. Since $\chi\left(\frac{x_i-T(y)}{d_{\min}}\right) = 0$ if $|x_i-T(y)| \leqslant d_{\min}/2$, the first term yields:

$$\int_{B(x_i,3W_\infty)}\chi\left(\frac{x_i-T(y)}{d_{\min}}\right)\frac{1}{|x_i-T(y)|^k}\varrho(t,dy) \leqslant C\|\varrho\|_\infty\frac{W_\infty^3}{d_{\min}^k}.$$

For the second term, we have $|x_i-T(y)| \geqslant |x_i-y|-|y-T(y)| \geqslant \frac{[x_i-y|}{2}$ and we get:

$$\int_{{}^cB(x_i,3W_\infty)}\chi\left(\frac{x_i-y}{d_{\min}}\right)\frac{1}{|x_i-T(y)|^k}\varrho(t,dy) \leqslant \|\varrho\|_\infty\int_{3W_\infty}^1\frac{1}{r^{k-2}}dr+\|\varrho\|_{L^1},$$

which yields the desired result. $\square$

2.B Estimates on $\mathcal{K}^N\varrho^N$, $\mathcal{K}\varrho$ and control of the minimal distance

In this part we present some estimates for the convergence of the velocity field $\mathcal{K}^N\varrho^N$ and its gradient towards $\mathcal{K}\varrho$ and its gradient. We estimate the ∞ norm of the error using the infinite Wasserstein distance between ϱ^N and ϱ in the spirit of [33, 34].
We recall that, according to [20][Theorem 5.6], at fixed time $t \geqslant 0$, there exists a (unique) optimal transport map T satisfying :

$$W_\infty := W_\infty(\varrho(t,\cdot), \varrho^N(t,\cdot)) = \varrho \text{ - esssup } |T(x) - x|,$$

with $\varrho^N(t,\cdot) = T\#\varrho(t,\cdot)$. This allows us to write $\mathcal{K}^N\varrho^N$ as follows

$$\mathcal{K}^N\varrho^N(x) = 6\pi r_0 \int \chi\Phi(x - T(y))\varrho(y)dy.$$

This important property allows us to show the following results.

Proposition 2.B.1 (Boundedness)**.** *Under the assumption that $\varrho \in W^{1,1} \cap W^{1,\infty}$, there exists a positive constant $C > 0$ independent of N such that:*

$$\|\mathcal{K}^N\varrho^N\|_{W^{2,\infty}} \leqslant C\left(\frac{W_\infty^3}{d_{\min}} + \frac{W_\infty^3}{d_{\min}^2} + \frac{W_\infty^3}{d_{\min}^3}\right)\|\varrho\|_{W^{1,\infty}\cap W^{1,1}}.$$

Remark 2.B.1. *The term $\frac{W_\infty^3}{d_{\min}^3}$ appears only for the second derivative of $\mathcal{K}^N\varrho^N$ which is needed for the proof of Theorem 2.1.2.*

Proof. Let $x \in \mathbb{R}^3$, we have :

$$\begin{aligned}\left|\mathcal{K}^N\varrho^N(x)\right| &\leqslant C\int |\chi\Phi(x - T(y))\varrho(y)dy|,\\ &\leqslant C\|\varrho\|_\infty \int_{B(x,3W_\infty)} |\chi\Phi(x - T(y))| + \int_{^cB(x,W_\infty)} |\chi\Phi(x - T(y))|\,|\varrho(y)|dy.\end{aligned}$$

Recall that for all $y \in B(x, 3W_\infty)$ such that $|x - T(y)| \leqslant d_{\min}/2$ we have $\chi\Phi(x - T(y)) = 0$. Hence in all cases we have the following bound for all $y \in B(x, 3W_\infty)$:

$$|\chi\Phi(x - T(y))| \leqslant \frac{C}{d_{\min}},$$

this yields the following bound

$$\int_{B(x,3W_\infty)} |\chi\Phi(x - T(y))| \leqslant C\frac{W_\infty^3}{d_{\min}}.$$

For all y ${}^cB(x,W_\infty)$ we have that $|x-T(y)| \geqslant |x-y| - |T(y)-y| \geqslant 2W_\infty \geqslant d_{\min}$. This ensures that $\chi\Phi(x-T(y)) = \Phi(x-T(y))$ on ${}^cB(x,W_\infty)$. Moreover we have

$$|x-T(y)| \geqslant |x-y| - W_\infty \geqslant \frac{1}{2}|x-y|,$$

which yields

$$\begin{aligned}\int_{{}^cB(x,W_\infty)} |\chi\Phi(x-T(y))|\,|\varrho(y)dy &\leqslant C\|\varrho\|_\infty \int_{{}^cB(x,W_\infty)\cap B(x,1)} \frac{dy}{|x-y|} + \|\varrho\|_{L^1},\\ &\leqslant C\|\varrho\|_{L^1\cap L^\infty}.\end{aligned}$$

Analogously we obtain a similar bound for $\nabla\mathcal{K}^N$. We focus now on the bound for $\nabla^2\mathcal{K}^N\varrho^N$. We have

$$\begin{aligned}\left|\nabla^2\mathcal{K}^N\varrho^N(x)\right| \leqslant C\|\varrho\|_\infty &\int_{B(x,3W_\infty)} \left|\nabla^2\chi\Phi(x-T(y))\right| dy\\ &+ \left|\int_{{}^cB(x,W_\infty)} \nabla^2\chi\Phi(x-T(y))\varrho(y)dy\right|.\end{aligned}$$

We use the same estimates as before to bound the first term by $\|\varrho\|_\infty \frac{W_\infty^3}{d_{\min}^3}$. For the second term we write

$$\begin{aligned}\left|\int_{{}^cB(x,W_\infty)} \nabla^2\chi\Phi(x-T(y))\varrho(y)dy\right| &\leqslant \left|\int_{{}^cB(x,W_\infty)} \nabla^2\Phi(x-y)\varrho(y)dy\right|\\ &+ \int_{{}^cB(x,W_\infty)} \left|\nabla^2\chi\Phi(x-T(y)) - \nabla^2\Phi(x-y)\right| |\varrho(y)|dy. \quad (2.64)\end{aligned}$$

Using an integration by parts for the first term in the right hand side of (2.64) we get

$$\begin{aligned}\left|\int_{{}^cB(x,W_\infty)} \nabla^2\Phi(x-y)\varrho(y)dy\right| &\leqslant \left|\int_{{}^cB(x,W_\infty)} \nabla\Phi(x-y)\nabla\varrho(y)dy\right|\\ &+ \int_{\partial B(x,W_\infty)} |\nabla\Phi(x-y)|\,|\varrho(y)|d\sigma(y)\,,\\ &\leqslant C\|\nabla\varrho\|_{L^1\cap L^\infty} + \|\varrho\|_\infty.\end{aligned}$$

Finally, for the second term in the right hand side of (2.64) we have

$$\begin{aligned}&\int_{{}^cB(x,W_\infty)} \left|\nabla^2\chi\Phi(x-T(y)) - \nabla^2\Phi(x-y)\right| |\varrho(y)|dy\\ &\leqslant \int_{{}^cB(x,W_\infty)} \left(\frac{1}{|x-y|^4} + \frac{1}{|x-T(y)|^4}\right) |y-T(y)||\varrho(y)|dy\\ &\leqslant C\|\varrho\|_{L^1\cap L^\infty}.\end{aligned}$$

□

The following convergence estimates are used in the proof of Theorem 2.1.2.

Proposition 2.B.2 (Convergence estimates)**.** *The following estimates hold true:*

$$
\begin{aligned}
\|\mathcal{K}^N \varrho^N - \mathcal{K}\varrho\|_{L^\infty} &\lesssim \|\varrho\|_\infty W_\infty(\varrho^N,\varrho)\left(1+\frac{W_\infty(\varrho^N,\varrho)^2}{d_{\min}}\right),\\
\|\nabla\mathcal{K}^N \varrho^N - \nabla\mathcal{K}\varrho\|_{L^\infty} &\lesssim \|\varrho\|_\infty W_\infty(\varrho^N,\varrho)\left(|\log W_\infty(\varrho^N,\varrho)|+\frac{W_\infty(\varrho^N,\varrho)^2}{d_{\min}^2}+1\right).
\end{aligned}
$$

Proof. We use in the proof the shortcut $W_\infty := W_\infty(\varrho^N,\varrho)$. Let $x\in\mathbb{R}^3$, we have

$$
\left|\mathcal{K}^N\varrho^N(x)-\mathcal{K}\varrho(x)\right| \leqslant 6\pi r_0 \int_{\operatorname{supp}\varrho} |\chi\Phi(x-T(y))-\Phi(x-y)|\,\varrho(y)dy.
$$

We split the integral into two disjoint domains $J := \{y\in\operatorname{supp}\varrho\,,\, |x-y|\leqslant 3W_\infty\}$ and its complementary. Note that on J, according to the definition of the truncation function χ, we have $\chi\Phi(x-T(y))=0$ for all $y\in J$ such that $|x-T(y)|\leqslant \frac{d_{\min}}{4}$. We can then bound directly the first integral as follows

$$
\begin{aligned}
\int_J |\chi\Phi(x-T(y))-\Phi(x-y)|\,\varrho(y)dy &\leqslant \int_J |\chi\Phi(x-T(y))|\,\varrho(y)dy + \int_J |\Phi(x-y)|\,\varrho(y)dy\\
&\lesssim \|\varrho\|_\infty\left(|B(x,3W_\infty)|\frac{4}{d_{\min}}+\int_{B(x,3W_\infty)}\frac{1}{|x-y|}dy\right).
\end{aligned}
$$

Direct computations yields

$$
\int_J |\chi\Phi(x-T(y))-\Phi(x-y)| \lesssim \|\varrho\|_\infty\left(\frac{W_\infty^3}{d_{\min}}+W_\infty^2\right).
$$

We focus now on the remaining term, note that for all $y\in {}^cJ := {}^cB(x,3W_\infty)$ we have

$$
|x-T(y)|\geqslant |x-y|-|T(y)-y|\geqslant 2W_\infty\geqslant d_{\min},
$$

which yields that $\chi\Phi(x-T(y))=\Phi(x-T(y))$ on ${}^cJ$. Moreover, we have $|x-T(y)|\geqslant\frac{1}{2}|x-y|$ on ${}^cJ$. We have then

$$
\begin{aligned}
\int_{{}^cJ} |\chi\Phi(x-T(y))-\Phi(x-y)| &= \int_{{}^cJ}|\Phi(x-T(y))-\Phi(x-y)|\,,\\
&\leqslant K\int_{{}^cJ}\left(\frac{1}{|x-T(y)|^2}+\frac{1}{|x-y|^2}\right)|y-T(y)|\varrho(y)dy,\\
&\lesssim W_\infty\|\varrho\|_\infty\int_{{}^cJ}\frac{1}{|x-y|^2}dy,\\
&\lesssim W_\infty\|\varrho\|_\infty.
\end{aligned}
$$

In the last line we use the fact that $\frac{1}{|x-y|^2}$ is integrable on ${}^cB(x,3W_\infty)$. The proof for the second estimate is analogous to the first one. The main difference occurs for the last estimate where the *log* term appears. This is due to the fact that we integrate $\frac{1}{|x-y|^3}$ on ${}^cB(x,3W_\infty)$. ☐

We present now an estimate for the conservation of the particle configuration. This estimate combined with Proposition 2.B.1 shows that the dilution regime is conserved provided that we have a control on the infinite Wasserstein distance.

Proposition 2.B.3. *For all $1 \leqslant i \leqslant N$ and $j \neq i$ we have*

$$\begin{aligned} |\dot{\xi}_i| &\lesssim \|\nabla \mathcal{K}^N \varrho^N\|_\infty |\xi_i| + O\left(d_{\min}\right), \\ \left|\dot{x}_+^i - \dot{x}_+^j\right| &\lesssim \|\nabla \mathcal{K}^N \varrho^N\|_\infty |x_+^i - x_+^j| + |\xi_i - \xi_j| + O(R), \\ \left|\dot{\xi}_i - \dot{\xi}_j\right| &\lesssim \|\nabla \mathcal{K}^N \varrho^N\|_\infty \left|\xi_i - \xi_j\right| + \|\nabla^2 \mathcal{K}^N \varrho^N\|_\infty \left|x_+^i - x_+^j\right| + O\left(d_{\min}\right). \end{aligned}$$

where

$$W_\infty := W_\infty(\varrho(t,\cdot), \bar{\varrho}^N(t,\cdot)) = \varrho \text{ - } \mathit{esssup}\, |T_t(x) - x|.$$

We remark that the conservation of the infinite Wasserstein distance, which is initially of order $\frac{1}{N^{1/3}}$, ensures the control of the particle distance. Unfortunately, due to the log term appearing in Proposition 2.B.2 we are not able to prove the conservation in time of the infinite Wasserstein distance.

2.C Existence, uniqueness and some stability properties

In this section we present some existence, uniqueness and stability estimates.

Proposition 2.C.1. *Let $p > 3$. Given $F_0 \in W^{2,p}$ and $u \in L^\infty(0,T;W^{3,p})$, there exists a time $T > 0$ such that $F \in L^\infty(0,T;W^{2,p})$ is the unique local solution of*

$$\left\{ \begin{array}{rcll} \partial_t F + \nabla F \cdot (\mathbb{A}^{-1}(F)\kappa g + u) &=& \nabla u \cdot F, & \text{on } [0,T] \times \mathbb{R}^3, \\ F(0,\cdot) &=& F_0, & \text{on } \mathbb{R}^3. \end{array} \right. \tag{2.65}$$

We have the following stability estimates

$$\|F_1 - F_2\|_{L^\infty(0,T;W^{1,p})} \leqslant C_1 T \|u_1 - u_2\|_{L^\infty(0,T;W^{2,p})} e^{C_2 T},$$

with C_1 and C_2 depending on $\|\mathbb{A}^{-1}\|_{2,\infty}$, $\|u_i\|_{L^\infty(0,T;W^{3,p})}$, $\|F_i\|_{L^\infty(0,T;W^{2,p})}$.

Proof. Since $p > 3$, we have $F_0 \in W^{2,p} \hookrightarrow W^{1,\infty}$ and $u \in W^{2,\infty}$. We can apply the existence proof analogous to the existence proof of Proposition 2.6.1 to get a unique solution $F \in L^\infty(0,T;W^{1,\infty})$ for a given $T > 0$. It remains to show that $F \in L^\infty(0,T;W^{2,p})$ for a finite time interval. We have for $\alpha = 0,1,2$

$$\partial_t D^\alpha F + \nabla D^\alpha F \left(\mathbb{A}^{-1}(F)\kappa g + u\right) = -\nabla F \cdot D^\alpha \left(\mathbb{A}^{-1}(F)\kappa g + u\right) + (D^\alpha \nabla u)F + (\nabla u) D^\alpha F.$$

Multiplying by $|D^\alpha F|^{p-1}$ and integrating by parts the second term using the fact that $\operatorname{div}(u) = 0$, we get

$$\begin{aligned}
&\frac{1}{p}\frac{d}{dt}\int |D^\alpha F|^p = \frac{1}{p}\int |D^\alpha F|^p \operatorname{div}\left(\mathbb{A}^{-1}(F)\right) + \nabla F \cdot |D^\alpha F|^{p-1}\left(D^\alpha \left[\mathbb{A}^{-1}(F)\right]\kappa g + D^\alpha u\right)\\
&+ (D^\alpha \nabla u) F |D^\alpha F|^{p-1} + (\nabla u) D^\alpha F |D^\alpha F|^{p-1},\\
&\lesssim \|F\|_{2,p}^p \left(\|\nabla \mathbb{A}^{-1}\|_\infty \|F\|_{1,\infty} + \|\nabla u\|_\infty\right)\\
&+ \|D^\alpha F\|^{p-1}\left(\|\mathbb{A}^{-1}\|_{2,\infty} + 1\right)\Bigg(\|\nabla F\|_\infty \left\{\|\nabla F\|_p + \|\nabla F\|_\infty \|\nabla F\|_p + \|\nabla^2 F\|_p + \|D^\alpha u\|_p\right\}\\
&+ \|F\|_\infty \|D^\alpha \nabla u\|_p\Bigg).
\end{aligned}$$

Since $\|F\|_{1,\infty} \lesssim \|F\|_{2,p}$, $\|u\|_{1,\infty} \lesssim \|F\|_{2,p}$, we get up to a constant depending on $\|\mathbb{A}^{-1}\|_{2,\infty}$

$$\frac{d}{dt}\|D^\alpha F\|_p^p \lesssim \|D^\alpha F\|_p^p \left(\|F\|_{2,p} + \|u\|_{3,p}\right) + \|D^\alpha F\|_p^{p-1}\|F\|_{2,p}\left(\|F\|_{2,p} + \|u\|_{3,p}\right).$$

Applying Young's inequality and summing over $\alpha = 0, 1, 2$ we get

$$\|F\|_{L^\infty(0,T;W^{2,p})} \lesssim \|F_0\|_{2,p} e^{C(p,\|F\|_{2,p},\|u\|_{3,p},\|\mathbb{A}^{-1}\|_{2,\infty})T},$$

which shows that $F \in L^\infty(0,T;W^{2,p})$ for a finite time $T > 0$. Now consider two divergence free velocity fields $u_1, u_2 \in L^\infty(0,T;W^{3,p})$ and denote by F_i the solution to (2.65). We have

$$\begin{aligned}
&\partial_t(F_1 - F_2) + (\nabla F_1 - \nabla F_2)(\mathbb{A}^{-1}(F_1)\kappa g + u_1)\\
&\qquad = \nabla F_2\left(\mathbb{A}^{-1}(F_1) - \mathbb{A}^{-1}(F_2) + u_1 - u_2\right) + (\nabla u_1 - \nabla u_2)F_1 + (F_1 - F_2)\nabla u_2.
\end{aligned}$$

Multiplying by $|F_1 - F_2|^{p-1}$ and integrating by parts the second term in the left hand side using the divergence free property of u, we get

$$\begin{aligned}
\frac{d}{dt}\|F_1 - F_2\|_p^p &\lesssim \|F_1 - F_2\|_p^p \left(\|\nabla \mathbb{A}^{-1}\|_\infty(\|\nabla F_1\|_\infty + \|\nabla F_2\|_\infty) + \|\nabla u_2\|_\infty\right)\\
&+ \|F_1 - F_2\|_p^{p-1}\|u_1 - u_2\|_{2,p}(\|\nabla F_1\|_\infty + \|\nabla F_2\|_\infty).
\end{aligned}$$

For the derivative we have

$$\begin{aligned}
&\partial_t(\nabla F_1 - \nabla F_2) + \nabla(\nabla F_1 - \nabla F_2)(\mathbb{A}^{-1}(F)\kappa g + u_1)\\
&= -(\nabla F_1 - \nabla F_2)(\nabla \mathbb{A}^{-1}(F_1)\nabla F_1 \kappa g + \nabla u_1) + \nabla^2 F_2\left(\mathbb{A}^{-1}(F_1) - \mathbb{A}^{-1}(F_2) + u_1 - u_2\right)\\
&+ \nabla F_2\left(\left\{\left[\nabla \mathbb{A}^{-1}(F_1) - \nabla \mathbb{A}^{-1}(F_2)\right]\nabla F_1 + \nabla \mathbb{A}^{-1}(F_2)(\nabla F_1 - \nabla F_2)\right\}\kappa g + \nabla u_1 - \nabla u_2\right)\\
&+ (\nabla^2 u_1 - \nabla^2 u_2)F_1 + (\nabla u_1 - \nabla u_2)\nabla F_1 + \nabla u_2(\nabla F_1 - \nabla F_2) + \nabla^2 u_2(F_1 - F_2).
\end{aligned}$$

Using the same estimates as previously, we obtain

$$\frac{d}{dt}\|F_1 - F_2\|_{1,p}^p \leqslant C_1\|F_1 - F_2\|_{1,p}^p + C_2\|F_1 - F_2\|_{1,p}^{p-1}\|u_1 - u_2\|_{2,p},$$

where C_1, C_2 depend on $\|\mathbb{A}^{-1}\|_{2,\infty}$, $\|u_i\|_{3,p}$, $\|F_i\|_{2,p}$. We conclude by integrating with respect to time and apply Gronwall's inequality. □

Proposition 2.C.2. *Let $T > 0$, $p > 3$. We consider $\varrho_0 \in W^{1,p}$, $u \in L^\infty(0,T;W^{3,p})$ and $F \in L^\infty(0,T;W^{2,p})$. There exists a unique solution $\varrho \in L^\infty(0,T;W^{1,p})$ to the transport equation*

$$\begin{cases} \partial_t\varrho + \operatorname{div}((\mathbb{A}^{-1}(F)\kappa g + u)\varrho) &= 0, \\ \varrho(0,\cdot) &= \varrho_0, \end{cases} \tag{2.66}$$

for all $T > 0$. ϱ satisfies

$$\|\varrho(t,\cdot)\|_{L^\infty(0,T;W^{1,p})} \leqslant \|\varrho_0\|_{1,p}e^{Ct},$$

where C depends on p, $\|\mathbb{A}^{-1}\|_{2,\infty}$, $\|F\|_{L^\infty(0,T;W^{2,p})}$, $\|u\|_{L^\infty(0,T;W^{2,p})}$. In addition, we have the following stability estimate

$$\|\varrho_1 - \varrho_2\|_{L^\infty(0,T;L^p)} \leqslant C_1 T\left(\|u_1-u_2\|_{L^\infty(0,T;W^{1,p})} + \|F_1 - F_2\|_{L^\infty(0,T;W^{1,p})}\right)e^{C_2T},$$

with constants depending on $\|\mathbb{A}^{-1}\|_{1,\infty}$, $\|\varrho_i\|_{L^\infty(0,T;W^{1,p})}$,$\|F_i\|_{L^\infty(0,T;W^{1,p})}$.

Remark 2.C.1. *If we assume in addition that ϱ_0 is compactly supported then classical transport theory ensures that $\varrho(t,\cdot)$ is compactly supported and using the characteristic flow, which is well defined since F, $u \in W^{1,\infty}$, one can show that*

$$\operatorname{diam}(\operatorname{supp}(\varrho(t,\cdot))) \leqslant \operatorname{diam}(\operatorname{supp}(\varrho_0))e^{Ct},$$

with $C = C(\|\nabla\mathbb{A}^{-1}\|_\infty, \|\nabla F\|_{L^\infty(0,t;L^\infty)}, \|\nabla u\|_{L^\infty(0,t;L^\infty)})$.

Proof. Since $g = -|g|e_3$, we have the following formula

$$\operatorname{div}(\mathbb{A}^{-1}(F)\kappa g) = -\nabla\mathbb{A}_3^{-1}(F)\cdot\nabla F\kappa|g|,$$

where $\mathbb{A}_3^{-1}$ is the third column of $\mathbb{A}^{-1}$. Note that since $p > 3$, we have the following Sobolev embedding

$$\|F\|_{1,\infty} \lesssim \|F\|_{2,p}, \quad \|u\|_{1,\infty} \lesssim \|u\|_{2,p}, \quad \|\varrho\|_\infty \lesssim \|\varrho\|_{1,p}. \tag{2.67}$$

The idea is to apply a fixed point argument. We define the operator A which maps any $\varrho \in L^\infty(0,T;W^{1,p})$ to the unique density $A(\varrho)$ solution of

$$\partial_t A(\varrho) + \nabla A(\varrho)\cdot(\mathbb{A}^{-1}(F)\kappa g + u) = \left(\nabla\mathbb{A}_3^{-1}(F)\cdot\nabla F\kappa|g|\right)\varrho. \tag{2.68}$$

Thanks to (2.67), $u \in W^{1,\infty}$ and $F \in W^{1,\infty}$, hence DiPerna-Lions renormalization theory ensures the existence of $\mathcal{A}(\varrho) \in L^\infty(0,T;L^p)$. Multiplying (2.68) by $|A(\varrho)|^{p-1}$, integrating by parts and using Young's inequality we get

$$\begin{aligned}\frac{1}{p}\|A(\varrho)\|_p^p &\leqslant \frac{1}{p}\|\varrho_0\|_p^p + \frac{1}{p}\int_0^t \|A(\varrho)\|_p^p\|\mathbb{A}^{-1}\|_\infty\|\nabla F\|_\infty + \int_0^t \|\mathbb{A}^{-1}\|_\infty\|\nabla F\|_\infty\|\varrho\|_p\|A(\varrho)\|_p^{p-1}, \\ &\leqslant \frac{1}{p}\|\varrho_0\|_p^p + C\int_0^t\left(\frac{1}{p}\|A(\varrho)\|_p^p + \frac{1}{p}\|\varrho\|_p^p + \frac{p-1}{p}\|A(\varrho)\|_p^p\right), \\ &\leqslant \frac{1}{p}\|\varrho_0\|_p^p + C\int_0^t \|A(\varrho)\|_p^p + \frac{C}{p}t\|\varrho\|_{L^\infty(L^p)}^p\end{aligned}$$

with $C = C(\|\mathbb{A}^{-1}\|_\infty, \|\nabla F\|_{L^\infty(0,T;L^\infty)})$. Hence, Gronwall's inequality yields

$$\|A(\varrho)\|_p \leqslant (\|\varrho_0\|_p + TC\|\varrho\|_p)e^{Ct}.$$

Moreover, we have

$$\begin{aligned}
&\partial_t \nabla A(\varrho) + \nabla(\nabla A(\varrho)) \cdot (\mathbb{A}^{-1}(F)\kappa g + u) \\
&= -\nabla A(\varrho)\nabla(\mathbb{A}^{-1}(F)\kappa g + u) + \nabla^2 \mathbb{A}_3^{-1}(F)\kappa|g|\nabla F \nabla F \varrho \\
&+ \nabla \mathbb{A}_3^{-1}(F)\kappa|g|\nabla^2 F \varrho + \nabla \mathbb{A}_3^{-1}(F) \cdot \nabla F \kappa|g|\nabla \varrho.
\end{aligned}$$

Multiplying by $|\nabla A(\varrho)|^{p-1}$ and reproducing the same computations as before we get

$$\|\nabla A(\varrho)\|_p \leqslant (\|\nabla \varrho_0\|_p + TC_1\|\varrho\|_{1,p})e^{C_2 t},$$

where we used (2.67). Hence, the constants C_1, C_2 depend on p, $\|\mathbb{A}^{-1}\|_{2,\infty}$,$\|u\|_{L^\infty(0,T;W^{2,p})}$, $\|F\|_{L^\infty(0,T;W^{2,p})}$ and $\|\varrho\|_{L^\infty(0,T;W^{1,p})}$. Gathering the two estimates we obtain

$$\|A(\varrho))\|_{L^\infty(0,T;W^{1,p})} \leqslant (\|\varrho_0\|_{1,p} + TC_1\|\varrho\|_{1,p})e^{C_2 T}. \tag{2.69}$$

Given ϱ_1, ϱ_2, since equation (2.68) is linear, $A(\varrho_1) - A(\varrho_2)$ satisfies the same equation with $\varrho_0 = 0$. Consequently, for $T > 0$ small enough, estimate (2.69) shows that the mapping A is a contraction and hence there exists a unique fixed point. Estimate (2.69) shows also global existence.

Let $u_i \in L^\infty(0, T, W^{3,p})$ and $F_i \in L^\infty(0, T, W^{2,p})$ for $i = 1, 2$. Denote by ϱ_i the unique solution to equation (2.66). We have

$$\begin{aligned}
&\partial_t(\varrho_1 - \varrho_2) + \nabla(\varrho_1 - \varrho_2) \cdot (\mathbb{A}^{-1}(F_1)\kappa g + u_1) \\
&= -\nabla \varrho_2 \cdot \big([\mathbb{A}^1(F_1) - \mathbb{A}^{-1}(F_2)]\kappa g + u_1 - u_2\big) \\
&+ (\varrho_1 - \varrho_2)\nabla \mathbb{A}_3^{-1}(F_1)\kappa|g| \\
&+ \varrho_1 \left(\left[(\nabla \mathbb{A}_3^{-1}(F_1) - \nabla \mathbb{A}_3^{-1}(F_2))\right] \nabla F_1 + \nabla \mathbb{A}_3^{-1}(F_2)(\nabla F_1 - \nabla F_2)\right) \kappa|g|.
\end{aligned}$$

Multiplying by $|\varrho_1 - \varrho_2|^{p-1}$ and integrating we get

$$\frac{d}{dt}\|\varrho_1 - \varrho_2\|_p^p \lesssim C_1\|\varrho_1 - \varrho_2\|_p^p + C_2\left(\|u_1 - u_2\|_\infty + \|F_1 - F_2\|_\infty + \|\nabla F_1 - \nabla F_2\|_p\right)\|\varrho_1 - \varrho_2\|_p^{p-1},$$

with constants depending on $\|\mathbb{A}^{-1}\|_{1,\infty}$, $\|\varrho_i\|_{1,p}$,$\|F_i\|_{1,p}$. We conclude using again the embedding $\|F_1 - F_2\|_\infty \leqslant C\|F_1 - F_2\|_{1,p}$ and analogously for $\|u_1 - u_2\|_\infty$. $\square$

Chapter 3

Fluid-kinetic modelling for respiratory aerosols with variable size and temperature

Abstract

In this paper, we propose a coupled fluid-kinetic model taking into account the radius growth of aerosol particles due to humidity in the respiratory system. We aim to numerically investigate the impact of hygroscopic effects on the particle behaviour. The air flow is described by the incompressible Navier-Stokes equations, and the aerosol by a Vlasov-type equation involving the air humidity and temperature, both quantities satisfying a convection-diffusion equation with a source term. Conservations properties are checked and an explicit time-marching scheme is proposed. Two-dimensional numerical simulations in a branched structure show the influence of the particle size variations on the aerosol dynamics.

Introduction

Aerosol therapy is one of the major curative way to treat chronic obstructive pulmonary diseases (COPD). Since *in vivo* observations of drug delivery in the human airways induce many difficulties, it appears crucial to model and to be able to numerically simulate the aerosol flow in the lung with a good enough accuracy, the main question being linked to the deposition phenomenon, and particularly its location.

The aerosol constitutes a set of very numerous particles. Those particles happen to have hygroscopic properties, *i.e.* abilities to exchange water with the bronchial air, which is full of humidity. Consequently, the aerosol particle sizes may vary in time, as it was assessed in [53, 51, 52]. Assuming that the droplets remain spherical, we intended to study the influence of radius growth on deposition (number of deposited particles, characteristic times of propagation/deposition inside a given realistic geometry, deposition areas...). It is worth noticing that those hygroscopic properties strongly rely on thermal effects, and the model we investigate involves both air and aerosol temperatures.

There are several kinds of models allowing to describe the aerosol motion in the air, two-phase models, agent-based ones and kinetic ones. In the first situation, the aerosol droplets are considered as a fluid which constitues a mixture with the ambient air in the lung. Then one focuses on the aerosol concentration in the air, see [7, 23] for instance. Nevertheless, with those models, it may be difficult to determine the aerosol deposition areas. The second situation, which is used in [63, 72] for instance, raises many difficulties to track the trajectory of numerous particles, in particular when there is a strong coupling between the particles and the air flow.

We here choose to use a kinetic approach, as in [9, 28], which is relevant from the modelling point of view: there are lots of particles in the aerosol, but their volume is negligible compared to the airways volume. In this framework, the aerosol behaviour is described through a distribution function which depends on macroscopic variables (time, space position) as well as on microscopic ones (velocity, for instance). The Vlasov-type equation satisfied by the distribution function is usually coupled with the incompressible Navier-Stokes equations to describe the airflow [17]. The model we present here is an extension of the latter one, where the air temperature, the mass fraction of the water vapour in the air and the dependence of the distribution function on both the size and temperature of the particles are taken into account. Note that it is also investigated from the mathematical point of view in [59].

This article is divided into four main parts. The first one aims to present the model(s) we study. In the brief second one, we formally check some relevant balance properties of our model. Then we discuss the numerical method we use to discretize our model in the third section. Eventually, the last section is dedicated to numerical experiments which point out the aerosol size growth importance in the deposition phenomenon.

3.1 Building the model

As stated above, this section aims to explain and present a model describing the behaviour of a therapeutic aerosol in the respiratory system, where the size of the aerosol particles can vary because of the ambient water vapour in the airflow.

We use a simplified fluid domain, denoted by Ω: in our setting, Ω can be chosen as a cylinder or a branch, and is assumed not to depend on time. Its boundary $\Gamma = \partial\Omega$ is divided into three subsets, the wall Γ^{wall}, the inlet Γ^{in} and the outlet Γ^{out}, see Figure 3.1.

As we already stated, we use a kinetic viewpoint to model the aerosol, which constitutes a dispersed phase. Let us consider a distribution function f representing the density of particles per unit volume in the domain of interest $\Omega \subset \mathbb{R}^3$. It depends on time $t \geqslant 0$, position $x \in \Omega$, velocity $v \in \mathbb{R}^3$, radius $r > 0$ and temperature $T > 0$. The usual dependence of f with respect to the variables t, x, and v is supplemented by the one with respect to the size and temperature of the droplets. Indeed, the condensation phenomenon which induces the size variation involves matter and thermal exchanges between the aerosol and the air. Note that we assume that the particles remain spherical and do not interact with each other. The latter hypothesis relies on the fact that there are not enough particles for their

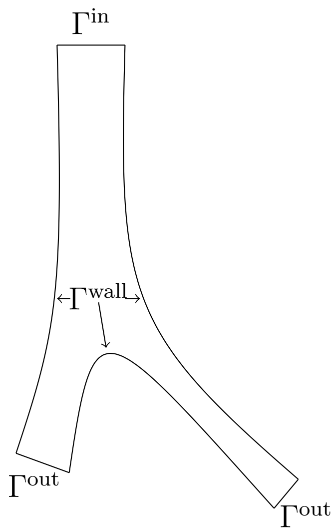

Figure 3.1 – Domain Ω

collisions to be significant.

In the respiratory system, the aerosol moves in the air, which can be assumed to be Newtonian and incompressible. In particular, this means that the air mass density ϱ_{air} is constant. The air flow is then classically described through the air velocity u and its pressure p.

In order to consider the growth of particles and describe the matter and thermal exchanges with the air, we also need to work with the water vapour mass fraction in the air $Y_{\mathrm{v,air}}$ and the air temperature T_{air}. All those quantities indexed by "air" depend on t and x (except ϱ_{air}, of course). Note that the water vapour mass density in the air considered as a gaseous mixture can be computed as $\varrho_{\mathrm{air}} Y_{\mathrm{v,air}}$.

Let us now focus on the various equations satisfied by the aerosol and air-related quantities, starting with the dispersed phase.

The aerosol density f satisfies a Vlasov-type equation, which can be written as:

$$\partial_t f + v \cdot \nabla_x f + \mathrm{div}_v \left[(\alpha(u-v) + \left(1 - \frac{\varrho_{\mathrm{air}}}{\varrho_d}\right) g) f \right] + \partial_r (af) + \partial_T (bf) = 0, \tag{3.1}$$

where g is the gravitational field, $\alpha(u-v)$ the drag acceleration undergone by the aerosol from the air, a and b respectively represent the radius and temperature growth evolutions of the particles, ϱ_{air} the mass density of the air and ϱ_d the mass density of the particle defined further by (3.4). The Vlasov equation is supplemented with the following boundary and initial conditions

$$\left\{ \begin{array}{rcll} f & = & f^{\mathrm{in}} & \text{on } \mathbb{R}_+ \times \Gamma^{\mathrm{in}} \times \mathbb{R}^3 \times \mathbb{R}_+^* \times \mathbb{R}_+^*, \\ f(t,\cdot) & = & 0 & \text{on } \Gamma^{\mathrm{wall}} \times \mathbb{R}^3 \times \mathbb{R}_+^* \times \mathbb{R}_+^*, \quad \text{if } v \cdot n \leqslant 0, \quad \text{a.e. } t, \\ f(0,\cdot) & = & f_{\mathrm{init}} & \text{on } \Omega \times \mathbb{R}^3 \times \mathbb{R}_+^* \times \mathbb{R}_+^*, \end{array} \right. \tag{3.2}$$

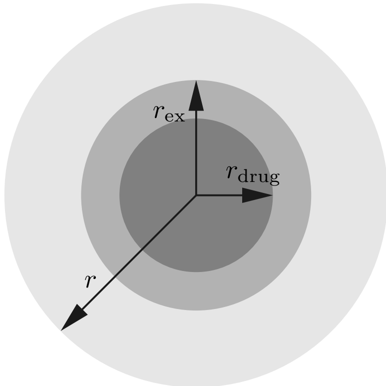

Figure 3.2 – Equivalent radii in a droplet

where $f^{\mathrm{in}} : \mathbb{R}_+ \times \Gamma^{\mathrm{in}} \times \mathbb{R}^3 \times \mathbb{R}_+^* \times \mathbb{R}_+^* \to \mathbb{R}$ and $f_{\mathrm{init}} : \Omega \times \mathbb{R}^3 \times \mathbb{R}_+^* \times \mathbb{R}_+^* \to \mathbb{R}$ are given. The boundary condition on Γ^{wall} is standard, it ensures that any droplet landing on the wall remains deposited on the wall afterwards.

We still need to define the functions α, a and b in (3.1). In order to do so, it is important to first understand how a particle behaves and what kind of phenomenon we deal with.

The main new phenomena taken into account in the model are the water vapour condensation on the droplet surface and the water evaporation from the droplet surface. In each particle, one can find active products (drug), excipient and water. Let us introduce some equivalent radii to simplify the situation. Denote by r_{drug} the radius such that $\frac{4}{3}\pi r_{\mathrm{drug}}^3 \varrho_{\mathrm{drug}}$ is the drug mass inside the droplet and by r_{ex} the one such that $\frac{4}{3}\pi (r_{\mathrm{ex}}^3 - r_{\mathrm{drug}}^3)\varrho_{\mathrm{ex}}$ is the excipient mass inside the droplet (see Figure 3.2). Obviously, ϱ_{drug} and ϱ_{ex} respectively are the (constant) drug and excipient mass densities. The latter equivalent radius r_{ex} will also be named the particle dry radius, in the sense that there is no water in a dry particle.

Denoting by ϱ_{w} the water mass density, assumed to be constant in the situations we investigate, it is now possible to define the mass and mass density of the particle, which both depend on r, *i.e.*

$$m(r) = \frac{4}{3}\pi \left[r_{\mathrm{drug}}^3 \varrho_{\mathrm{drug}} + (r_{\mathrm{ex}}^3 - r_{\mathrm{drug}}^3)\varrho_{\mathrm{ex}} + (r^3 - r_{\mathrm{ex}}^3)\varrho_{\mathrm{w}} \right], \tag{3.3}$$

$$\varrho_{\mathrm{d}}(r) = \frac{1}{r^3} \left[r_{\mathrm{drug}}^3 \varrho_{\mathrm{drug}} + (r_{\mathrm{ex}}^3 - r_{\mathrm{drug}}^3)\varrho_{\mathrm{ex}} + (r^3 - r_{\mathrm{ex}}^3)\varrho_{\mathrm{w}} \right]. \tag{3.4}$$

For the definition of α we have, as in [17],

$$\alpha(r) = \frac{6\pi\eta r}{m(r)}, \tag{3.5}$$

where η is the constant air dynamic viscosity, so that the drag force satisfies the Stokes law.

We rely on [52] to build the functions a and b. Since we want to take into account condensation and evaporation, the key physical quantities are the heat fluxes between the air and the droplets, the convective one Q_d and the evaporating one $L_\mathrm{v}N_\mathrm{d}$, where L_v is the latent heat of water vaporisation. The convective flux depends on r, T, but also on t and x through T_air. The evaporating heat flux involves the water mass flux N_d at the droplet surface. This flux depends on r, T, and also on t and x again, but this time through $Y_\mathrm{v,air}$, and also governs the size evolution of the droplets. The expressions of the functions a and b can then be written in terms of N_d and Q_d as

$$a(r,T,Y_\mathrm{v,air}(t,x)) = -\frac{N_\mathrm{d}(r,T,Y_\mathrm{v,air}(t,x))}{\varrho_\mathrm{w}}, \tag{3.6}$$

$$b(r,T,Y_\mathrm{v,air}(t,x),T_\mathrm{air}(t,x)) = \\ \frac{3}{\varrho_\mathrm{d}(r)c_{P_\mathrm{d}}r}(-Q_\mathrm{d}(r,T,T_\mathrm{air}(t,x)) - L_\mathrm{v}N_\mathrm{d}(r,T,Y_\mathrm{v,air}(t,x))), \tag{3.7}$$

where c_{P_d} is the constant specific heat of the droplet.

Let us now detail the expressions of Q_d and N_d. We can first write

$$Q_\mathrm{d}(r,T,T_\mathrm{air}(t,x)) = \frac{\mathrm{Nu}\,\kappa_\mathrm{air}\,C_T}{2r}(T - T_\mathrm{air}(t,x)), \tag{3.8}$$

where Nu is the droplet Nusselt number in the air, κ_air the thermal conductivity of the air as a gaseous mixture, and C_T the Knudsen correlation for non-continuum effects, all of them being considered as constants in our case.

Second, the water mass flux N_d involves $Y_\mathrm{v,air}$ and also the mass fraction $Y_\mathrm{v,surf}$ of water vapour at the droplet surface, which depends on r and T. That quantity $Y_\mathrm{v,surf}$ is quite intricate to be defined from the modelling viewpoint. We do not provide any detailed explanation on the model itself, the reader is invited to refer to [52] for more details. We first need the water vapour saturation pressure, which depends on T, and is here expressed in the cgs unit system:

$$P_\mathrm{v,sat}(T) = 10\exp\left(23.196 - \frac{3816.44}{T - 46.13}\right). \tag{3.9}$$

Then the influence of the Kelvin effect on the droplet surface concentration of water vapor is expressed thanks to

$$K(r,T) = \exp\left(\frac{2\sigma}{r\varrho_\mathrm{d}(r)R_\mathrm{v}T}\right), \tag{3.10}$$

where R_v is the gas constant of water vapour and the droplet surface tension σ is assumed to be constant too in our framework (in particular not depending on T). Eventually, we need the water activity coefficient given by

$$S(r) = \frac{\dfrac{\varrho_\mathrm{w}(r^3 - r_\mathrm{ex}^3)}{M_\mathrm{w}}}{\dfrac{\varrho_\mathrm{w}(r^3 - r_\mathrm{ex}^3)}{M_\mathrm{w}} + i_\mathrm{drug}\dfrac{\varrho_\mathrm{drug}r_\mathrm{drug}^3}{M_\mathrm{drug}} + i_\mathrm{ex}\dfrac{\varrho_\mathrm{ex}(r_\mathrm{ex}^3 - r_\mathrm{drug}^3)}{M_\mathrm{ex}}}, \tag{3.11}$$

where M_{w}, M_{drug} and M_{ex} respectively denote the molar masses of water, drug and excipient, and the constants i_{drug} and i_{ex} are the so-called van't Hoff factors of the drug and the excipient, allowing to take into account the molecular dissociation during dissolution. Note that the previous expression S is different from the one in [52]. Indeed, S equals 0 when the particle is dry, *i.e.* when $r = r_{\mathrm{ex}}$, which was not possible in [52], but otherwise, of course, we recover the same value for S. We can now write the expression of $Y_{\mathrm{v,surf}}$, that is

$$Y_{\mathrm{v,surf}}(r,T) = \frac{S(r)K(r,T)P_{\mathrm{v,sat}}(T)}{\varrho_{\mathrm{d}}(r)R_{\mathrm{v}}T}. \tag{3.12}$$

The expression of the water mass flux subsequently comes

$$N_{\mathrm{d}}(r,T,Y_{\mathrm{v,air}}(t,x)) = \varrho_{\mathrm{air}} \frac{\mathrm{Sh}\, D_{\mathrm{v}}(T_{\mathrm{air}})\, C_m}{2r} \frac{Y_{\mathrm{v,surf}}(r,T) - Y_{\mathrm{v,air}}(t,x)}{1 - Y_{\mathrm{v,surf}}(r,T)}, \tag{3.13}$$

where Sh is the Sherwood number describing the water transfer between the air and the droplet, C_m is the mass Knudsen number correction, and the binary diffusion coefficient D_{v} of water vapour in the air is given, in the cgs unit system, by

$$D_{\mathrm{v}}(T_{\mathrm{air}}(t,x)) = 0.216 \left(\frac{T_{\mathrm{air}}(t,x)}{273.15}\right)^{1.8}. \tag{3.14}$$

Remark 3.1.1. *The definitions* (3.6)–(3.8) *and* (3.13) *of a, b, Q_{d} and N_{d} allow to determine lower bounds for the support of the distribution function with respect to both r and T. We know that a governs the time evolution of this support. Assume that, at initial time, the droplets all have a radius greater than r_{ex}. In that situation, if r somehow reaches the value r_{ex}, as we already pointed out, we have $S(r_{\mathrm{ex}}) = 0$ and subsequently $Y_{\mathrm{v,surf}} = 0$, which implies $N_{\mathrm{d}} \leqslant 0$ and $a \geqslant 0$. That ensures that r cannot go below r_{ex} in the model. For the support of f with respect to T, from the mathematical viewpoint, even if the formulae leading to* (3.13) *do not hold in the considered temperature range, one can check that if T somehow reaches* 46.13 *K (the value in $P_{\mathrm{v,sat}}$), N_{d} is non positive, since $Y_{\mathrm{v,surf}} = 0$ again. And Q_{d} is clearly non positive too. That ensures that T cannot go below* 46.13 *K in the model. Anyway, if all the functions involved are smooth enough, if f_{init} is chosen with a compact support in all its variables, that compactness property should hold at least for small times. Note that, from the physical viewpoint, it seems relevant to assume that all the temperatures remain around* 300 *K, and that $Y_{\mathrm{v,air}}$ remains positive.*

Remark 3.1.2. *Thanks to formula* (3.4) *and the fact that $r \geqslant r_{ex} \geqslant r_{drug}$ according to Remark 3.1.1, we have*

$$\min(\varrho_w, \varrho_{ex}, \varrho_{drug}) \leqslant \varrho_d \leqslant \max(\varrho_w, \varrho_{ex}, \varrho_{drug}),$$

this allows us to neglect the term $\frac{\varrho_{air}}{\varrho_d}$ appearing in equation (3.1) *in our numerical simulations due to its smallness, see 3.A.1 for the physical values of ϱ_{drug}, ϱ_{ex}, ϱ_w, ϱ_{air}.*

Let us now tackle the air equations. To begin with, the fluid velocity $u(t,x) \in \mathbb{R}^3$ and its pressure $p(t,x) \in \mathbb{R}$ classically [17] satisfy the incompressible Navier-Stokes equations

$$\varrho_{\mathrm{air}}[\partial_t u + (u \cdot \nabla_x u)] - \eta \Delta_x u + \nabla_x p = F, \tag{3.15}$$

$$\mathrm{div}_x\, u = 0, \tag{3.16}$$

on $\mathbb{R}_+ \times \Omega$, completed with the following boundary and initial conditions:

$$\begin{cases} u = u^{\mathrm{in}} & \text{on } \mathbb{R}_+ \times \Gamma^{\mathrm{in}}, \\ u = 0 & \text{on } \mathbb{R}_+ \times \Gamma^{\mathrm{wall}}, \\ \sigma(u,p) \cdot n = 0 & \text{on } \mathbb{R}_+ \times \Gamma^{\mathrm{out}}, \\ u(0,\cdot) = u_{\mathrm{init}} & \text{on } \Omega, \end{cases} \tag{3.17}$$

where $\sigma(u,p) = \nabla_x u + (\nabla_x u)^\intercal - p\,\mathrm{Id}$ is the stress tensor, n is the outgoing normal vector from Γ, $u^{\mathrm{in}} : \mathbb{R}_+ \times \Gamma^{\mathrm{in}} \to \mathbb{R}^3$ is chosen to be a Poiseuille flow and $u_{\mathrm{init}} : \Omega \to \mathbb{R}^3$ is the initial datum. Eventually, the aerosol retroaction F on the air is given by

$$F(t,x) = -\iiint_{\mathbb{R}^3 \times \mathbb{R}_+ \times \mathbb{R}} m(r)\alpha(r)(u(t,x) - v) f(t,x,v,r,T)\,\mathrm{d}v\,\mathrm{d}r\,\mathrm{d}T$$

$$= -\iiint_{\mathbb{R}^3 \times \mathbb{R}_+^* \times \mathbb{R}_+^*} 6\pi\eta r(u(t,x) - v) f(t,x,v,r,T)\,\mathrm{d}v\,\mathrm{d}r\,\mathrm{d}T.$$

Remark 3.1.3. *In our numerical simulations, that latter term will be neglected ($F = 0$) because of its smallness related to the investigated particle size range, see [17], but we keep it for the time being, in order to remain consistent with respect to the total momentum conservation of our system.*

We still need to write equations to describe the evolution of the air temperature T_{air} and the water vapour mass fraction $Y_{\mathrm{v,air}}$ in the air. The water vapor mass fraction $Y_{\mathrm{v,air}}$ satisfies an advection-diffusion equation including a source term S_Y which accounts for the water mass exchanges between the bronchial air and the aerosol. Other effects such as turbulence effects could also be taken into account (see [53, 51]). Thus, we write, on $\mathbb{R}_+ \times \Omega$,

$$\varrho_{\mathrm{air}}[\partial_t Y_{\mathrm{v,air}} + (u \cdot \nabla_x) Y_{\mathrm{v,air}}] - \mathrm{div}_x(D_{\mathrm{v}}(T_{\mathrm{air}}) \nabla_x Y_{\mathrm{v,air}}) = S_Y, \tag{3.18}$$

completed with the following boundary and initial conditions

$$\begin{cases} Y_{\mathrm{v,air}} = Y_{\mathrm{v,air}}^{\mathrm{in}} & \text{on } \mathbb{R}_+ \times \Gamma^{\mathrm{in}}, \\ Y_{\mathrm{v,air}} = Y_{\mathrm{v,wall}} & \text{on } \mathbb{R}_+ \times \Gamma^{\mathrm{wall}}, \\ \nabla_x Y_{\mathrm{v,air}} \cdot n = 0 & \text{on } \mathbb{R}_+ \times \Gamma^{\mathrm{out}}, \\ Y_{\mathrm{v,air}}(0,\cdot) = Y_{\mathrm{v,air,init}} & \text{on } \Omega, \end{cases} \tag{3.19}$$

where $Y_{\mathrm{v,air,init}}$, $Y_{\mathrm{v,air}}^{\mathrm{in}}$, $Y_{\mathrm{v,wall}} > 0$ are given. The boundary condition on Γ^{wall} ensures that the wall continuously provides water vapour to the air mixture. The source side term S_Y

of (3.18) is defined, very similarly to the one from [52], as

$$S_Y(t,x) = \varrho_{\mathrm{w}} \iiint\limits_{\mathbb{R}^3\times\mathbb{R}_+^*\times\mathbb{R}_+^*} 4\pi r^2 N_{\mathrm{d}}(r,T,Y_{\mathrm{v,air}}(t,x))\, f(t,x,v,r,T)\,\mathrm{d}v\,\mathrm{d}r\,\mathrm{d}T. \tag{3.20}$$

Finally, the air temperature also satisfies an advection-diffusion equation on $\mathbb{R}_+\times\Omega$, which writes

$$\varrho_{\mathrm{air}} c_{P_{\mathrm{air}}}[\partial_t T_{\mathrm{air}} + (u\cdot\nabla_x)T_{\mathrm{air}}] - \kappa_{\mathrm{air}}\Delta_x T_{\mathrm{air}} = S_T, \tag{3.21}$$

completed with the following boundary and initial conditions

$$\left\{\begin{array}{rcll} T_{\mathrm{air}} &=& T_{\mathrm{air}}^{\mathrm{in}} & \text{on } \mathbb{R}_+\times\Gamma^{\mathrm{in}},\\ T_{\mathrm{air}} &=& T_{\mathrm{wall}} & \text{on } \mathbb{R}_+\times\Gamma^{\mathrm{wall}},\\ \nabla_x T_{\mathrm{air}}\cdot n &=& 0 & \text{on } \mathbb{R}_+\times\Gamma^{\mathrm{out}},\\ T_{\mathrm{air}}(0,\cdot) &=& T_{\mathrm{air,init}} & \text{on } \Omega, \end{array}\right. \tag{3.22}$$

where $T_{\mathrm{air,init}}$, $T_{\mathrm{air}}^{\mathrm{in}}$, $T_{\mathrm{wall}} > 0$ are given. The source side term S_T of (3.21) represents the heat transfer between the air and the aerosol through the water vapour, and is given, again very similarly to the one from [52], by

$$S_T(t,x) = \iiint\limits_{\mathbb{R}^3\times\mathbb{R}_+^*\times\mathbb{R}_+^*} 4\pi r^2\, Q_{\mathrm{d}}(r,T,T_{\mathrm{air}}(t,x))\, f(t,x,v,r,T)\,\mathrm{d}v\,\mathrm{d}r\,\mathrm{d}T. \tag{3.23}$$

In what follows, equations (3.1)–(3.23), which include all the effects related to aerosol size and temperature variation, will be referred to as the (ARAT) model, see Remarks 3.1.2 and 3.1.3 for the neglected terms. If we drop the temperature effects, the (ARST) model is given by (3.1)–(3.6) and (3.9)–(3.20), with $b = 0$. And for the (SRST) model, where no aerosol size or temperature variation is allowed, we consider equations (3.1)–(3.5) and (3.15)–(3.17) with $a = 0$ and $b = 0$. To summarise the models under study, we rewrite below the PDEs for each one of them, without the boundary and initial conditions:

$$\left\{\begin{array}{l} \partial_t f + v\cdot\nabla_x f + \mathrm{div}_v[(\alpha(u-v)+g)f] + \partial_r(af) + \partial_T(bf) = 0,\\ \varrho_{\mathrm{air}}[\partial_t u + (u\cdot\nabla_x u)] - \eta\Delta_x u + \nabla_x p = 0, \quad \mathrm{div}_x\, u = 0,\\ \varrho_{\mathrm{air}}[\partial_t Y_{\mathrm{v,air}} + (u\cdot\nabla_x)Y_{\mathrm{v,air}}] - \mathrm{div}_x(D_{\mathrm{v}}(T_{\mathrm{air}})\nabla_x Y_{\mathrm{v,air}}) = S_Y,\\ \varrho_{\mathrm{air}} c_{P_{\mathrm{air}}}[\partial_t T_{\mathrm{air}} + (u\cdot\nabla_x)T_{\mathrm{air}}] - \kappa_{\mathrm{air}}\Delta_x T_{\mathrm{air}} = S_T, \end{array}\right. \quad \begin{array}{c}\text{varying size}\\ \text{and temperature}\\ \text{(ARAT)},\end{array}$$

$$\left\{\begin{array}{l} \partial_t f + v\cdot\nabla_x f + \mathrm{div}_v[(\alpha(u-v)+g)f] + \partial_r(af) = 0,\\ \varrho_{\mathrm{air}}[\partial_t u + (u\cdot\nabla_x u)] - \eta\Delta_x u + \nabla_x p = 0, \quad \mathrm{div}_x\, u = 0,\\ \varrho_{\mathrm{air}}[\partial_t Y_{\mathrm{v,air}} + (u\cdot\nabla_x)Y_{\mathrm{v,air}}] - \mathrm{div}_x(D_{\mathrm{v}}(T_{\mathrm{air}})\nabla_x Y_{\mathrm{v,air}}) = S_Y, \end{array}\right. \quad \begin{array}{c}\text{varying size}\\ \text{no temperature}\\ \text{variation (ARST)},\end{array}$$

$$\left\{\begin{array}{l} \partial_t f + v\cdot\nabla_x f + \mathrm{div}_v[(\alpha(u-v)+g)f] = 0,\\ \varrho_{\mathrm{air}}[\partial_t u + (u\cdot\nabla_x u)] - \eta\Delta_x u + \nabla_x p = 0, \quad \mathrm{div}_x\, u = 0, \end{array}\right. \quad \begin{array}{c}\text{no size}\\ \text{nor temperature}\\ \text{variation (SRST)}.\end{array}$$

3.2 Checking the physical conservations

In this section, we discuss the physical conservations of various quantities related to the (ARAT) system, and we focus on two quantities which involve water vapour. The first one focuses on the water vapour mass exchange. More precisely, the water vapour coming from the air is supposed to lead to a size variation of the aerosol droplets. That property is stated in the following proposition.

Proposition 3.2.1. *Assume that $u = 0$ and $\nabla_x Y_{\mathrm{v,air}} \cdot n = 0$ on $\partial\Omega$, and that $f = 0$ on $\partial\Omega \times \mathbb{R}^3 \times \mathbb{R}_+^* \times \mathbb{R}_+^*$. Then we have*

$$\frac{\mathrm{d}}{\mathrm{d}t}\left[\int_\Omega \left(\varrho_{\mathrm{air}} Y_{\mathrm{v,air}}(t,x) + \iiint\limits_{\mathbb{R}^3\times\mathbb{R}_+^*\times\mathbb{R}_+^*} m(r) f(t,x,v,r,T)\,\mathrm{d}v\,\mathrm{d}r\,\mathrm{d}T\right)\mathrm{d}x\right] = 0.$$

Proof. On the one hand, multiplying (3.1) by $m(r)$, integrating with respect to all the variables except t, and eliminating the conservative terms through integrations by parts, we obtain

$$\begin{aligned}\frac{\mathrm{d}}{\mathrm{d}t}&\left[\int_\Omega \iiint\limits_{\mathbb{R}^3\times\mathbb{R}_+^*\times\mathbb{R}_+^*} m(r) f(t,x,v,r,T)\,\mathrm{d}v\,\mathrm{d}r\,\mathrm{d}T\,\mathrm{d}x\right] \\ &= \int_\Omega \iiint\limits_{\mathbb{R}^3\times\mathbb{R}_+^*\times\mathbb{R}_+^*} m'(r)\, a(r,T,Y_{\mathrm{v,air}}(t,x))\, f(t,x,v,r,T)\,\mathrm{d}v\,\mathrm{d}r\,\mathrm{d}T\,\mathrm{d}x.\end{aligned}$$

On the other hand, integrating (3.18) on Ω, we get, thanks to (3.20),

$$\begin{aligned}\frac{\mathrm{d}}{\mathrm{d}t}\left[\int_\Omega \varrho_{\mathrm{air}} Y_{\mathrm{v,air}}(t,x)\,\mathrm{d}x\right] &= \int_\Omega S_Y(t,x)\,\mathrm{d}x \\ &= \int_\Omega \iiint\limits_{\mathbb{R}^3\times\mathbb{R}_+^*\times\mathbb{R}_+^*} 4\pi r^2 \varrho_{\mathrm{w}} N_{\mathrm{d}}(r,T,Y_{\mathrm{v,air}}(t,x))\, f(t,x,v,r,T)\,\mathrm{d}v\,\mathrm{d}r\,\mathrm{d}T\,\mathrm{d}x \\ &= -\int_\Omega \iiint\limits_{\mathbb{R}^3\times\mathbb{R}_+^*\times\mathbb{R}_+^*} m'(r)\, a(r,T,Y_{\mathrm{v,air}}(t,x))\, f(t,x,v,r,T)\,\mathrm{d}v\,\mathrm{d}r\,\mathrm{d}T\,\mathrm{d}x.\end{aligned}$$

That clearly concludes the formal proof. □

The exchanges of thermal energy associated to water transfers between the air and the aerosol are more intricate to understand. The following proposition holds.

Proposition 3.2.2. *Assume that $u = 0$ and $\nabla_x T_{\mathrm{air}} \cdot n = 0$ on $\partial\Omega$, and that $f = 0$ on $\partial\Omega \times \mathbb{R}^3 \times \mathbb{R}_+^* \times \mathbb{R}_+^*$. Then we have*

$$\frac{\mathrm{d}}{\mathrm{d}t}\left[\int_\Omega \left(\varrho_{\mathrm{air}} c_{P_{\mathrm{air}}} T_{\mathrm{air}}(t,x) + \iiint\limits_{\mathbb{R}^3\times\mathbb{R}_+^*\times\mathbb{R}_+^*} m(r) c_{P_{\mathrm{d}}} T f(t,x,v,r,T)\,\mathrm{d}v\,\mathrm{d}r\,\mathrm{d}T\right)\mathrm{d}x\right]$$
$$= -\int_\Omega \iiint\limits_{\mathbb{R}^3\times\mathbb{R}_+^*\times\mathbb{R}_+^*} 4\pi r^2 (L_{\mathrm{v}} + c_{P_{\mathrm{d}}} T) N_{\mathrm{d}}(r,T,Y_{\mathrm{v,air}}(t,x))\, f(t,x,v,r,T)\,\mathrm{d}v\,\mathrm{d}r\,\mathrm{d}T\,\mathrm{d}x. \quad (3.24)$$

Proof. On the one hand, we integrate (3.21) over Ω to obtain

$$\frac{\mathrm{d}}{\mathrm{d}t}\left[\int_\Omega \varrho_{\mathrm{air}} c_{P_{\mathrm{air}}} T_{\mathrm{air}}(t,x)\,\mathrm{d}x\right] = \int_\Omega S_T(t,x)\,\mathrm{d}x.$$

Then we multiply (3.1) by $m(r)c_{P_{\mathrm{d}}}T$ and integrate it with respect to all the variables except t to get

$$\frac{\mathrm{d}}{\mathrm{d}t}\left[\int_\Omega \iiint\limits_{\mathbb{R}^3\times\mathbb{R}_+^*\times\mathbb{R}_+^*} m(r) c_{P_{\mathrm{d}}}\, T\, f(t,x,v,r,T)\,\mathrm{d}v\,\mathrm{d}r\,\mathrm{d}T\,\mathrm{d}x\right]$$
$$= \int_\Omega \iiint\limits_{\mathbb{R}^3\times\mathbb{R}_+^*\times\mathbb{R}_+^*} \big[m'(r) c_{P_{\mathrm{d}}}\, T\, a(r,T,Y_{\mathrm{v,air}}(t,x))\, f(t,x,v,r,T)$$
$$+ m(r)\, b(r,T,Y_{\mathrm{v,air}}(t,x),T_{\mathrm{air}}(t,x))\, f(t,x,v,r,T)\big]\,\mathrm{d}v\,\mathrm{d}r\,\mathrm{d}T\,\mathrm{d}x.$$

Then we sum both previous equalities to recover (3.24), noticing that the term involving Q_{d} vanishes, keeping two terms involving N_{d}: one with L_{v} to take the change of physical state into account and one with the added thermal energy in the aerosol due to the mass exchange. □

For the total momentum conservation, when the retroaction term is involved, in fact, the formal proof is exactly the same as in [17]. We do not present any more details about the conservation of this quantity and the total kinetic energy decreasing.

3.3 Numerical method

Before studying some relevant physical situations from the computational viewpoint, let us describe, in this section, the numerical scheme we implemented to solve system (ARAT).

We proceed in the same way as in [17], by using a time-marching scheme and uncoupling the fluid and aerosol equations. First, we solve the three fluid equations (3.15)–(3.16), (3.18) and (3.21) with the source terms computed at the previous time step for both equations for $Y_{\mathrm{v,air}}$ and T_{air} (recall that F is chosen equal to 0). Then we solve the Vlasov equation (3.1) using the updated fluid quantities. For the fluid equations, we use a finite-element method, and the aerosol is computed thanks to a particle method. All the computations are performed in a two-dimensional setting with FreeFem++ [35], on a time interval $[0,\tau]$, where $\tau > 0$ is given. For a time step $\Delta t > 0$ such that $\tau/\Delta t \in \mathbb{N}^*$, we denote $t^n = n\Delta t$ for any n, with $0 \leqslant n \leqslant N$. The domain Ω is discretized as a tetrahedric mesh Ω_h.

Let us provide more details about the numerical solving. As already stated, we start by solving the fluid equations, and use a finite element method to do so. If we write weak formulations of those equations, we introduce the following test functions: $\chi \in L^2(\Omega)$ for (3.16), and ν, ψ, $\phi \in H^1(\Omega)$, vanishing on Γ^{in} and Γ^{wall}, respectively for (3.15), (3.18) and (3.21). Then, for the discretization, we are led to use $\mathbb{P}_2$ functions for the velocities u and ν and $\mathbb{P}_1$ functions for p, $Y_{\mathrm{v,air}}$, T_{air}, χ, ψ and ϕ.

To go from t^n to t^{n+1}, assume that u^n, $Y^n_{\mathrm{v,air}}$, T^n_{air}, S^n_T and S^n_Y are known. In order to handle the convective term in (3.15), we introduce the approximated characteristic flow X^n, which approximates the solution X to the Cauchy problem, set on $[t^n, t^{n+1}]$,

$$\dot{X}(s) = u^n(s, X(s)), \qquad X(t^{n+1}) = x,$$

for any $x \in \Omega_h$. The approximation X^n is computed thanks to the FreeFem++ command convect. Hence, we define u^{n+1} as the solution to the following discrete weak formulation

$$\varrho_{\mathrm{air}} \int_\Omega \frac{u^{n+1} - u^n \circ X^n}{\Delta t} \cdot \nu \,\mathrm{d}x + \eta \int_\Omega \nabla_x u^{n+1} : \nabla_x \nu \,\mathrm{d}x \\ - \int_\Omega p^{n+1} \operatorname{div}_x \nu \,\mathrm{d}x + \int_\Omega \operatorname{div}_x u^{n+1} \chi \,\mathrm{d}x = 0. \quad (3.25)$$

We proceed in the same way to define $Y^{n+1}_{\mathrm{v,air}}$ and T^{n+1}_{air} as the solutions to the discrete weak formulations

$$\begin{aligned} \varrho_{\mathrm{air}} \int_\Omega \frac{Y^{n+1}_{\mathrm{v,air}} - Y^n_{\mathrm{v,air}} \circ X^n}{\Delta t} \phi \,\mathrm{d}x + D_{\mathrm{v}} \int_\Omega \nabla_x Y^{n+1}_{\mathrm{v,air}} \cdot \nabla_x \phi \,\mathrm{d}x &= \int_\Omega S^n_Y \phi \,\mathrm{d}x, \\ \varrho_{\mathrm{air}} c_{P_{\mathrm{air}}} \int_\Omega \frac{T^{n+1}_{\mathrm{air}} - T^n_{\mathrm{air}} \circ X^n}{\Delta t} \psi \,\mathrm{d}x + \kappa_{\mathrm{air}} \int_\Omega \nabla_x T^{n+1}_{\mathrm{air}} \cdot \nabla_x \psi \,\mathrm{d}x &= \int_\Omega S^n_T \psi \,\mathrm{d}x. \end{aligned}$$

Note that, in the considered air temperature range, the value of D_{v}, which theoretically depends on T_{air}, only has a 2 % variation, so we choose not to update D_{v} with respect to T_{air} in this equation.

Next comes the aerosol numerical solving. Since we use a particle method, we discretize the distribution function f as a weighted sum of Dirac masses in the position, velocity, radius and temperature variables. More precisely, we consider $N_{\mathrm{num}} \in \mathbb{N}^*$ numerical particles, each of them having the representativity $\omega \in \mathbb{N}^*$, so that the total number of physical particles is $N_{\mathrm{aero}} = \omega N_{\mathrm{num}}$. Note that, for obvious computational cost reasons, N_{num} must be chosen to be small with respect to N_{aero}, but large enough to faithfully represent the distribution of the aerosol particles.

The distribution function is then approximated by

$$f(t,x,v,r,T) \simeq \omega \sum_{p=1}^{N_{\text{num}}} \delta_{x_p(t)} \otimes \delta_{v_p(t)} \otimes \delta_{r_p(t)} \otimes \delta_{T_p(t)}(x,v,r,T),$$

where $x_p(t)$, $v_p(t)$, $r_p(t)$, $T_p(t)$ are the coordinates, in the space phase of f, of the numerical particle $p \in \{1,\ldots,N_{\text{num}}\}$ at time t.

The particle coordinates solve the following differential system

$$\left\{\begin{array}{rcl} \dot{x}_p(t) &=& v_p(t), \\ \dot{v}_p(t) &=& \alpha(r_p(t))(u(t,x_p(t)) - v_p(t)) + g, \\ \dot{r}_p(t) &=& a(r_p(t), T_p(t), Y_{\text{v,air}}(t,x_p(t))), \\ \dot{T}_p(t) &=& b(r_p(t), T_p(t), Y_{\text{v,air}}(t,x_p(t)), T_{\text{air}}(t,x_p(t))), \end{array}\right. \tag{3.26}$$

supplemented with initial data chosen to fit the distribution of droplets given by f_{init}.

The ODE on r_p is solved thanks to a RK4 scheme, in order to remain very accurate for the radii computations, involving the newly computed value $Y_{\text{v,air}}^{n+1}$ at the current position of the particle x_p^n. The velocity and temperature ODEs are solved with a semi-implicit Euler scheme, respectively involving u^{n+1}, and $Y_{\text{v,air}}^{n+1}$, T_{air}^{n+1}, all of them again being valued at x_p^n. Eventually, the position x_p^{n+1} is updated using the newly computed v_p^{n+1}.

Once we know $(x_p^{n+1}, v_p^{n+1}, r_p^{n+1}, T_p^{n+1})$ for all $p = 1,\ldots,N_{\text{num}}$, we define the source terms for the next time step t^{n+1} as

$$\begin{array}{rcl} S_Y^{n+1} &=& \omega \varrho_{\text{w}} \displaystyle\sum_{p=1}^{N_{\text{num}}} 4\pi \left(r_p^{n+1}\right)^2 N_{\text{d}}(r_p^{n+1}, T_{\text{air}}^{n+1}(x_p^{n+1}), Y_{\text{v,air}}^{n+1}(x_p^{n+1}))\delta_{x_p^{n+1}}, \\ S_T^{n+1} &=& \omega \displaystyle\sum_{p=1}^{N_{\text{num}}} 4\pi \left(r_p^{n+1}\right)^2 Q_{\text{d}}(r_p^{n+1}, T_p^{n+1}, T_{\text{air}}^{n+1}(x_p^{n+1}))\delta_{x_p^{n+1}}. \end{array}$$

In order to take into account the deposition or exiting conditions from (3.2), in the previous definition of the discrete source terms at time t^{n+1}, we drop the indices p such that x_p^{n+1} is outside the domain Ω_h in the sum $p \in \{1,\ldots,N_{\text{num}}\}$. It means that, at time t^{n+1}, the corresponding particle p either deposited on the wall or went out of the domain through the outlet (depending on its distance to Γ^{wall} and Γ^{out} at time t^n) . Note that a particle p is also considered to be deposited if the distance between x_p and Γ^{wall} is smaller that r_p. The same goes for Γ^{out} for exiting the domain. Once the particle is deposited or out, it is of course not treated numerically anymore.

It appears mandatory to perform a time-subcycling for the aerosol computations. Without that subcycling, the particle would be able to go across various cells during the same (fluid) time step. Moreover, it is particularly relevant when dealing with the particle temperatures because, if we compute the coefficients involved, we can check that the temperature ODE is very stiff.

3.4 Numerical simulations

In this section, we numerically investigate various situations. Let us first provide the specific setting of our numerical experiments. Note that the values of the physical constants appearing in our models are gathered in Appendix 3.A.

3.4.1 Experimental context, reference situation

The final time is set at $\tau = 1$ s. Our domain is supposed to represent the trachea and the first bifurcation in the human airways, see Figure 3.1). Its characteristic sizes and shape are the ones described in [71, 68], taking into account a 3D-2D correction coefficient for each branch length. More precisely, the diameter of the trachea is set at $D_0 = 1.80$ cm, and its length at $\ell_0 = 7.52$ cm. The right-hand bronchus has an angle of 25∘ with the tracheal axis, it is quite short ($\ell_{10} = 3.75$ cm), but its diameter quite large, $D_{10} = 1.50$ cm. The left-hand bronchus has an angle of 45∘ with the tracheal axis, it is longer than the first one ($\ell_{01} = 6.75$ cm), but its diameter is smaller, with $D_{01} = 1.00$ cm. Let us emphasize that the right-hand bronchus is the left branch on Figure 3.1, and conversely: we have the outsider's view, not the patient's.

The middle of the boundary inlet Γ^{in} is the origin of the space coordinate system, with horizontal and vertical axes.

Let us now provide the boundary and initial conditions for the fluid equations. The velocity fluid is initialized at $u_{\text{init}} = 0$, and, at the inlet, u^{in} follows a Poiseuille law, *i.e.* it is vertically oriented from up to bottom and its modulus is given, for any $x \in \Gamma^{\text{in}}$, by

$$|u^{\text{in}}(x)| = \frac{4u_0}{{D_0}^2}\left(\frac{{D_0}^2}{4} - {x_1}^2\right),$$

where $u_0 = 50.0$ cm.s^{-1}. The air temperature uses the following values

$$T_{\text{air,init}} = 37^\circ\text{C} = 310 \text{ K}, \quad T_{\text{air}}^{\text{in}} = 24^\circ\text{C} = 297 \text{ K}, \quad T_{\text{wall}} = 37^\circ\text{C} = 310 \text{ K}.$$

The initial and boundary values of $Y_{\text{v,air}}$ uses the ones of the relative humidities in the airways, here chosen as $\text{RH}_{\text{lung}} = 0.990$ and $\text{RH}_{\text{wall}} = 1.00$. Then we write

$$Y_{\text{v,air,init}} = \frac{\text{RH}_{\text{lung}} P_{\text{v,sat}}(T_{\text{air,init}})}{\varrho_{\text{air}} R_{\text{v}} T_{\text{air,init}}}, \qquad Y_{\text{v,air}}^{\text{in}} = \frac{\text{RH}_{\text{lung}} P_{\text{v,sat}}(T_{\text{air}}^{\text{in}})}{\varrho_{\text{air}} R_{\text{v}} T_{\text{air}}^{\text{in}}},$$

$$Y_{\text{v,wall}} = \frac{\text{RH}_{\text{wall}} P_{\text{v,sat}}(T_{\text{wall}})}{\varrho_{\text{air}} R_{\text{v}} T_{\text{wall}}}.$$

Figure 3.1 shows the values of $|u|$, $Y_{\text{v,air}}$ and T_{air} at final time, where some kind of stationary state is reached for the fluid. Let us next describe the computational and experimental parameters for the aerosol. We consider 5 injections in the domain of 100 numerical particles each with representativity $\omega = 10^4$, periodically released between initial time and $t = 0.25$ s. Hence, we deal with $N_{\text{num}} = 500$ numerical particles and $N_{\text{aero}} = 5\ 10^6$ physical particles.

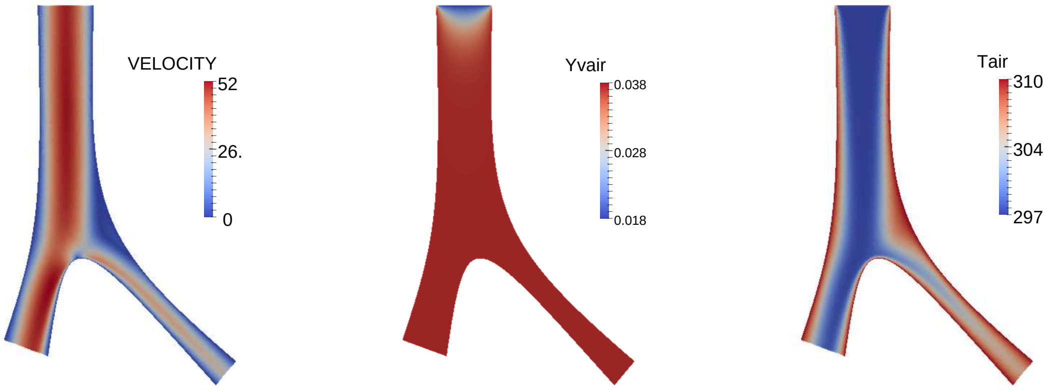

(a) (b) (c)

Table 3.1 – Distribution of the velocity $|u|$, water vapor mass fraction in the air $Y_{\mathrm{v,air}}$ and temperature T_{air} at final time $\tau = 1$ s.

All the numerical particles initially have the same vertical velocity $v_{p,2}(0) = -100$ cm.s^{-1}, the same radius $r_p(0) = 2.25\ 10^{-5}$ cm, and the same temperature $T_p(0)$, equal to the air temperature $T_{\mathrm{air}}^{\mathrm{in}}$ at the inlet. They are released from random positions $x_p(0) \in \Gamma^{\mathrm{in}}$ with its first coordinate in $[-D_0/4, D_0/4]$, following a uniform law. We choose this latter interval instead of $[-D_0/2, D_0/2]$ so that it allows a larger deposition phenomenon. Since we use a particle method, it is mandatory, in order to obtain meaningful results, to perform averaging computations over several initial randomly chosen distributions of droplets, in our case, 10 different distributions.
This parameter set defines what we name the *reference situation*, which was first used to validate the code. Indeed, we checked, at the computational level, the total mass conservation in the water vapour exchange between air and aerosol and the thermal energy balance implied by the thermodynamic state change of water vapour. The next subsection also lies in the framework of the reference situation, in order to give an almost exhaustive overview of all the phenomena.

3.4.2 Numerical tests

We first show, for the (ARAT) model, the behaviour of the air velocity u and temperature T_{air} at different times, as well as the movement in the domain of the various aerosol releases, in Figures 3.3–3.4. We do not provide snapshots for the water vapor mass fraction $Y_{\mathrm{v,air}}$ because they would look like Figure 3.1(b): $Y_{\mathrm{v,air}}$ seems to reach a stationary state very fast, whereas u and T_{air} only do so near time 0.48 s.

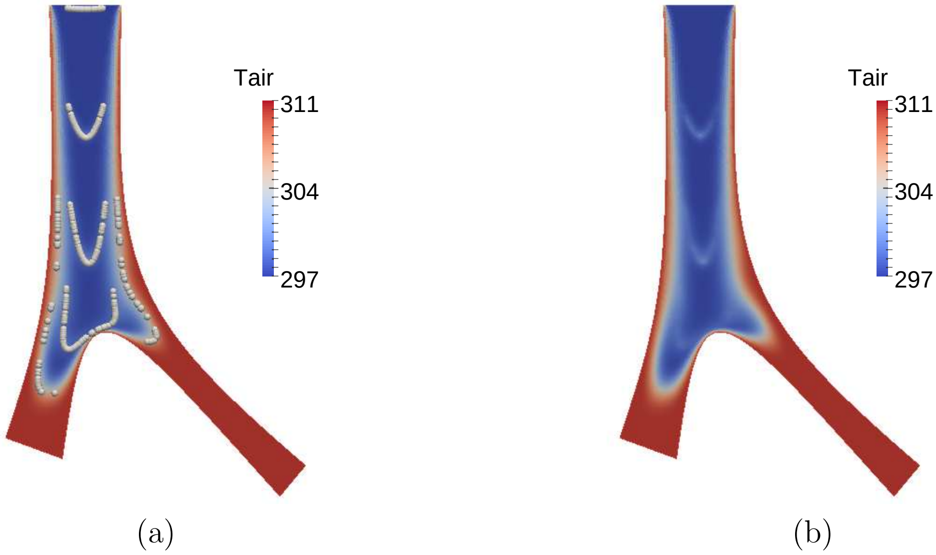

Figure 3.5 – Local effects of the aerosol on the air temperature, here at time $0.25 + \Delta t$ (in seconds).

Figure 3.5, where the air temperature is shown just after the last aerosol release at time 0.25 s, plotting or not the particle positions, allows to point out an effect which could not be seen in the snapshots from Figure 3.4, because of the plotting of the particles in the domain. Indeed, for all aerosol releases except for the first one, there is a local air temperature increasing at the location of the particles. This effect is clearly not explained by direct thermal phenomena, hence it comes from the water vapour mass exchange between the humidified air and the droplets.

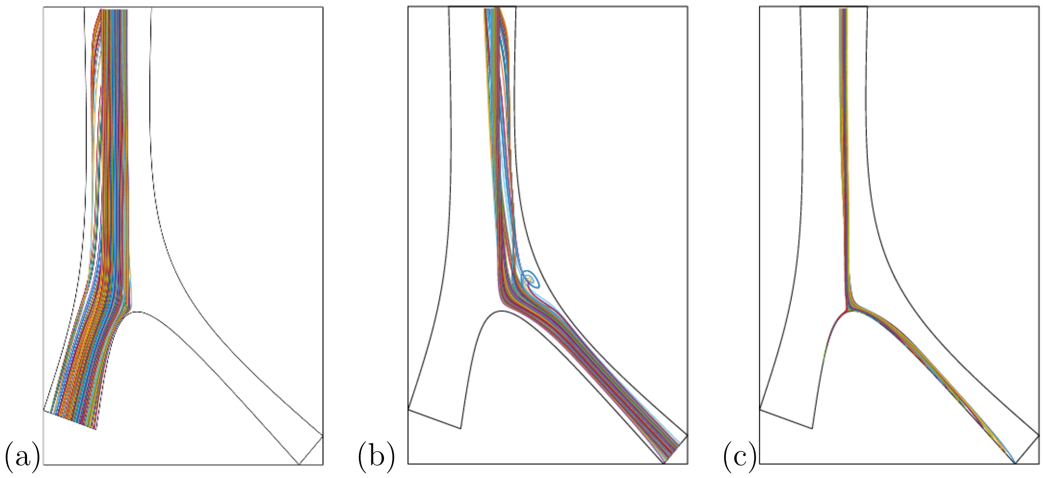

Figure 3.6 – Particle trajectories (a) towards the left branch, (b) towards the right branch, (c) deposition.

On Figure 3.6, we represent the particle trajectories obtained with the (ARAT) model. In this example, most of the droplets (348 over 500) go out of the domain through the left branch. A less significant number of particles (98) go out through the right branch, and a smaller part of them (47) deposit on the wall (more precisely, on the "internal" wall of the left branch). There are still 7 droplets in the domain at final time. The major exit at the left branch is of course no surprise: because of its diameter, the branch is the most natural way out for the aerosol.

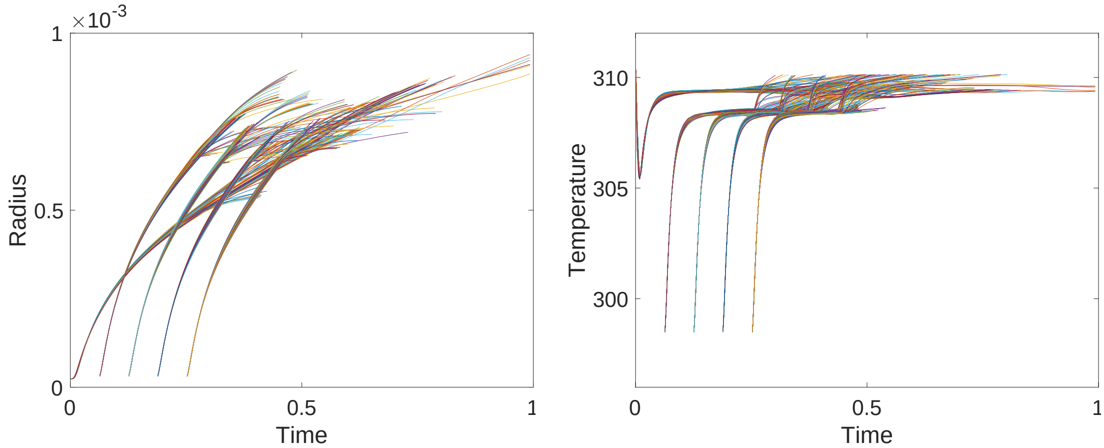

Figure 3.7 – Radius and temperature evolution of all the particles with respect to time.

Let us now focus on Figure 3.7. The plots show the time evolution of (a) the radius and (b) the temperature of all the numerical particles from one of the initial distributions we used, in the (ARAT) model. It is clear from Figure 3.7(a) that, at first, the droplets from the first release do not behave in the same way as the ones from the other releases: the size growth happens more slowly. The difference is confirmed by Figure 3.7(b): the temperature plots for the first release again behave very differently from the others. In particular, even if the temperatures of the first injected particles are initially 297 K, they almost instantaneously become close to 310 K because they move in an air at 310 K, see Figure 3.4(a). On the contrary, the other releases live in a cooler air, see Figure 3.4(b)–(e), and hence are not submitted to a thermal shock. Then, we can check on Figure 3.7 that each plot seems to have a characteristic time of behaviour change. It is definitively clear on Figure 3.7(b). For all releases except for the first one, there is a temperature jump which is, for the second one, located in time at approximately 0.25 s. If we observe the temperature snapshot 3.4(d), we can see that the corresponding time, which is 0.24 s, is approximately the one when the second release goes into the branches, where the diameters are significantly smaller than in the trachea, and where the wall effect consequently appears stronger. This explains the fact that the particle temperatures increase more.

Then, on Figures 3.8–3.10, we compare the radius and temperature evolution, with respect to time, of particular droplets of the second release evolving in models (ARAT), (ARST) and (SRST). Figure 3.8 focuses on a droplet exiting the domain through the left branch with the (ARAT) model, Figure 3.9 through the right branch, and Figure 3.10 on a droplet depositing. Note that those same particles share the same future in models (ARAT) and (SRST), but are all deposited in the (ARST) model. Let us first comment Figures 3.8(b)–3.10(b), *i.e.* the temperature plots. Of course, in the (ARST) and (SRST) models, the temperature remains constant, whereas, in the (ARAT) model, the particle temperature grows until it (approximately) reaches T_{wall}. This may seem peculiar. Indeed, the aerosol enters the domain at 297 K, and, except for the first aerosol release, it evolves in a cooled air. Since the droplet temperature variations cannot be explained because of the ambient air temperature, it means that they are triggered by hygroscopic phenomena. This leads us to study more carefully Figures 3.8(a)–3.10(a). As one can see, in the three situations, model (ARST) induces a larger size growth than model (ARAT): this may explain the fact that the particle deposits in model (ARST). The hygroscopic effects imply radius variations for both models, but a part of this variation existing in the (ARST) model also has a temperature effect in the (ARAT) model, which justifies that the radius for (ARAT) is smaller than the one for (ARST).

Let us finally provide some statistical behaviours of the aerosol for each model. In Table 3.2, we first give the following values, all of them being computed from the 10 initial aerosol distributions used to solve the Vlasov equation:

— the droplets mean radius and temperature at “final” time (in the sense that, when a particle exits or deposits during the computation, its radius and temperature do not change anymore until the end of the simulation),

— the mean percentage of deposited particles and of particles reaching the boundaries Γ^{out} (right and left) among the 500 particles,

— the corresponding mean event time, *i.e.* the time when the particles exit or deposit.

Models	(ARAT)	(ARST)	(SRST)
Mean radius (cm)	$6.55\ 10^{-4}$	$1.67\ 10^{-3}$	$2.25\ 10^{-5}$
Mean temperature (K)	309	297	297
Deposited particles	7.6%	35.5%	0.0%
Left exiting particles	69.0%	64.5%	69.6%
Right exiting particles	22.4%	0.0%	24.7%
Mean depos. time (s)	0.409	0.270	–
Mean left exit time (s)	0.289	0.261	0.296
Mean right exit time (s)	0.509	–	0.461

Table 3.2 – Statistics in the reference case.

As seen in Figures 3.8(a)–3.10(a), the particle mean radius in the (ARAT) model is intermediate between the ones from (SRST) and (ARST), and, as already emphasized, when we neglect the temperature effects, the particle radius must bear the whole hygroscopic effect in the (ARST) model. Besides, the size growth between (SRST) and (ARAT) is significant. It seems to be the main reason for aerosol deposition in that case. Otherwise, (ARAT) and

(SRST) models have closer mean behaviours, which may imply that the (ARST) model is not relevant.

Finally, Table 3.3 gives the droplets mean radius at final time depending on their evolution (deposition, left/right exiting) for (ARAT) and (ARST) models, since the radius remains constant to 2.25 10^{-5} cm with the (SRST) model. There exists a significant variation of the radius, which can be linked to the mean event times in Table 3.2. In the (ARAT) model, the particles going out through the right branch remain longer in the domain, thus undergoing a larger radius growth. For the (ARST) model, deposition or exiting happen more or less at the same time, leading to very similar radii for the particles.

	Deposited particles	Left exiting particles	Right exiting particles
Mean radius (cm) with model (ARAT)	6.43 10^{-4}	6.25 10^{-4}	7.42 10^{-4}
Mean radius (cm) with model (ARST)	1.68 10^{-3}	1.67 10^{-3}	–

Table 3.3 – Statistics for the particles depending on their future (depositing/exiting).

3.5 Conclusion

The previous section allowed to point out the relevance of model (ARAT) compared to (ARST) and (SRST) to properly take into account the hygroscopic effects on aerosols in the airways.

Besides, in our opinion, there are plenty of situations remaining to investigate, which should be addressed in further works. Let us mention some of them below.

First, observe that the source term modelled by function b given by (3.7), which drives the behaviour of the aerosol particles, is naturally composed of two terms, which we may denote by b_1 and b_2 (the first one involves Q_d and the second one N_d). In fact, b_1 and b_2 happen to have opposite signs and the same order of magnitude, around 2 10^5 K/s at initial time, whereas b approximately equals 400 K/s (see Figure 3.11). Even if the model seems to behave nicely with respect to temperatures (the temperature of the corresponding numerical particle is given on Figure 3.12), it is only because we used a very fine subcycling time step to guarantee numerical accuracy in the description of the thermal effects. From the computational viewpoint, this can probably be improved.

We did not provide any numerical tests with the presence of excipient in the aerosol, *i.e.* we chose $r_\mathrm{ex} = r_\mathrm{drug}$, though we wrote the (ARAT) model involving the excipient. Nevertheless, since standard values of ϱ_drug and ϱ_ex are close to each other, it is unlikely that the excipient implies major behaviour changes on the aerosol.

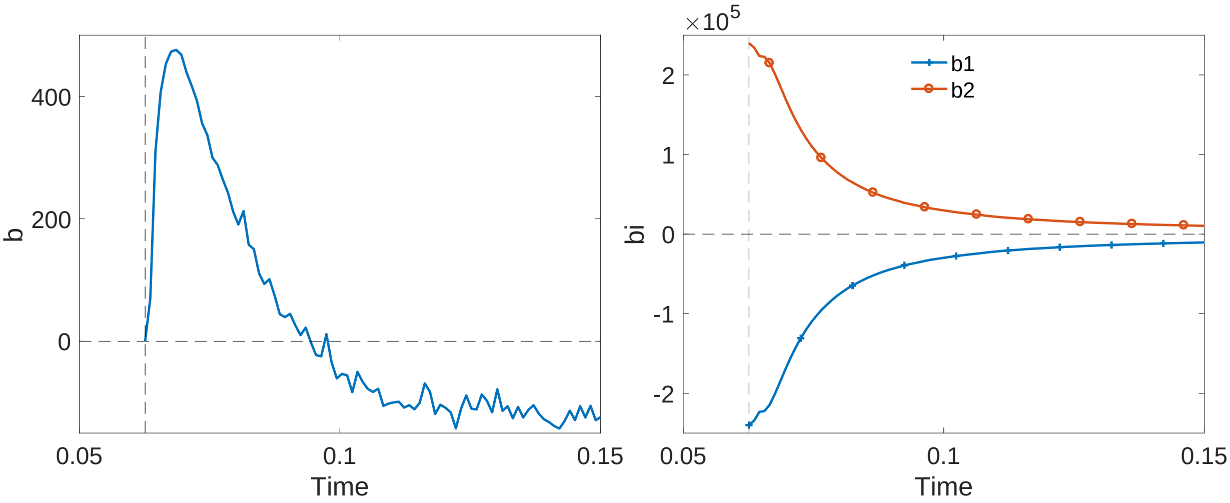

Figure 3.11 – Order of magnitude of each thermal effect b_1 and b_2 for a given particle.

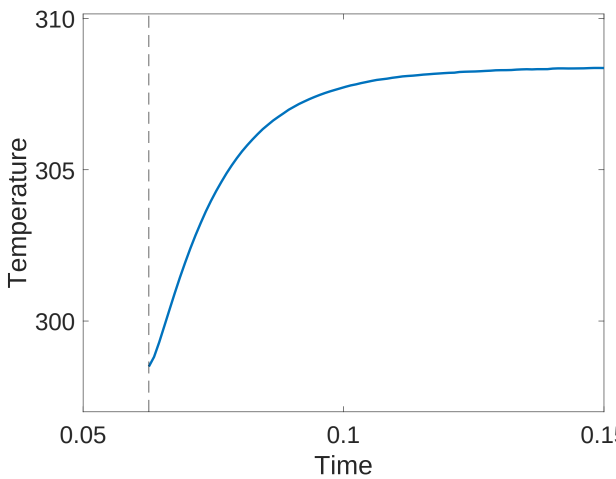

Figure 3.12 – Temperature evolution of the chosen particle in Figure 3.11.

Moreover, the air flow we here studied was only related to the inspiration part of the respiration. However, it seems difficult to tackle the expiration part, because boundary conditions on f at Γ^{out} are then unclear.

The computational domain here represents the upper part of the airways, including the trachea. It would be relevant to study the model behaviour within other domains, not necessarily with a vertical main axis, to understand the effect of the geometrical variability.

Eventually, as it was emphasized in [17] where 3D computations are performed, compared to [16] in a 2D domain, two-dimensional simulations tend to increase the aerosol deposition phenomenon. In order to study the model very faithfully, it is probably mandatory to work in a 3D setting.

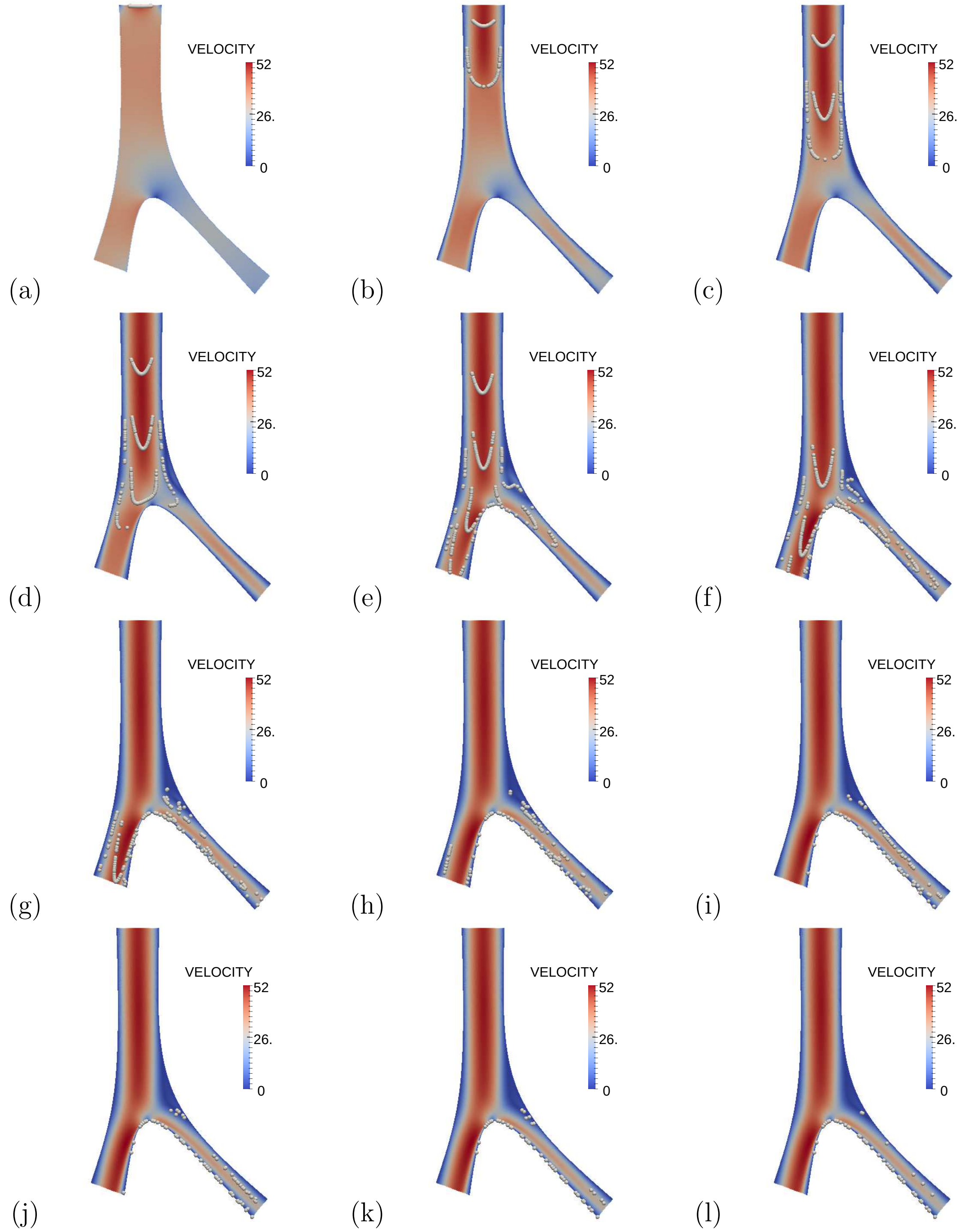

Figure 3.3 – Dynamics of the particles with the air velocity, at time t = 0.00, 0.08, 0.16, ..., 0.80 s and at final time τ = 1 s.

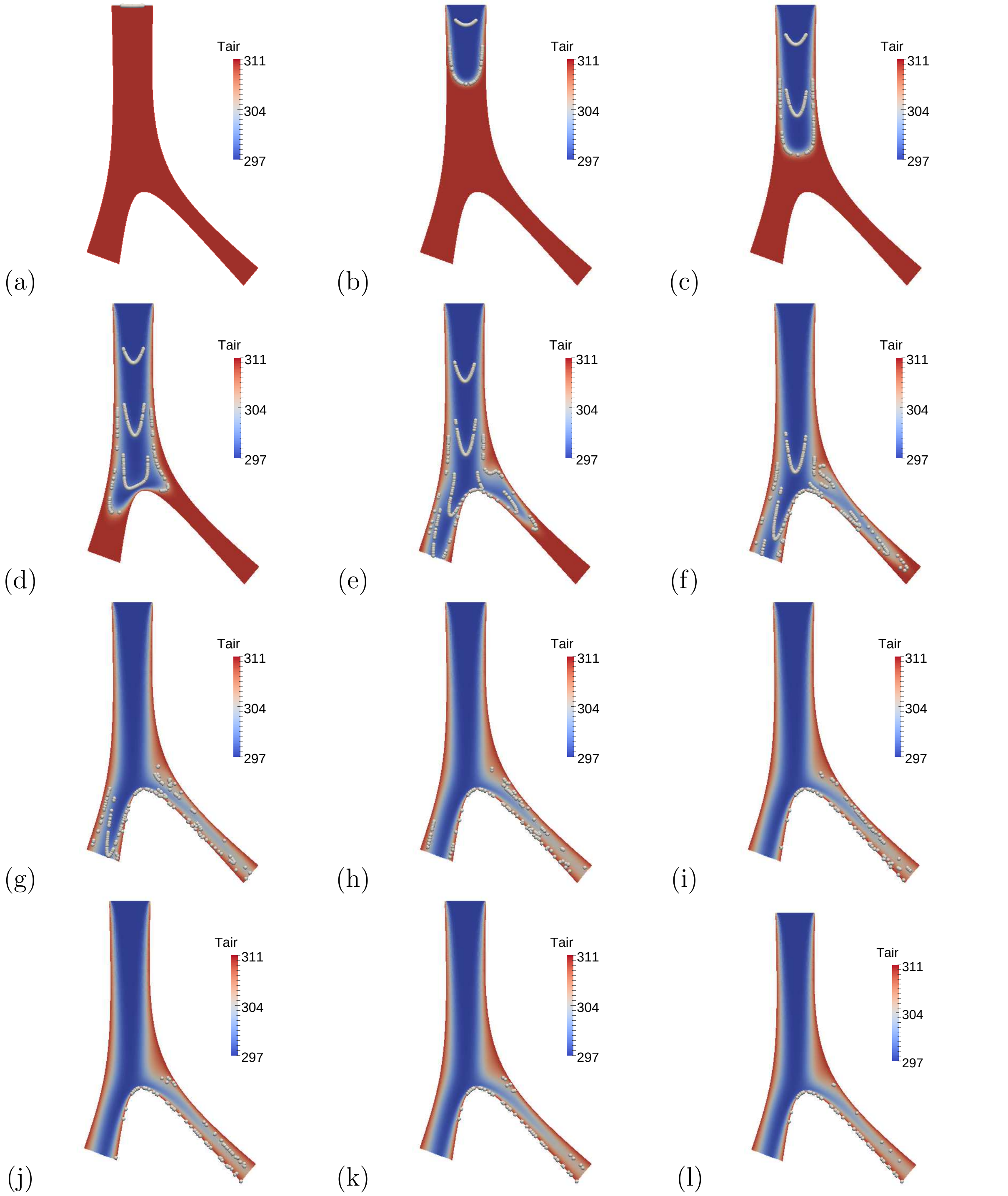

Figure 3.4 – Dynamics of the particles with the air temperature, at time t = 0.00, 0.08, 0.16, ..., 0.80 s and at final time $\tau = 1$ s.

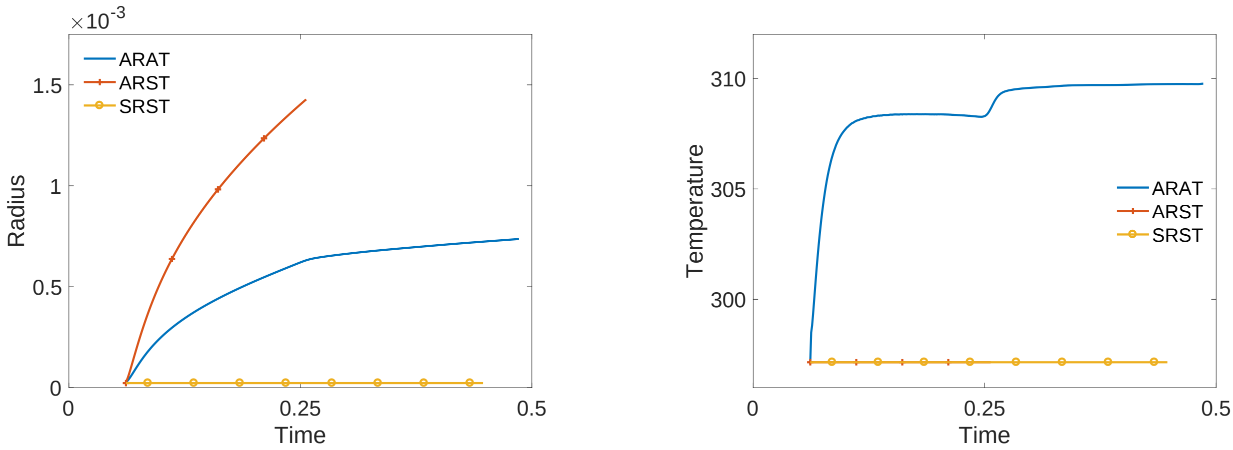

Figure 3.8 – Radius and temperature evolution of a particular droplet which goes out through the left branch, comparison in the three models.

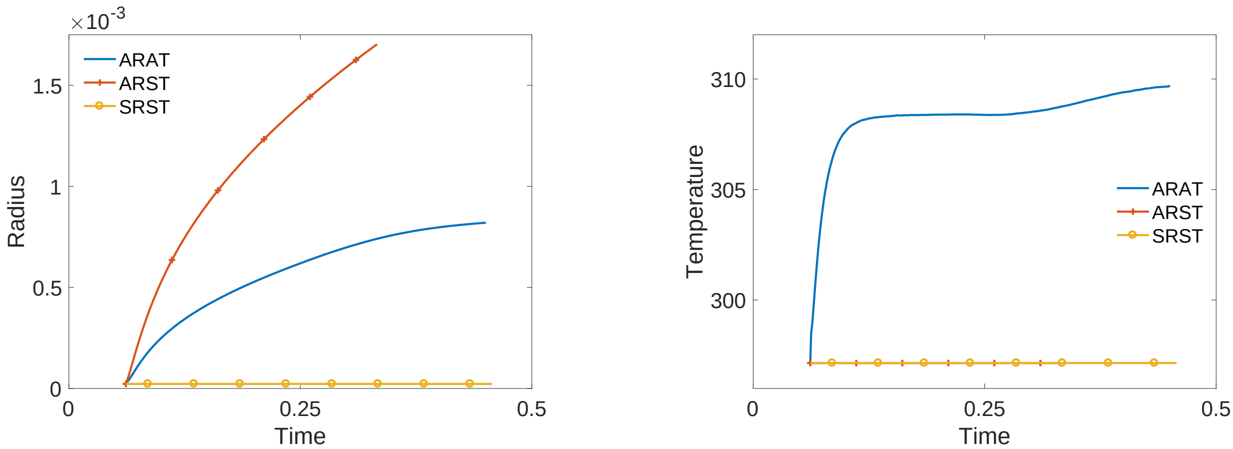

Figure 3.9 – Radius and temperature evolution of a particular droplet which goes out through the right branch, comparison in the three models.

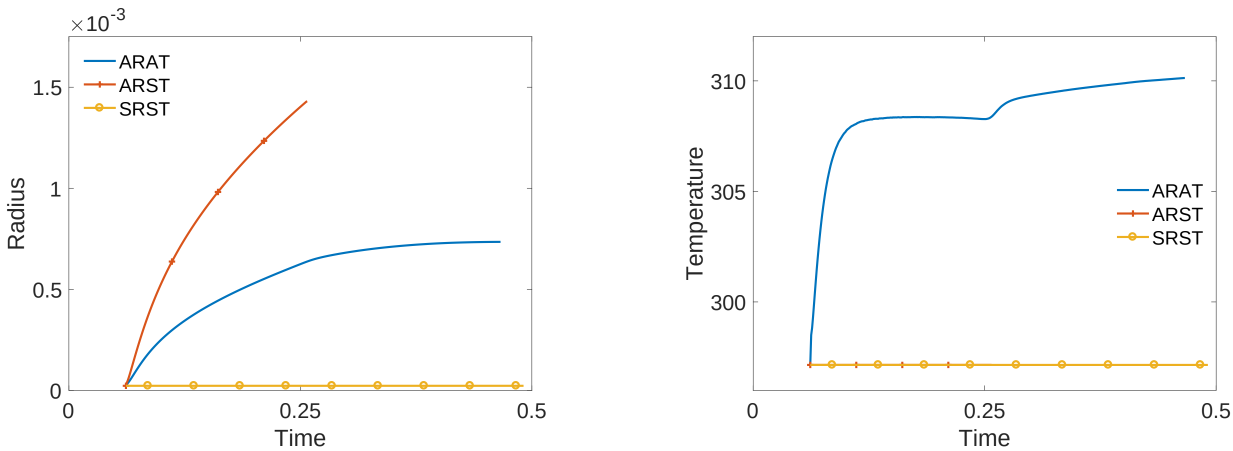

Figure 3.10 – Radius and temperature evolution of a particular droplet which deposits, comparison in the three models.

Appendix

3.A Values of the physical constants

All the values of the physical constants used in our numerical simulations are given in Table 3.A.1.

Quantity	**Symbol**	**Value**	**Unit** (cgs)
Gravitation	$\|g\|$	980	cm.s^{-2}
Air mass density	ϱ_{air}	1.18 10^{-3}	g.cm^{-3}
Air specific heat	$c_{P_{\mathrm{air}}}$	1.01 10^{7}	cm^{2}.s^{-2}.K^{-1}
Air thermal conductivity	κ_{air}	2.60 10^{3}	g.cm.s^{-3}.K^{-1}
Air dynamic viscosity	η	1.18 10^{-4}	g.cm^{-1}.s^{-1}
Water mass density	ϱ_{w}	0.997	g.cm^{-3}
Drug mass density	ϱ_{drug}	1.34	g.cm^{-3}
Excipient mass density	ϱ_{ex}	2.17	g.cm^{-3}
Water molar mass	M_{w}	18.0	g.mol^{-1}
Drug molar mass	M_{drug}	577	g.mol^{-1}
Excipient molar mass	M_{ex}	58.4	g.mol^{-1}
Drug van't Hoff coefficient	i_{drug}	2.10	–
Excipient van't Hoff coefficient	i_{ex}	2.10	–
Droplet specific heat	$c_{P_{\mathrm{d}}}$	4.18 10^{7}	cm^{2}.s^{-2}.K^{-1}
Droplet mass Knudsen number correction	C_m	1.00	–
Droplet temperature Knudsen correlation	C_T	1.00	–
Droplet Nusselt number	Nu	2.00	–
Droplet Sherwood number	Sh	2.00	–
Water vaporization latent heat	L_{v}	2.26 10^{10}	cm^{2}.s^{-2}
Droplet surface tension	σ	72.0	dyn.cm^{-1}
Water vapor specific gas constant	R_{v}	4.61 10^{6}	cm^{2}.s^{-2}.K^{-1}

Table 3.A.1 – Value of the physical constants.

Chapter 4

Analysis of the transport-Stokes equation

Abstract

This chapter is dedicated to the analysis of the transport-Stokes equation derived in the first chapter. First we present a global existence and uniqueness result for $L^1 \cap L^\infty$ initial densities with finite first moment. Secondly, we consider the case where the initial data is the characteristic function of a droplet and investigate the regularity of its surface. We present a local existence and uniqueness result for the surface parametrization. Finally, we consider the case where the initial domain is the unit ball and present some numerical computations that shows the droplet regularity breakup.

4.1 Introduction

In this chapter, we consider the sedimentation of a cloud of rigid particles in a viscous fluid. At the mesoscopic scaling, It has been showed that the equation describing the dynamics is the transport-Stokes problem in the case where inertia of both fluid and particles is neglected:

$$\left\{ \begin{array}{rcll} \partial_t \varrho + \operatorname{div}((u + \kappa g)\varrho) & = & 0\,, & \text{on } \mathbb{R}^+ \times \mathbb{R}^3, \\ -\Delta u + \nabla p & = & 6\pi r_0 \kappa \varrho g\,, & \text{on } \mathbb{R}^3, \\ \operatorname{div} u & = & 0\,, & \text{on } \mathbb{R}^3, \\ \varrho(0, \cdot) & = & \varrho_0\,, & \text{on } \mathbb{R}^3. \end{array} \right. \tag{4.1}$$

Here, the function ϱ stands for the density of the particles, (u, p) are the velocity and pressure of the fluid, r_0 is the homogenized particles radius, g is the gravity vector and κg represents the fall speed of one particle sedimenting under gravitational force. The rigorous proof of convergence of this model starting from the microscopic one is established in [38], [41], [57].

At the microscopic scaling, the motion and shape evolution of a blob has been studied in [55, 58, 62]. Experimental and numerical investigations lead to the conclusion that a

spherical cloud of particles slowly evolves to a torus. Precisely, the particles at top of the cloud leak away from the cluster and form a vertical tail. The decrease of the number of particles at the vertical axis of the cloud leads to the apparition of the toroidal form. Moreover, it has been observed that the unstable torus breaks into two secondary droplets which deform into tori themselves in a repeating cascade.
We are interested in observing this phenomena on the mesoscopic model. The idea is to consider equation (4.1) when the initial density of the cloud is the characteristic function of a bounded domain B_0. Existence and uniqueness of (4.1) has been proved in [38] for regular initial data ϱ_0. Hence, the first step of this study is to extend the result for less regular data allowing to tackle blob distribution.
Note that, if (ϱ, u) are solutions to equation (4.1), then

$$(\tilde{\varrho}(t,x), \tilde{u}(t,x)) = (\varrho(t, x + t\kappa g), u(t, x + t\kappa g)),$$

is solution to

$$\begin{cases} \partial_t \varrho + \operatorname{div}(\varrho u) &= 0\,, & \text{on } \mathbb{R}^+ \times \mathbb{R}^3, \\ -\Delta u + \nabla p &= 6\pi r_0 \kappa \varrho g\,, & \text{on } \mathbb{R}^3, \\ \operatorname{div} u &= 0\,, & \text{on } \mathbb{R}^3, \\ \varrho(0,\cdot) &= \varrho_0\,, & \text{on } \mathbb{R}^3. \end{cases}$$

Since $6\pi r_0 \kappa g = -6\pi r_0 \kappa |g| e_3$, without loss of generality, we consider in this chapter the following transport-Stokes problem:

$$\begin{cases} \partial_t \varrho + \operatorname{div}(\varrho u) &= 0\,, & \text{on } \mathbb{R}^+ \times \mathbb{R}^3, \\ -\Delta u + \nabla p &= -\varrho e_3\,, & \text{on } \mathbb{R}^3, \\ \operatorname{div} u &= 0\,, & \text{on } \mathbb{R}^3, \\ \varrho(0,\cdot) &= \varrho_0\,, & \text{on } \mathbb{R}^3. \end{cases} \tag{4.2}$$

where e_3 is the third vector of the standard basis in $\mathbb{R}^3$.
The organization of the chapter is the following one. The first section is dedicated to the existence and uniqueness of the transport-equation (4.2). In the first subsection we recall some classical results and estimates regarding the transport and Stokes equations. The second subsection is dedicated to the proof of the first Theorem. The second section concerns the analysis of the regularity of the contour of a blob. In the first subsection we provide a local existence and uniqueness of a contour parametrization. In the second subsection, we present some numerical results that show the droplet regularity breakup.

4.2 Existence and uniqueness of the transport-Stokes equation

The main result of this section is the following Theorem

Theorem 4.2.1. *Let $\varrho_0 \in L^1(\mathbb{R}^3) \cap L^\infty(\mathbb{R}^3)$ a measure with finite first moment. There exits a unique couple $(\varrho, u) \in L^\infty(0,T; L^1(\mathbb{R}^3) \cap L^\infty(\mathbb{R}^3)) \times L^\infty(0,T; W^{1,\infty}(\mathbb{R}^3))$ satisfying the* *transport-Stokes equation* (4.2) *for all* $T \geqslant 0$*. Moreover, there exists a unique characteristic flow* X *such that*

$$\varrho(t,\cdot) = X(t,0,\cdot)\#\varrho_0.$$

In order to prove the main Theorem we recall some existence, uniqueness and stability estimates for Stokes and transport equations.

4.2.1 Reminder on the Steady Stokes and transport equations

Equation (4.2) is a steady Stokes problem coupled with a transport equation. We recall here some properties concerning the Stokes problem on $\mathbb{R}^3$ and the transport equations.

Proposition 4.2.2. *Let* $\eta \in L^\infty(\mathbb{R}^3) \cap L^1(\mathbb{R}^3)$*, The unique velocity field* u *solution to the Stokes equation:*

$$\begin{cases} -\Delta u + \nabla p &= \eta\,, \quad \text{on } \mathbb{R}^3 \\ \quad \operatorname{div}(u) &= 0\,, \quad \text{on } \mathbb{R}^3, \end{cases}$$

is given by the convolution of the source term η *with the Oseen tensor* Φ *defined in chapter 1, see* (1.26) *for the definition*

$$u = \Phi * \eta.$$

Moreover, $u \in W^{1,\infty}(\mathbb{R}^3)$ *and there exists a positive constant independent of the data such that:*

$$\|u\|_\infty + \|\nabla u\|_\infty \leqslant C\|\eta\|_{L^1\cap L^\infty}. \tag{4.3}$$

A proof can be found in [38, Lemma 3.18] in the case $\eta \in X_\beta$ where X_β is defined in [38, Definition 2.5] and recalled in the first chapter, Section 1.5.1. The proof is mainly the same when considering $\eta \in L^1 \cap L^\infty$. We recall now a stability estimate using the first Wasserstein distance W_1 which is well defined for measures with finite first moment. The following Proposition uses arguments similar to [34, Proposition 3] and [33, Theorem 3.1].

Proposition 4.2.3 (Steady-Stokes stability estimates)**.** *Let* $\eta_1, \eta_2 \in L^1(\mathbb{R}^3) \cap L^\infty(\mathbb{R}^3)$ *and denote by* u_1 *and* u_2 *the associated Stokes solution. For all compact subset* $K \subset \mathbb{R}^3$ *one can show that there exists a constant depending on* K *such that*

$$\|u_1 - u_2\|_{L^1(K)} + \|\nabla u_1 - \nabla u_2\|_{L^1(K)} \leqslant C(K)\, W_1(\eta_1,\eta_2).$$

Moreover, given a density $\varrho \in L^1 \cap L^\infty$*, there exists a positive constant independent of the data such that:*

$$\int_{\mathbb{R}^3} |u_1(x) - u_2(x)|\varrho(dx) \leqslant C\|\varrho\|_{L^1\cap L^\infty} W_1(\eta_1,\eta_2) \tag{4.4}$$

Since similar computations will be used thereafter, we present the proof of the former Proposition.

Proof. According to [66, Theorem 1.5], there exists an optimal transport map T such that $\eta_2 := T\#\eta_1$ and we have:

$$W_1(\eta_1, \eta_2) = \int_{\mathbb{R}^3} |T(y) - y|\, \eta_1(dy).$$

This yields:

$$\begin{aligned}
\int_K |u_2(x) - u_1(x)|\, dx &= \int_K \left| \int_{\mathbb{R}^3} \Phi(x-y)\eta_1(dy) - \int_{\mathbb{R}^3} \Phi(x - T(y))\eta_1(dy) \right| dx \\
&\leqslant C \int_K \int_{\mathbb{R}^3} \frac{|T(y) - y|}{\min(|x-y|^2, |x - T(y)|^2)} \eta_1(dy)dx \\
&\leqslant \int_{\mathbb{R}^3} \int_K \left(\frac{1}{|x-y|^2} + \frac{1}{|x - T(y)|^2} \right) dx |T(y) - y|\, \eta_1(dy) \\
&\leqslant C(K) W_1(\eta_1, \eta_2).
\end{aligned}$$

The proof of the last formula (4.4) is analogous to the estimate above where we replace $C(K)$ by $\|\varrho\|_{L^1 \cap L^\infty}$. $\square$

Given a velocity field having the same regularity as above, we recall now an existence, uniqueness and stability estimates for the transport equations. The stability estimate presented below is analogous to [34, Proposition 3] which is adapted from [50].

Proposition 4.2.4. *Let $u \in L^\infty(0,T; W^{1,\infty}(\mathbb{R}^3))$ and $\varrho_0 \in L^1 \cap L^\infty$, for all $T > 0$ there exists a unique solution $\eta \in L^\infty(0,T; L^1 \cap L^\infty)$ to the transport equation*

$$\left\{ \begin{array}{rcl} \partial_t \varrho + \operatorname{div}(\varrho u) &=& 0\,, \\ \varrho(0, \cdot) &=& \varrho_0\,. \end{array} \right. \tag{4.5}$$

Moreover, given two velocity fields u_i, $i = 1, 2$, if we denote by ϱ_i the solutions to the associated transport equation , we have for all $t \geqslant s \geqslant 0$:

$$\begin{aligned}
&W_1(\varrho_1(t), \varrho_2(t)) \\
&\qquad \leqslant \left(W_1(\varrho_1(s), \varrho_2(s)) + \int_s^t \int_{\mathbb{R}^3} |u_2(\tau, x) - u_1(\tau, x)|\, \varrho_1(\tau, x) dx d\tau \right) e^{Q_2(t-s)},
\end{aligned} \tag{4.6}$$

where $Q_i := \|u_i\|_{L^\infty(0,T;W^{1,\infty})}$.

Proof. Classical transport theory ensures the existence and uniqueness. Precisely, the characteristic flow satisfying

$$\left\{ \begin{array}{rcll} \partial_t X(t,s,x) &=& u(s, X(t,s,x)), & \forall\, t, s \in [0,T], \\ X(s,s,x) &=& x, & \forall\, s \in [0,T], \end{array} \right. \tag{4.7}$$

is well defined in the sense of Carathéodory since u is L^∞ in time and Lipschitz regarding the space variable. Moreover, the following formula hods true

$$\varrho(t, \cdot) = X(t, s, \cdot)\#\varrho(s, \cdot). \tag{4.8}$$

Now, consider two velocity fields $u_i \in L^\infty(0,T;W^{1,\infty})$ and denote by X_i its associated characteristic flow. For all $x \neq y$, $i = 1,2$ we have:

$$\begin{aligned}|X_i(t,s,x) - X_i(t,s,y)| &\leqslant |x-y| + \int_s^t |u_i(\tau, X_i(\tau,s,x)) - u_i(\tau, X_i(\tau,s,y))| d\tau \\ &\leqslant |x-y| + Q_i \int_s^t |X_i(\tau,s,x) - X_i(\tau,s,y)| d\tau\,,\end{aligned}$$

which yields, using Gronwall's inequality, for all $t \geqslant s \geqslant 0$:

$$\mathrm{Lip}(X_i(s,t,\cdot)) \leqslant e^{Q_i(t-s)}.$$

We recall that at time $s \geqslant 0$, according to [66, Theorem 1.5], one can choose an optimal mapping T_s such that $\varrho_2(s) = T_s\#\varrho_1(s)$ and

$$W_1(\varrho_1(s), \varrho_2(s)) := \int |T_s(y) - y| \varrho_1(s,dy),$$

on the other hand, thanks to the flows X_i we can construct a mapping T_t at time $t \geqslant s$ such that $\varrho_2(t) = T_t\#\varrho_1(t)$ defined by

$$T_t := X_2(t,s,\cdot) \circ T_s \circ X_1(s,t,\cdot). \tag{4.9}$$

According to the definition of the Wasserstein distance and formulas (4.8), (4.9) we have:

$$\begin{aligned}W_1(\varrho_1(t), \varrho_2(t)) &\leqslant \int |T_t(x) - x|\, \varrho_1(t,dx) \\ &= \int |T_t(X_1(t,s,y)) - X_1(t,s,y)|\, \varrho_1(s,dy) \\ &= \int |X_2(t,s,T_s(y)) - X_1(t,s,y)|\, \varrho_1(s,dy) \\ &\leqslant \mathrm{Lip}(X_2(t,s,\cdot)) W_1(\varrho_1(s), \varrho_2(s)) + \int |X_2(t,s,y) - X_1(t,s,y)|\, \varrho_1(s,dy).\end{aligned}$$

Now we have:

$$\begin{aligned}&\int |X_2(t,s,y) - X_1(t,s,y)|\, \varrho_1(s,dy) \\ &\leqslant \int_s^t \int |u_2(\tau, X_2(\tau,s,y)) - u_1(\tau, X_1(\tau,s,y)|\, \varrho_1(s,dy) d\tau \\ &\leqslant Q_2 \int_s^t \int |X_2(\tau,s,y) - X_1(\tau,s,y))|\, \varrho_1(s,dy) d\tau + \int_s^t \int |u_2(\tau,x) - u_1(\tau,x)|\, \varrho_1(\tau,dx) d\tau.\end{aligned}$$

Gronwall's inequality yields:

$$\int_{\mathbb{R}^3} |X_2(t,s,y) - X_1(t,s,y)|\, \varrho_1(s,dy) \leqslant \left(\int_s^t \int_{\mathbb{R}^3} |u_2(\tau,x) - u_1(\tau,x)|\, \varrho_1(\tau,dx) d\tau \right) e^{Q_2(t-s)}.$$

Finally we get

$$
\begin{aligned}
W_1(\varrho_1(t), \varrho_2(t)) \leqslant & \operatorname{Lip}(X_2(t,s,\cdot)) W_1(\varrho_1(s), \varrho_2(s)) \\
& + \left(\int_s^t \int_{\mathbb{R}^3} |u_2(\tau, x) - u_1(\tau, x)| \, \varrho_1(\tau, dx) d\tau \right) e^{Q_2(t-s)},
\end{aligned}
$$

with $\operatorname{Lip}(X_2(s,t,\cdot)) \leqslant e^{Q_2(t-s)}$. □

4.2.2 proof of the existence and uniqueness result

Proof of Theorem 4.2.1. Let $T \geqslant 0$ and $\varrho_0 \in L^\infty \cap L^1$ a measure with finite first moment. We construct a sequence of solutions as follows : Given ϱ^N we define (u^N, ϱ^{N+1}) as the solution to the system:

$$
\begin{cases}
\partial_t \varrho^{N+1} + \operatorname{div}(u^N \varrho^{N+1}) &= 0\,, & \text{on } [0,T] \times \mathbb{R}^3, \\
-\Delta u^N + \nabla p^N &= -\varrho^N e_3\,, & \text{on } [0,T] \times \mathbb{R}^3, \\
\operatorname{div} u^N &= 0\,, & \text{on } [0,T] \times \mathbb{R}^3, \\
\varrho^{N+1}(0,\cdot) &= \varrho_0\,, & \text{on } \mathbb{R}^3,
\end{cases}
$$

here u^N is given by $u^N = -\Phi * \varrho^N e_3$ and p^N its associated pressure. We choose $\varrho^0(t,\cdot) = \varrho_0$ as first step. Since ϱ^N is transported by an incompressible fluid we have for all time $t \in [0,T]$:

$$
\|\varrho^N(t)\|_{L^1 \cap L^\infty} \leqslant \|\varrho_0\|_{L^1 \cap L^\infty}.
$$

Formula (4.3) from Proposition 4.2.2 yields

$$
\|u^N\|_{W^{1,\infty}} \leqslant C \|\varrho^N\|_{L^1 \cap L^\infty}.
$$

This shows that u^N is uniformly bounded in $W^{1,\infty}$ and admits a weakly-* converging subsequence to a limit u.
On the other hand, applying formula (4.6) from Proposition 4.2.4 together with formula (4.4) from Proposition 4.2.3, we have:

$$
\begin{aligned}
W_1(\varrho^{N+1}, \varrho^N) &\leqslant e^{Q_N t} \int_0^t \int_{\mathbb{R}^3} |u^N(\tau, x) - u^{N+1}(\tau, x)| \varrho^N(t, dx) d\tau\,, \\
&\leqslant C e^{Q_N t} \|\varrho^N\|_{L^1 \cap L^\infty} \int_0^t W(\varrho^N(\tau), \varrho^{N-1}(\tau)) d\tau,
\end{aligned}
$$

with

$$
Q_N := \sup_{\tau \leqslant t} \operatorname{Lip}(u^{N+1}(\tau,\cdot)) \leqslant \sup_{\tau \leqslant t} \|u^{N+1}(\tau,\cdot)\|_{W^{1,\infty}} \leqslant C \sup_{\tau \leqslant t} \|\varrho^N\|_{L^1 \cap L^\infty} \leqslant C \|\varrho_0\|_{L^1 \cap L^\infty}.
$$

Hence

$$
\|W_1(\varrho^{N+1}, \varrho^N)\|_{L^\infty[0,T]} \leqslant \left(e^{C\|\varrho_0\| T} C \|\varrho_0\|_{L^1 \cap L^\infty} T \right)^N \|W_1(\varrho^1, \varrho^0)\|_{L^\infty[0,T]}. \tag{4.10}
$$

Note that, if we set X^N the characteristic flow associated to u^N, we have

$$\int |x|\varrho^{N+1}(dx) = \int |X^N(t,0,x)|\varrho_0(dx) \leqslant \int |x|\varrho_0(dx) + T\sup_{[0,T]}\|u^N(t,\cdot)\|_\infty \|\varrho_0\|_1,$$

which ensures that the sequence $(\varrho^N)_{N\in\mathbb{N}}$ is in the space of finite first moment measures. If we take T small enough, formula (4.10) shows that ϱ^N is a Cauchy sequence in the (complete) space of L^∞ functions from $[0,T]$ in the complete space of finite first moment measures metrized by the Wasserstein distance W_1, see [70, Theorem 6.16]. Hence there exists a limit ϱ such that:

$$\|W_1(\varrho^N,\varrho)\|_{L^\infty[0,T]} \underset{N\to\infty}{\to} 0.$$

Recall that for all compact sets K we have for all $M > N \geqslant 0$

$$\|u^N - u^M\|_{L^\infty([0,T],L^1(K))} + \|\nabla u^N - \nabla u^M\|_{L^\infty(0,T;L^1(K))} \leqslant C(K)\,\|W_1(\varrho^N,\varrho^M)\|_{L^\infty[0,T]}.$$

Hence, $u^N_{|K}$ and $\nabla u^N_{|K}$ are Cauchy sequences in $L^\infty(0,T;L^1(K))$ and admit a limit in $L^\infty(0,T;W^{1,\infty}(K))$. Finally $u \in L^\infty(0,T;W^{1,\infty} \cap W^{1,1}_{\mathrm{loc}})$.
Thanks to the convergence, in the space of measure-valued functions, of ϱ^N to ϱ and the strong convergence of u^N towards u in $L^\infty(0,T;W^{1,1}_{\mathrm{loc}})$ one can show that (u,ϱ) satisfies weakly the system:

$$\begin{cases} \partial_t\varrho + \mathrm{div}(u\varrho) &= 0, & \text{on } [0,T]\times\mathbb{R}^3,\\ -\Delta u + \nabla p &= -\varrho e_3, & \text{on } [0,T]\times\mathbb{R}^3,\\ \mathrm{div}\, u &= 0, & \text{on } [0,T]\times\mathbb{R}^3,\\ \varrho(0,\cdot) &= \varrho_0, & \text{on } \mathbb{R}^3. \end{cases}$$

Moreover, if we assume that there exists two fixed-points (u_i,ϱ_i), $i = 1,2$, then estimate (4.10)

$$\|W_1(\varrho_1,\varrho_2)\|_{L^\infty[0,T]} \leqslant CT\|\varrho_1\|e^{C\|\varrho_0\|T}\|W_1(\varrho_1,\varrho_2)\|_{L^\infty[0,T]},$$

ensures uniqueness for $T > 0$ small enough. In order to show the global existence in time we need to show that the solutions ϱ and u do not blow up in finite time and this is ensured by the following estimates:

$$\begin{aligned} \|\varrho(t)\|_{L^1\cap L^\infty} &\leqslant \|\varrho_0\|_{L^\infty\cap L^1},\\ \|u(t)\|_{L^\infty} + \|\nabla u(t)\|_{L^\infty} &\leqslant C\|\varrho(t)\|_{L^1\cap L^\infty}. \end{aligned}$$

□

4.3 Analysis of the regularity of the contour of a blob

In this section we consider the special case where the initial measure ϱ_0 is the characteristic function of a regular bounded domain B_0. Since the measure ϱ_0 has finite first moment and satisfies $\varrho_0 \in L^\infty \cap L^1$, Theorem 4.2.1 ensures the existence and uniqueness of ϱ and classical transport theory shows that the measure ϱ is transported along the flow thanks to formula

$$\varrho(t,\cdot) = X(t,0,\cdot)\#\varrho_0,$$

where X is the characteristic flow satisfying equation (4.7). This ensures that $\varrho(t,\cdot)$ is the characteristic function of the transported domain $B_t := X(t,0,B_0)$. The aim now is to investigate the behaviour of the blob B_t in time. Keeping in mind that the motivation is to recover the instability properties described in the experimental and numerical investigations [55, 58, 62] at the microscopic scaling. First, we emphasize that the regularity of the velocity field u prevents the breaking of the blob B_t. Indeed, the flow X is a diffeomorphism in our case. Hence, the idea is to investigate the behaviour of the regularity of the contour ∂B_t.

4.3.1 Contour evolution: local existence and uniqueness

In what follows we use the notation $\mathbb{S}^2 := \partial B(0,1) \subset \mathbb{R}^3$. We consider $\tilde{X}_0$ an initial parametrization of ∂B_0:

$$\partial B_0 = \{\tilde{X}_0(\omega), \omega \in \mathbb{S}^2\},$$

and we set:

$$\partial B_t = \{\tilde{X}(t,\omega), \omega \in \mathbb{S}^2\}.$$

Since the domain moves with the flow, a natural choice of $\tilde{X}$ is the Lagrangian parametrization:

$$\begin{cases} \dot{\tilde{X}}(\omega) &= u\left[\tilde{X}\right](\omega)\,, \\ \tilde{X}(0,\cdot) &= \tilde{X}_0\,, \end{cases} \tag{4.11}$$

where $u\left[\tilde{X}\right](\omega) := u(\tilde{X}(\omega))$ and u is the solution to the Stokes equation associated to the source term $-e_3 1_{B_t}$. We recall the convolution formula for the velocity field u

$$u(x) = -\frac{1}{8\pi}\int_{B_t} \frac{1}{|x-y|}e_3 + \frac{(x-y)\cdot e_3}{|x-y|^3}(x-y).$$

Using the fact that $\nabla_y \frac{1}{|x-y|} = \frac{x-y}{|x-y|^3}$, the second term in the right hand side yields using an integration by parts

$$\begin{aligned} \int_{B_t} \frac{x-y}{|x-y|^3}(x-y)\cdot e_3 &= \int_{B_t} \left(\nabla_y \frac{1}{|x-y|}\right)(x-y)\cdot e_3, \\ &= -\int_{B_t}\int \frac{1}{|x-y|}(-e_3) + \int_{\partial B_t} \frac{(x-y)\cdot e_3}{|x-y|} n d\sigma(y). \end{aligned}$$

Hence, we get

$$u(x) = -\frac{1}{8\pi}\left(\int_{B_t} \frac{2}{|x-y|} dy e_3 + \int_{\partial B_t} \frac{(x-y)\cdot e_3}{|x-y|} n d\sigma(y)\right),$$

for the first term in the right hand side we use the fact that $\operatorname{div}_y \frac{x-y}{|x-y|} = -\frac{2}{|x-y|}$ to get

$$u(x) = -\frac{1}{8\pi}\int_{\partial B_t}\left(-\frac{(x-y)\cdot n(y)}{|x-y|}e_3 + \frac{(x-y)\cdot e_3}{|x-y|}n\right)d\sigma(y). \tag{4.12}$$

We can now define $u\left[\tilde{X}\right](\bar{\omega})$ for all $\bar{\omega}\in\mathbb{S}^2$ using formula (4.12) and the parametrization $\tilde{X}$ of ∂B_t. We set p the stereographic projection of $\mathbb{S}^2\backslash\{N\}$ where $N=(0,0,1)$

$$\begin{aligned} p\colon \qquad & \mathbb{S}^2 && \longrightarrow \mathbb{R}^2 \\ & w=(x,y,z) && \mapsto (u,v) = \left(\frac{x}{1-z},\frac{y}{1-z}\right). \end{aligned} \tag{4.13}$$

Its inverse p^{-1} provides a parametrization of $\mathbb{S}^2$ and is defined as

$$p^{-1}(u,v) = \left(2u,2v,u^2+v^2-1\right)\frac{1}{1+u^2+v^2}. \tag{4.14}$$

We define the surface integral on ∂B_t using the parametrization $\tilde{X}\circ p^{-1}$ as follows

$$\begin{aligned} u(x) = -\frac{1}{8\pi}\int_{\mathbb{R}^2}&\Bigg(\frac{(x-\tilde{X}\circ p^{-1}(u,v))\cdot e_3}{|x-\tilde{X}\circ p^{-1}(u,v)|}n\left[\tilde{X}\right](u,v) \\ &- \frac{(x-\tilde{X}\circ p^{-1}(u,v))\cdot n\left[\tilde{X}\right](u,v)}{|x-\tilde{X}\circ p^{-1}(u,v)|}e_3\Bigg)\left|s\left[\tilde{X}\right](u,v)\right|dudv, \end{aligned}$$

where

$$\begin{aligned} s\left[\tilde{X}\right](u,v) &= \partial_u\left(\tilde{X}\circ p^{-1}(u,v)\right)\times\partial_v\left(\tilde{X}\circ p^{-1}(u,v)\right) \\ &= \nabla\tilde{X}\circ p^{-1}\cdot p_u^{-1}(u,v)\times\nabla\tilde{X}\circ p^{-1}\cdot p_v^{-1}(u,v). \end{aligned}$$

$\left|s\left[\tilde{X}\right](u,v)\right|$ is the surface element of ∂B_t and the unit normal vector $n\left[\tilde{X}\right]$ on ∂B_t is defined as

$$n\left[\tilde{X}\right] = \frac{s\left[\tilde{X}\right]}{\left|s\left[\tilde{X}\right]\right|},$$

see for instance [64, Section 13.3]. Simplifying $n\left[\tilde{X}\right]\left|s\left[\tilde{X}\right]\right|$ by $s\left[\tilde{X}\right]$, we get the following formula

$$\begin{aligned} u\left[\tilde{X}\right](\omega) = -\frac{1}{8\pi}\int_{\mathbb{R}^2}&\Bigg(\frac{(\tilde{X}(\omega)-\tilde{X}\circ p^{-1}(u,v))\cdot e_3}{|\tilde{X}(\omega)-\tilde{X}\circ p^{-1}(u,v)|}s\left[\tilde{X}\right](u,v) \\ &- \frac{(\tilde{X}(\omega)-\tilde{X}\circ p^{-1}(u,v))\cdot s\left[\tilde{X}\right](u,v)}{|\tilde{X}(\omega)-\tilde{X}\circ p^{-1}(u,v)|}e_3\Bigg)dudv, \end{aligned} \tag{4.15}$$

The problem encountered herein is similar to the global existence problem for the vorticity formulation of the 2D Euler equations, see [21]. In this section, we state an existence and uniqueness result for the contour $\tilde{X}$. We follow the idea of proof introduced in [14] or [56, Section 8.3.2.] and assume that $\tilde{X}_0 \in \mathcal{C}^1(\mathbb{S}^2;\mathbb{R}^3)$ and is such that :

$$|\tilde{X}|_* := \inf_{\omega \neq \omega'} \frac{|\tilde{X}(\omega) - \tilde{X}(\omega')|}{|\omega - \omega'|} > 0 \,, \tag{4.16}$$

which means that the mapping is bijective.

Remark 4.3.1. *Since $\nabla \tilde{X}$ is invertible, we have*

$$|s\left[\tilde{X}\right]| \lesssim |\nabla \tilde{X}|^2 |\partial_u p^{-1} \times \partial_v p^{-1}|,$$

here $|\partial_u p^{-1} \times \partial_v p^{-1}|$ is the surface element of $\mathbb{S}^2$. Moreover, according to the definition of p^{-1} in (4.14), one can show that $\nabla p^{-1} \in L^\infty \cap L^2$. Indeed direct computations yield

$$|\nabla p^{-1}(u,v)| \leqslant \frac{C}{1+u^2+v^2}.$$

The main result of the subsection is the following Theorem

Theorem 4.3.1. *Let $\tilde{X}_0 \in \mathcal{C}^1(\mathbb{S}^2;\mathbb{R}^3)$ such that $|\tilde{X}_0|_* > 0$. There exists a time $T > 0$ such that equation (4.11) has a unique local solution $\tilde{X} \in \mathcal{C}^1(0,T;\mathcal{C}^1(\mathbb{S}^2;\mathbb{R}^3))$. Moreover, global existence is ensured as long as we have control on $|\tilde{X}|_*$ and $\|\nabla \tilde{X}\|_0$.*

The idea is to apply the method of proof of [56, Chapter 8]. Precisely, we apply the following Picard Theorem [56, Theorem 8.3].

Theorem 4.3.2 (Picard Theorem on a Banach Space)**.** *Let $O \subset \mathcal{B}$ be an open subset of a Banach space $\mathcal{B}$ and let F be a nonlinear operator satisfying the following criteria*

1. *F maps O to $\mathcal{B}$.*
2. *F is locally Lipschitz continuous, i.e. for any $X \in O$, there exists $L > 0$ and a neighborhoud $U_X \subset \mathcal{O}$ of X such that*

$$\|F(\tilde{X}) - F(\hat{X})\|_{\mathcal{B}} \leqslant L\|\tilde{X} - \hat{X}\|_{\mathcal{B}}, \text{ for all } \hat{X}, \tilde{X} \in U_X$$

.

Then for any $X_0 \in O$, there exists a time T such that the ODE

$$\frac{d}{dt}X = F(X), \quad X_{|t=0} = X_0,$$

has a unique (local) solution $X \in \mathcal{C}^1(0,T;O)$.

Proof of Theorem 4.3.1. We introduce the subspace

$$O := \{\tilde{X} \in \mathcal{C}^1(\mathbb{S}^2;\mathbb{R}^3),\ |\tilde{X}|_* > \frac{1}{\lambda},\ \|\nabla\tilde{X}\|_{\mathcal{C}^0} < \lambda\},$$

for some positive constant $\lambda > 1$. One can show that the mapping $|\cdot|_*$ is continuous for the $\mathcal{C}^{0,1}$ norm and hence the $\mathcal{C}^1$ norm. This ensures that O is a non-empty open subset of the Banach space $\mathcal{C}^1(\mathbb{S}^2;\mathbb{R}^3)$ containing the identity map. We consider the mapping A defined for any $\tilde{X} \in \mathcal{B}$ as follows

$$A(\tilde{X}) = u\left[\tilde{X}\right].$$

where $u\left[\tilde{X}\right]$ is given by (4.15). The idea is to show that $A(O) \subset \mathcal{C}^1$ and A is locally Lipschitz. Theorem 4.3.1 is then a direct application of Picard Theorem 4.3.2. We set $z = (u,v) \in \mathbb{R}^2$ and define the following function on $\mathbb{S}^2 \times \mathbb{R}^2$

$$\begin{aligned} G(\bar{\omega}, z) = &\frac{(\tilde{X}(\bar{\omega}) - \tilde{X}\circ p^{-1}(u,v))\cdot e_3}{|\tilde{X}(\bar{\omega}) - \tilde{X}\circ p^{-1}(u,v)|} s\left[\tilde{X}\right](u,v) \\ &- \frac{(\tilde{X}(\bar{\omega}) - \tilde{X}\circ p^{-1}(u,v))\cdot s\left[\tilde{X}\right](u,v)}{|\tilde{X}(\bar{\omega}) - \tilde{X}\circ p^{-1}(u,v)|} e_3. \end{aligned}$$

G is continuous in $\bar{\omega}$ for almost all $z \in \mathbb{R}^2$ and we have using Remark 4.3.1

$$|G(\bar{\omega}, z)| \leqslant 2|s[\tilde{X}](z)| \leqslant C\|\nabla\tilde{X}\|_0 |\nabla p^{-1}(z)|^2,$$

where $\nabla p^{-1} \in L^2(\mathbb{R}^2)$ according to Remark 4.3.1. This shows that $\bar{\omega} \mapsto A[\tilde{X}](\bar{\omega})$ is continuous. Moreover, $\bar{\omega} \mapsto G(\bar{\omega}, z)$ is differentiable for almost all $z \in \mathbb{R}^2$ and we have

$$\begin{aligned} |\nabla_{\bar{\omega}} G(\bar{\omega}, z)| &\leqslant C\left\|\nabla\tilde{X}\right\|_0 \frac{|\partial_u p^{-1} \times \partial_v p^{-1}|}{|\tilde{X}(\bar{\omega}) - \tilde{X}\circ p^{-1}(z)|}, \\ &\leqslant C\frac{\left\|\nabla\tilde{X}\right\|_0}{|\tilde{X}|_*} \frac{|\partial_u p^{-1} \times \partial_v p^{-1}|}{|\bar{\omega} - p^{-1}(z)|}, \end{aligned}$$

which is integrable. Indeed, for all $\bar{\omega} \in \mathbb{S}^2$

$$\int_{\mathbb{R}^2} \frac{|\partial_u p^{-1} \times \partial_v p^{-1}|}{|\bar{\omega} - p^{-1}(z)|} dz = \int_{\mathbb{S}^2} \frac{d\omega}{|\omega - \bar{\omega}|},$$

is uniformly bounded with respect to $\bar{\omega}$ according to Lemma (4.A.1). Reproducing the same arguments, the derivative is continuous and we have $A(O) \subset \mathcal{C}^1(\mathbb{S}^2)$. It remains to check that A is locally lipschitz. A sufficient condition is to show that the operator is Fréchet differentiable and that the derivative denoted by DA is bounded in O. Let $\tilde{X}, h \in \mathcal{C}^1$ we have

$$
\begin{aligned}
&-8\pi\left(A(\tilde{X}+h)(\bar{\omega})-A(\tilde{X})(\bar{\omega})\right)\\
&=\int_{\mathbb{R}^2}\left(\frac{(\tilde{X}(\bar{\omega})-\tilde{X}\circ p^{-1}+h(\bar{\omega})-h\circ p^{-1})\cdot e_3}{|\tilde{X}(\bar{\omega})-\tilde{X}\circ p^{-1}+h(\bar{\omega})-h\circ p^{-1}|}s\left[\tilde{X}+h\right]-\frac{(\tilde{X}(\bar{\omega})-\tilde{X}\circ p^{-1})\cdot e_3}{|\tilde{X}(\bar{\omega})-\tilde{X}\circ p^{-1}|}s\left[\tilde{X}\right]\right)\\
&-\int_{\mathbb{R}^2}\left(\frac{(\tilde{X}(\bar{\omega})-\tilde{X}\circ p^{-1}+h(\bar{\omega})-h\circ p^{-1})\cdot s\left[\tilde{X}+h\right]}{|\tilde{X}(\bar{\omega})-\tilde{X}\circ p^{-1}+h(\bar{\omega})-h\circ p^{-1}|}-\frac{(\tilde{X}(\bar{\omega})-\tilde{X}\circ p^{-1})\cdot s\left[\tilde{X}\right]}{|\tilde{X}(\bar{\omega})-\tilde{X}\circ p^{-1}|}\right)e_3,\\
&=I_1[\tilde{X}](h)(\bar{\omega})+I_2[\tilde{X}](h)(\bar{\omega}).
\end{aligned}
$$

We have

$$
s\left[\tilde{X}+h\right]=s[\tilde{X}]+\nabla\tilde{X}\cdot p_u^{-1}\times\nabla h\cdot p_v^{-1}+\nabla h\cdot p_u^{-1}\times\nabla\tilde{X}\cdot p_v^{-1}+s[h]. \tag{4.17}
$$

We write I_1 as follows

$$
\begin{aligned}
&I_1[\tilde{X}](h)(\bar{\omega})\\
&=\int_{\mathbb{R}^2}\frac{(\tilde{X}(\omega)-\tilde{X}\circ p^{-1})\cdot e_3}{|\tilde{X}(\omega)-\tilde{X}\circ p^{-1}|}\left(s\left[\tilde{X}+h\right]-s\left[\tilde{X}\right]\right)\\
&+\int_{\mathbb{R}^2}\left(\frac{(\tilde{X}(\omega)-\tilde{X}\circ p^{-1}+h(\bar{\omega})-h\circ p^{-1})\cdot e_3}{|\tilde{X}(\omega)-\tilde{X}\circ p^{-1}+h(\bar{\omega})-h\circ p^{-1}|}-\frac{(\tilde{X}(\omega)-\tilde{X}\circ p^{-1})\cdot e_3}{|\tilde{X}(\omega)-\tilde{X}\circ p^{-1}|}\right)s\left[\tilde{X}+h\right]
\end{aligned}
$$

For the first term we get using (4.17)

$$
\begin{aligned}
&\int_{\mathbb{R}^2}\frac{(\tilde{X}(\bar{\omega})-\tilde{X}\circ p^{-1})\cdot e_3}{|\tilde{X}(\bar{\omega})-\tilde{X}\circ p^{-1}|}\left(s\left[\tilde{X}+h\right]-s\left[\tilde{X}\right]\right)\\
&=\int_{\mathbb{R}^2}\frac{(\tilde{X}(\bar{\omega})-\tilde{X}\circ p^{-1})\cdot e_3}{|\tilde{X}(\bar{\omega})-\tilde{X}\circ p^{-1}|}\left(\nabla\tilde{X}\cdot p_u^{-1}\times\nabla h\cdot p_v^{-1}+\nabla h\cdot p_u^{-1}\times\nabla\tilde{X}\cdot p_v^{-1}\right)\\
&+\int_{\mathbb{R}^2}\frac{(\tilde{X}(\bar{\omega})-\tilde{X}\circ p^{-1})\cdot e_3}{|\tilde{X}(\bar{\omega})-\tilde{X}\circ p^{-1}|}\left(s\left[h\right]\right),\\
&=\mathcal{O}_{1,1}[\tilde{X}](h)(\bar{\omega})+\mathcal{E}_{1,1}[\tilde{X}](h)(\bar{\omega}).
\end{aligned}
$$

Analogously, for the second term in the right hand side of I_1 we have

$$
\begin{aligned}
&\int_{\mathbb{R}^2}\left(\frac{(\tilde{X}(\bar{\omega})-\tilde{X}\circ p^{-1}+h(\bar{\omega})-h\circ p^{-1})}{|\tilde{X}(\bar{\omega})-\tilde{X}\circ p^{-1}+h(\bar{\omega})-h\circ p^{-1}|}-\frac{(\tilde{X}(\bar{\omega})-\tilde{X}\circ p^{-1})}{|\tilde{X}(\bar{\omega})-\tilde{X}\circ p^{-1}|}\right)\cdot e_3\,s\left[\tilde{X}+h\right]\\
&=\mathcal{O}_{1,2}[\tilde{X}](\bar{\omega})+\mathcal{E}_{1,2}[\tilde{X}](h)(\bar{\omega}).
\end{aligned}
$$

with

$$\mathcal{O}_{1,2}[\tilde{X}](\bar{\omega}) = \int_{\mathbb{R}^2} \left(\frac{(h(\bar{\omega}) - h \circ p^{-1}) \cdot e_3}{|\tilde{X}(\bar{\omega}) - \tilde{X} \circ p^{-1}|} \right.$$
$$\left. - \frac{\left[(\tilde{X}(\bar{\omega}) - \tilde{X} \circ p^{-1}) \cdot (h(\bar{\omega}) - h \circ p^{-1})\right] \left[(\tilde{X}(\bar{\omega}) - \tilde{X} \circ p^{-1}) \cdot e_3\right]}{|\tilde{X}(\bar{\omega}) - \tilde{X} \circ p^{-1}|^3} \right) s\left[\tilde{X}\right].$$

The operators $\mathcal{O}_{1,i}[\tilde{X}]$, $i = 1, 2$ are linear on $\mathcal{C}^1$ and we have using estimates similar to the previous ones

$$\|\mathcal{O}_{1,i}[\tilde{X}](h)\|_1 \lesssim \|\nabla \tilde{X}\|_0 \left(1 + \frac{\|\nabla \tilde{X}\|_0}{|\tilde{X}|_*} + \frac{\|\nabla \tilde{X}\|_0^2}{|\tilde{X}|_*^2}\right) \|h\|_1.$$

For the error terms we get

$$\begin{aligned}
&\|\mathcal{E}_{1,1}[\tilde{X}](h)\|_{\mathcal{C}^1} + \|\mathcal{E}_{1,2}[\tilde{X}](h)\|_{\mathcal{C}^1} \lesssim \|h\|_1^2 \left(\|\nabla \tilde{X}\|_0^2 + \|\nabla h\|_0^2\right) (1 + \|h\|_1) \left(1 + \frac{1}{|\tilde{X}|_*}\right) \times \\
&\left(\left[1 + \frac{1}{|\tilde{X}|_*} + \frac{1}{|\tilde{X}|_*^2} + \frac{1}{|\tilde{X}|_*^3}\right] (1 + \|\nabla \tilde{X}\|_0) \right. \\
&\left. + \frac{1}{|\tilde{X}|_* |\tilde{X} + h|_*} \left(1 + \frac{\|\nabla \tilde{X}\|_0}{|\tilde{X}|_*} + \frac{\|\nabla (\tilde{X} + h)\|_0}{|\tilde{X} + h|_*}\right) \right).
\end{aligned} \tag{4.18}$$

This shows that the term corresponding to I_1 is Fréchet differentiable. The term I_2 is analogous to the first one with the role of e_3 and $s\left[\tilde{X}\right]$ reversed and we denote by $\mathcal{E}_{2,i}[\tilde{X}]$, $i = 1, 2$ the associated error terms for future reference. Finally, A is Fréchet differentiable and we have

$$\|DA[\tilde{X}]\|_1 \lesssim \|\nabla \tilde{X}\|_0 \left(1 + \frac{\|\nabla \tilde{X}\|_0}{|\tilde{X}|_*} + \frac{\|\nabla \tilde{X}\|_0^2}{|\tilde{X}|_*^2}\right). \tag{4.19}$$

Moreover, given $\tilde{X}_1$, $\tilde{X}_2 \in O$, we set $h = X_1 - X_2$ and we have

$$\begin{aligned}
A[\tilde{X}_1] - A[\tilde{X}_2] &= A[\tilde{X}_2 + h] - A[\tilde{X}_2] \\
&= DA[\tilde{X}_2](h) + \sum_{i=1}^{2} \mathcal{E}_{1,i}[\tilde{X}](h) + \mathcal{E}_{2,i}[\tilde{X}](h).
\end{aligned}$$

Using (4.18) for the error terms and (4.19) for the derivative we get

$$\|A[\tilde{X}_1] - A[\tilde{X}_2]\|_1 \leqslant C(\|\nabla \tilde{X}_2\|_0, |\tilde{X}_2|_*, |\tilde{X}_2 + h|_*, \|\nabla h\|_0) \|[\tilde{X}_1] - [\tilde{X}_2]\|_1,$$

we conclude using the fact that $\tilde{X}_2$ and $\tilde{X}_2 + h = \tilde{X}_1$ are in O to get a uniform bound depending only on λ. $\square$

4.3.2 Case of spherical contour parametrization

In this part we investigate the contour evolution in the case where the initial blob is the unit ball. We would like to compare the behaviour of the contour with the observations encountered in the microscopic model, see [58], [55], [62]. We set then

$$B_0 = B(0,1),$$

and keep the same notation B_t for the domain at time t. We set $c(t)$ the position at time t of the center of the domain and write $B_t = c(t) + \tilde{B}_t$. The center $c(t)$ is transported along the flow meaning that $\dot{c} = u(t,c)$. Using the change of variable $x = c(t) + \tilde{x} \in B_t$, the weak formulation of the transport equation writes

$$\int_0^T \int_{\tilde{B}_t} \partial_t \psi + \nabla\psi \cdot (u(c(t)+\cdot) - \dot{c}) d\tilde{x} = 0\,, \forall \psi \in \mathcal{C}_c^\infty([0,T]\times \tilde{B}_t).$$

Since the flow preserves the rotational invariance, we define the spherical parametrization of $\tilde{B}_t$ as follows:

$$\tilde{B}_t = \left\{ (\varrho, \theta, \phi)\,, r \leqslant r(t,\theta) \right\}.$$

Note that the function r is independent of the azimuthal angle ϕ thanks to the rotational invariance. The weak formulation of the transport equation yields:

$$n_t + (u - \dot{c})\cdot n = 0\,, \text{ on } \partial\tilde{B}_t\ ,$$

where n (resp. n_t) is the unit normal on the boundary of $\tilde{B}_t$ with respect to space (resp. time). Since $\partial\tilde{B}_t = \{(r,\theta,\phi)\,, r = r(t,\theta)\}$, this yields:

$$\partial_t r = (u(c+\cdot) - \dot{c})_r - r'(u(c+\cdot) - \dot{c})_\theta := A_2[r] - r' A_1[r].$$

Using the convolution formula for the velocity field u and the spherical parametrization we get

Lemma 4.3.3. *r satisfies the following transport equation*

$$\left\{ \begin{array}{rcl} \partial_t r + r' A_1[r] &=& A_2[r], \\ r(0,\cdot) &=& 1. \end{array} \right. \tag{4.20}$$

where $A_1[r]$ and $A_2[r]$ are defined as follows

$$\begin{aligned} A_1[r](\bar{\theta}) := -\frac{1}{8\pi}\int_0^{2\pi}\int_0^{\pi} & \frac{r(\theta)\sin(\theta) - r'(\theta)\cos(\theta)}{\beta[r](\theta,\bar{\theta},\phi)} r\sin(\theta)\Big(r(\bar{\theta})\cos(\phi) \\ & - r(\theta)\Big\{\cos(\theta)\cos(\bar{\theta})\cos(\phi) + \sin(\theta)\sin(\bar{\theta})\Big\}\Big) d\theta d\phi \\ & - \frac{1}{4}\sin(\bar{\theta})\int_0^{\pi} r^2(\theta)\sin(\theta)\left(1 - \frac{1}{2}\sin^2(\theta)\right) d\theta. \end{aligned} \tag{4.21}$$

$$A_2[r](\bar{\theta}) := -\frac{1}{8\pi}\int_0^{2\pi}\int_0^{\pi} \frac{r(\theta)\sin(\theta) - r'(\theta)\cos(\theta)}{\beta[r](\theta,\bar{\theta},\phi)} r\sin(\theta)\Big(- r(\theta)\sin(\bar{\theta})\cos(\theta)\cos(\phi) + r(\theta)\cos(\bar{\theta})\sin(\theta)\Big) d\theta d\phi + \frac{1}{4}\cos(\bar{\theta})\int_0^{\pi} r^2(\theta)\sin(\theta)\left(1-\frac{1}{2}\sin^2(\theta)\right)d\theta\,. \quad (4.22)$$

$$\beta[r](\theta,\bar{\theta},\phi)^2 = r^2(\theta) + r^2(\bar{\theta}) - 2r(\theta)r(\bar{\theta})(\sin(\theta)\sin(\bar{\theta})\cos(\phi) + \cos(\theta)\cos(\bar{\theta})).$$

Moreover, the center of the droplet $c = (0,0,c_3)$ satisfies

$$\begin{cases} \dot{c}_3(t) &= -\frac{1}{4}\int_0^{\pi} r^2(\theta)\sin(\theta)\left(1-\frac{1}{2}\sin^2(\theta)\right)d\theta, \\ c_3(0) &= 0, \end{cases} \quad (4.23)$$

The computations for the proof of the former result are gathered in the Appendix. Note that, we have non negativity of the radius.

Lemma 4.3.4 (non-negativity)**.** *If there exists a time $t^* \geqslant 0$ and $\bar{\theta}^* \in [0,\pi]$ such that $r(t^*,\bar{\theta}^*) = 0$, then*

$$\partial_t r(t^*,\bar{\theta}^*) = 0.$$

Proof. We keep the same notations as in the proof of Lemma 4.3.3. If $r(t^*,\bar{\theta}^*) = 0$, then:

$$N(\theta,\bar{\theta}^*,\phi) = \Big(r(\theta)\sin(\theta) - r'(\theta)\cos(\theta)\Big)\sin(\theta),$$

hence the terms in formula (4.20) involving ϕ vanish and we obtain:

$$\begin{aligned}\partial_t r(t^*,\bar{\theta}^*) &= -\frac{1}{4}\int_0^{\pi}\Big(r(\theta)\sin(\theta) - r'(\theta)\cos(\theta)\Big) r(\theta)\sin^2(\theta)d\theta \times \Big[r'(t,\bar{\theta}))\sin(\bar{\theta}) + \cos(\bar{\theta})\Big] \\ &\quad - \Big(\cos(\bar{\theta}) + r'(\bar{\theta}\sin(\bar{\theta}))\Big)\dot{c}_3\,, \\ &= -\frac{1}{4}\left\{\int_0^{\pi}\Big(r^2(\theta)\sin^3(\theta) + \frac{1}{2}r^2(\theta)(-\sin^3(\theta) + 2\sin(\theta)\cos^2(\theta)\Big)d\theta\right\} \\ &\quad \times \Big[r'(t,\bar{\theta}))\sin(\bar{\theta}) + \cos(\bar{\theta})\Big] - \Big(\cos(\bar{\theta}) + r'(\bar{\theta})\sin(\bar{\theta})\Big)\dot{c}_3\,, \\ &= 0,\end{aligned}$$

according to formula (4.23). □

Numerical simulations In what follows we set $T > 0$. In order to provide a qualitative behaviour of the contour we consider $N, M, L \in \mathbb{N}^*$ and define

$$(dt, h_1, h_2) = \left(\frac{T}{N-1}, \frac{\pi}{M-1}, \frac{2\pi}{L-1}\right)$$

we set for $i = 1, \cdots, M,\ j = 1, \cdots, L,\ n = 1, \cdots, N$

$$\theta_i = h_1(i-1), \quad \phi_j = h_2(j-1), \quad t^n = dt(n-1).$$

$(\theta_i)_{1\leqslant i\leqslant M}$ is a subdivision of $[0,\pi]$, $(t^n)_{1\leqslant n\leqslant N}$ a subdivision of $[0,T]$ and $(\phi)_{1\leqslant j\leqslant P}$ a subdivision of $[0,2\pi]$. We discretise the radius and the center by setting

$$r(t,\theta) \sim (r_i^n)_{1\leqslant i\leqslant M}^{1\leqslant n\leqslant N}\,, r_i^n = r(t^n,\theta_i)\,, c(t) \sim (c^n)_{1\leqslant n\leqslant N}$$

Given $(r_i^n)_{1\leqslant i\leqslant N}$ we define $(r_i^{n+1})_{1\leqslant i\leqslant N}$ as

$$\frac{r_i^{n+1}-r_i^n}{dt} = A_2^{i,n} - A_1^{i,n}\Delta r_i^n - \Big(\cos(\theta_i) + \Delta r_i^n \sin(\theta_i)\Big)\Delta c^n\,, i = 2,\cdots,M\,,$$

with $r_1^{n+1} = r_2^{n+1}$ and

$$\Delta r_i = \frac{r_i^n - r_{i-1}^n}{h_1}, i = 2,\cdots,M, \quad \Delta c^n = \dot{c}_3(t^n)\,, \tag{4.24}$$

$$\begin{aligned} A_1^{i,n} = -\frac{1}{8\pi}\sum_{k=1}^{M}\sum_{j=1}^{L} h_1h_2\frac{r_k\sin(\theta_k)-\Delta r_k\cos(\theta_k)}{\beta_{i,j,k}^n} r_k\sin(\theta_k)\Big(r_i\cos(\phi_j) \\ - r_k\Big\{\cos(\theta_k)\cos(\theta_i)\cos(\phi_j)+\sin(\theta_k)\sin(\theta_i)\Big\}\Big) - \sin(\theta_i)\Delta c^n, \end{aligned}$$

$$\begin{aligned} A_2^{i,n} := -\frac{1}{8\pi}\int_0^{2\pi}\sum_{k=1}^{M}\sum_{j=1}^{L} h_1h_2\frac{r_k\sin(\theta_k)-\Delta r_k\cos(\theta_k)}{\beta_{i,j,k}^n} r_k\sin(\theta_k)\Big(-r_k\sin(\theta_i)\cos(\theta_k)\cos(\phi_j) \\ + r_k\cos(\theta_i)\sin(\theta_k)\Big) + \cos(\theta_i)\Delta c^n, \end{aligned}$$

$$\beta_{i,j,k}^n = \sqrt{(r_i^n)^2 + (r_k^n)^2 - 2r_i^n r_k^n(\sin(\theta_i)\sin(\theta_k)\cos(\phi_j)+\cos(\theta_i)\cos(\theta_k)},$$

$$\frac{c^{n+1}-c^n}{dt} = \Delta c^n = -\frac{1}{4}\sum_{k=1}^{M} h_1 r_k^2\sin(\theta_k)\left(1-\frac{1}{2}\sin^2(\theta_k)\right).$$

We present below the evolution of the shape of the blob on the interval time $[0,50]$ with a time step of $dt = 0.01$. Figures 4.1 and 4.2 corresponds to the vertical section of the surface of the droplet defined by $\theta \mapsto (r(t,\theta)\sin(\theta), r(t,\theta)\cos(\theta))$. We remark the formation of a singularity at the north and south points of the droplet. Precisely, the value of $r(t,0)$ increases in time whereas $r(t,\pi)$ is decreasing. A numerical loss of the droplet volume is noticed. We gather in Table 4.1 the evolution of radius value at $\theta = 0$, $\theta = \pi$ and the volume relative error E.

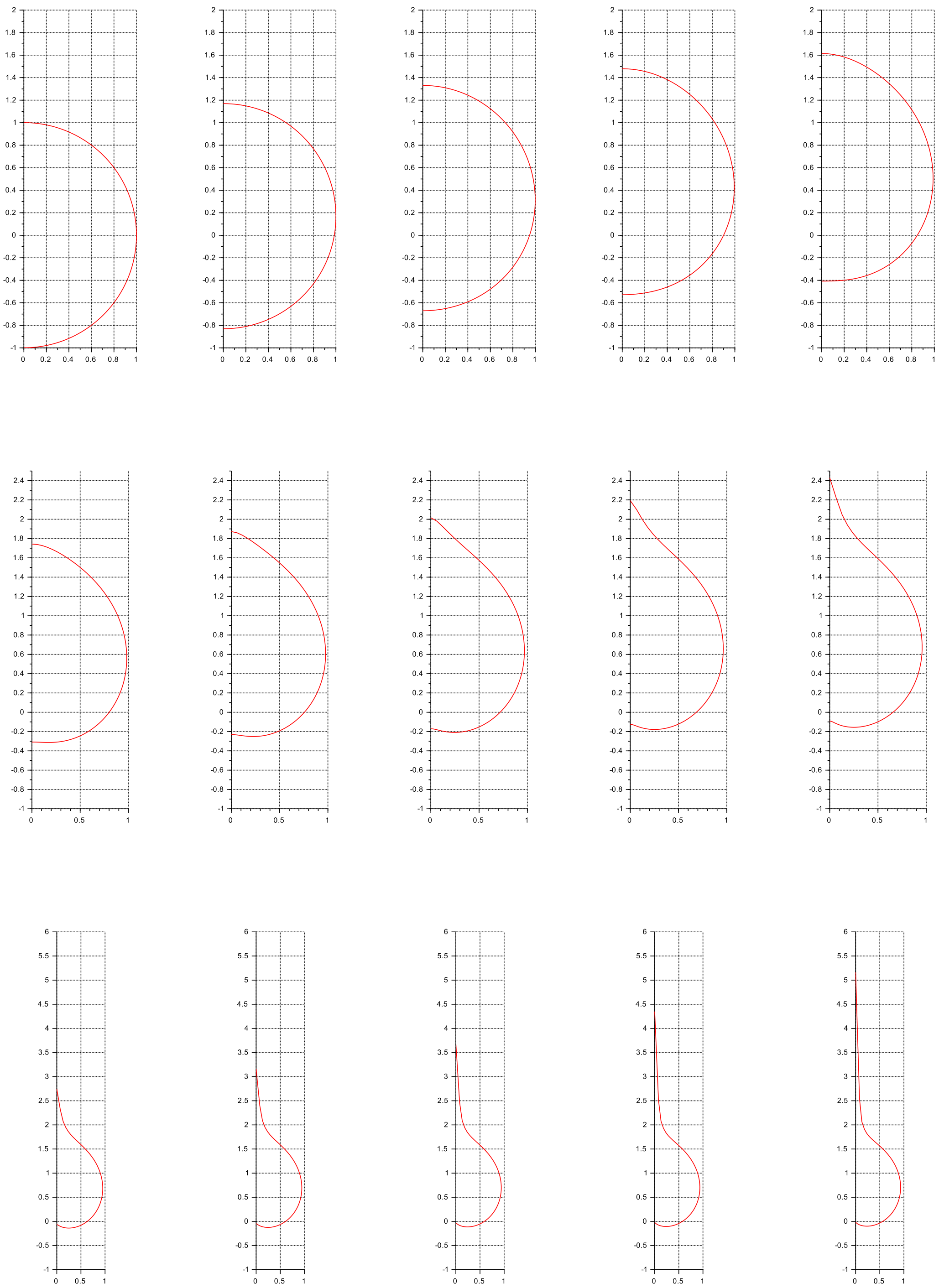

Figure 4.1 – Droplet evolution for $t = 0, 2.5, \cdots, 35$

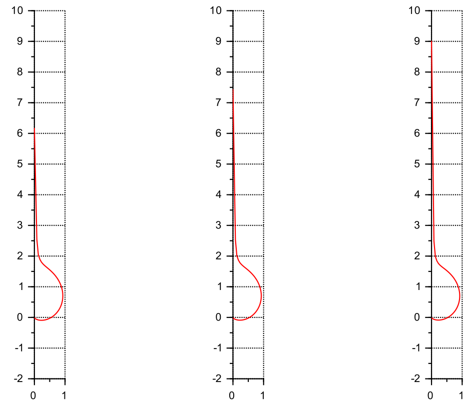

$t = 37.5$ $\quad$ $t = 40$ $\quad$ $t = 42.5$

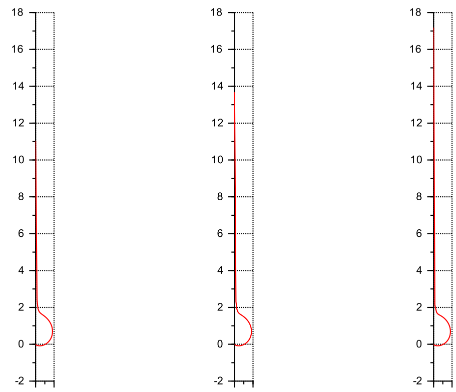

$t = 45$ $\quad$ $t = 47.5$ $\quad$ $t = 50$

Figure 4.2 – Droplet evolution

t	0	20	40	60	80	100
$r(t,0)$	1	1.62	2.2	3.7	7.44	17.19
$r(t,\pi)$	1	0.4	0.12	3.510^{-2}	1.610^{-2}	3.1610^{-2}
$E(t)$	0	0.01	0.07	0.14	0.2	0.25

Table 4.1 – Evolution of $r(t,0)$, $r(t,\pi)$ and the volume relative error $E(t)$

Appendix

4.A Technical lemmas

We recall the following lemma

Lemma 4.A.1. *There exists a positive constant $C > 0$ such that*

$$\sup_{\bar{\omega}\in\mathbb{S}^2}\int_{\mathbb{S}^2}\frac{d\omega}{|\omega-\bar{\omega}|}\leqslant C.$$

Proof. Let $(\bar{x},\bar{y},\bar{z}) = \bar{\omega} = p^{-1}(\bar{u},\bar{v}) \in \mathbb{S}^2$, without loss of generality, we can assume that $\bar{z} \leqslant 0$ and consider the stereographic projection p as defined in (4.13). Using Remark 4.3.1 we get for fixed $\alpha < 1/2$

$$\begin{aligned}
I(\bar{\omega}) &= \int_{\mathbb{S}^2}\frac{d\omega}{|\omega-\bar{\omega}|},\\
&= \int_{\mathbb{R}^2}\frac{|\nabla p^{-1}|^2}{|p^{-1}(u,v)-p^{-1}(\bar{u},\bar{v})|}du\,dv,\\
&\leqslant \int_{O(\bar{\omega},\alpha)}\frac{|\nabla p^{-1}|^2}{|p^{-1}(u,v)-p^{-1}(\bar{u},\bar{v})|}du\,dv + \frac{C}{\alpha}\int_{\mathbb{R}^2}\frac{dudv}{(1+u^2+v^2)^2},\\
&\leqslant \int_{O(\bar{\omega},\alpha)}\frac{|\nabla p^{-1}|^2}{|p^{-1}(u,v)-p^{-1}(\bar{u},\bar{v})|}du\,dv + \frac{C}{\alpha},
\end{aligned}$$

where

$$O(\bar{\omega},\alpha) = \{(u,v)\in\mathbb{R}^2, |p^{-1}(\bar{u},\bar{v})-p^{-1}(u,v)|\leqslant\alpha\}.$$

This yields

$$\begin{aligned}
|(u,v)-(\bar{u},\bar{v})| &= |p(\omega)-p(\bar{\omega})|,\\
&\leqslant \sup_{B(\bar{\omega},\alpha)}|\nabla p|\,|\omega-\bar{\omega}|,\\
&\leqslant \alpha\sup_{B(\bar{\omega},\alpha)}|\nabla p|.
\end{aligned}$$

Since $\bar{z}\leqslant 0$ we have $B(\bar{\omega},\alpha)\subset\{\omega\in\mathbb{S}^2, z\leqslant\alpha\}$, we get

$$\sup_{B(\bar{\omega},\alpha)}|\nabla p| \leqslant \sup_{\{\omega\in\mathbb{S}^2, z\leqslant\alpha\}}|\nabla p| \leqslant L_1(\alpha), \tag{4.25}$$

this shows that

$$O(\bar{\omega},\alpha) \subset B((\bar{u},\bar{v}),\alpha L_1(\alpha)).$$

Moreover, since $\bar{z} \leqslant 0$ this yields $(\bar{u},\bar{v}) \in B(0,1)$ and hence

$$B((\bar{u},\bar{v}),\alpha L_1(\alpha)) \subset B(0,1+\alpha L_1(\alpha)),$$

this yields a uniform bound for ∇p^{-1}

$$\sup_{B((\bar{u},\bar{v}),\alpha L_1(\alpha))} |\nabla p^{-1}| \leqslant \sup_{B(0,1+\alpha L_1(\alpha))} |\nabla p^{-1}| \leqslant L_2(\alpha). \tag{4.26}$$

finally we get using (4.25), (4.26)

$$\begin{aligned}\int_{O(\bar{\omega},\alpha)} \frac{|\nabla p^{-1}|^2}{|p^{-1}(u,v)-p^{-1}(\bar{u},\bar{v})|}du\,dv &\leqslant L_2(\alpha)^2 \int_{O(\bar{\omega},\alpha)} \frac{\sup\limits_{B(\bar{\omega},\alpha)} |\nabla p|}{|(u,v)-(\bar{u},\bar{v})|}du\,dv,\\ &\leqslant L_2(\alpha)^2 L_1(\alpha) \int_{B((\bar{u},\bar{v}),\alpha L_1(\alpha))} \frac{du\,dv}{|(u,v)-(\bar{u},\bar{v})|},\end{aligned}$$

this yields the desired result since $x \mapsto \frac{1}{|x|}$ is locally integrable on $\mathbb{R}^2$. □

We present now the computations related to Lemma 4.3.3.

Proof of Lemma 4.3.3. We recall that r satisfies

$$\partial_t r = (u(c+\cdot)-\dot{c})_r - r'(u(c+\cdot)-\dot{c})_\theta, \tag{4.27}$$

with $\dot{c} = u(c)$. We have for all $x \in \mathbb{R}^3$:

$$u(x) = -\frac{1}{8\pi}\int_{\partial B_t} \left(\frac{(x_3-y_3)}{|x-y|}n(\sigma) - \frac{(x-y)\cdot n(\sigma)}{|x-y|}e_3 \right) d\sigma(y).$$

We reformulate the integral using a spherical parametrization of $\partial \tilde{B}_t$. We set $y = c+\tilde{y}$, where $\tilde{y} = r(t,\theta)e(\theta,\phi)$, $\theta \in [0,\pi]$, $\phi \in [0,2\pi]$ with:

$$e(\theta,\phi) = \begin{pmatrix} \cos(\phi)\,\sin(\theta) \\ \sin(\phi)\,\sin(\theta) \\ \cos(\theta) \end{pmatrix}.$$

Direct computation yields

$$n = \partial_\theta \tilde{y} \times \partial_\phi \tilde{y} = r^2\,\sin(\theta)\,e(\theta,\phi) - r'(\theta)\,r(\theta)\,\sin(\theta)\,\partial_\theta e(\theta,\phi).$$

We set:

$$x = c+\tilde{x} = c + r(t,\bar{\theta})\,e(\bar{\theta},\bar{\phi}) \in \partial B_t\ ,\ (\bar{\theta},\bar{\phi}) \in [0,\pi]\times[0,2\pi].$$

Hence, the velocity field is given by

$$u(r(t,\bar{\theta})e(\bar{\theta},\bar{\phi})) = -\frac{1}{8\pi}\int_{[0,\pi]\times[0,2\pi]}\left(\frac{\big(r(\bar{\theta})e(\bar{\theta},\bar{\phi})-r(\theta)e(\theta,\phi)\big)\cdot e_3}{\big|r(\bar{\theta})e(\bar{\theta},\bar{\phi})-r(\theta)e(\theta,\phi)\big|}n[r](\theta)\right.$$
$$\left. - \frac{\big(r(t,\bar{\theta})e(\bar{\theta},\bar{\phi})-r(\theta)e(\theta,\phi)\big)\cdot n[r](\theta)}{\big|r(\bar{\theta})e(\bar{\theta},\bar{\phi})-r(\theta)e(\theta,\phi)\big|}e_3\right). \quad (4.28)$$

For sake of clarity we use the shortcut

$$\beta = |x-y| = |\tilde{x}-\tilde{y}| = |r(\bar{\theta})e(\bar{\theta},\bar{\phi})-r(\theta)e(\theta,\phi)|,$$

and we have:

$$\beta^2 = r^2(\theta) + r^2(\bar{\theta}) - 2r(\theta)r(\bar{\theta})\Big(cos(\phi-\bar{\phi})\sin(\theta)\sin(\bar{\theta}) + \cos(\theta)\cos(\bar{\theta})\Big). \quad (4.29)$$

This yields:

$$u_1 = -\frac{1}{8\pi}\int_0^{2\pi}\int_0^{\pi}\frac{r(\bar{\theta})cos(\bar{\theta}) - r(\theta)\cos(\theta)}{\beta}r(\theta)\sin(\theta)$$
$$\times\Big(r(\theta)\sin(\theta) - r'(\theta)\cos(\theta)\Big)\cos(\phi)d\theta d\phi\,,$$

$$u_2 = -\frac{1}{8\pi}\int_0^{2\pi}\int_0^{\pi}\frac{r(\bar{\theta})\cos(\bar{\theta}) - r(\theta)\cos(\theta)}{\beta}r(\theta)\sin(\theta)$$
$$\times\Big(r(\theta)\sin(\theta) - r'(\theta)\cos(\theta)\Big)\sin(\phi)d\theta d\phi\,,$$

$$u_3 = -\frac{1}{8\pi}\int_0^{2\pi}\int_0^{\pi}\frac{r(\theta)\sin(\theta) - r'(\theta)\cos(\theta)}{\beta}r(\theta)\sin(\theta)$$
$$\times\Big\{-r(\bar{\theta})\sin(\bar{\theta})\cos(\phi-\bar{\phi}) + r(\theta)\sin(\theta)\Big\}d\theta d\phi$$

We also recall that $u_r = u\cdot e(\bar{\theta},\bar{\phi})$ and $u_\theta = u\cdot\partial_\theta e(\bar{\theta},\bar{\phi})$. We get:

$$u_r = -\frac{1}{8\pi}\int_0^{2\pi}\int_0^{\pi}\frac{r(\theta)\sin(\theta) - r'(\theta)\cos(\theta)}{\beta}r\sin(\theta)\Big(-r(\theta)\sin(\bar{\theta})\cos(\theta)\cos(\bar{\phi}-\phi)$$
$$+ r(\theta)\cos(\bar{\theta})\sin(\theta)\Big)d\theta d\phi\,, \quad (4.30)$$

$$u_\theta = -\frac{1}{8\pi}\int_0^{2\pi}\int_0^{\pi}\frac{r(\theta)\sin(\theta) - r'(\theta)\cos(\theta)}{\beta}r\sin(\theta)\Big(r(\bar{\theta})\cos(\phi-\bar{\phi})$$
$$- r(\theta)\Big\{\cos(\theta)\cos(\bar{\theta})\cos(\phi-\bar{\phi}) + \sin(\theta)\sin(\bar{\theta})\Big\}\Big)d\theta d\phi\,. \quad (4.31)$$

This shows that u_θ and u_r do not depend on $\bar{\phi}$. On the other hand, since $\dot{c} = u(c)$ we get:

$$\dot{c} = u(c) = -\frac{1}{8\pi}\int_{\partial \tilde{B}_t} \left(\frac{-\tilde{y}_3}{[\tilde{y}|} n(\sigma) + e_3 \frac{\tilde{y}\cdot n(\sigma)}{|\tilde{y}|} \right) d\sigma(\tilde{y})$$

recall that $|\tilde{y}| = r(\theta)$ and since $e \perp \partial_\theta e$ we get:

$$\begin{aligned}
\tilde{y}\cdot n(\sigma) &= r(\theta)e(\theta,\phi)\cdot \big(r^2(\theta)\, \sin(\theta)\, e(\theta,\phi) - r'(\theta)\, r(\theta)\, \sin(\theta)\, \partial_\theta e(\theta,\phi)\big) \\
&= r^3(\theta)\sin(\theta).
\end{aligned}$$

This yields:

$$\begin{aligned}
\dot{c}_1 &= -\frac{1}{8\pi}\int\int -cos(\theta)\, \big(r^2(\theta)\, \sin(\theta)\, \cos(\phi)\sin(\theta) - r'(\theta)\, r(\theta)\, \sin(\theta)\, \cos(\phi)\cos(\theta)\big) = 0\,, \\
\dot{c}_2 &= -\frac{1}{8\pi}\int\int -cos(\theta)\, \big(r^2(\theta)\, \sin(\theta)\, \sin(\phi)\sin(\theta) - r'(\theta)\, r(\theta)\, \sin(\theta)\, \sin(\phi)\cos(\theta)\big) = 0\,.
\end{aligned}$$

$$\begin{aligned}
\dot{c}_3 &= -\frac{1}{8\pi}\int_0^{2\pi}\int_0^{\pi} \Big(- cos(\theta)\, \big(r^2(\theta)\, \sin(\theta)\, \cos(\theta) + r'(\theta)\, r(\theta)\, \sin^2\, (\theta)\big) \\
&+ r^2(\theta)\sin(\theta)\Big) d\theta d\phi\,, \\
&= -\frac{1}{4}\int_0^{\pi} \big(r^2(\theta)\sin^3(\theta) - r'(\theta) r(\theta)\cos(\theta)\sin^2(\theta)\big)\, d\theta\,, \\
&= -\frac{1}{4}\int_0^{\pi} \bigg(r^2(\theta)\sin^3(\theta) + \frac{1}{2} r^2(\theta)\Big(- \sin^3(\theta) + 2\cos^2(\theta)\sin(\theta)\Big)\bigg)\, d\theta\,, \\
&= -\frac{1}{4}\int_0^{\pi} \frac{1}{2} r^2(\theta)\Big(- \sin^3(\theta) + 2\sin(\theta)\Big) d\theta\,, \\
&= -\frac{1}{4}\int_0^{\pi} r^2(\theta)\sin(\theta)\Big(1 - \frac{1}{2}\sin^2(\theta)\Big) d\theta < 0.
\end{aligned}$$

Thus,

$$\dot{c}_r = \cos(\bar{\theta})\dot{c}_3 \quad , \quad \dot{c}_\theta = -\sin(\bar{\theta})\dot{c}_3. \tag{4.32}$$

We conclude by replacing formulas (4.30), (4.31), (4.32) in (4.27). $\square$

Bibliography

[1] G. Allaire, *Homogenization of the navier stokes equations in open sets perforated with tiny holes i. abstract framework, a volume distribution of holes*, Arch. Rational Mech. Anal. 113, (1991), pp. [209,259].

[2] ——, *Shape optimization by the homogenization method*, Springer Verlag, New York, 2001.

[3] ——, *A brief introduction to homogenization and miscellaneous applications, mathematical and numerical approaches for multiscale problem*, ESAIM Proceedings, 37 (2012), pp. [1,49].

[4] F. Alouges, A. DeSimone, and A. Lefebvre, *Biological fluid dynamics: swimming at low reynolds numbers*, Encyclopedia of Complexity and System Science, Springer Verlag, (2008).

[5] ——, *Optimal strokes for low reynolds number swimmers : an example*, J Nonlinear Sci, 18 (2008), pp. [277,302].

[6] ——, *Optimal strokes for axisymmetric microswimmers*, Eur. Phys. J. E, 28 (2009), pp. [279,284].

[7] B. Asgharian, W. Hofmann, and R. Bergmann, *Particle deposition in a multiple-path model of the human lung*, Aerosol Sci. Tech., 34 (2001), pp. 332–339.

[8] N. Bakhvalov and G. Panasenko, *Homogenization: Averaging Processes in Periodic Media*, Springer Netherlands, Dordrecht, 1989.

[9] C. Baranger, L. Boudin, P.-E. Jabin, and S. Mancini, *A modeling of biospray for the upper airways*, in CEMRACS 2004—mathematics and applications to biology and medicine, vol. 14 of ESAIM Proc., EDP Sci., Les Ulis, 2005, pp. 41–47.

[10] G. K. Batchelor, *An introduction to fluid dynamics*, Cambridge University Press, 1967.

[11] ——, *Sedimentation in a dilute dispersion of spheres*, J . Fluid Mech. vol. 52, part 2,, (1972), pp. [245,268].

[12] G. K. Batchelor and J. Green, *The determination of the bulk stress in a suspension of spherical particles to order c*, J. Fluid 1Mech, vol. 56, part 3, (1972), pp. [401–427].

[13] A. Bensoussan, J. L. Lions, and G. Papanicolau, *Asymptotic analysis for periodic structures*, AMS Chelsea Publishing, (1978).

[14] A. L. Bertozzi and P. Constantin, *Global regularity for vortex patches*, Commun.Math. Phys. Volume 152, (1993), pp. [19,28].

[15] L. Boudin, L. Desvillettes, C. Grandmont, and A. Moussa, *Global existence of solutions for the coupled Vlasov and Navier-Stokes equations*, Differential Integral Equations, 22(11-12), (2009), pp. [1247,1271].

[16] L. Boudin, C. Grandmont, B. Grec, and D. Yakoubi, *Influence of the spray retroaction on the airflow*, in CEMRACS 2009 – Mathematical Modelling in Medicine, vol. 30 of ESAIM Proc., EDP Sci., Les Ulis, 2010, pp. 153–165.

[17] L. Boudin, C. Grandmont, A. Lorz, and A. Moussa, *Modelling and numerics for respiratory aerosols*, Commun. Comput. Phys., 18 (2015), pp. 723–756.

[18] H. Brenner and M. E. O'neill, *On the stokes resistance of multiparticle systems in a linear shear field*, Chemical Engineering Science, Vol. 27, (1972), pp. [1421,1439].

[19] H. C. Brinkman, *A calculation of the viscous force exerted by a flowing fluid on a dense swarm of particles*, Flow, Turbulence and Combustion, (1949), pp. [1,27].

[20] T. Champion, L. D. Pascale, and P. Juutinen, *The ∞-Wasserstein distance: local solutions and existence of optimal transport maps*, SIAMJ. Math. Anal. 40, (2008), pp. [1,20].

[21] J. Y. Chemin, *Persistance de structures géométriques dans les fluides incompressibles bidimensionnels*, Ann. Sci. Éc. Norm. Supér. série 4, tome 26, n4, (1993), pp. [517,542].

[22] D. Cioranescu and F. Murat, *Un terme étrange venu d'ailleurs*, In "Nonlinear partial differential equations and their applications", collège de France Seminar, Vol. 2, Reasearch Notes in Mathematics, 60, (1982), pp. [98,138].

[23] A. Comerford, G. Bauer, and W. A. Wall, *Nanoparticle transport in a realistic model of the tracheobronchial region*, Int. J. Numer. Method Biomed. Eng., 26 (2010), pp. 904–914.

[24] L. Desvillettes, F. Golse, and V. Ricci, *The mean field limit for solid particles in a Navier-Stokes flow*, J. Stat. Phys., (2008).

[25] R. Dobrushin, *Vlasov equations*, Func. Anal. Appl. 13, (1979), pp. [115,123].

[26] S. Faure, S. Martin, B. Maury, and T. Takahashi, *Towards the simulation of dense suspensions: a numerical tool*, ESAIM: Proceedings, 28 (2009), pp. [55,79].

[27] G. P. Galdi, *An introduction to the mathematical theory of the Navier-Stokes equations*, Springer Monographs in Mathematics.Springer, New York,, second edition ed., 2011. Steady-state problems.

[28] T. Gemci, T. E. Corcoran, and N. Chigier, *A numerical and experimental study of spray dynamics in a simple throat model*, Aerosol Sci. Technol., 36 (2002), pp. 18–38.

[29] F. Golse, *The mean-field limit for the dynamics of large particle systems*, Journées équations aux dérivées partielles,Tome (2003), pp. [1,47].

[30] E. Guazzelli and J. F. Morris, *A Physical Introduction To Suspension Dynamics*, Cambridge Texts In Applied Mathematics, 2012.

[31] K. Hamdache, *Global existence and large time behaviour of solutions for the Vlasov-Stokes equations*, Japan J. Indust. Appl. Math., 15(1), (1998), pp. [51,74].

[32] J. Happel and H. Brenner, *Low Reynolds number hydrodynamics*, Martinus Nijhoff, 1983. with special applications to particulate media.

[33] M. Hauray, *Wasserstein distances for vortices approximation of Euler-type equations*, Math. Models Methods Appl. Sci. 19, (2009), pp. [1357,1384].

[34] M. Hauray and P. E. Jabin, *Particle approximation of Vlasov equations with singular forces : propagation of chaos*, Ann. Sci. Éc. Norm. Supér. (4), (2015).

[35] F. Hecht, *New development in FreeFem++*, J. Numer. Math., 20 (2012), pp. 251–265.

[36] M. Hillairet, *On the homogenization of the stokes problem in a perforated domain*, Arch Rational Mech Anal, 230, (2018), pp. 1179,1228.

[37] M. Hillairet, A. Moussa, and F. Sueur, *On the effect of polydispersity and rotation on the Brinkman force induced by a cloud of particles on a viscous incompressible flow*, arXiv:1705.08628v1 [math.AP], (2017).

[38] R. M. Höfer, *Sedimentation of inertialess particles in Stokes flows*, Commun. Math. Phys. 360, (2018), pp. 55,101.

[39] R. M. Höfer and J. J. L. Velàzquez, *The method of reflections, homogenization and screening for Poisson and Stokes equations in perforated domains*, Arch Rational Mech Anal, 227, (2018), pp. 1165,1221.

[40] W. Hofmann, *Modelling inhaled particle deposition in the human lung – a review*, J. Aerosol Sci., 42 (2011), pp. 693–724.

[41] P. E. Jabin and F. Otto, *Identification of the dilute regime in particle sedimentation*, Communications in Mathematical Physics, (2004).

[42] D. J. Jeffrey and Y. Onishi, *Calculation of the resistance and mobility functions for two unequal spheres in low-Reynolds-number flow*, J . Fluid Meoh. vol. 139, (1984), pp. [261,290].

[43] V. Jikov, S. Kozlov, and O. Oleinik, *Homogenization of Differential Operators*, Springer-Verlag Berlin Heidelberg, 1994.

[44] S. Kim and S. J. Karrila, *Microhydrodynamics : Principles and Selected Applications*, Courier Corporation, 2005.

[45] P. Laurent, G. Legendre, and J. Salomon, *On the method of reflections*, https://hal.archives-ouvertes.fr/hal-01439871, (2017).

[46] A. Lefebvre, *Fluid-particle simulations with freefem++*, ESAIM: PROCEEDINGS, 18 (2007), pp. [120,132].

[47] A. Lefebvre and B. Maury, *Apparent viscosity of a mixture of a newtonian fluid and interacting particles, fluid-solid interactions: modeling, simulation, bio-mechanical applications*, Comptes Rendus Mecanique, 333 (2005), pp. [923,933].

[48] ——, *Micro-macro modelling of an array of spheres interacting through lubrication forces*, Adv. Math. Sci. Appl., 21 (2011), pp. [535,557].

[49] A. Lefebvre-Lepot, *Numerical simulation of suspensions: lubrication correction, including fluid correction*, Actes du colloque Edp-Normandie, (2017).

[50] G. Loeper, *Uniqueness of the solution to the Vlasov-Poisson system with bounded density*, J. Math. Pures Appl. 86, (2006), pp. [68,79].

[51] P. W. Longest and M. Hindle, *CFD simulations of enhanced condensational growth (ECG) applied to respiratory drug delivery with comparisons to in vitro data*, J. Aerosol Sci., 41 (2010), pp. 805–820.

[52] ——, *Numerical model to characterize the size increase of combination drug and hygroscopic excipient nanoparticle aerosols*, Aerosol Sci. Technol., 45 (2011), pp. 884–899.

[53] P. W. Longest and C. Kleinstreuer, *Computational models for simulating multicomponent aerosol evaporation in the upper respiratory airways*, Aerosol Sci. Tech., 39 (2005), pp. 124–138.

[54] J. H. C. Luke, *Convergence of a multiple reflection method for calculating Stokes flow in a suspension*, Society for Industrial and Applied Mathematics, (1989).

[55] G. Machu, W. Meile, L. C. Nitsche, and U. Schaflinger, *Coalescence, torus formation and breakup of sedimenting drops: experiments and computer simulations*, J . Fluid Mech. Volume 447, (25 November 2001), pp. [299,336].

[56] A. J. Majda and A. L. Bertozzi, *Vorticity and Incompressible Flow*, Cambridge University Press, 2010.

[57] A. Mecherbet, *Sedimentation of particles in stokes flow*, arXiv:1806.07795.

[58] B. Metzger, M. Nicolas, and . Guazzelli, *Falling clouds of particles in viscous fluids*, J . Fluid Mech. Volume 580, (10 June 2007), pp. [283,301].

[59] D. Michel, *Analyse mathématique de couplages fluide-cinétique*, PhD thesis, Sorbonne Université, work in progress since 2018.

[60] G. Milton, *The theory of composites*, Cambridge University Press, Cambridge, 2001.

[61] A. Moussa, *Étude mathématique et numérique du transport d'aérosols dans le poumon humain*, PhD thesis, École Normale Supérieure de Cachan, 2009.

[62] J. M. Nitsche and G. K. Batchelor, *Break-up of a falling drop containing dispersed particles*, J . Fluid Mech. Volume 340, (10 June 1997), pp. [161,175].

[63] J. M. Oakes, A. L. Marsden, C. Grandmont, S. C. Shadden, C. Darquenne, and I. E. Vignon-Clémentel, *Airflow and particle deposition simulations in health and emphysema: From in vivo to in silico animal experiments*, Ann. Biomed. Eng., 42 (2014), pp. 899–914.

[64] A. Pressley, *Elementary Differential Geometry*, Springer-Verlag London, 2010.

[65] E. Sanchez-Palencia, *Non-Homogeneous Media and Vibration Theory*, Springer, Berlin, Heidelberg, 1980.

[66] F. Santambrogio, *Introduction to optimal transport theory*, hal-00519456, (2009).

[67] M. Smoluchowski, *Über die Wechselwirkung von Kugeln, die sich in einer zähen Flüssigkeit bewegen*, Bull. Acad. Sci. Cracovie A 1, (1911), pp. [28,39].

[68] T. Soong, P. Nicolaides, C. P. Yu, and S. C. Soong, *A statistical description of the human tracheobronchial tree geometry*, Resp. Physiol., 37 (1979), pp. 161–172.

[69] L. Tartar, *The general theory of homogenization. A personalized introduction*, Springer-Verlag Berlin Heidelberg, 2009.

[70] C. Villani, *Optimal transport, old and new*, Springer-Verlag, Berlin, 2009.

[71] E. R. Weibel, *Morphometry of the human lung*, Springer Verlag and Academic Press, New York, 1963.

[72] Z. Zhang, C. Kleinstreuer, and C. S. Kim, *Airflow and nanoparticle deposition in a 16-generation tracheobronchial airway model*, Ann. Biomed. Eng., 36 (2008), pp. 2095–2110.

Résumé. Dans cette thèse, nous nous intéressons à la modélisation et l'analyse mathématique de certains problèmes liés aux écoulements en suspension. Le premier chapitre concerne la justification du modèle de type transport-Stokes pour la sédimentation de particules sphériques dans un fluide de Stokes où l'inertie des particules est négligée et leur rotation est prise en compte. Ce travail est une extension des résultats antérieurs pour un ensemble plus général de configurations de particules. Le deuxième chapitre concerne la sédimentation d'une distribution d'amas de paires de particules dans un fluide de Stokes. Le modèle dérivé est une équation de transport-Stokes décrivant l'évolution de la position et l'orientation des amas. Nous nous intéressons par la suite au cas où l'orientation des amas est initialement corrélée aux positions. Un résultat d'existence locale et d'unicité pour le modèle dérivé est présenté. Dans le troisième chapitre, nous nous intéressons à la dérivation d'un modèle de type fluide-cinétique pour l'évolution d'un aérosol dans les voies respiratoires. Ce modèle prend en compte la variation du rayon des particules et leur température due à l'échange d'humidité entre l'aérosol et l'air ambiant. Les équations décrivant le mouvement de l'aérosol est une équation de type Vlasov-Navier Stokes couplée avec des équations d'advection diffusion pour l'évolution de la température et la vapeur d'eau dans l'air ambiant. Le dernier chapitre traite de l'analyse mathématique de l'équation de transport-Stokes dérivée au premier chapitre. Nous présentons un résultat d'existence et d'unicité globale pour des densités initiales de type $L^1 \cap L^\infty$ ayant un moment d'ordre un fini. Nous nous intéressons ensuite à des densités initiales de type fonction caractéristique d'une gouttelette et montrons un résultat d'existence locale et d'unicité d'une paramétrisation régulière de la surface de la gouttelette. Enfin nous présentons des simulations numériques montrant l'aspect instable de la gouttelette.

Mots clés. Écoulements de fluides multiphasiques, écoulements en suspension, écoulement de Stokes, sédimentation, équations de (Navier) Stokes, équations de type Vlasov, équations de transport, système d'interaction de particules, méthode de réflexions, théorie de champ moyen, homogéneisation, existence locale et unicité.

Abstract. This thesis is devoted to the modelling and mathematical analysis of some aspects of suspension flows. The first chapter concerns the justification of the transport-Stokes equation describing the sedimentation of spherical rigid particles in a Stokes flow where particles rotation is taken into account and inertia is neglected. This work is an extension of former results for a more general set of particles configurations. The second chapter is dedicated to the sedimentation of clusters of particle pairs in a Stokes flow. The derived model is a transport-Stokes equation describing the time evolution of the position and orientation of the cluster. We also investigate the case where the orientation of the cluster is initially correlated to its position. A local existence and uniqueness result for the limit model is provided. In the third chapter, we propose a coupled fluid-kinetic model taking into account the radius growth of aerosol particles due to humidity in the respiratory system. We aim to numerically investigate the impact of hygroscopic effects on the particle behaviour. The air flow is described by the incompressible Navier-Stokes equations, and the aerosol by a Vlasov-type equation involving the air humidity and temperature, both quantities satisfying a convection-diffusion equation with a source term. The last chapter is dedicated to the analysis of the transport-Stokes equation derived in the first chapter. First we present a global existence and uniqueness result for $L^1 \cap L^\infty$ initial densities with finite first moment. Secondly, we consider the case where the initial data is the characteristic function of a droplet. We present a local existence and uniqueness result for a regular parametrization of the droplet surface. Finally, we provide some numerical computations that show the regularity breakup of the droplet.

Keywords. Multiphase fluid flows, suspension flows, Stokes flows, sedimentation, (Navier) Stokes equations, Vlasov-like equations, transport equations, system of interacting particles, method of reflections, mean field limit, homogenization, local existence and uniqueness.